NITROGEN IN THE ENVIRONMENT

EDITED BY: Muhammad Shaaban, Ryusuke Hatano,
Rosa María Martínez-Espinosa and Yupeng Wu

PUBLISHED IN: Frontiers in Environmental Science

frontiers Research Topics

ISSN 1664-8714
ISBN 978-2-88974-809-9
DOI 10.3389/978-2-88974-809-9

About Frontiers

Frontiers is more than just an open-access publisher of scholarly articles: it is a pioneering approach to the world of academia, radically improving the way scholarly research is managed. The grand vision of Frontiers is a world where all people have an equal opportunity to seek, share and generate knowledge. Frontiers provides immediate and permanent online open access to all its publications, but this alone is not enough to realize our grand goals.

Frontiers Journal Series

The Frontiers Journal Series is a multi-tier and interdisciplinary set of open-access, online journals, promising a paradigm shift from the current review, selection and dissemination processes in academic publishing. All Frontiers journals are driven by researchers for researchers; therefore, they constitute a service to the scholarly community. At the same time, the Frontiers Journal Series operates on a revolutionary invention, the tiered publishing system, initially addressing specific communities of scholars, and gradually climbing up to broader public understanding, thus serving the interests of the lay society, too.

Dedication to Quality

Each Frontiers article is a landmark of the highest quality, thanks to genuinely collaborative interactions between authors and review editors, who include some of the world's best academicians. Research must be certified by peers before entering a stream of knowledge that may eventually reach the public - and shape society; therefore, Frontiers only applies the most rigorous and unbiased reviews.
Frontiers revolutionizes research publishing by freely delivering the most outstanding research, evaluated with no bias from both the academic and social point of view. By applying the most advanced information technologies, Frontiers is catapulting scholarly publishing into a new generation.

What are Frontiers Research Topics?

Frontiers Research Topics are very popular trademarks of the Frontiers Journals Series: they are collections of at least ten articles, all centered on a particular subject. With their unique mix of varied contributions from Original Research to Review Articles, Frontiers Research Topics unify the most influential researchers, the latest key findings and historical advances in a hot research area! Find out more on how to host your own Frontiers Research Topic or contribute to one as an author by contacting the Frontiers Editorial Office: frontiersin.org/about/contact

NITROGEN IN THE ENVIRONMENT

Topic Editors:
Muhammad Shaaban, Bahauddin Zakariya University, Pakistan
Ryusuke Hatano, Hokkaido University, Japan
Rosa María Martínez-Espinosa, University of Alicante, Spain
Yupeng Wu, Huazhong Agricultural University, China

Citation: Shaaban, M., Hatano, R., Martínez-Espinosa, R. M., Wu, Y., eds. (2022). Nitrogen in the Environment. Lausanne: Frontiers Media SA.
doi: 10.3389/978-2-88974-809-9

Table of Contents

frontiers in Environmental Science

EDITORIAL
published: 20 January 2022
doi: 10.3389/fenvs.2021.829104

Editorial: Nitrogen in the Environment

Muhammad Shaaban[1]*, *Ryusuke Hatano*[2], *Rosa María Martínez-Espinosa*[3] and *Yupeng Wu*[4]

[1]Key Laboratory of Mountain Surface Processes and Ecological Regulation, Institute of Mountain Hazards and Environment, Chinese Academy of Sciences, Chengdu, China, [2]Research Faculty of Agriculture, Hokkaido University, Sapporo, Japan, [3]Division of Biochemistry and Molecular Biology, Department of Agrochemistry and Biochemistry, University of Alicante, Alicante, Spain, [4]College of Resources and Environment, Huazhong Agricultural University, Wuhan, China

Keywords: environment, soil, nitrogen, processes, challenge

Editorial on the Research Topic

Nitrogen in the Environment

Nitrogen (N) is essential for life of all living organisms in the universe. Every year, about 67.84 million tons of nitrogen is applied to agricultural land all over the world (Liu et al., 2010). Nitrogen is the only essential element which exists in several forms in soil. The transformations of N takes place by several interactive factors and microbes. The interaction among factors therefore plays a pivotal role in functional maintenance of environment. Nitrogen is always not beneficial to living organisms; excess concentration of N might act as pollutant, thus N may also affect human and environmental health (Robertson and Groffman, 2015). Understanding the importance of N in various ecosystems is thus essential for understanding sustainable development and productivity. In terrestrial ecosystems, N exists in nine different chemical forms corresponding to different oxidative states. Dinitrogen gas (N_2) is the inert form of N and the most abundant in the biosphere. N_2 is transformed to organic N through biological N_2 fixation, and enters biological pools of soil. Subsequently, the fixed-N undergoes several microbial processes; mineralization, immobilization, nitrification, denitrification. Löhnis (1913) was the first scientist who developed the concept of N cycle illustrating that N is transformed from one form to another (Löhnis, 1913; Robertson and Groffman, 2015). Anthropogenic activities have seriously perturbed the global nitrogen cycle. Excessive use of nitrogen for crop production has negatively impacted soil biological diversity, climate, and human health (Liu et al., 2013). However, nitrogen shortage leads us to fall short of proper food demands by limiting both the quantity and quality of crops. The disturbance of the global nitrogen cycle at a large scale presents substantial challenges and requires immediate implementation of strategies for appropriate nitrogen management. Understanding nitrogen transformations and the soil microbes that perform them, as well as proper management of nitrogen for crops, are thus essential for understanding and managing ecosystem health and productivity. Biological and industrial N_2 fixation have far outpaced record denitrification rates in the history and is identified as main reason of N pollution in the environment (Galloway et al., 2008). Therefore, it is an environmental challenge to make managed ecosystems with rational use of N (Robertson and Vitousek, 2009).

In this Research Topic, we received total 13 articles, and finally eight articles after peer review were recommended for publication in Research Topic (N in the environment) by Guest Editors. Among eight published articles, two are review articles, one is method, and five are original research articles. The published articles focused various aspects of N in the environment.

The first article recommended for the publication was authored by Nadeem et al., They studied nitrification and denitrification kinetics and the abundance of ammonia oxidizing bacteria (AOB) and ammonia oxidizing archaea (AOA) in soils sampled from a field experiment 2–3 years after liming. The $N_2O/(N_2O+N_2)$ product ratio of heterotrophic denitrification declined with increasing pH, and the potential nitrification rate and its N_2O yield (YN_2O: $N_2O\text{-}N/NO_3^-\text{-}N$), as measured in fully oxic soil slurries, increased with pH, and both correlated strongly with the AOB/AOA gene

OPEN ACCESS

Edited and reviewed by:
Vera I. Slaveykova,
Université de Genève, Switzerland

***Correspondence:**
Muhammad Shaaban
shabanbzu@hotmail.com

Specialty section:
This article was submitted to Biogeochemical Dynamics, a section of the journal Frontiers in Environmental Science

Received: *04 December 2021*
Accepted: *23 December 2021*
Published: *20 January 2022*

Citation:
Shaaban M, Hatano R, Martínez-Espinosa RM and Wu Y (2022) Editorial: Nitrogen in the Environment. Front. Environ. Sci. 9:829104. doi: 10.3389/fenvs.2021.829104

abundance ratio. They proposed that while low emissions from nitrification in well-drained soils may be enhanced by liming, the spikes of high N_2O emission induced by ammonium fertilization at high soil moisture may be reduced by liming, because the heterotrophic N_2O reduction is enhanced by high pH. Another article authored by Xu et al., which explored the comparison of N_2O emission from a cold waterlogged and normal paddy field. They revealed that N_2O emissions from cold waterlogged paddy fields were significantly lower than those of normal rice fields due to the low temperature and higher water content; there may also be complete denitrification that may lead to a decrease in N_2O emissions. In the review article, Mejías et al., reviewed the potential use as an innovative approach to improve nitrogen use efficiency and reduce N losses to the wider environment, analyzing potential shortcomings and future considerations for animal food chains. Su et al., used a fully automated system to continuously measure soil N_2O emissions for 2 years and suggested that sampling between 9:00 am and 10: 00 am is the best empirical sampling time for the intermittent manual measurements. Hayakawa et al., examined sulfur-driven NO_3^- reduction using streambank soils in a headwater catchment underlain by marine sedimentary rock. Many denitrifying sulfur-oxidizing bacteria were detected which dominated up to 5% of the entire microbial population, suggesting that these bacteria are widespread in sulfide-rich soil layers in the catchment. They concluded that the catchment with abundant sulfides in the subsoil possessed the potential for sulfur-driven NO_3^- reduction, which could widely influence N cycling in and NO_3^- export from the headwater catchment. In a review article, Moeller et al., described the current picture of the function of regulatory sRNAs in biogeochemical cycles, with specific focus on the nitrogen cycle. Non-coding small RNAs (sRNAs) regulate a wide range of physiological processes in microorganisms that allow them to rapidly respond to changes in environmental conditions. sRNAs have predominantly been studied in a few model organisms, however it is becoming increasingly clear that sRNAs play a crucial role in environmentally relevant pathways. For example, several sRNAs have been shown to control important enzymatic processes within the nitrogen cycle and many more have been identified in nitrogen cycling organisms that remain to be characterized. Alongside these studies meta-transcriptomic data indicated both known and putative sRNA are expressed in microbial communities and are potentially linked to changes in environmental processes in these habitats. Schleppi and Wessel analyzed the statistical and practical considerations for the design of labeling experiments and also for assessments of natural ^{15}N abundance. According to their findings, the stable isotope ^{15}N is an extremely useful tool for studying the nitrogen (N) cycle of terrestrial ecosystems. Banik et al., conducted a study based on the hypothesis that the combined amendment of biochar and manure could be a better soil amendment than conventional manure application. Manure-biochar treatments significantly increased soil total C, N, and improved soil bulk density. Overall, the manure-biochar application enabled biochar to stabilize the C and N from manure. The authors suggested that biochar could be used to solve N related environmental and agronomic challenges and further improve N use efficiency for sustainable crop production.

All articles published in this Research Topic employed advanced techniques and interesting for the readership of the journal. The Guest Editors of this Research Topic would like to thank all authors, reviewers, and the Editorial team and technical staff of Frontiers in Environmental Science. All of them have collaborated with their great work and involvement in the development of this Research Topic.

AUTHOR CONTRIBUTIONS

MS, RH, RM-E and YW wrote and finally proofed the reading of the document.

REFERENCES

Galloway, J. N., Townsend, A. R., Erisman, J. W., Bekunda, M., Cai, Z., Freney, J. R., et al. (2008). Transformation of the Nitrogen Cycle: Recent Trends, Questions, and Potential Solutions. *Science* 320, 889–892. doi:10.1126/science.1136674

Liu, J., You, L., Amini, M., Obersteiner, M., Herrero, M., Zehnder, A. J. B., et al. (2010). A High-Resolution Assessment on Global Nitrogen Flows in Cropland. *Proc. Natl. Acad. Sci. USA* 107, 8035–8040. doi:10.1073/pnas.0913658107

Liu, X., Zhang, Y., Han, W., Tang, A., Shen, J., Cui, Z., et al. (2013). Enhanced Nitrogen Deposition over China. *Nature* 494, 459–462. doi:10.1038/nature11917

Löhnis, F. (1913). *Vorlesungen über landwirtschaftliche Bakteriologie*. Stuttgart: Gebrüder Borntraeger.

Robertson, G. P., and Groffman, P. (2015). "Nitrogen Transformations," in *Soil Microbiology, Ecology and Biochemistry*. Editor A. Paul (Amsterdam, Netherlands: Elsevier), 341–364. doi:10.1016/b978-0-12-415955-6.00014-1

Robertson, G. P., and Vitousek, P. M. (2009). Nitrogen in Agriculture: Balancing the Cost of an Essential Resource. *Annu. Rev. Environ. Resour.* 34, 97–125. doi:10.1146/annurev.environ.032108.105046

Conflict of Interest: The authors declare that the research was conducted in the absence of any commercial or financial relationships that could be construed as a potential conflict of interest.

Publisher's Note: All claims expressed in this article are solely those of the authors and do not necessarily represent those of their affiliated organizations, or those of the publisher, the editors and the reviewers. Any product that may be evaluated in this article, or claim that may be made by its manufacturer, is not guaranteed or endorsed by the publisher.

frontiers in Environmental Science

ORIGINAL RESEARCH
published: 04 December 2020
doi: 10.3389/fenvs.2020.598513

Contingent Effects of Liming on N_2O-Emissions Driven by Autotrophic Nitrification

Shahid Nadeem[1], Lars R. Bakken[2], Åsa Frostegård[2], John C. Gaby[2] and Peter Dörsch[1]*

[1] Faculty of Environmental Sciences and Natural Resource Management, Norwegian University of Life Sciences (NMBU), Ås, Norway, [2] Faculty of Chemistry, Biotechnology and Food Science, Norwegian University of Life Sciences (NMBU), Ås, Norway

OPEN ACCESS

Edited by:
Muhammad Shaaban, Bahauddin Zakariya University, Pakistan

Reviewed by:
Alessandro Florio, Institut National de Recherche pour l'Agriculture, l'alimentation et l'Environnement (INRAE), France
Meihua Deng, ZheJiang Academy of Agricultural Sciences, China

****Correspondence:***
Lars R. Bakken
lars.bakken@nmbu.no

Specialty section:
This article was submitted to Soil Processes, a section of the journal Frontiers in Environmental Science

Received: *24 August 2020*
Accepted: *11 November 2020*
Published: *04 December 2020*

Citation:
Nadeem S, Bakken LR, Frostegård Å, Gaby JC and Dörsch P (2020) Contingent Effects of Liming on N_2O-Emissions Driven by Autotrophic Nitrification. Front. Environ. Sci. 8:598513. doi: 10.3389/fenvs.2020.598513

Liming acidic soils is often found to reduce their N_2O emission due to lowered $N_2O/(N_2O + N_2)$ product ratio of denitrification. Some field experiments have shown the opposite effect, however, and the reason for this could be that liming stimulates nitrification-driven N_2O production by enhancing nitrification rates, and by favoring ammonia oxidizing bacteria (AOB) over ammonia oxidizing archaea (AOA). AOB produce more N_2O than AOA, and high nitrification rates induce transient/local hypoxia, thereby stimulating heterotrophic denitrification. To study these phenomena, we investigated nitrification and denitrification kinetics and the abundance of AOB and AOA in soils sampled from a field experiment 2–3 years after liming. The field trial compared traditional liming (carbonates) with powdered siliceous rocks. As expected, the $N_2O/(N_2O + N_2)$ product ratio of heterotrophic denitrification declined with increasing pH, and the potential nitrification rate and its N_2O yield (Y_{N2O}: N_2O-N/NO_3^--N), as measured in fully oxic soil slurries, increased with pH, and both correlated strongly with the AOB/AOA gene abundance ratio. Soil microcosm experiments were monitored for nitrification, its O_2-consumption and N_2O emissions, as induced by ammonium fertilization. Here we observed a conspicuous dependency on water filled pore space (WFPS): at 60 and 70% WFPS, Y_{N2O} was 0.03-0.06% and 0.06–0.15%, respectively, increasing with increasing pH, as in the aerobic soil slurries. At 85% WFPS, however, Y_{N2O} was more than two orders of magnitude higher, and decreased with increasing pH. A plausible interpretation is that O_2 consumption by fertilizer-induced nitrification cause hypoxia in wet soils, hence induce heterotrophic nitrification, whose Y_{N2O} decline with increasing pH. We conclude that while low emissions from nitrification in well-drained soils may be enhanced by liming, the spikes of high N_2O emission induced by ammonium fertilization at high soil moisture may be reduced by liming, because the heterotrophic N_2O reduction is enhanced by high pH.

Keywords: soil pH, nitrification, N_2O-reductase, N_2O, moisture

INTRODUCTION

Although soils are buffered by ion exchange reactions and weathering of minerals (Chadwick and Chorover, 2001), they become gradually acidified by cultivation, primarily due to ammoniacal nitrogen fertilization and loss of base cations (von Uexküll and Mutert, 1995; Guo et al., 2010). Soil acidification is commonly counteracted by carbonate addition, either as frequent low doses or as infrequent heavy dressings (Shaaban et al., 2014; Goulding, 2016). Crop plants display substantial variation in acid tolerance (Goulding, 2016), and even cultivars within one species may vary in their tolerance to soil acidity (Kochian et al., 2004). Thus, the target pH for sustaining high yields will depend on the crop, with the minimum given by its tolerance to acidity and the maximum by the micronutrient availability of the soil at elevated pH (White and Robson, 1989). Liming may also serve other purposes than securing an agronomic minimum pH for crop production. Heavy dressings of CaO (or $Ca(OH)_2$) reduce soil erosion by improving the structure of heavy clay soils (Ulén and Etana, 2014), while the effect on crop growth appears variable, possibly due to reduced manganese availability at high pH in some soils (Blomquist et al., 2018).

Liming beyond the minimum for crops has also been proposed as a means of reducing N_2O emissions, since soil acidification leads to high N_2O/N_2 product ratios of denitrification under standardized anoxic incubations. This was first observed by Wijler and Delwiche (1954), and corroborated by subsequent investigations, although the reason remained obscure (Čuhel and Šimek, 2011). Recent studies of transcription and enzyme kinetics have provided compelling evidence that this is a post-transcriptional phenomenon: the making of functional N_2O-reductase is increasingly impaired with increasing proton concentrations (Liu et al., 2014).

Numerous field and microcosm experiments have been conducted to determine if N_2O emission can be reduced by increasing soil pH, be it by carbonates (Shaaban et al., 2014, 2015, 2018; Oo et al., 2018), or biochar (reviewed by Cayuela et al., 2014). Although the investigations generally corroborate the hypothesis, there are also cases where N_2O emissions were either unaffected or even increased in response to elevated soil pH (see review by Qu et al., 2014). One reason for the variable effect of liming on N_2O emissions from soils could be the production of N_2O by ammonia oxidizing organisms. The three known groups of ammonia oxidizing organisms are the ammonia oxidizing bacteria (AOB), the ammonia oxidizing archaea (AOA) and the recently discovered comammox group (Daims et al., 2015), which oxidizes NH_3 all the way to NO_3^- While little is known about the ecology and N_2O production of comammox, the biochemistry and ecophysiology of AOB and AOA and their N_2O production have been subject to intense studies. AOA are frequently found to outnumber AOB in soils with low availability of NH_4^+ and low pH, while AOB appear to thrive in response to high pH and fertilization with NH_4^+ (Nicol et al., 2008). Thus, liming acid soils should favor AOB over AOA, which would enhance N_2O production by nitrification because AOB produce much more N_2O per mole N oxidized than AOA, as pointed out by Hink et al. (2017a).

Next to the prevalence of AOB and AOA, the amount of N_2O produced per mole N oxidized could also be affected by the rate of nitrification: nitrification consumes oxygen and produces NO_2^- and NO_3^-, hence potentially inducing denitrification, either by heterotrophic or nitrifying organisms (Kool et al., 2011a,b; Huang et al., 2014). Isotope tracing data have been taken to suggest that *nitrifier denitrification* is more significant than heterotrophic denitrification in soils (Zhu et al., 2013; Wrage-Mönning et al., 2018), but the validity of this has been challenged recently by Bakken and Frostegård (2017), who claim that the isotope tracing method cannot be used to distinguish between the two pathways. This distinction is important in the context of pH management because the net production of N_2O by heterotrophic denitrification is strongly dependent on pH, while that by *nitrifier denitrification* is not: denitrification by nitrifying organisms produces pure N_2O regardless of pH, because they lack the gene for N_2O reductase (*nosZ*) (Klotz and Stein, 2011).

While increasing soil pH was expected to reduce the N_2O emission from denitrification by enhancing the synthesis of functional N_2O reductase, we hypothesized that it would have the opposite effect on N_2O emission from nitrification, both by increasing its N_2O yield (mol N_2O per mol NO_3^- produced) and by enhancing the potential nitrification rate. The latter would lead to high oxygen consumption after fertilization with ammonium, hence increasing the risk for hypoxia and denitrification if the soil moisture content is high. Such nitrification induced denitrification would be a strong N_2O source, hypothetically enhanced by increasing the soil pH, unless effectively counteracted by enhanced synthesis of N_2O reductase at high pH. To shed light on the potential stimulation of N_2O emission from nitrification after liming, we conducted a series of laboratory incubations with soils sampled over a period of 2 years from a field trial, in which carbonates were compared with siliceous rock powders as agents to increase the soil pH (Nadeem et al., 2015). The motive for testing powdered siliceous rocks was to explore the possibility of using carbonate-free minerals, thus avoiding the emission of carbonate-CO_2. In addition, we describe the effect of the rock powders on the AOB/AOA ratio as a function of increasing soil pH.

While corroborating the well-known effect of pH-increase on the synthesis of functional N_2O reductase (hence reducing N_2O emission from denitrification), the strictly oxic incubations demonstrated that the rate of nitrification and its N_2O yield increased with soil pH. We further demonstrate that nitrification-induced denitrification increases with soil moisture, and provide evidence that oxygen consumption by nitrification induces heterotrophic denitrification, rather than *nitrifier-denitrification*. The results are important because they explain why the effect of liming on the N_2O emission induced by ammonium fertilization depends on the soil moisture content: at very high soil moisture content, ammonium fertilization may cause high N_2O emission by inducing heterotrophic denitrification, and this emission can be reduced by liming. At modest/low moisture content, ammonium fertilization induces modest

N_2O emission from nitrification alone, and this is enhanced by liming.

MATERIALS AND METHODS

Experimental Site and Soil Sampling

Soils were sampled from a field trial established in autumn 2014, to test the effect of finely ground siliceous minerals as alternatives to liming. The trial is situated on the research farm of the Norwegian University of Life Sciences (NMBU) at Ås (59° 49′ N, 10° 47′ E, 75 m a.s.l) in southeast Norway. Mean annual temperature is 7.7°C and mean annual precipitation is 1,083 mm (Hansen and Grimenes, 2015). The field had been under crop rotation including leys since 1953, and the soil (clay loam) had not been limed since 1970. The field trial consists of six treatments: two types of calcareous lime (calcite and dolomite), and three types of siliceous rock powders (olivine, norite, and larvikite) and an untreated control. Each treatment was replicated four times and randomly distributed in two blocks (same blocks as the previous crop rotation experiment). Soil pH and content of soil organic matter measured prior to liming is given in **Supplementary Table 1**. Minerals were applied during autumn 2014 at a rate of 30 t ha^{-1} (siliceous rock powders and calcite) and 23 t ha^{-1} (dolomite). The siliceous minerals were Olivine: Blueguard 63, particle size <63 μm, from the company Sibelco Nordic AS Norway; Larvikite: rock cutting dust from Lundhs AS Norway, which was further ball milled and wet sieved to achieve a particle size <63 μm; Norite: waste material from titanium enrichment process (cyclone removal of particles), from Titania AS Norway, particle size <300 μm (∼50% W/W <63 μm); Calcite obtained as a suspension of colloidal particles (0.4–1.5 μm) from OMYA-Hustadmarmor AS; and Dolomite, obtained as an agricultural lime from Franzefoss A/S Norway. The mineral materials were mixed evenly into the upper 20 cm of the soil by plowing after adding half of the material, then harrowing after adding the second half. Winter wheat was sown in late autumn 2014, but failed to establish, and the field was plowed again in the late spring of 2015. Barley (*Hordeum vulgar*, cultivar Sunita) was sown on June 5 as a cover crop together with a grass mixture (20% *Phleum pratense*, 25% *Lolium perenne*, 25% *Festuca pratensis*, 20% *Festuca arundinacea schreb*, 10% *Poa pratense L*), fertilized with 100 kg N ha^{-1} (mineral fertilizer, NPK 22:3:10). The cover crop was harvested after 8 weeks. Ley growth was poor in the year of establishment, but improved in subsequent years. The ley was fertilized with 270 kg N ha^{-1} y^{-1} as NPK or CAN, split into 120 kg N in spring, 90 kg N after the 1st harvest and 60 kg N after the 2nd harvest. Soil samples were collected in 2015 and 2016 (during summer and late autumn), at 15, 21, and 27 months after liming. A composite sample (2–10 cm) was taken from each replicate plot by pooling at least 6 auger cores per plot. The soil samples were immediately transferred to the laboratory, sieved (2 mm), and stored in plastic bags at 4°C, until used for analyses and laboratory incubations (1–5 days after collection).To determine soil pH, 10 g soil were thoroughly dispersed in 25 mL 0.01 M $CaCl_2$ (hand shaken). The slurry was left to settle overnight, then shaken again, and finally left to settle for 15 min before measuring the pH.

Nitrification and Denitrification Kinetics

Soil Slurry Experiments

Soil slurries were used for potential nitrification and denitrification experiments. Equivalents of 4 g dry weight soil were transferred to 120 ml serum flasks and dispersed in 40 ml 1 mM NH_4Cl (for nitrification) or KNO_3 solution (for denitrification). All flasks were equipped with Teflon coated magnetic stirrers, and crimp-sealed with Teflon-coated silicone septa for nitrification experiments (to avoid inhibition of nitrification), and butyl rubber septa for denitrification experiments.

To ensure low initial NO_3^- concentrations in the nitrification assay, the soils were first flooded with deionized water and drained by vacuum in 500 ml filter funnels (Millipore) with 0.45 μm filters, then transferred to the vials (4 g dry weight equivalents). The nitrification assay was performed at 23°C, while shaking the flasks horizontally on a reciprocal shaker (125 rpm) to ensure that fully oxic condition were maintained throughout the incubation. To measure N_2O, the bottles were removed from the shaker once or twice per day and placed for a short period in a temperature-controlled water bath (23°C) of the incubation robot (Molstad et al., 2007). The robot sampled the headspace (∼1 mL) with a hypodermic needle, to determine O_2 and N_2O concentrations. After each sampling, an equal volume of He was pumped back to the headspace to keep the flask pressure at ∼1 atm. We used the new version of the robot, described by Molstad et al. (2016), equipped with an Agilent GC-7890A gas chromatograph with three detectors (FID, TCD, ECD) for determining the concentrations of O_2, N_2, N_2O, and CO_2, and with a chemiluminescence detector (Teledyne NO/NO_x analyzer mod 200E) for detection of NO. After each gas analysis, the flasks were returned to the reciprocal shaker. Oxygen concentrations in the headspace were monitored throughout, and pure oxygen was added when O_2 concentration fell below 16 vol% in the headspace, thus maintaining O_2 concentration between 15 and 20 vol%.

Denitrification kinetics were measured by frequent sampling from the headspace of 120 ml serum flasks containing 4 g dry weight soil and 40 ml of 1 mM KNO_3. The flasks were placed in the water bath of the incubation robot, and the slurries were stirred continuously (400 rpm). Before the incubation, all flasks were washed with He by repeated evacuation and filling. The final He overpressure was released by using a syringe without plunger containing water. The observed gas kinetics were corrected for dilution and leakage as outlined by Molstad et al. (2007). Soil pH for each replicate sample was measured at the beginning and end of the incubation, and the average of these two values was used for further calculations.

NO_2^- and NO_3^- Measurements

Nitrification rates were determined from the accumulation of NO_3^- and NO_2^- in the soil slurries over time. Once per day, 0.5 ml of the soil slurry was removed with a syringe and centrifuged at 10,000 *g* for 15 min at 4°C. NO_3^- and NO_2^- concentrations in the supernatant were determined immediately by colorimetry using a microplate reader (Infinite F50, TECAN Austria GmbH) at 540 nm. Both NO_3^- and NO_2^- were measured by Griess reaction (Keeney and Nelson, 1982),

with NO_3^- being converted to NO_2^- by vanadium chloride (Doane and Horwath, 2003).

Calculations

Nitrification rates were calculated from $NO_2^- + NO_3^-$ accumulation, while denitrification rates were calculated as the sum of NO, N_2O and N_2 accumulation. N_2O emission potentials from each process were estimated by calculating the N_2O yield as $N_2O/(NO_2^- + NO_3^-)$ for nitrification and the N_2O production index (I_{N2O}) for denitrification. The N_2O index of denitrification was calculated as described in Liu et al. (2010).

$$I_{N2O} = \frac{\int_0^T N_2O\, dt}{\int_0^T (N_2O + N_2) dt} \quad (1)$$

where N_2O (t) is the accumulated flux of N_2O at any time t, N_2 (t) is the accumulated flux of N_2 at any time, and T is the time when a certain amount of NO_3^--N kg^{-1} soil was recovered as gaseous N (NO_2^-, NO, N_2O, and N_2). I_{N2O} was calculated for two time periods, T_{10} and T_{25}; i.e., the time point when 10 and 25 μmol NO_3^-, respectively, had been denitrified to gaseous *N*.

Incubation Experiments With Remolded Soil

To study nitrification and denitrification under more realistic conditions than in slurries, we conducted a series of incubations with remolded soils.

Aerobic incubation was used to study nitrification (and its N_2O emission): 10 g of sieved soil from each plot (15 months after liming) was added to 120 ml serum flasks, packed to a bulk density of 1 g cm^{-3} and adjusted to 60% water filled pore space (WFPS). To induce nitrification, the soil was amended with a concentrated $(NH_4)_2SO_4$ solution equivalent to 110 mg N kg^{-1} soil by carefully distributing the solution throughout the soil volume, by using a syringe with a long needle. The flasks were incubated with air in the headspace at 20°C for 150 h, and O_2 consumption and N_2O production were monitored by the robotized incubation system described above. Nitrification was estimated from NO_3^- and NO_2^- accumulation in parallel offline incubation flasks covered with aluminum foil, which were subsampled periodically for determination of NO_3^- and NO_2^- concentrations (0.5 g soil was transferred to Eppendorf tubes with 1 ml deionized water, shaken, and centrifuged). The experiment was repeated at higher WFPS values (70 and 85%) with soils collected 27 months after liming to quantify the net N_2O emissions under conditions supporting coupled nitrification-denitrification, i.e., the reduction of NO_3^- or NO_2^- from nitrification by denitrification.

Anaerobic incubation of remolded soil was used to study denitrification: Prior to incubation, the soils were flooded with 2 mM KNO_3 solution and then drained, as described by Liu et al. (2010). After drainage an equivalent of 20 g dry weight soil was loosely packed into 120 ml serum flasks. Headspace gas was replaced with He. Headspace gasses were monitored as described above.

SSU rRNA Gene Sequence Analysis

DNA was extracted according to the protocol of Lim et al. (2016). To determine the relative proportion of AOB vs. AOA, we conducted amplicon sequencing of the SSU rRNA gene from the microbial communities in the different field plots as sampled December, 2016. Briefly, the V4 region of the 16S rRNA gene was amplified with the 515f (5′-GTGYCAGCMGCCGCGGTAA-3′) and 806rB (5′-GGACTACNVGGGTWTCTAAT-3′) primers (Apprill et al., 2015; Parada et al., 2016) by following the Earth Microbiome Project protocol[1], and amplicons were sequenced on an Illumina MiSeq instrument using a 600 cycle kit, v3 (2 × 300 bp paired-end reads). A total of 36 samples were sequenced, which includes field plots that were sequenced in triplicate (**Supplementary File 1**) as technical replicates. The number of sequence reads per sample ranged from 81,276 to 457,377 with a mean of 299,296 and standard deviation of 99,835. The demultiplexed FASTQ files were obtained from the sequencer and analyzed in the statistical software R^2 using the packages DADA2 (Callahan et al., 2016) and Phyloseq (McMurdie and Holmes, 2013). Taxonomy of the resultant Amplicon Sequence Variants (ASVs) was established by reference to the Silva SSU rRNA database release 132 (Yilmaz et al., 2014). We then identified ammonia-oxidizers by searching for the term "nitroso" among all levels of the taxonomic hierarchy, whereby we determined that the ammonia-oxidizing *Archaea* consisted solely 42 ASVs in 2 classes of the phylum *Thaumarchaeota*, *Nitrososphaeria* and "Group_1.1c". Similarly, we identified ammonia-oxidizing *Bacteria* as consisting of 77 ASVs within the family *Nitrosomonadaceae* within the phylum *Gammaproteobacteria*. The abundances of these ASVs in the different samples were tallied to obtain the relative abundance of AOB and AOA and thus to determine the AOB/AOA ratio. To identify nitrite oxidizing bacteria, we similarly searched for their taxonomic descriptors and identified *Nitrospira*, *Nitrobacter*, and *Candidatus* Nitrotoga as present in the dataset. A total of 20 *Nitrospira* ASVs were detected while only one sample contained one *Nitrobacter* ASV and another sample contained a single *Candidatus* Nitrotoga ASV.

[1]http://www.earthmicrobiome.org/emp-standard-protocols/16s/

TABLE 1 | Soil pH as affected by the mineral treatments.

Treatment	Soil pH_{CaCl2}	ΔpH
Control	5.01 ± 0.05	–
Larvikite	5.02 ± 0.04	0.01 ± 0.01
Norite	5.12 ± 0.04	0.11 ± 0.02
Olivine	5.17 ± 0.03	0.16 ± 0.03
Dolomite	5.55 ± 0.04	0.58 ± 0.04
Calcite	6.62 ± 0.06	1.57 ± 0.08

The table shows the average soil pH_{CaCl2} (n = 14 ± SE) throughout the 2 years after incorporation of lime and minerals, and the average increase in pH by each mineral treatment relative to the control (ΔpH). Pairwise t-tests for difference between mineral treatments and control (ΔpH) showed significant effects ($p < 0.05$) for all minerals except Larvikite. Fluctuations in pH and ΔpH throughout the 2 years are shown in ***Supplementary Figure 1****.*

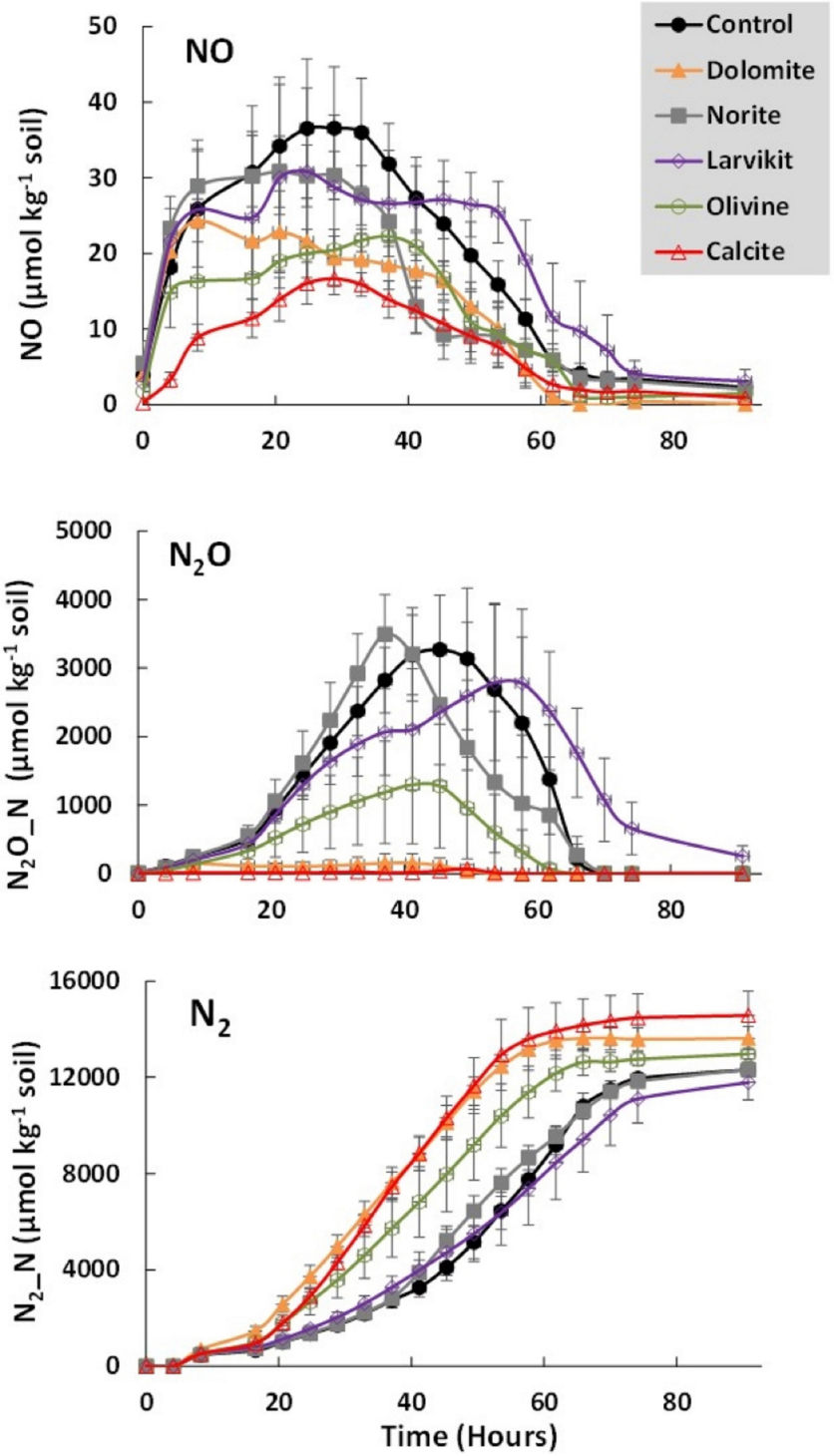

FIGURE 1 | Denitrification in soil slurries. NO and N_2O are shown as measured, while N_2 is the cumulative production (measured values corrected for sampling loss, see Molstad et al., 2007). Plotted values are means and standard errors of four field-replicates for each treatment, sampled 27 months after mineral applications in the field experiment. Samples taken 15 months after mineral treatment showed very similar response to soil pH whereby the N_2O production index (I_{N2O}) declined with soil pH. I_{N2O} for individual soil samples in both experiments are shown in **Supplementary Figure 4**.

Accession Numbers

The sequence data analyzed in this study is available for download at the Sequence Read Archive (SRA) under BioProject accession PRJNA541961, which corresponds to BioSample accessions SAMN12414160 to SAMN12414195 and SRA accessions SRS5197145 to SRS5197180.

RESULTS

Soil pH

Average soil pH measured in the field plots throughout the 26 months after application of lime and siliceous minerals are shown in **Table 1**. The pH increased 1.57 units in the calcite treatment, 0.58 in the dolomite, 0.16 in the olivine and 0.11 in the norite treatment. Larvikite had no significant effect on the soil pH ($p = 0.12$ for pairwise t-test of larvikite versus control). The calcite effect decreased over time by 0.5 units (**Supplementary Figure 1**).

Denitrification Kinetics in Anoxic Slurry Incubations

The gas kinetics in anoxic slurries of soils sampled 27 months after incorporation of lime and rock powder (**Figure 1**) showed transient accumulation of both NO and N_2O which clearly declined in magnitude with increasing soil pH, more dramatically so for N_2O than for NO. Stable plateaus of N_2, reached after ∼60 h indicated depletion of N oxides since the levels largely accounted for the initial amount of NO_3^--N present in the flasks (∼14 mmol N kg^{-1}; the soil contained ∼4 mmol NO_3^- kg^{-1}). **Table 2** summarizes the maximum denitrification rates, maximum NO and N_2O accumulation, and the N_2O index (I_{N2O}) for incubation experiments carried out with soils sampled 15, 21, and 27 months after liming. Denitrification rates were lowest in samples taken during winter 2015 (the year of ley establishment), and largest in summer of the first production year, after which they decreased again in the following winter. Denitrification rates exhibited a slight but statistically significant increase with soil pH (**Supplementary Figure 3**), while the transient accumulation of NO declined with pH. The influence of soil pH on the $N_2O/(N_2O + N_2)$ ratio of denitrification was examined by plotting the N_2O index (I_{N2O}) across pH, revealing a marked decrease with increasing pH (**Supplementary Figure 4**).

Nitrification and N_2O Yield in Oxic Slurry Incubations

Figure 2 shows the kinetics of oxygen consumption, transient accumulation of NO_2^- and the accumulation of $N_2O + NO_3^-$ in oxic slurries of soils sampled in December 2015 and 2016 (15 and 27 months after incorporation of lime and siliceous minerals). Similar kinetics were observed for soils sampled 21 months after liming and **Table 3** summarizes essential variables for all three sampling dates. The oxygen consumption rate was largest in calcite and dolomite treated soils, followed by olivine

TABLE 2 | Denitrification rates and transient NO and N_2O accumulation in anoxic slurry incubations.

Treatment	Denitrification rate μmol N kg^{-1} h^{-1}	Max NO μmol N kg^{-1}	Max N_2O μmol N kg^{-1}	I_{N2O25}
December 2015 (15 months)				
Control	69 ± 3	46 ± 6	1749 ± 351	0.22 ± 0.04
Larvikite	63 ± 3	41 ± 3	906 ± 185	0.11 ± 0.03
Norite	60 ± 5	47 ± 4	1390 ± 428	0.20 ± 0.07
Olivine	69 ± 6	45 ± 7	1460 ± 451	0.19 ± 0.05
Dolomite	90 ± 6	26 ± 2	247 ± 77	0.03 ± 0.01
Calcite	91 ± 7	16 ± 1	5 ± 1	<0.01
July 2016 (21 months)				
Control	376 ± 18	40 ± 4	5724 ± 665	0.33 ± 0.04
Larvikite	354 ± 29	40 ± 1	5384 ± 853	0.26 ± 0.05
Norite	409 ± 20	43 ± 3	5886 ± 1454	0.22 ± 0.02
Olivine	398 ± 9	38 ± 3	2844 ± 832	0.18 ± 0.04
Dolomite	424 ± 15	35 ± 3	224 ± 54	0.10 ± 0.03
Calcite	413 ± 7	27 ± 2	111 ± 74	0.01 ± 0.00
December 2016 (27 months)				
Control	204 ± 15	39 ± 8	3620 ± 748	0.42 ± 0.04
Larvikite	191 ± 17	35 ± 11	3201 ± 893	0.34 ± 0.06
Norite	207 ± 12	35 ± 4	3627 ± 539	0.44 ± 0.08
Olivine	255 ± 23	26 ± 4	1421 ± 870	0.18 ± 0.10
Dolomite	263 ± 26	27 ± 4	265 ± 102	0.04 ± 0.01
Calcite	293 ± 33	18 ± 2	97 ± 60	<0.01 ± 0.00

Denitrification rates (μmol N kg^{-1} soil h^{-1}) are given as average values (n = 4, ±SE) for the first 50 h of incubation. Maximum amounts of NO and N_2O are given as μmol N kg^{-1} soil. The N_2O index (I_{N2O}) is a proxy for the propensity of N_2O emission from denitrification calculated by equation (1) for the period until the total amount of gaseous N ($NO + N_2O + N_2$) accumulation reaches the specific limit indicated by the subscript (I_{N2O25}: 25 μmol N-gas $vial^{-1}$ = 6.3 mmol N-gas kg^{-1} soil). Rates and I_{N2O25} for individual soil samples in both experiments are shown in ***Supplementary Figures 3, 4****, respectively.*

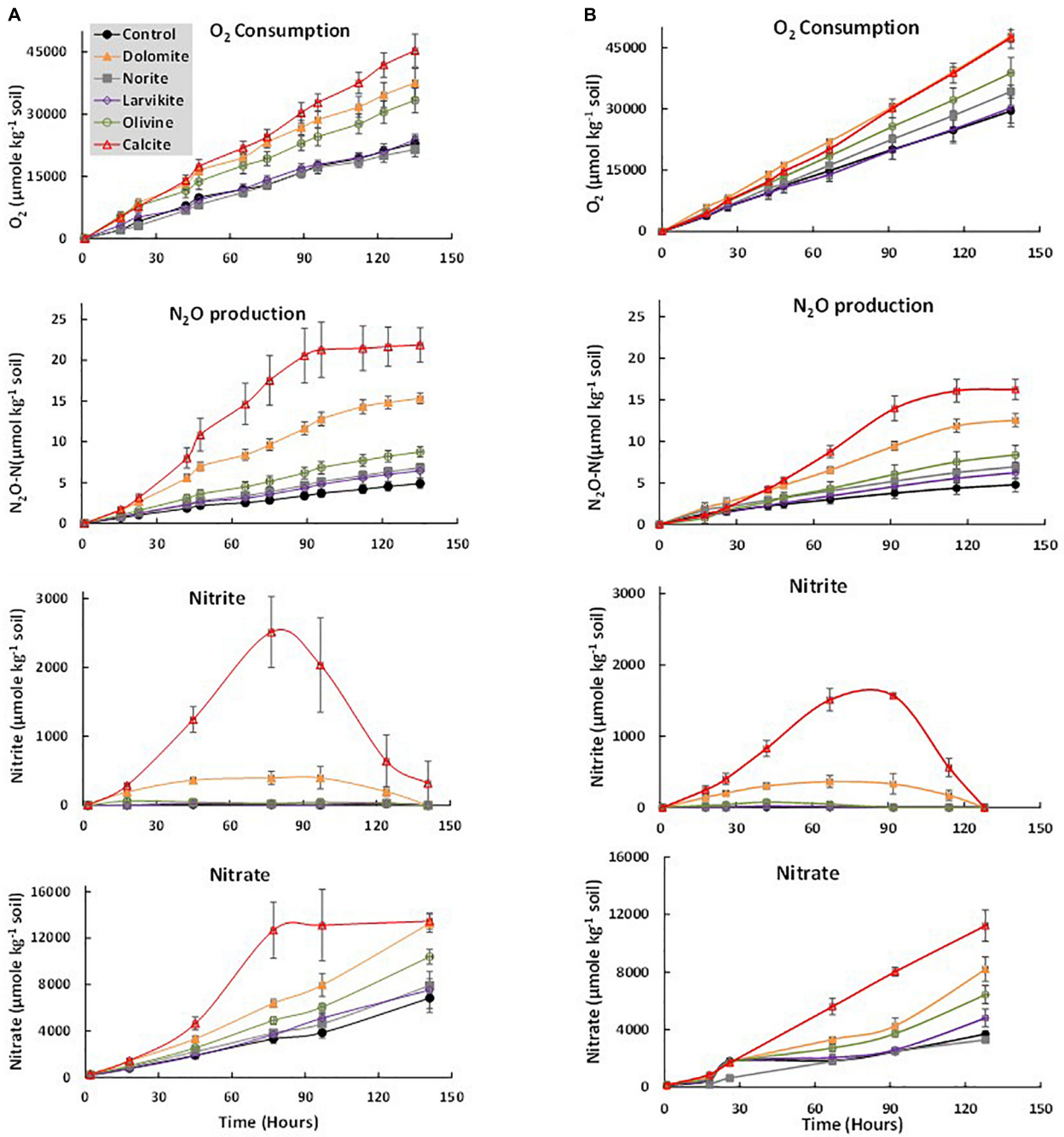

FIGURE 2 | Nitrification in oxic soil slurries. Oxygen consumption (cumulative), and production of N_2O nitrite and nitrate oxic soil slurries. Plotted values are the means and standard errors of four field replicates of each mineral treatment. Plotted gas kinetics are from two incubations experiments with soil collected from the field December 2015 (Panel **A**) and 2016 (Panel **B**) (15 and 27 months after application of minerals).

($p < 0.0005$), whereas larvikite and norite treatments were indistinguishable from the control.

The NH_4^+ oxidation rates (measured as $NO_2^- + NO_3^-$ accumulation) increased linearly with pH (**Figure 3**). NH_4^+ was evidently not depleted during the incubation, except for the calcite-amended soil sampled 15 months after mineral application (**Figure 2**: the NO_3^- plateaus reached after 60–90 h match the initial amounts of NH_4^+, which was 1.4 mmol NH_4^+ kg^{-1}). Transient accumulation of NO_2^- was substantial in the high pH soils (calcite > dolomite), whereas it was marginal in the other treatments and was found to increase exponentially with pH (**Supplementary Figure 4**). The calculated N_2O yield (Y_{N2O}) ranged from 0.09 to 0.34% and was significantly higher in the calcite and dolomite treatments than in the other treatments.

TABLE 3 | Rates of O_2 consumption, ammonium oxidation, N_2O production, NO_2^- accumulation and N_2O yield (Y_{N2O}) in oxic slurry incubations.

Treatment	O_2 μmol kg^{-1} h^{-1}	NH_4^+ oxid. † μmol N kg^{-1} h^{-1}	N_2O prod. † μmol N kg^{-1} h^{-1}	max NO_2^- μmol N kg^{-1}	Y_{N2O} (%)
December 2015 (15 months)					
Control	176 ± 19	41 ± 6	0.04 ± 0.01	25 ± 7	0.09 ± 0.01
Larvikite	181 ± 8	61 ± 2	0.05 ± 0.01	31 ± 3	0.08 ± 0.01
Norite	168 ± 16	51 ± 5	0.05 ± 0.01	36 ± 5	0.10 ± 0.00
Olivine	238 ± 20	69 ± 6	0.07 ± 0.01	110 ± 66	0.10 ± 0.01
Dolomite	276 ± 23	86 ± 9	0.14 ± 0.01	471 ± 133	0.14 ± 0.01
Calcite	340 ± 37	165 ± 28	0.25 ± 0.04	2687 ± 550	0.15 ± 0.01
July 2016 (21 months)					
Control	189 ± 22	32 ± 3	0.04 ± 0.00	nd††	0.12 ± 0.00
Larvikite	198 ± 47	31 ± 3	0.05 ± 0.01	nd	0.15 ± 0.01
Norite	207 ± 24	38 ± 4	0.05 ± 0.01	nd	0.14 ± 0.01
Olivine	198 ± 20	49 ± 4	0.10 ± 0.01	nd	0.19 ± 0.01
Dolomite	249 ± 9	77 ± 3	0.22 ± 0.01	423 ± 78	0.28 ± 0.03
Calcite	269 ± 53	99 ± 2	0.35 ± 0.04	1461 ± 135	0.34 ± 0.06
December 2016 (27 months)					
Control	213 ± 26	24 ± 5	0.04 ± 0.01	1 ± 1	0.14 ± 0.01
Larvikite	216 ± 27	31 ± 5	0.05 ± 0.00	17 ± 12	0.16 ± 0.02
Norite	246 ± 13	39 ± 2	0.06 ± 0.00	23 ± 7	0.13 ± 0.01
Olivine	281 ± 25	44 ± 4	0.07 ± 0.01	71 ± 22	0.15 ± 0.01
Dolomite	343 ± 11	64 ± 5	0.10 ± 0.00	411 ± 107	0.16 ± 0.01
Calcite	347 ± 22	84 ± 7	0.13 ± 0.01	1563 ± 66	0.18 ± 0.03

Data were averaged over the entire incubation period. Results for three experiments with soil sampled 15, 21, and 27 months after incorporation of lime and rock powders. Presented values are means of four field replicates and standard error. Maximum NO_2^- concentrations for individual field plot samples plotted against soil pH are shown in ***Supplementary Figure 4****. †NH_4^+ oxid., ammonium oxidation rate; N_2O prod., N_2O production rate.††nd, not detected.*

Assuming that the oxidation of 1 mole of NH_3 to NO_3^- consumes 2 moles of O_2, the measured nitrification accounted for 20–90% of the measured oxygen consumption rate (consistently highest for calcite).

Anoxic Incubations of Remolded Soil

For loosely remolded soil sampled 27 months after liming and incubated under fully anoxic conditions, denitrification gas kinetics exhibited similar N gas accumulation patterns as observed in the anoxic soil slurries. Calcite and dolomite treated soils accumulated less N_2O than any other treatment (**Figure 4**). Denitrification rate, maximum N_2O and N_2O index (I_{N2O}) in remolded soil experiments are shown in **Table 4**. Denitrification rates were calculated for the period 0–50 h of incubation, and the N_2O index for the time point when 500 μmol N kg^{-1} soil was recovered as NO + N_2O + N_2-N.

Oxic Incubations of Remolded Soils

The O_2 consumption rates, NH_4^+ oxidation rates, maximum NO_2^- concentrations, and the N_2O yields for these incubations are all summarized in **Table 5**, and the N_2O kinetics is shown in **Figure 5A**. The O_2 consumption rate increased gradually with increasing soil moisture content: the average O_2 consumption rates (all treatments) were 75, 106, and 153 μmol O_2 kg^{-1} soil h^{-1} at 60, 70, and 85% WFPS, respectively. The higher O_2 consumption rate at 70% than at 60% WFPS likely reflects a higher concentration of available organic carbon: soils used for the 60% WFPS experiments were sampled in December 2015, while the 70 and 85% WFPS experiments used soil samples taken in December 2016, when the ley was fully established. This is confirmed by oxygen consumption rates measured in oxic soil slurries (**Table 3**): the average rates for the December samples were 230 and 274 μmol O_2 kg^{-1} soil h^{-1} in 2015 and 2016, respectively, i.e., a 20% increase from 2015 to 2016.

The percentage of O_2 consumption theoretically accounted for by NH_3 oxidation (assuming 2 mol O_2 consumed per mol NH_4^+ oxidized) varied between 20 and 40% at 60% WFPS, which is somewhat lower than in the soil slurries. For the 85% WFPS treatment, much lower percentages were calculated, reflecting that NO_3^- consumption by denitrification resulted in grossly underestimated nitrification rates.

On average, the estimated N_2O yield (Y_{N2O}) at 70% WFPS was twice as high as at 60% WFPS (0.088 versus 0.043%, **Table 5**). The Y_{N2O} values for 70% WFPS are uncertain, however, since they are based on the assumption that nitrification rates were the same as at 60% WFPS. The 85% WFPS treatment differed markedly from the two other moisture levels in that O_2 consumption rates were larger, rates of NO_2^- + NO_3^- accumulation were lower, and N_2O production rates were two orders of magnitude higher. The apparent N_2O yields calculated for the initial 75 h (**Table 5**) were high, ranging from 2 to 15%, and approximately twice as high if calculated for the first 45 h of incubation, except for calcite, for which the N_2O production was low compared to the others, and more constant throughout. The pH response of the N_2O production rate in the 85% WFPS treatment differed fundamentally from those of the lower WFPS treatments (**Figure 5B**): while the N_2O production rates increased with pH at 60 and 70% WFPS, they declined sharply at 85% WFPS.

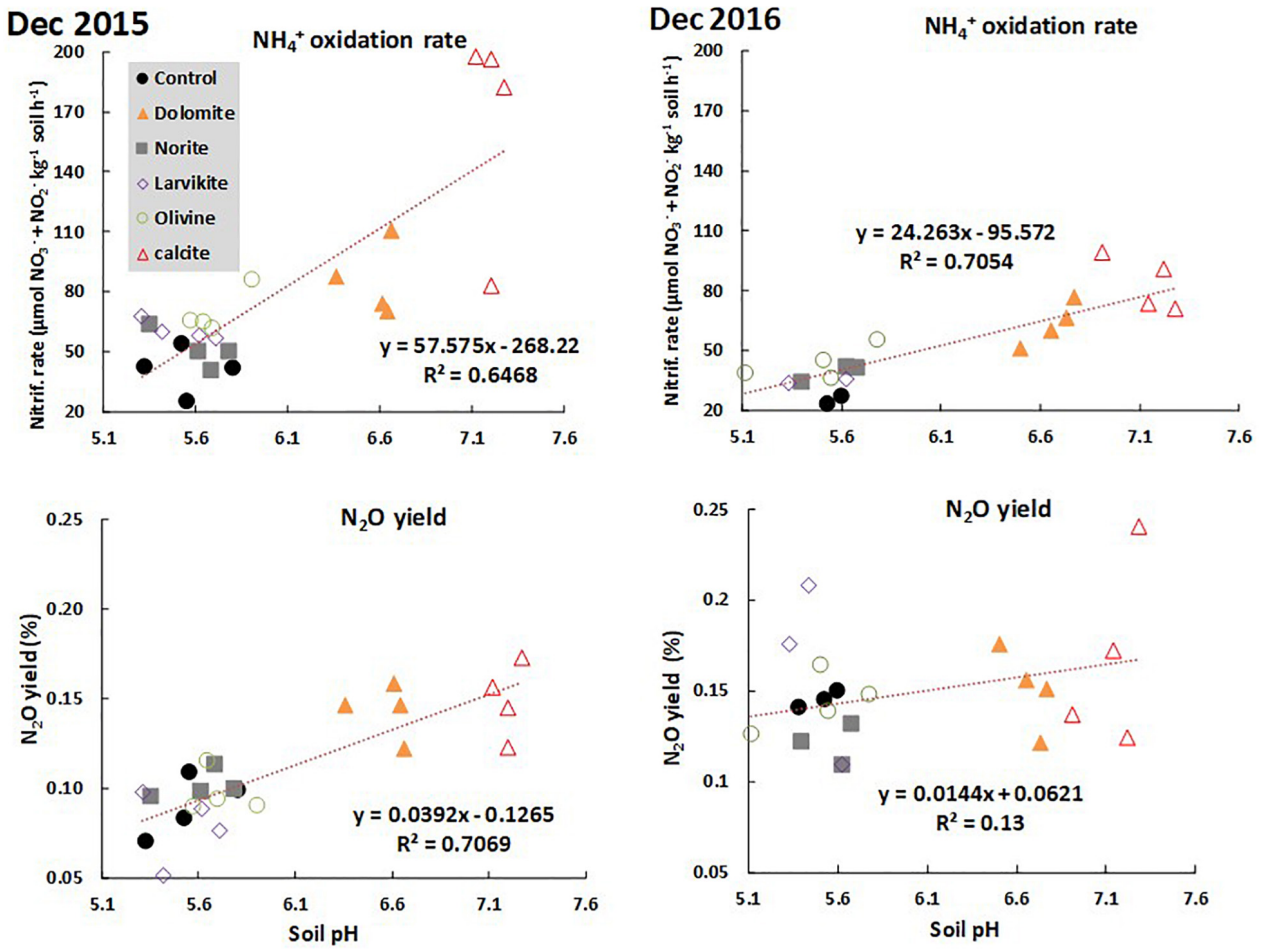

FIGURE 3 | Relationship between soil slurry pH, NH_4^+ oxidation rate and N_2O yield (% of oxidized N emitted as N_2O-N) in oxic nitrification assays. The plotted values are single flask values for four field replicates of each treatment. Plotted values are from two incubation experiments with soils collected from field 15 and 27 months after application of minerals.

AOA, AOB, and Nitrite Oxidizer Abundances

The relative abundance of AOA-, AOB-, and NOB-SSU in the overall bacterial community, as indicated by SSU rRNA amplicon sequencing, are shown in **Figure 6**. AOA identified in the samples consisted of 42 ASVs in the phylum *Thaumarchaeota* including the genera *Candidatus Nitrosotalea*, *Nitrososphaera* and *Nitrocosmicus*, as well as undescribed taxa within the phylum (**Supplementary File 1**). The identified AOB consisted of 77 ASVs from the family *Nitrosomonadaceae* within the phylum *Proteobacteria* and consisted of the genera *Nitrosomonas* and *Nitrosospira*, as well as several uncharacterized genera (**Supplementary File 1**). We also identified SSU rRNA genes affiliated to the phylum *Nitrospirae* and the genus *Nitrospira*, which are nitrite oxidizers (**Supplementary File 1** and **Supplementary Figure 8**). Regression analyses showed that the relative abundances of AOB and NOB increased significantly with soil pH ($p < 0.001$ for both), while AOA declined with pH ($p = 0.02$), and the AOB/AOA abundance ratio increased with pH ($p < 0.001$). SSU rRNA identified as *Nitrospira* may include *comammox*, i.e., organisms that oxidize ammonium to nitrate (Daims et al., 2015), but the ability of a given *Nitrospira* to carry out comammox as opposed to only nitrite oxidation may only be discerned by analysis of their functional genes (Daims et al., 2015). Hence, our SSU rRNA analysis cannot discern whether the *Nitrospira* ASVs detected are simple NOB or comammox.

DISCUSSION

It has become increasingly clear that the reason why emissions of N_2O from soils increase with acidity (Wang et al., 2018) is that the synthesis of functional N_2O reductase is impeded by low pH (Liu et al., 2014). Therefore, liming of acidic soil should reduce N_2O emissions and would justify the use of high doses of lime/biochar to mitigate these emissions, hence reducing the climate forcing that occurs as a result of fertilizer use in crop production. In theory, this beneficial effect of liming on climate forcing could be outweighed by emission of carbonate-CO_2,

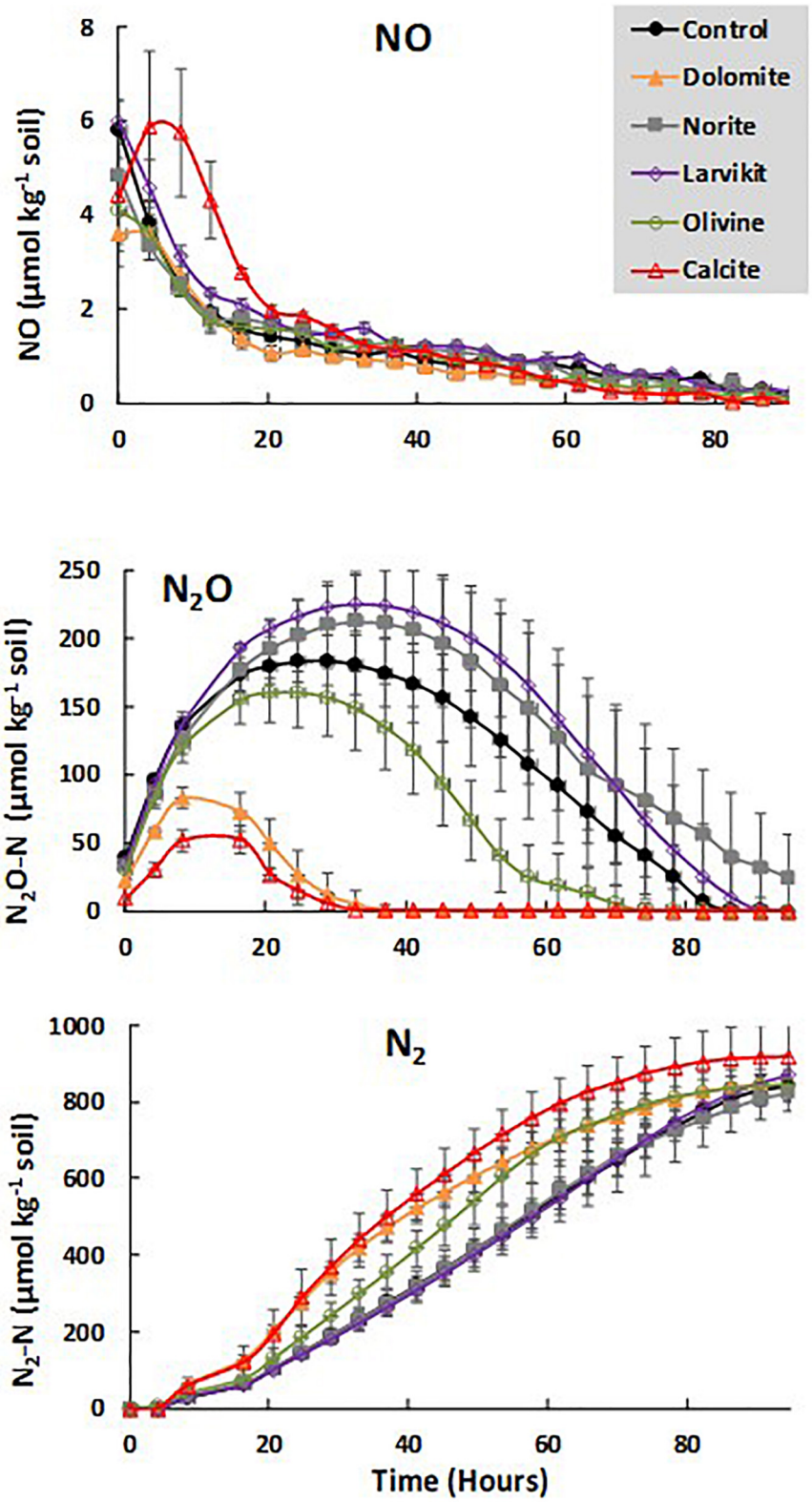

FIGURE 4 | Gas kinetics of denitrification in remolded soil under anoxic conditions. Plotted values are the means and standard error of four field replicates. Soil samples were collected in December 2016 (27 months after application of minerals).

TABLE 4 | Denitrification rate and production of NO and N_2O during anoxic incubation of remolded soils amended with nitrate.

Treatment	Denitrification μmol N kg^{-1} soil h^{-1}	Max. NO μmol N kg^{-1} soil	Max N_2O μmol N kg^{-1} soil	$I_{N2O}10$ (10)
Control	13 ± 0.4	6 ± 0.6	193 ± 20	0.43 ± 0.04
Larvikite	13 ± 0.6	6 ± 0.5	234 ± 29	0.50 ± 0.04
Norite	13 ± 1.4	5 ± 0.8	228 ± 33	0.46 ± 0.07
Olivine	15 ± 1.0	4 ± 0.6	166 ± 27	0.34 ± 0.06
Dolomite	14 ± 0.8	5 ± 0.4	90 ± 11	0.10 ± 0.05
Calcite	14 ± 1.8	6 ± 1.5	62 ± 10	0.10 ± 0.02

The N_2O index (I_{N2O}) is a proxy for the propensity of N_2O emission calculated by equation (1) for the period until the total amount of gaseous N ($NO + N_2O + N_2$) reached a specific limit indicated by the subscript (I_{N2O10}: 10 μmol N vial = 500 μmol kg^{-1} soil). Mean values of four field replicates (±SE) are given.

TABLE 5 | Rates of O_2 consumption, net $NO_2^- + NO_3^-$ accumulation, maximum NO_2^- accumulation and N_2O production rate during oxic incubation of remolded soils amended with ammonium at 60, 70, and 85% WFPS.

Treatment	O_2 rate μmol kg^{-1} soil h^{-1}	$NO_2^- + NO_3^-$ accum.-rate μmol N kg^{-1} soil h^{-1}	N_2O rate μmol N kg^{-1} soil h^{-1}	Max NO_2^- μmol N kg^{-1} soil	Y_{N2O} %
December 2015 (60% WFPS)					
Control	77 ± 9	22 ± 3	0.007 ± 0.0001	nd†	0.03 ± 0.004
Larvikite	63 ± 8	19 ± 2	0.007 ± 0.0004	nd	0.04 ± 0.004
Norite	62 ± 8	25 ± 5	0.007 ± 0.0008	nd	0.04 ± 0.007
Olivine	88 ± 6	27 ± 4	0.015 ± 0.0037	2 ± 2	0.06 ± 0.013
Dolomite	69 ± 6	26 ± 2	0.008 ± 0.0003	5 ± 5	0.03 ± 0.003
Calcite	90 ± 15	40 ± 5	0.021 ± 0.0025	117 ± 40	0.06 ± 0.014
December 2016 (70% WFPS)					
Control	102 ± 8	nd†	0.015 ± 0,004	nd	0.07††
Larvikite	86 ± 3	nd	0.018 ± 0.002	nd	0.10
Norite	96 ± 4	nd	0.014 ± 0.002	nd	0.06
Olivine	105 ± 7	nd	0.016 ± 0.004	nd	0.07
Dolomite	126 ± 6	nd	0.021 ± 0.002	nd	0.08
Calcite	131 ± 9	nd	0.050 ± 0.012	nd	0.15
December 2016 (85% WFPS)					
Control	142 ± 17	4 ± 1	0.74 ± 0.47	nd	8 ± 4
Larvikite	123 ± 14	3 ± 0	1.48 ± 0.86	nd	15 ± 9
Norite	137 ± 13	4 ± 1	1.24 ± 1.20	nd	8 ± 7
Olivine	166 ± 12	3 ± 1	0.45 ± 0.25	nd	6 ± 3
Dolomite	193 ± 6	4 ± 0	0.43 ± 0.22	nd	5 ± 2
Calcite	157 ± 29	3 ± 0	0.06 ± 0.03	213 ± 40	2 ± 1

*The N_2O yield (Y_{N2O}) is the percentage of N_2O-N relative to net accumulation of oxidized N ($NO_2^- + NO_3^- + N_2O$) at the end of the incubation. The N_2O emission from soils without NH_4^+ amendment was ≤10% of that with NH_4^+ (**Supplementary Table 3**). Presented values are means and standard error of four field replicates. †nd, not detected. ††NO_2^- and NO_3^- were not measured in this incubation. Y_{N2O} was estimated assuming identical nitrification rates as measured at 60% WFPS, hence standard deviations were not estimated.*

although the assumption that all carbonate-C is released as CO_2 has been contested (Hamilton et al., 2007; Page et al., 2009). Nevertheless, the emission of carbonate-CO_2 was our motive for testing finely ground siliceous minerals as alternatives to carbonates. The weathering of siliceous minerals will increase the pH of acidic soils, but our results so far are discouraging: while the carbonate materials caused a substantial increase in soil pH, larvikite had no significant effect, and norite and olivine increased the pH by only 0.11 and 0.16 pH units, respectively (**Table 1** and **Supplementary Figure 1**). Thus, although demonstrating the potential for two of the siliceous minerals, the weathering rates were obviously too low to achieve substantial increase in soil pH within 3 years after application. Improvement could have been achieved by grinding the minerals to finer particle size, since the weathering rate is proportional to the surface area, but the cost would be prohibitively high (van Noort et al., 2018).

N_2O emission from denitrification typically occurs during hypoxic/anoxic spells and is caused by transiently high soil moisture, high oxygen consumption rates, or both. The N_2O emissions during such "hot events," or in "hot spots" if localized in microsites with high oxygen consumption rates (Schlüter et al., 2019) depends on the enzyme kinetics: early/efficient synthesis of active N_2O reductase secures a low $N_2O/(N_2 + N_2O)$ product ratio, hence minimizing emission of N_2O, whereas delayed synthesis will lead to a high N_2O product ratio and emission. Since the synthesis of functional N_2O reductase is severely impeded/delayed by low pH (Liu et al., 2014),

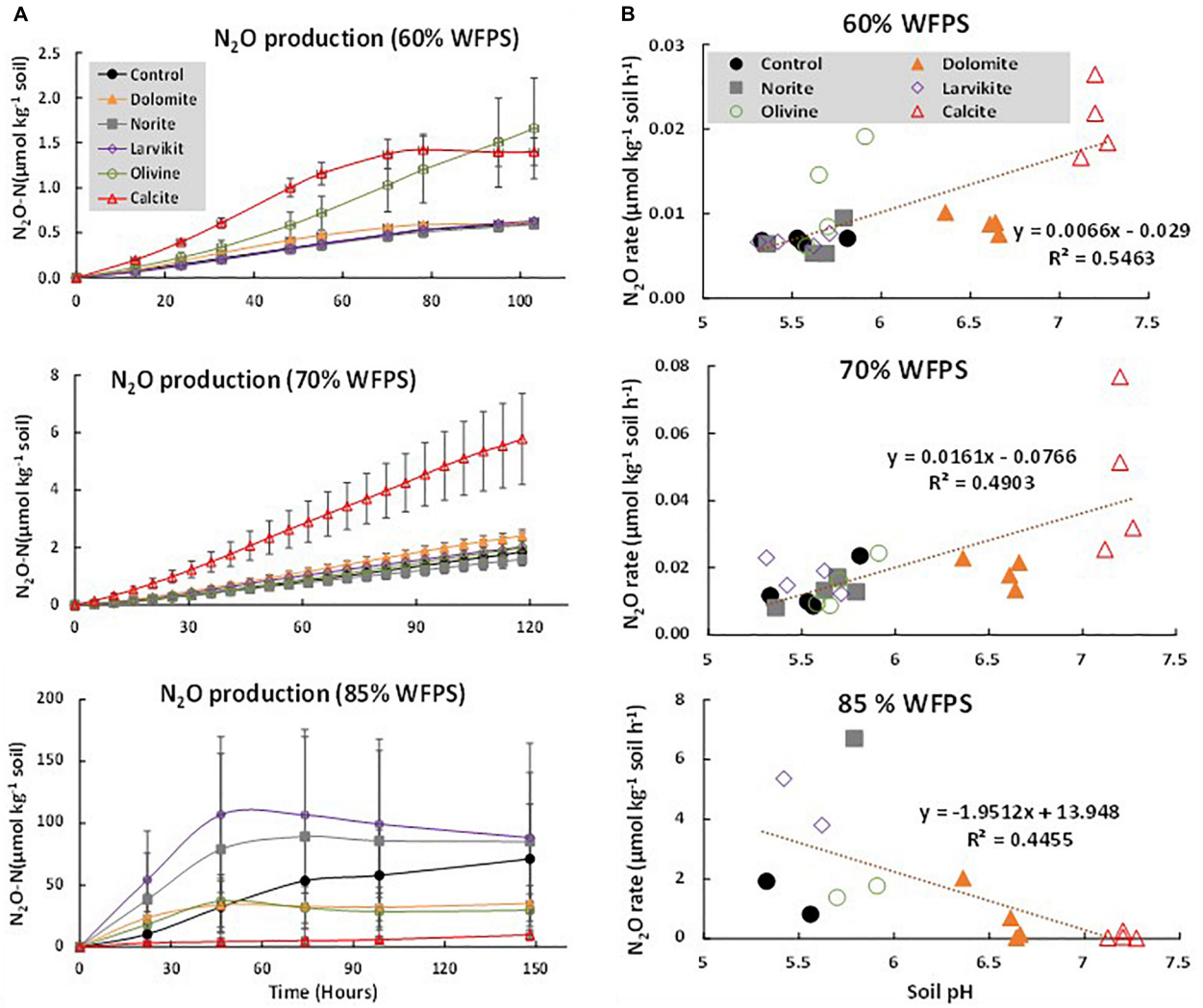

FIGURE 5 | N_2O accumulation during oxic incubations of remolded soils amended with NH_4^+. Panel **(A)** shows the N_2O kinetics throughout the incubations at the three moisture levels (means and standard error, $n = 4$). Panel **(B)** shows the N_2O production rates during the first 50 h of incubation plotted against the pH of the soils (individual flasks). Soils were collected from the field 15 months after liming (December 2015) for the 60% WFPS experiment and 27 months after liming (December 2016) for the 70 and 85% WFPS experiment. The NO_2^- + NO_3^- accumulation throughout the incubations at 60 and 85% WFPS are shown in **Supplementary Figure 6**.

the emission of N_2O will decrease with increasing soil pH. Anoxic soil incubations are commonly used to mimic anoxic spells, and such experiments have invariably shown that the transient accumulation of N_2O is controlled by pH (Čuhel and Šimek, 2011; Raut et al., 2012; Qu et al., 2014). The present result is no exception: increasing the pH by liming clearly lowered the $N_2O/(N_2O + N_2)$ product ratio during anaerobic incubations of both soil slurries (**Figure 1** and **Table 2**) and remolded soil (**Figure 4**). Thus, our findings corroborate previous investigations of denitrification as affected by pH. Our main aim, however, was to investigate the effect of liming on both denitrification and nitrification, and their contribution to N_2O emission.

Based on Hink et al. (2018) we hypothesized that increasing the pH by using lime or siliceous minerals would increase the potential nitrification rates in the soil, and selectively stimulate bacterial (AOB) over archaeal ammonia oxidizers (AOA). We further hypothesized that the N_2O yield of nitrification (Y_{N2O}) would increase with soil pH (as observed previously by Mørkved et al., 2007), because AOB have an inherently higher Y_{N2O} than AOA (Hink et.al. 2017a). The SSU rRNA gene quantification corroborated the hypothesis regarding selective stimulation of AOB (**Figure 6**). The effect of soil pH on AOA and AOB abundances has also been studied by Hu et al. (2013), who observed that the qPCR-determined ratio of AOA/AOB decreased with increasing soil pH, and hence the inverse of that ratio, or

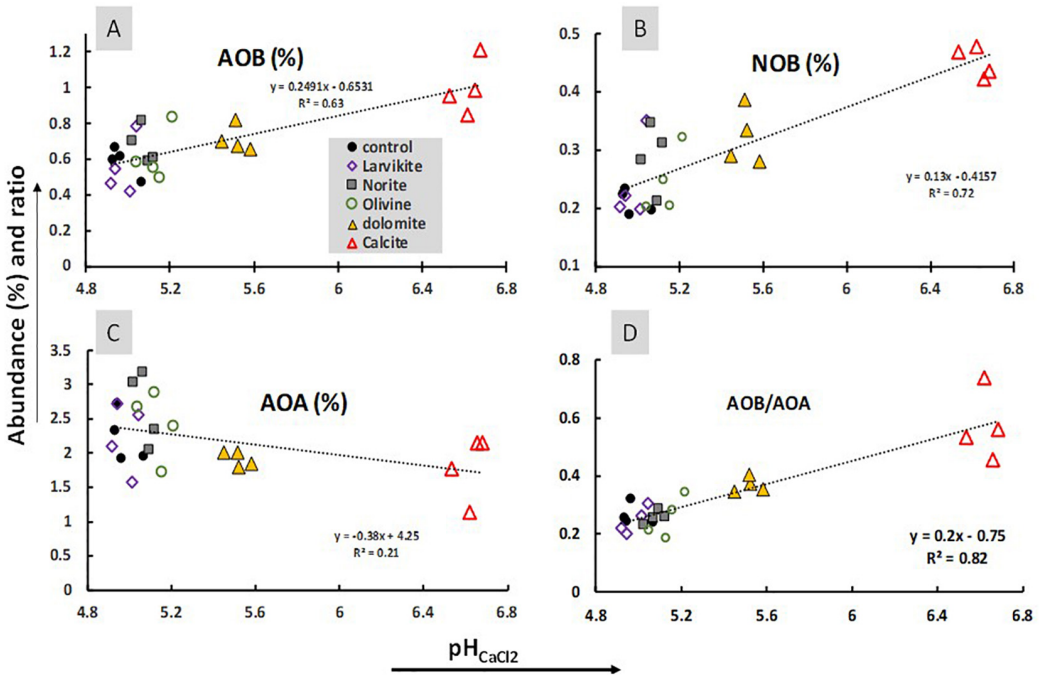

FIGURE 6 | The relative abundance (%) of nitrifying organisms as affected by soil pH. The figures show the relative abundance SSU rRNA copies (%) for AOB **(A)**, NOB **(B)** and AOA **(C)**, and the ratio between AOB and AOA abundance **(D)**; all plotted against pH measured in 0.01 M $CaCl_2$. Each point represents one individual field plot. The equation for the linear regression is included (all were significant, $p < 0.05$). The abundance of dominating groups within AOA and AOB are shown in **Supplementary Table 4**. The N_2O yield of nitrification in soil slurries (Y_{N2O}. mol N_2O-N per mol oxidized NH_4^+) correlated strongly with the AOB/AOA ratio (**Supplementary Figure 7**).

the AOB/AOA ratio increases, which supports our findings (**Figure 6**). The AOA taxa included several candidatus genera as well as a number of uncharacterized taxa, suggesting that there remains considerable diversity to be explored among AOA, whereas for the AOB, all the ASVs were from the *Nitrosomonadaceae* and mostly affiliated with named genera, although most were apparently uncultivated phylotypes such as "mle1-7," "MND1," etc. (**Supplementary File 1**). In addition, the slurry experiments confirmed the effect on nitrification rates and N_2O yields (**Figure 3**). The soil slurry experiments were designed to secure oxic conditions, thus eliminating denitrification as a source of N_2O. This is important, because it means that the N_2O produced in these experiments largely reflects the inherent N_2O production by the ammonia oxidation pathways. A similar increase in abundance of the nitrite-oxidizing *Nitrospira* (**Supplementary Figure 8**) with increasing pH was observed by Rousk et al. (2010), although in that study the r^2 between pH and *Nitrospira* relative abundance was 0.16 with $P = 0.20$.

We further hypothesized that the enhancement of nitrification by liming would increase the risk that the oxygen consumption by nitrification creates hypoxic/anoxic microsites in soil, thus inducing heterotrophic denitrification. This would be aggravated by high soil moisture content (Schurgers et al., 2006). The results with remolded soils shed some light on this (**Table 5**): at low soil moisture content (60 and 70% WFPS), Y_{N2O} was lower than in the soil slurries, but increased with soil pH (as in the soil slurries) thus suggesting that nitrification was the main dominating process. At high soil moisture content (85% WFPS), the apparent Y_{N2O} was 2–3 orders of magnitude higher than in the low moisture (60 and 70% WFPS) experiments, plausibly because oxygen consumption by nitrification along with high WFPS resulted in hypoxic/anoxic microsites and hence denitrification. This N_2O-production by denitrification could be expected to be promoted by high soil pH because of the higher nitrification rate (providing NO_2^- and NO_3^- for denitrification), but the opposite was the case; the N_2O production rates clearly declined with soil pH. Our interpretation of this finding is that, while denitrification was induced at all pH levels, the $N_2O/(N_2 + N_2O)$ product ratio declined with increasing soil pH due to more efficient synthesis of functional N_2O reductase at high pH (Liu et al., 2014). This necessarily implies that heterotrophic denitrification, rather than *nitrifier denitrification* must have been dominating, because ammonia oxidizing bacteria lack the gene for N_2O-reductase. A recent study of the electron flow to denitrification in ammonia oxidizing bacteria support this interpretation, showing that although the electron flow to nitrite- and nitric oxide reductase in these organisms increased in response to hypoxia, it never amounted to more than 1.2% of the total electron flow (Hink et al., 2017b). This finding lends little support to the common notion that *nitrifier denitrification* is a

[2]https://www.r-project.org/

strong source of N_2O in soils under partially hypoxic conditions (Zhu et al., 2013; Mushinski et al., 2019). As argued elsewhere (Bakken and Frostegård, 2017), the evidence for significant N_2O production by *nitrifier denitrification* is in fact rather weak. The notion emerged as a result of circumstantial evidence (co-occurrence, and selective inhibition of ammonia oxidation), and later by employing $^{18}O/^{15}N$ tracing to differentiate between N_2O from *nitrifier denitrification* and heterotrophic denitrification (Wrage-Mönning et al., 2018). The differentiation is based on the assumption that nitrite produced by ammonia oxidizers is exclusively reduced by the ammonia oxidizers themselves, because heterotrophs prefer nitrate. This is highly improbable, however: a fraction of the denitrifying heterotrophs carrying nitrite reductase lack nitrate reductase (Lycus et al., 2017), and those with nitrate reductase will reduce external nitrite along with nitrate because nitrite is a free intermediate that is reduced outside the cytoplasmic membrane. This, together with the fact that heterotrophic denitrifiers grossly outnumber ammonia oxidizing organisms, and that nitrifiers allocate miniscule fractions of the electron flow to denitrification (Hink et al., 2017a), suggests the opposite: under hypoxic conditions the nitrite produced by ammonia oxidizers is more likely to be reduced by heterotrophs than by ammonia oxidizers themselves.

Our results are important because they explain why increasing the pH of acidic soils (by lime or biochar) has a contingent effect on their N_2O emission. Highly variable effects may be expected for systems/conditions where N_2O emission is driven by high ammonium oxidation rates such as urine patches (Clough et al., 2004; Carter, 2007; Khan et al., 2011), while consistent reduction of the N_2O emission can be expected for systems/conditions where heterotrophic denitrification is dominant. Laboratory experiments may be designed to isolate nitrification- and denitrification driven N_2O emissions, but in agronomically realistic field experiments, the contributions of nitrification and denitrification merge and fluctuate (Russenes et al., 2016), being further modulated by a plethora of other factors (Butterbach-Bahl et al., 2013; Saggar et al., 2013; Rochette et al., 2018). As a result, the net effect of pH management on N_2O emissions in single field experiments is to some extent anecdotic, and the evaluation of pH management as a mitigation option should be based on ensembles of well-designed field experiments. Unfortunately, most of the existing emission data are from field experiments designed to test other factors than pH. Nevertheless, a recent meta-study by Wang et al. (2018), which used emission data from 117 studies worldwide, demonstrated an overall reduction of N_2O emission by increasing soil pH, creating a basis for recommending liming for mitigating N_2O emissions from acidified soils.

DATA AVAILABILITY STATEMENT

The datasets generated for this study can be found in online repositories. The names of the repository/repositories and accession number(s) can be found in the article/**Supplementary Material**.

AUTHOR CONTRIBUTIONS

SN: experimental design and writing, did the laboratory work, and analyses of kinetics. LB: experimental design and writing. ÅF: molecular analyses and writing. JG: bioinformatic analyses and writing. PD: experimental design and writing. All authors contributed to the article and approved the submitted version.

FUNDING

This research was financed by the Norwegian Research Council; project number 234382 (MIGMIN). PD received funding from the FACCE-ERA-GAS project MAGGE-pH under the Grant Agreement No. 696356.

ACKNOWLEDGMENTS

We thank Trygve Fredriksen for support during the field sampling, and Natalie Y. N. Lim for conducting the DNA extractions.

SUPPLEMENTARY MATERIAL

The Supplementary Material for this article can be found online at: https://www.frontiersin.org/articles/10.3389/fenvs.2020.598513/full#supplementary-material

REFERENCES

Apprill, A., Mcnally, S., Parsons, R., and Weber, L. (2015). Minor revision to V4 region SSU rRNA 806R gene primer greatly increases detection of SAR11 bacterioplankton. *Aquat. Microb. Ecol.* 75, 129–137. doi: 10.3354/ame01753

Bakken, L. R., and Frostegård, Å (2017). Sources and sinks for N2O, can microbiologist help to mitigate N2O emissions? *Environ. Microbiol.* 19, 4801–4805. doi: 10.1111/1462-2920.13978

Blomquist, J., Simonsson, M., Etana, A., and Berglund, K. (2018). Structure liming enhances aggregate stability and gives varying crop responses on clayey soils. *Acta Agric. Scand. B Soil Plant Sci.* 68, 311–322. doi: 10.1080/09064710.2017.1400096

Butterbach-Bahl, K., Baggs, E. M., Dannemann, M., Kiese, R., and Zechmeister-Boltenstern, S. (2013). Nitrous oxide emissions from soils: how well do we understand the processes and controls? *Philos. Trans. R. Soc. B* 368:20130122. doi: 10.1098/rstb.2013.0122

Callahan, B. J., McMurdie, P. J., Rosen, M. J., Han, A. W., Johnson, A. J., and Holmes, S. P. (2016). DADA2: High-resolution sample inference from Illumina amplicon data. *Nat. Methods* 13, 581–583. doi: 10.1038/nmeth.3869

Carter, M. S. (2007). Contribution of nitrification and denitrification to N_2O emissions from urine patches. *Soil Biol. Biochem.* 39, 2091–2102. doi: 10.1016/j.soilbio.2007.03.013

Cayuela, M. L., Zwieten, L., Singh, B. P., Jeffery, S., Roig, A., and Sanchez-Mondero, M. A. (2014). Biochar's role in mitigating soil nitrous oxide emissions: a review and metaanalysis. *Agric. Ecosyst. Environ.* 191, 5–16. doi: 10.1016/j.agee.2013.10.009

Chadwick, O. A., and Chorover, J. (2001). The chemistry of pedogenic thresholds. *Geoderma* 100, 321–353. doi: 10.1016/s0016-7061(01)00027-1

Clough, T. C., Kelliher, F. M., Sherlock, R. R., and Ford, C. D. (2004). Lime and soil moisture effects on nitrous oxide emissions from a urine patch. *Soil Soc. Am. J.* 68, 1600–1609. doi: 10.2136/sssaj2004.1600

Čuhel, J., and Šimek, M. (2011). Proximal and distal control by pH of denitrification rate in a pasture soil. *Agric. Ecosyst. Environ.* 141, 230–233. doi: 10.1016/j.agee.2011.02.016

Daims, H., Lebedeva, E. V., Pjevac, P., Han, P., Herbold, C., Albertsen, M., et al. (2015). Complete nitrification by *Nitrospira bacteria*. *Nature* 528, 504–509. doi: 10.1038/nature16461

Doane, T. A., and Horwath, W. R. (2003). Spectrophotometric determination of nitrate with a single reagent. *Anal. Lett.* 36, 2713–2722. doi: 10.1081/al-120024647

Goulding, K. W. T. (2016). Soil acidification and the importance of liming agricultural soils with particular reference to the United Kingdom. *Soil Use Manag.* 32, 390–399. doi: 10.1111/sum.12270

Guo, J., Liu, X., Zhang, Y., Shen, J., Han, W., Zhang, W., et al. (2010). Significant acidification in major Chinese croplands. *Science* 327, 1008–1010. doi: 10.1126/science.1182570

Hamilton, S. K., Kurzman, A. L., Arango, C., Jin, L., and Robertson, G. P. (2007). Evidence for carbon sequestration by agricultural liming. *Glob. Biogeochem. Cycles* 21:GB2021. doi: 10.1029/2006GB002738

Hansen, V. T., and Grimenes, A. A. (2015). *Meteorologisk Data for Ås 2014*. Oslo: Norwegian Meteorological Institute.

Hink, L., Gubry-Rangin, C., Nicol, G. W., and Prosser, J. I. (2018). The consequences of niche and physiological differentiation of archaeal and bacterial ammonia oxidizers for nitrous oxide emissions. *ISME J.* 12, 1048–1093.

Hink, L., Lycus, P., Gubry-Rangin, C., Frostegård, Å, Nicol, G. W., Prosser, J. I., et al. (2017b). Kinetics of NH3-oxidation, NO-turnover, N2O production and electron flow during oxygen depletion in model bacterial and archaeal ammonia oxidisers. *Environ. Microbiol.* 19, 4882–4896. doi: 10.1111/1462-2920.13914

Hink, L., Nicol, G. W., and Prosser, J. I. (2017a). Archaea produce lower yields of N2O than bacteria during aerobic ammonia oxidation in soil. *Environ. Microbiol.* 19, 4829–4837. doi: 10.1111/1462-2920.13282

Hu, H. W., Zhang, L. M., Dai, Y., Di, H. J., and He, J. Z. (2013). pH-dependent distribution of soil ammonia oxidizers across a large geographical scale as revealed by high-throughput pyrosequencing. *J. Soils Sediments* 13, 1439–1449. doi: 10.1007/s11368-013-0726-y

Huang, T., Gao, B., Hu, X. K., Lu, X., Well, R., Christie, P., et al. (2014). Ammonia-oxidation as an engine to generate nitrous oxide in an intensively managed calcareous Fluvo-aquic soil. *Sci. Rep.* 4:3950. doi: 10.1038/srep03950

Keeney, D. R., and Nelson, D. W. (1982). "Nitrogen inorganic forms," in *Methods of Soil Analysis, Part 2- Chemical and Microbiological Properties*, eds A. L. Page, R. H. Miller, and D. R. Keeney (Madison, WI: American Society of Agronomy Inc), 643–698. doi: 10.2134/agronmonogr9.2.2ed.c33

Khan, S., Clough, T. J., Goh, K. M., and Sherlock, R. R. (2011). Influence of soil pH on NOx and N2O emissions from bovine urine applied to soil columns. *New Zeal. J. Agric. Res.* 54, 285–301. doi: 10.1080/00288233.2011.607831

Klotz, M. G., and Stein, L. Y. (2011). "Genomics of ammonia−oxidizing bacteria and insights into their evolution," in *Nitrification*, eds B. B. Ward, D. J. Arp, and M. G. Klotz (Washington, DC: ASM Press), doi: 10.1128/9781555817145.ch4

Kochian, L. V., Hoekenga, A., and Pineros, M. A. (2004). How do crop plants tolerate acid soils? Mechanisms of aluminum tolerance and phosphorous efficiency. *Annu. Rev. Plant Biol.* 55, 459–493. doi: 10.1146/annurev.arplant.55.031903.141655

Kool, D. M., Dolfing, J., Wrage, N., and Van Groeningen, J. W. (2011b). Nitrifier denitrification as a distinct and significant source of nitrous oxide from soil. *Soil Biol. Biochem.* 43, 174–178. doi: 10.1016/j.soilbio.2010.09.030

Kool, D. M., van Groenigen, J. W., and Wrage, N. (2011a). Source determination of nitrous oxide based on nitrogen and oxygen isotope tracing: dealing with oxygen exchange. *Methods Enzymol.* 496, 139–160. doi: 10.1016/b978-0-12-386489-5.00006-3

Lim, N. Y. N., Roco, A. C., and Frostegård, Å (2016). Transparent DNA/RNA co-extraction workflow protocol suitable for inhibitor-rich environmental samples that focuses on complete DNA removal for transcriptomic analyses. *Front. Microbiol.* 7:1588. doi: 10.3389/fmicb.2016.01588

Liu, B., Frostegård, Å, and Bakken, L. R. (2014). Impaired reduction of N2O to N2 in acid soil is due to a post-transcriptional interference with the expression of nosZ. *mBio* 5:e01383-14. doi: 10.1128/mBio.01383-14

Liu, B., Mørkved, P. T., Frostegård, Å, and Bakken, L. R. (2010). Denitrification gene pools, transcription and kinetics of NO, N2O and N2 production as affected by soil pH. *FEMS Microbiol. Ecol.* 72, 407–417. doi: 10.1111/j.1574-6941.2010.00856.x

Lycus, P., Bøthun, K. L., Bergaust, L., Shapleigh, J. P., Bakken, L. R., Frostegård, Å., et al. (2017). Phenotypic and genotypic richness of denitrifiers revealed by a novel isolation strategy. *ISME J.* 11, 2219–2232. doi: 10.1038/ismej.2017.82

McMurdie, P. J., and Holmes, S. (2013). Phyloseq: an R package for reproducible interactive analysis and graphics of microbiome census data. *PLoS One* 8:e61217. doi: 10.1371/journal.pone.0061217

Molstad, L., Dörsch, P., and Bakken, L. R. (2007). Robotized incubation system for monitoring gases (O2, NO, N2O and N2) in denitrifying cultures. *J. Microbiol. Methods* 71, 202–211. doi: 10.1016/j.mimet.2007.08.011

Molstad, L., Dörsch, P., and Bakken, L. R. (2016). *Report: New Improved Robot for Gas Kinetics in Batch Cultures*. Berlin: Research Gate, doi: 10.13140/RG.2.2.30688.07680

Mørkved, P. T., Dörsch, P., and Bakken, L. R. (2007). The N2O product ratio of nitrification and its dependence on long-term changes in soil pH. *Soil Biol. Biochem.* 39, 2048–2057. doi: 10.1016/j.soilbio.2007.03.006

Mushinski, R. M., Phillips, R. P., Payne, Z. C., Avney, R. B., Jo, I., Fei, S., et al. (2019). Microbial mechanisms and ecosystem flux estimation for aerobic NOy emissions from deciduous forest soils. *Proc. Natl. Acad. Sci. U.S.A.* 116, 2138–2145. doi: 10.1073/pnas.1814632116

Nadeem, S., Bakken, L. R., Köster, J. R., Mørkved, P. T., Simon, N., and Dörsch, P. (2015). Soil pH management without lime, a strategy to reduce greenhouse gas emissions from cultivated soils. *Geophys. Res. Abstracts* 17, EGU2015–EGU9790.

Nicol, G. W., Leininger, S., Schleper, C., and Prosser, J. I. (2008). The influence of soil pH on the diversity, abundance and transcriptional activity of ammonia oxidizing archaea and bacteria. *Environ. Microbiol.* 10, 2966–2978. doi: 10.1111/j.1462-2920.2008.01701.x

Oo, A. Z., Sudo, S., Akiyama, H., Win, K. T., Shibata, A., Yamamoto, A., et al. (2018). Effect of dolomite and biochar addition on N2O and CO2 emissions from acidic tea field soil. *PLoS One* 13:e0192235. doi: 10.1371/journal.pone.0192235

Page, K. L., Allen, D. E., Dalal, R. C., and Slattery, W. (2009). Processes and magnitude of CO2, CH4, and N2O fluxes from liming of Australian acidic soils: a review. *Soil Res.* 47, 747–762. doi: 10.1071/sr09057

Parada, A. E., Needham, D. M., and Fuhrman, J. A. (2016). Every base matters: Assessing small subunit rRNA primers for marine microbiomes with mock communities, time series and global field samples. *Environ. Microbiol.* 18, 1403–1414. doi: 10.1111/1462-2920.13023

Qu, Z., Wang, J., Almøy, T., and Bakken, L. R. (2014). Excessive use of nitrogen in Chinese agriculture results in high N2O/(N2O+ N2) product ratio of denitrification, primarily due to acidification of the soils. *Glob. Change Biol.* 20, 1685–1698. doi: 10.1111/gcb.12461

Raut, N., Dörsch, P., Sitaula, B. K., and Bakken, L. R. (2012). Soil acidification by intensified crop production in South Asia results in higher $N_2O/(N_2 + N_2O)$ product ratios of denitrification. *Soil Biol. Biochem.* 55, 104–112. doi: 10.1016/j.soilbio.2012.06.011

Rochette, P., Liang, C., Pelster, D., Bergeron, O., Lemke, R., Kroebel, R., et al. (2018). Soil nitrous oxide emissions from agricultural soils in Canada: exploring relationships with soil, crop and climate variables. *Agric. Ecosyst. Environ.* 254, 69–81. doi: 10.1016/j.agee.2017.10.021

Rousk, J., Bååth, E., Brookes, P. C., Lauber, C. L., Lozupone, C., Caporaso, J. G., et al. (2010). Soil bacterial and fungal communities across a pH gradient in an arable soil. *ISME J.* 4, 1340–1351. doi: 10.1038/ismej.2010.58

Russenes, A. L., Korsaeth, A., Bakken, L. R., and Dörsch, P. (2016). Spatial variation in soil pH controls off-season N2O emission in an agricultural soil. *Soil Biol. Biochem.* 99, 36–46. doi: 10.1016/j.soilbio.2016.04.019

Saggar, S., Jha, N., Deslippe, J., Bolan, N. S., Luo, J., Giltrap, D. L., et al. (2013). Denitrification and N2O:N2 production in temperate grasslands: processes, measurements, modelling and mitigating negative impacts. *Sci. Total Environ.* 465, 173–195. doi: 10.1016/j.scitotenv.2012.11.050

Schlüter, S., Zawallich, J., Vogel, H. J., and Dörsch, P. (2019). Physical constraints for respiration in microbial hotspots in soil and their importance for denitrification. *Biogeosciences* 16, 3665–3678. doi: 10.5194/bg-2019-2

Schurgers, G., Dörsch, P., Bakken, L. R., Leffelaar, P., and Haugen, L. E. (2006). Modelling soil anaerobiosis from water retention characteristics and soil respiration. *Soil Biol. Biochem.* 39, 2637–2644. doi: 10.1016/j.soilbio.2006.04.016

Shaaban, M., Peng, Q., Hu, R., Wu, Y., Lin, S., and Zhao, J. (2015). Dolomite application to acidic soils: a promising option for mitigating N2O emissions. *Environ. Sci. Pollut. Res.* 22, 19961–19970. doi: 10.1007/s11356-015-5238-4

Shaaban, M., Peng, Q., Lin, S., Wu, Y., Zhao, J., and Hu, R. (2014). Nitrous oxide emission from two acidic soils as affected by dolomite application. *Soil Res.* 52, 841–848. doi: 10.1071/sr14129

Shaaban, M., Wu, Y., Khalid, M. S., Peng, Q., Xu, X., Wu, L., et al. (2018). Reduction in soil N2O emissions by pH manipulation and enhanced nosZ gene transcription under different water regimes. *Environ. Pollut.* 235, 625–631. doi: 10.1016/j.envpol.2017.12.066

Ulén, B., and Etana, A. (2014). Phosphorus leaching from clay soils can be counteracted by structure liming. *Acta Agric. Scand. B Soil Plant Sci.* 64, 425–433. doi: 10.1080/09064710.2014.920043

van Noort, R., Mørkved, P. T., and Dundas, S. H. (2018). Acid neutralization by mining waste dissolution under conditions relevant for agricultural applications. *Geosciences* 8:380. doi: 10.3390/geosciences8100380

von Uexküll, H. R., and Mutert, E. (1995). Global extent, development and economic impact of acid soils. *Plant Soil* 171, 1–15. doi: 10.1007/bf00009558

Wang, Y., Guo, J., Vogt, R. D., Mulder, J., Wang, J., and Zhang, X. (2018). Soil pH as the chief modifier for regional nitrous oxide emissions: new evidence and implications for global estimates and mitigation. *Glob. Change Biol.* 24, e617–e626.

White, P. F., and Robson, A. D. (1989). Rhizosphere acidification and Fe^{3+} reduction in lupins and peas: Iron deficiency in lupins is not due to a poor ability to reduce Fe^{3+}. *Plant and Soil* 119, 163–175. doi: 10.1007/BF02370281

Wijler, J., and Delwiche, C. C. (1954). Investigations on the denitrifying process in soil. *Plant Soil* 5, 155–169. doi: 10.1007/bf01343848

Wrage-Mönning, N., Horn, M., Well, R., Müller, C., Velthof, G., and Oenema, O. (2018). The role of nitrifier denitrification in the production of nitrous oxide revisited. *Soil Biol. Biochem.* 123, A3–A16.

Yilmaz, P., Parfrey, L. W., Yarza, P., Gerken, J., Pruesse, E., Quast, C., et al. (2014). The SILVA and "all-species living tree project (LTP)" taxonomic frameworks. *Nucleic Acids Res.* 42, D643–D648. doi: 10.1093/nar/gkt1209

Zhu, X., Burger, M., Doane, T. A., and Horwath, W. R. (2013). Ammonia oxidation pathways and nitrifier denitrification are significant sources of N2O and NO under low oxygen availability. *Proc. Natl. Acad. Sci. U.S.A.* 110, 6328–6333. doi: 10.1073/pnas.1219993110

Conflict of Interest: The authors declare that the research was conducted in the absence of any commercial or financial relationships that could be construed as a potential conflict of interest.

frontiers in Environmental Science

MINI REVIEW
published: 19 March 2021
doi: 10.3389/fenvs.2021.635114

Nanofertilizers: A Cutting-Edge Approach to Increase Nitrogen Use Efficiency in Grasslands

*J. H. Mejias[1], F. Salazar[2], L. Pérez Amaro[3], S. Hube[2], M. Rodriguez[2] and M. Alfaro[2]**

[1]Instituto de Investigaciones Agropecuarias, INIA Carillanca, Temuco, Chile, [2]Instituto de Investigaciones Agropecuarias, INIA Remehue, Osorno, Chile, [3]Ecocompatible Polymeric Materials Laboratory, LMPE, Capannori, Italy

Nitrogen (N) is the most critical element limiting agricultural production at a global scale. Despite many efforts, the N use efficiency (NUE) in agriculture remains in a range of less than 50%. Reaching targeted crop yields has resulted in N overuse, which is an economic and environmental concern worldwide. The continuous exploration of innovative solutions has led to the synthesis of novel nanomaterials, resulting in a powerful tool for the development of new technological products. Nanofertilizers are one of the most promising engineered materials that are being tested, either for soil or foliar applications. Encouraging results have been obtained using nanofertilizers in different plant species, however, limited information has been reported about its use in grasslands. Commonly, N is applied to grassland soils as granular fertilizers, which may result in significant losses via surface runoff or leaching, ammonia (NH_3) volatilization and N oxides (N_2O, NO, NO_x) emissions. Nitrogen nanofertilizers are expected to increase NUE by improving the effectiveness of N delivery to plants and reducing N losses to the environment. Information on the efficiency of the use of N nanofertilizers in grasslands species is scarce and the application strategies that can be used to avoid N losses are poorly understood. New scenarios of increasing economic and environmental constraints may represent an opportunity for N nanofertilizers application in grasslands. This article reviews its potential use as an innovative approach to improve NUE and reduce N losses to the wider environment, analyzing potential shortcomings and future considerations for animal food chains.

Keywords: nitrogen nanofertilizers, nitrogen losses, nitrogen use efficiency, nanofertilizers in grasslands, nitrogen based nanomaterials

OPEN ACCESS

Edited by:
Yupeng Wu,
Huazhong Agricultural University, China

Reviewed by:
Mahmud Hossain,
Bangladesh Agricultural University, Bangladesh
Yufei Li,
Institute of Plant Nutrition and Resource, China
Kemo Jin,
China Agricultural University, China

****Correspondence:***
M. Alfaro
malfaro@inia.cl

Specialty section:
This article was submitted to Biogeochemical Dynamics, a section of the journal Frontiers in Environmental Science

Received: *29 November 2020*
Accepted: *08 February 2021*
Published: *19 March 2021*

Citation:
Mejias J H, Salazar F, Pérez Amaro L, Hube S, Rodriguez M and Alfaro M (2021) Nanofertilizers: A Cutting-Edge Approach to Increase Nitrogen Use Efficiency in Grasslands. Front. Environ. Sci. 9:635114. doi: 10.3389/fenvs.2021.635114

INTRODUCTION

The world population is estimated to exceed 9.7 billion by 2050 (FAO, 2018). Accordingly, it has been anticipated that current crop production needs to be increased by up to 70% to satisfy future food demands (Hunter et al., 2017). This great challenge will require combined efforts to preserve natural resources to support intensive agriculture while limiting detrimental impact on the environment (Lee et al., 2006; Hunter et al., 2017; Xie et al., 2019). The intensive use of mineral fertilizers and organic amendments has negatively affected soil and water quality worldwide (Bashir et al., 2020). In particular, the use of conventional N fertilizers has caused substantial N losses to the environment, triggering eutrophication of waters, soil acidification, and biodiversity loss (Banger et al., 2017).

Since the industrial revolution, the use of synthetic N fertilizers has led to the increase of atmospheric N_2O, one of the most important anthropogenic greenhouse gases causing global warming (Davidson, 2009). Despite previous efforts, the Nitrogen Use Efficiency (NUE) in agricultural systems has remained low, meaning that on a global scale, more than 50% of the N applied to agricultural soils is potentially lost into the environment (Lassaletta et al., 2014). One of the major challenges of modern agriculture is to satisfy actual and future global food demands efficiently. The current NUE needs to be improved substantially by increasing the efficiency of agricultural systems, adopting environmentally sound agronomic practices, and exploring disrupting technologies.

Nanotechnology is the study, design, creation, synthesis, manipulation and application of nanometric scale materials, having one or more dimensions with sizes smaller than 100°nm (Lee and Moon, 2020). Nanomaterials differ from their original materials, and alterations in their physic-chemical properties are expected, acquiring exceptional properties, functionalities, and high reactivity given by its high surface area-volume ratio (Andrews et al., 2019). In the last few decades, nanotechnology has been considered a projecting technology with plentiful applications (Marchiol et al., 2020). A wide range of materials has been used to create nanoparticles like metal oxides, ceramics, magnetic materials, semiconductor, quantum dots, lipids, polymers (synthetic or natural), dendrimers and emulsions (Benelmekki, 2015; Kumar et al., 2018; Ruiz-Cañas et al., 2020). Accordingly, several nanotechnology applications have been developed and tested as potential agrochemicals such as bactericides, fungicides, growth regulators and fertilizers (Peters et al., 2014; Pestovsky and Martínez-Antonio, 2017). Nanofertilizers are defined as materials in the nanometer scale, usually in the form of nanoparticles, containing macro and micronutrients that are delivered to crops in a controlled mode (DeRosa et al., 2010; Adisa et al., 2019; Shang et al., 2019).

According to the type of formulation, nanofertilizers are classified into three categories: 1) nanoscale fertilizer, which corresponds to the conventional fertilizer reduced in size typically in the form of nanoparticles; 2) nanoscale additive fertilizer, is a traditional fertilizer containing a supplement nanomaterial; and 3) nanoscale coating fertilizer, refers to nutrients encapsulated by nanofilms or intercalated into nanoscale pores of a host material (Mastronardi et al., 2015). Encapsulated nutrients by films or held in nanopores within a carrier material such as clays have been used to form nanocomposite structures for controlling the nutrient release (Golbashy et al., 2016; Kottegoda et al., 2017; Borges et al., 2019; Tarafder et al., 2020).

Nanotechnology applications in agriculture appear to be a promising approach, fostering the transformation of conventional production systems into upgraded agricultural practices with a clear emphasis on the development of more efficient and environmentally friendly methodologies (Duhan et al., 2017; Lowry et al., 2019). Nanofertilizers could be a crucial development in the protection of the environment because they can be applied in smaller quantities compared to traditional fertilizers (Adisa et al., 2019), hence reducing leaching, runoff, and gas emissions to the atmosphere (Manjunatha et al., 2016). At present, uncertainty exists about the production costs of nanofertilizers compared to conventional fertilizers, as well as the magnitude of the possible disruption in the existing conventional fertilizer industry (Dimkpa and Brindraban, 2018).

A comprehensive analysis of the potential benefits of using nitrogenous nanofertilizer in grasslands and its impact on N losses to the environment has to be addressed, considering, among others, its agronomic and physiological properties, growing rates, plant architecture and use, compared to annual and/or perennial crops, given that in perennial crops nutrient carryover is usually seen from one season to the next one due to retranslocation from the annual plant parts, which can naturally increase NUE (Weih et al., 2011) Additionally, perennial crops tend to have longer photosynthetic seasons resulting from earlier canopy development and longer green leaf duration, increasing seasonal light interception efficiencies and precipitation interception (Tilman et al., 2009), including retention of potential foliar applications. There are important factors to assess when using these new formulations applied to grass, to improve NUE use efficiency and losses, like N molecules type and size, temperature, specific surface area, and urease activity, among other considerations (Bowman and Paul, 1992; Ryle and Stanley, 1992; Henning et al., 2013a). This review focuses on the potential use of N nanofertilizers as a novel approach to improve NUE in grasslands and their role in reducing environmental impact, with a focus on the decrease of N losses into the environment.

NITROGEN USE EFFICIENCY IN GRASSLAND SYSTEMS

Nitrogen use efficiency (NUE) is commonly used to estimate the conversion of N inputs into agricultural products and to indicate the risk of N losses to the broader environment (Oenema et al., 2014; Norton et al., 2015). The NUE is considered an easy-to-use indicator applicable to agriculture and food production-consumption systems (EU Nitrogen Expert Panel, 2015). It is expressed as a ratio of outputs over inputs and can be estimated using a range of metrics, such as plant growth per unit of N applied (e.g. fertilizer and manure); meat or milk production per unit of animal N intake; N exported from a farm per unit of N imported; or N consumed in food per unit of N used to produce the food (de Klein et al., 2017). The NUE values have to be interpreted in relation to productivity (N output) and N surplus (i.e., the difference between N input and harvested N output). The NUE may allow decision makers to examine differences in NUE between farms, between specific systems, between countries, and between years. It also allows identifying technical progress and the efficiency of policy measures. As such, NUE can serve as a valuable indicator for monitoring sustainable development in relation to food production and environmental challenges (EU Nitrogen Expert Panel, 2015). This parameter can be also used to express the amount of N applied as fertilizer, which is harvested in crop or pasture (de Klein et al., 2017), varying mostly around 30–35%. Nitrogen use efficiency increases significantly by synchronizing, as much as possible, N availability supply with

N demand (e.g. Maddux and Barnes, 1985). Nanomaterials, given they may provide a slow, steady, and time-dependent release of essential nutrients, including N, represent an opportunity to improve NUE, also reducing N leaching or losses as NH_3 volatilization, in agreement with Preetha and Balakrishnan (2017). Furthermore, an increase of up to threefold as well as an improvement in productivity by promoting seed germination, seedling growth, N metabolism, photosynthetic activity, protein synthesis, antioxidant defense among other benefits (Iqbal et al., 2019).

Nitrogen Losses From Grasslands

Nitrogen could be easily lost to the wider environment. The main pathways of N losses in grassland are gaseous emissions (NH_3 and N_2O) and nitrate leaching and runoff (NO_3^- and organic N) (Cameron et al., 2013). Agriculture is recognized as a major source of atmospheric NH_3, which has been associated with soil acidification, acid particulate matter and rainfall, odors (Aneja et al., 2009), and it is also indirectly linked to N_2O and global warming (IPCC, 2015). As an example, agriculture is a key contributor to NH_3 volatilization, representing the main source of NH_3 emissions in different countries (Pan et al., 2016), averaging 31% of the N applied to crops and grasslands (Silva et al., 2017). Another important pathway of N loss is denitrification as N_2O, which is a potent greenhouse gas (GHG) contributing to the depletion of the ozone layer (Matheyarasu et al., 2016). Worldwide, 12% of N_2O losses are attributed to synthetic fertilizers applied to agricultural soils (IPCC, 2015).

It has been estimated that agriculture due to leaching and surface runoff of NO_3^- represents between 37 and 82% of the N input into surface waters of Western Europe (Isermann, 1990), where the livestock sector in this continent contributes 73% of water pollution for both N and P (Leip et al., 2015). Traditionally, N has been applied to crops and pastures as granular formulation, and integrated into the soil nutrients cycle, where it can be absorbed by plants, fixed by the soil components, or lost from the soil-plant system through different pathways (Jadon et al., 2018). There are only a few studies evaluating N losses on grass species, focusing mainly on NH_3 losses (Henning et al., 2013b; Schlossberg et al., 2018), and NH_3 and N_2O loss (Alfaro et al., 2018). Foliar N application, using traditional or enhanced fertilizers dissolved in water, and more recently, the use of nanoformulations, has been evaluated to increase NUE (Dimkpa et al., 2020).

Potential Role of Nanofertilizers in Increasing Nitrogen Use Efficiency in Grasslands

The increasing demand for food globally will require more productive systems that use suitable and reliable technologies, ensuring low environmental impact in terms of soil and water pollution (Jyothi and Hebsur, 2017). Many agricultural management practices such as split N application, N localization, precision farming, use of liquid formulations, foliar sprays, and liming applications have been proposed to improve NUE (Sharma and Bali, 2018; Egan et al., 2019) in annual crops such as potato (Souza et al., 2020) and mix crop-livestock systems (Ershadia et al., 2020). In the case of grasslands, several management options have been studied including the traditional 4R approach for the use of fertilizer application (Right source, Right time, Right rate, Right place) (Snyder, 2017), the optimization of plant combinations according to the final purpose of the animal system including the more efficient cultivars and species (Pijlman et al., 2020), and the integration of the soil-plant-animal system, considering more efficient grazing regimes and N inputs on animal feed and manures as a source of organic fertilizer (Oenema et al., 2014; de Klein et al., 2017). Fertilizers and manures NUE may vary between 50 and 80% depending on agro-climatic conditions, soil parameters, types of pastures, and other factors (Powell et al., 2010). Authors agree that in pasture-based systems major progress in eco-efficiency will be achieved through the implementation of tailor-made aspects associated with operational management. Málinas et al. (2020), concluded that a combination of forage mixture with lower to medium N inputs could significantly contribute to increase NUE from *c.* 50–86%, and from 45 to 53%, respectively, while providing sustainable long-term grass yields across managed grasslands.

Nanofertilizers have been projected as a tool to meet sustainable intensification criteria in agricultural activities in the next 30 years due to the feasibility of synchronizing the release mechanism of nutrients (N and phosphorus, P) with an increment in crop yields and forage production while reducing the fertilization inputs (Kalia et al., 2019). Nanofertilizers can boost NUE by enabling a slow and constant release of nutrients thus assisting nutrient plant uptake (Jyothi and Hebsur, 2017; Kalia and Sharma, 2019). It has been reported that the use of nanofertilizers can improve crop production by up to 30% compared with traditional chemical fertilizers (Kah et al., 2018); however, there are also studies showing no advantage to using nanofertilizers over conventional fertilizers (Kopittke et al., 2019).

NANOFERTILIZER TYPES AND POTENTIAL NANOSTRUCTURES TO BE USED IN PASTURES

Nanofertilizers can be classified in nanoscale fertilizers, nanoscale additives, and nanoscale coatings (Mikkelsen, 2018). The release of nutrients that are immobilized or/and encapsulated into a particular nanocarrier (biologic, chemical and physical) is activated by three different factors. The biological factors are bacteria, fungi and other microorganisms that biodegrade the coating based on a biodegradable or synthetic polymeric material, thus allowing the release of nutrients and its fixation into the soil. The chemical-triggered mechanisms are moisture, solubilization, pH variation, soil type (Weeks and Hettiarachchi, 2019; Ramzan et al., 2020), and ion exchange reactions (Ribeiro and Carmo, 2019). The physical factors are ultrasound, magnetic field, heat and diffusion-controlled release (Mikkelsen, 2018; Ribeiro and Carmo, 2019).

Nanostructured 2D clays can be considered good candidates to carry nutrients because they are ionic systems characterized by the presence of anions and cations that compensate each other, leading to neutrality (Lazaratou et al., 2020). The ionic nature of the clays as well as their ability to host a wide range of organic and inorganic ions in combination with an elevated ion exchange

TABLE 1 | Potential advantages of nanofertilizers as an alternative to increasing nitrogen use efficiency.

Agronomic impact	
Increase crop productivity	Kopittke et al. (2019), Kottegoda et al. (2011), Abd El-Azeim et al. (2020)
Reduction of N rate applied	Raguraj et al. (2020)
Increase bioavailability of nutrients	Liu and Lal (2015), Kah et al. (2018)
Increase N use efficiency	Perrin et al. (1998), Raguraj et al. (2020)
Environmental impact	
Reduction of NO_3^- leaching	Malekian et al. (2011), Jadon et al. (2018)
Reduction of NH_3^+ volatilization	Jadon et al. (2018)
Reduction of N_2O emissions	Pereira et al. (2015)
Characteristics of nanomaterials	
Slow-release source according to plant demands	Ureña-Amate et al. (2011), Chhowalla (2017), Tarafder et al. (2020)
Use of biodegradable materials	Kusumastuti et al. (2019)
Possibility to use different N molecules and formulations	Sarkar et al. (2014), Benício et al. (2016), Golbashy et al. (2016)
Favors penetration through nanopores and stomatal openings in plant leaves	Abdel-Aziz et al. (2016), Mahil and Kumar (2019)
Facilitates transport and delivery of nutrients through plasmodesmata	Eichert et al. (2008), Pérez-de-Luque (2017)

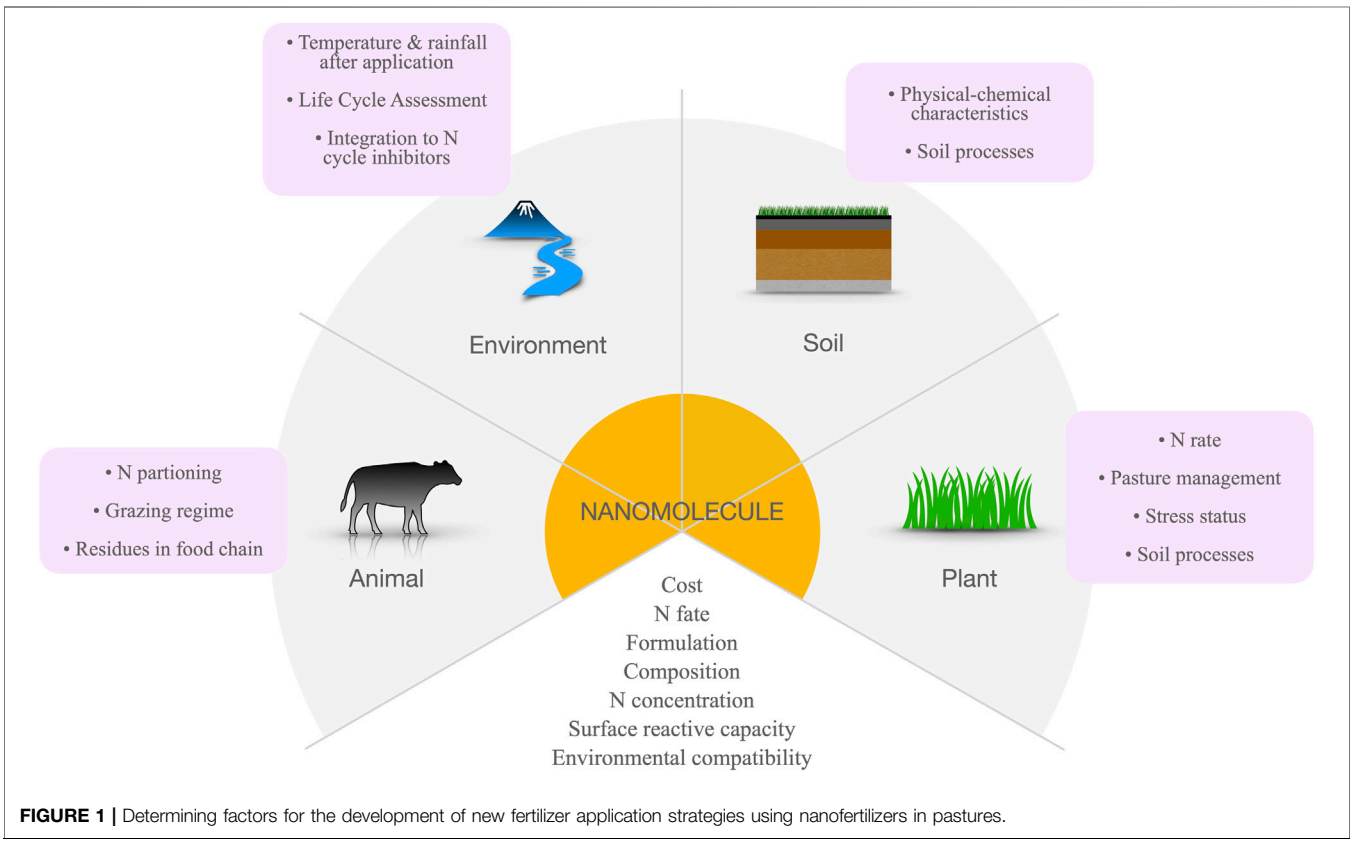

FIGURE 1 | Determining factors for the development of new fertilizer application strategies using nanofertilizers in pastures.

capacity, may render them suitable for controlled or slow nutrients release and thus increasing NUE (**Table 1**). For example, Layered Double Hydroxide (LDH) (Ureña-Amate et al., 2011; Berber et al., 2013; Koilraj et al., 2013; Borges et al., 2019; Jiang et al., 2019), montmorillonite (MMT) (Golbashy et al., 2016), and Zeolite ((Manjaiah et al., 2019) are good examples of a 2D nanostructure clay with promising opportunities as nanofertilizers for grasslands. Another suitable nanomaterial, due to its intrinsic nutrient capacity is the Hydroxyapatite (HT), a nanoparticle that can supply P in a faster and more prolonged manner (biphasic pattern) (Montalvo et al., 2015; Kottegoda et al., 2017). The LDH has also been reported to have the ability to uptake P and to provide a beneficial effect in the soil due to buffer properties (Torres-Dorante et al., 2009; Silva et al., 2014; Benício et al., 2016).

STRATEGIES FOR N BASED NANOFERTILIZERS USE IN GRASSLANDS

Because grassland ecosystems present unique features compared to traditional annual or perennial crops, the approach for

applying nanofertilizers should follow a particular strategy (**Figure 1**), considering grass harvest by cattle and the different grazing patterns during the year, with short (*c.* 10–14 days) or long periods (*c.* 40–60 days) between grazing cycles in managed systems in temperate regions (Whitehead, 2000). Commonly, pastures are composed of a mixture of plant species, each with a different nutrient demand, with annual, biannual or perennial species participating in the grassland ecosystem. Thus, the growth pattern varies among grassland types and so does their nutrients demand (Blair et al., 2014). The pasture type depends on animal system needs, such as grazing oriented, forage conservation or both. Nanofertilizers could be applied to the soil or directly over the plant as foliar sprays (Mahil and Kumar, 2019). Soil applied nanofertilizers enable the movement of nutrients in the soil, facilitating its release and penetration into the roots. Controlled-release and slow-release nanofertilizers are used to supply nutrients in suitable concentration to plants over a prolonged interval of time, avoiding the continuous fertilizer application, and reducing the environmental risks (Jiang et al., 2019; Jia et al., 2020; Yoon et al., 2020).

Reduction of N losses has been reported using N charged porous nanomaterials, such as zeolites (Manikandan and Subramanian, 2017), clays (Sarkar et al., 2014), or biodegradable polymers such as chitosan (Sharif et al., 2018). These could be related to a gradual release rate of NH_4^+ and/or NO_3^-, that in turn limits soil available N, which could potentially be lost to the environment in agreement with Cardenas et al. (2013). Foliar application, on the other hand, has proven to be useful to supply small quantities of fertilizer to the crops and it is especially beneficial in the correction of micronutrient deficiency, while in the case of macronutrients it can supplement soil conventional fertilization, particularly when soils have limiting factors (Fageria et al., 2009). Within foliar fertilizers, urea dissolved in water has been commonly used as the main N source for foliar application in perennial and annual crops, and to a lesser extent, in grassland species (Bowman and Paul, 1992; Stiegler et al., 2011; Ramírez-Rodríguez et al., 2020), however, N volatilization losses could be high, which could limit its use. Because nutrients in foliar applications are delivered directly to the target in small amounts, foliar fertilization is potentially more beneficial to the environment compared to traditional root treatments. Nevertheless, even if foliar nutrient application presents several advantages and has increasing importance in agriculture. Many mechanisms controlling the penetration of nutrients to the plant are not fully understood and plant response to foliar applications varies widely (Lv et al., 2019).

CONCLUDING REMARKS AND PERSPECTIVES

Although encouraging NUE results have been found when using nanofertilizers, some limitations and adverse effects have also been reported (Iqbal et al., 2019). Most of the research has also only been carried out at a laboratory scale (Kah et al., 2018). Examples of shortcomings in the use of foliar fertilizers are that they require an available leaf area to be effective, and may cause scorching or burning if the concentration of the spray is too high (Achari and Kowshik, 2018). They also require perfect timing for the application, since climatic conditions affect effectiveness. The costs of multiple applications can be too high to be profitable, the standardization of the nanoformulations, and lack of size uniformity of the nanoparticles (Iqbal, 2019), and optimizing foliar applications of nanofertilizers are challenges that need to be addressed in future research.

Further research is required to better understand the role of different N forms in supplying these molecules (i.e. NO_3^-, NH_4^+) and their impact on NUE in pastures, including N transformation within the plant and their effect on reducing N losses to the environment. Additionally, the integration of this technology with the use of N cycling inhibitors may represent an opportunity by creating favoring synergetic effects (**Figure 1**). More information is required to understand whether nanofertilizers are fully transformed into ionic forms in the plant and later incorporated into proteins and different metabolites, or if some of them remain intact and reach consumers through the food chain (Iqbal, 2019).

A better understanding of the advantages of nanomaterials is needed (**Table 1**), more and higher quality data is required on materials characterization, comprehensive comparisons with non-nano formulations, and field studies (Kah et al., 2018). Additionally, adapted nutrient fertilizer application strategies will need to be adjusted to take advantage of the benefits provided, to consider the inclusion of precision agriculture, such as drones fitted with cameras to gather multispectral images detecting N concentration in the grass within the paddock, avoiding over-application (e.g. urine patches), and repeated applications at low rates, with a potential increase in costs. All these factors will need to be addressed in an integrated manner (**Figure 1**) to account for potential downfalls and take full advantage of the opportunities and synergies the use of nanofertilizers may provide for the sustainable future of grassland production. The future development and adoption of these molecules as an answer for increasing food production with higher nutrient efficiency will need to balance economic and environmental costs of production with the potential reduction of environmental impact and yield increases. For this, a Life Cycle Assessment (LCA) may represent an opportunity for an integrated analysis of its use, considering yield productivity, environmental implications, and impact on food chains. The need to validate the pros and cons of nanofertilizers under representative field grasslands conditions to address the questions arising from stakeholders also remains as a pending task before the widespread adoption of this technology.

AUTHOR CONTRIBUTIONS

MA was the research leader for the FONDECYT Grant 1180775, and contributed to the manuscript, including NUE in grasslands concepts section of the manuscript, and contributed to the discussion, as well as the general editing of the manuscript. JM was a researcher on the nano fertilizer project and coordinated and contributed to manuscript conceptualization;

writing-original draft preparation; writing-review and editing. FS was a researcher on the nano fertilizer project and was responsible for the N losses section of the manuscript and contributed to the discussion and editing of the manuscript. LPA led the manuscript sections on nanofertilizer types and the potential nanostructures used in pastures. SH participated in the manuscript sections on nanofertilizer types and the potential nanostructures that could be used in pastures. MR contributed to the general discussion and provided a practical overview of nanoformulations and their use in grasslands.

FUNDING

We would like to acknowledge Fondo Nacional de Desarrollo Científico y Tecnológico de Chile (FONDECYT), grant 1180775.

ACKNOWLEDGMENTS

The authors would like to thank the Instituto de Investigaciones Agropecuarias-Chile.

REFERENCES

Abd El-Azeim, M. M., Sherif, M. A., Hussien, M. S., Tantawy, I. A. A., and Bashandy, S. O. (2020). Impacts of nano- and non-nanofertilizers on potato quality and productivity. *Acta Ecol. Sin.* 40, 388. doi:10.1016/j.chnaes.2019.12.007

Abdel-Aziz, H. M. M., Hasaneen, M. N. A., and Omer, A. M. (2016). Nano chitosan-NPK fertilizer enhances the growth and productivity of wheat plants grown in sandy soil. *Span J. Agric. Res.* 14, e0902. doi:10.5424/sjar/2016141-8205

Achari, G. A., and Kowshik, M. (2018). Recent developments on nanotechnology in agriculture: plant mineral nutrition, health, and interactions with soil microflora. *J. Agric. Food Chem.* 66, 8647–8661. doi:10.1021/acs.jafc.8b00691

Adisa, I. O., Pullagurala, V. L. R., Peralta-Videa, J. R., Dimkpa, C. O., Elmer, W. H., Gardea-Torresdey, J. L., et al. (2019). Recent advances in nano-enabled fertilizers and pesticides: a critical review of mechanisms of action. *Environ. Sci. Nano* 6, 2002–2030. doi:10.1039/C9EN00265K

Alfaro, M., Salazar, F., Hube, S., Ramírez, L., and Mora, M. S. (2018). Ammonia and nitrous oxide emissions as affected by nitrification and urease inhibitors. *J. Soil Sci. Plant Nutr.* 18, 479–486. doi:10.4067/S0718-95162018005001501

Andrews, D., Nann, T., and Lipson, R. H. (2019). *Comprehensive nanoscience and nanotechnology*. Cambridge, MA: Academic Press.

Aneja, V. P., Schlesinger, W. H., and Erisman, J. W. (2009). Effects of agriculture upon the air quality and climate: research, policy, and regulations. *Environ. Sci. Technol.* 43, 4234–4240. doi:10.1021/es8024403

Banger, K., Yuan, M., Wang, J., Nafziger, E. D., and Pittelkow, C. M. (2017). A vision for incorporating environmental effects into nitrogen management decision support tools for U.S. Maize production. *Front. Plant Sci.* 8, 1270. doi:10.3389/fpls.2017.01270

Bashir, I., Lone, F. A., Bhat, R. A., Mir, S. A., Dar, Z. A., and Dar, S. A. (2020). Concerns and threats of contamination on aquatic ecosystems. in *Bioremediation and Biotechnology, Sustainable Approaches to Pollution Degradation*, Berlin, Germany: Springer. 1–26. doi:10.1007/978-3-030-35691-0_1

Benelmekki, M. (2015). "An introduction to nanoparticles and nanotechnology," in *Designing hybrid nanoparticles* (San Rafael, CA: Morgan & Claypool Publishers), 1. doi:10.1088/978-1-6270-5469-0ch1

Benício, L. P. F., Constantino, V. R. L., Pinto, F. G., Vergütz, L., Tronto, J., and da Costa, L. M. (2016). Layered double hydroxides: new technology in phosphate fertilizers based on nanostructured materials. *ACS Sustain. Chem. Eng.* 5, 399. doi:10.1021/acssuschemeng.6b01784

Berber, M. R., Hafez, I. H., Minagawa, K., and Mori, T. (2013). A sustained controlled release formulation of soil nitrogen based on nitrate-layered double hydroxide nanoparticle material. *J. Soils Sediments* 14, 60–66. doi:10.1007/s11368-013-0766-3

Blair, J., Nippert, J., and Briggs, J. (2014). Grassland ecology. *Ecol. Environ.* 389–423. doi:10.1007/978-1-4614-7501-9_14

Borges, R., Wypych, F., Petit, E., Forano, C., and Prevot, V. (2019). Potential sustainable slow-release fertilizers obtained by mechanochemical activation of MgAl and MgFe layered double hydroxides and K2HPO4. *Nanomaterials* 9, 183. doi:10.3390/nano9020183

Bowman, D. C., and Paul, J. L. (1992). Foliar absorption of urea, ammonium, and nitrate by perennial ryegrass tryegrass turf. *jashs* 117, 75–79. doi:10.21273/JASHS.117.1.75

Cameron, K. C., Di, H. J., and Moir, J. L. (2013). Nitrogen losses from the soil/plant system: a review. *Ann. Appl. Biol.* 162, 145–173. doi:10.1111/aab.12014

Cardenas, L. M., Hatch, D. J., Scholefield, D., Jhurreea, D., Clark, I. M., Hirsch, P. R., et al. (2013). Potential mineralization and nitrification in volcanic grassland soils in Chile. *Soil Sci. Plant Nutr.* 59, 380–391. doi:10.1080/00380768.2013.789395

Chhowalla, M. (2017). Slow release nanofertilizers for bumper crops. *ACS Cent. Sci.* 3, 156−157. doi:10.1021/acscentsci.7b00091

Davidson, E. A. (2009). The contribution of manure and fertilizer nitrogen to atmospheric nitrous oxide since 1860. *Nat. Geosci.* 2, 156–157. doi:10.1038/ngeo608

de Klein, C. A. M., Monaghan, R. M., Alfaro, M., Gourley, C. J. P., Oenema, O., and Powell, J. M. (2017). Nitrogen performance indicators for dairy production systems. *Soil Res.* 55, 479. doi:10.1071/SR16349

DeRosa, M. C., Monreal, C., Schnitzer, M., Walsh, R., and Sultan, Y. (2010). Nanotechnology in fertilizers. *Nat. Nanotechnol.* 5, 91. doi:10.1038/nnano.2010.2

Dimkpa, C. O., and Bindraban, P. S. (2018). Nanofertilizers: new products for the industry? *J. Agric. Food Chem.* 66, 6462–6473. doi:10.1021/acs.jafc.7b02150

Dimkpa, C. O., Fugice, J., Singh, U., and Lewis, T. D. (2020). Development of fertilizers for enhanced nitrogen use efficiency - trends and perspectives. *Sci. Total Environ.* 731, 139113. doi:10.1016/j.scitotenv.2020.139113

Duhan, J. S., Kumar, R., Kumar, N., Kaur, P., Nehra, K., and Duhan, S. (2017). Nanotechnology: the new perspective in precision agriculture. *Biotechnol. Rep.* 15, 11–23. doi:10.1016/j.btre.2017.03.002

Egan, G., Mckenzie, P., Crawley, M., and Fornara, D. A. (2019). Effects of grassland management on plant nitrogen use efficiency (NUE): evidence from a long-term experiment. *Basic Appl. Ecol.* 41, 33. doi:10.1016/j.baae.2019.10.001

Eichert, T., Kurtz, A., Steiner, U., and Goldbach, H. E. (2008). Size exclusion limits and lateral heterogeneity of the stomatal foliar uptake pathway for aqueous solutes and water-suspended nanoparticles. *Physiol. Plant* 134, 151–160. doi:10.1111/j.1399-3054.2008.01135.x

Ershadi, S. Z., Dias, G., Heidari, M. D., and Pelletier, N. (2020). Improving nitrogen use efficiency in crop-livestock systems: a review of mitigation technologies and management strategies, and their potential applicability for egg supply chains. *J. Clean. Prod.* 265, 121671. doi:10.1016/j.jclepro.2020.121671

EU Nitrogen Expert Panel (2015). *Nitrogen Use Efficiency (NUE) - an indicator for the utilization of nitrogen in agriculture and food systems*. Wageningen, Netherlands: Wageningen University.

Fageria, N. K., Filho, M. P. B., Moreira, A., and Guimarães, C. M. (2009). Foliar fertilization of crop plants. *J. Plant Nutr.* 32, 1044–1064. doi:10.1080/01904160902872826

FAO (2018). *The future of food and agriculture – Alternative pathways to 2050. Summary version*. Rome, Italy, 60 Licence: CC BY-NC-SA 3.0 IGO. Available at: http://www.fao.org/3/CA1553EN/ca1553en.pdf.

Golbashy, M., Sabahi, H., Allahdadi, I., Nazokdast, H., and Hosseini, M. (2016). Synthesis of highly intercalated urea-clay nanocomposite via domestic montmorillonite as eco-friendly slow-release fertilizer. *Arch. Agron. Soil Sci.* 63, 84. doi:10.1080/03650340.2016.1177175

Henning, S. W., Branham, B. E., and Mulvaney, R. L. (2013b). Response of turfgrass to urea-based fertilizers formulated to reduce ammonia volatilization and nitrate conversion. *Biol. Fertil. Soils* 49, 51–60. doi:10.1007/s00374-012-0696-z

Henning, S. W., Mulvaney, R. L., and Branham, B. E. (2013a). Factors affecting foliar nitrogen uptake by creeping bentgrass. *Crop Sci.* 53, 1778. doi:10.2135/cropsci2012.11.0650

Hunter, M. C., Smith, R. G., Schipanski, M. E., Atwood, L. W., and Mortensen, D. A. (2017). Agriculture in 2050: recalibrating targets for sustainable intensification. *BioScience* 67, 386–391. doi:10.1093/biosci/bix010

Iqbal, M. A. (2019). *Nano-fertilizers for sustainable crop production under changing climate: a global perspective*. London, United Kingdom: IntechOpen, doi:10.5772/intechopen.89089

Iqbal, M., Umar, S., and Mahmooduzzafar (2019). Nano-fertilization to enhance nutrient use efficiency and productivity of crop plants. *in Nanomater. Plant Potential*, 473–505. doi:10.1007/978-3-030-05569-1_19

Isermann, K. (1990). Share of agriculture in nitrogen and phosphorus emissions into the surface waters of Western Europe against the background of their eutrophication. *Fertilizer Res.* 26, 253–269. doi:10.1007/BF01048764

Jadon, P., Selladurai, R., Yadav, S. S., Coumar, M. V., Dotaniya, M. L., Singh, A. K., et al. (2018). Volatilization and leaching losses of nitrogen from different coated urea fertilizers. *J. Soil Sci. Plant Nutr.* 18, 1036–1047. doi:10.4067/S0718-95162018005002903

Jia, C., Lu, P., and Zhang, M. (2020). Preparation and characterization of environmentally friendly controlled release fertilizers coated by leftovers-based polymer. *Processes* 8, 417. doi:10.3390/pr8040417

Jiang, X., Yan, B., Chen, J., Li, W., Hu, J., and Guan, Y. (2019). Transport and retention of phosphorus in soil with addition of Mg-Al layered double hydroxides: effects of material dosage, flow velocity and pH. *Chem. Eng. J.* 378, 122154. doi:10.1016/j.cej.2019.122154

Jyothi, T. V., and Hebsur, N. S. (2017). Effect of nanofertilizers on growth and yield of selected cereals - a review. *Ag* 38. doi:10.18805/ag.v38i02.7942

Kah, M., Kookana, R. S., Gogos, A., and Bucheli, T. D. (2018). A critical evaluation of nanopesticides and nanofertilizers against their conventional analogues. *Nat. Nanotechnol.* 13, 677–684. doi:10.1038/s41565-018-0131-1

Kalia, A., Sharma, S. P., and Kaur, H. (2019). "Nanoscale fertilizers: harnessing boons for enhanced nutrient use efficiency and crop productivity," in *Nanobiotechnology applications in plant protection: volume 2 nanotechnology in the Life sciences.* Editors K. A. Abd-Elsalam and R. Prasad (Cham, Switzerland: Springer International Publishing)), 191–208. doi:10.1007/978-3-030-13296-5_10

Kalia, A., and Sharma, S. P. (2019). "Nanomaterials and vegetable crops: realizing the concept of sustainable production," in *Nanoscience for sustainable agriculture*. Editors R. N. Pudake, N. Chauhan, and C. Kole (Cham, Switzerland: Springer International Publishing), 323–353. doi:10.1007/978-3-319-97852-9_15

Koilraj, P., Antonyraj, C. A., Gupta, V., Reddy, C. R. K., and Kannan, S. (2013). Novel approach for selective phosphate removal using colloidal layered double hydroxide nanosheets and use of residue as fertilizer. *Appl. Clay Sci.* 86, 111–118. doi:10.1016/j.clay.2013.07.004

Kopittke, P. M., Lombi, E., Wang, P., Schjoerring, J. K., and Husted, S. (2019). Nanomaterials as fertilizers for improving plant mineral nutrition and environmental outcomes. *Environ. Sci. Nano* 6, 3513–3524. doi:10.1039/C9EN00971J

Kottegoda, N., Sandaruwan, C., Priyadarshana, G., Siriwardhana, A., Rathnayake, U. A., Berugoda Arachchige, D. M., et al. (2017). Urea-Hydroxyapatite nanohybrids for slow release of nitrogen. *ACS Nano* 11, 1214–1221. doi:10.1021/acsnano.6b07781

Kottegoda, N., Munaweera, I., Madusanka, N., and Karunaratne, V. (2011). A green slow-release fertilizer composition based on urea-modified hydroxyapatite nanoparticles encapsulated wood. *Curr. Sci.* 101, 73–78.

Kumar, R., Ashfaq, M., and Verma, N. (2018). Synthesis of novel PVA-starch formulation-supported Cu-Zn nanoparticle carrying carbon nanofibers as a nanofertilizer: controlled release of micronutrients. *J. Mater. Sci.* 53, 7150–7164. doi:10.1007/s10853-018-2107-9

Kusumastuti, Y., Istiani, A., Rochmadiand Purnomo, C. W. (2019). Chitosan-based polyion multilayer coating on NPK fertilizer as controlled released fertilizer. *Adv. Mater. Sci. Engineering* 2019, 1. doi:10.1155/2019/2958021

Lazaratou, C. V., Vayenas, D. V., and Papoulis, D. (2020). The role of clays, clay minerals and clay-based materials for nitrate removal from water systems: a review. *Appl. Clay Sci.* 185, 105377. doi:10.1016/j.clay.2019.105377

Lee, D. R., Barrett, C. B., and McPeak, J. G. (2006). Policy, technology, and management strategies for achieving sustainable agricultural intensification. *Agric. Econ.* 34, 123–127. doi:10.1111/j.1574-0864.2006.00112.x

Lee, Y.-C., and Moon, J.-Y. (2020). Introduction to nanotechnology and bionanotechnology," in *Introduction to bionanotechnology*. Editors Y.-C. Lee and J.-Y. Moon (Singapore: Springer), 1–14. doi:10.1007/978-981-15-1293-3_1

Leip, A., Billen, G., Garnier, J., Grizzetti, B., Lassaletta, L., Reis, S., et al. (2015). Impacts of European livestock production: nitrogen, sulphur, phosphorus and greenhouse gas emissions, land-use, water eutrophication and biodiversity. *Environ. Res. Lett.* 10, 115004. doi:10.1088/1748-9326/10/11/115004

Liu, R., and Lal, R. (2015). Potentials of engineered nanoparticles as fertilizers for increasing agronomic productions. *Sci. Total Environ.* 514, 131–139. doi:10.1016/j.scitotenv.2015.01.104

Lowry, G. V., Avellan, A., and Gilbertson, L. M. (2019). Opportunities and challenges for nanotechnology in the agri-tech revolution. *Nat. Nanotechnol.* 14, 517–522. doi:10.1038/s41565-019-0461-7

Lv, J., Christie, P., and Zhang, S. (2019). Uptake, translocation, and transformation of metal-based nanoparticles in plants: recent advances and methodological challenges. *Environ. Sci. Nano* 6, 41–59. doi:10.1039/C8EN00645H

Maddux, L., and Barnes, P. (1985). Effects of time and rate of applied nitrogen and nitrapyrin on irrigated corn. *J. Fertil. issues* 2, 124–129.

Mahil, E. I. T., and Kumar, B. N. A. (2019). *Foliar application of nanofertilizers in agricultural crops – a review*. 11.

Malekian, R., Abedi-Koupai, J., and Eslamian, S. S. (2011). Influences of clinoptilolite and surfactant-modified clinoptilolite zeolite on nitrate leaching and plant growth. *J. Hazard. Mater.* 185, 970–976. doi:10.1016/j.jhazmat.2010.09.114

Malinas, A., Rotar, I., Vidican, R., Iuga, V., Pacurar, F., Malinas, C., et al. (2020). Designing a sustainable temporary grassland system by monitoring nitrogen use efficiency. *Agronomy* 10 (1), 149. doi:10.3390/agronomy10010149

Manikandan, A., and Subramanian, K. S. (2017). Study on mitigation of ammonia volatilization loss in urea through adsorbents. *Jans* 9, 688–692. doi:10.31018/jans.v9i2.1258

Manjaiah, K., Mukhopadhyay, R., Paul, R., Datta, S., Periyamuthu, K., and Sarkar, B. (2019). *Clay minerals and zeolites for environmentally sustainable agriculture*. in *Modified clay and zeolite nanocomposite materials*. Amsterdam, Netherlands: Elsevier. 309–329. doi:10.1016/B978-0-12-814617-0.00008-6

Manjunatha, S. B., Biradar, D., and Aladakatti, Y. (2016). Nanotechnology and its applications in agriculture: a review. *J. Farm Sci.* 29, 1–13.

Marchiol, L., Iafisco, M., Fellet, G., and Adamiano, A. (2020). "Chapter Two - nanotechnology support the next agricultural revolution: perspectives to enhancement of nutrient use efficiency," in *Advances in agronomy*. Editor D. L. Sparks (Cambridge, MA: Academic Press), 27–116. doi:10.1016/bs.agron.2019.12.001

Mastronardi, E., Tsae, P., Zhang, X., Monreal, C., and Derosa, M. (2015). *Strategic role of nanotechnology in fertilizers: potential and limitations*. Berlin, Germany: Springer. 25–67. doi:10.1007/978-3-319-14024-7_2

Matheyarasu, R., Seshadri, B., Bolan, N. S., and Naidu, R. (2016). Assessment of nitrogen losses through nitrous oxide from abattoir wastewater-irrigated soils. *Environ. Sci. Pollut. Res. Int.* 23, 22633–22646. doi:10.1007/s11356-016-7438-y

Mikkelsen, R. (2018). Nanofertilizer and Nanotechnology: a quick look. *Better Crops* 102, 18–19. doi:10.24047/BC102318

Montalvo, D., McLaughlin, M. J., and Degryse, F. (2015). Efficacy of hydroxyapatite nanoparticles as phosphorus fertilizer in andisols and oxisols. *Soil Sci. Soc. America J.* 79, 551–558. doi:10.2136/sssaj2014.09.0373

Norton, R., Davidson, E., and Roberts, T. (2015). "Nitrogen use efficiency and nutrient performance indicators," in *Glob. Partnersh. Nutr. Manag.* (Washington, DC: Task Team Workshop Wash. DC), 1–14.

IPCC (2015). *Climate change 2014: mitigation of climate change ; summary for policymakers technical Summary ; part of the working group III contribution to the fifth asessment rreport of the intergovernmental panel on climate change*. O. Edenhofer, R. Pichs-Madruga, Y. Sokona, J. C. Minx, E. Farahani, S. Kadner, et al. (Geneva, Switzerland: Intergovernmental Panel on Climate Change).

Oenema, O., de Klein, C., and Alfaro, M. (2014). Intensification of grassland and forage use: driving forces and constraints. *Crop Pasture Sci.* 65, 524–537. doi:10.1071/cp14001

Pan, B., Lam, S. K., Mosier, A., Luo, Y., and Chen, D. (2016). Ammonia volatilization from synthetic fertilizers and its mitigation strategies: a global synthesis. *Agric. Ecosyst. Environ.* 232, 283–289. doi:10.1016/j.agee.2016.08.019

Pereira, E. I., da Cruz, C. C. T., Solomon, A., Le, A., Cavigelli, M. A., and Ribeiro, C. (2015). Novel slow-release nanocomposite nitrogen fertilizers: the impact of polymers on nanocomposite properties and function. *Ind. Eng. Chem. Res.* 54, 3717–3725. doi:10.1021/acs.iecr.5b00176

Pérez-de-Luque, A. (2017). Interaction of nanomaterials with plants: what do we need for real applications in agriculture? *Front. Environ. Sci.* 5, 12. doi:10.3389/fenvs.2017.00012

Perrin, T. S., Drost, D. T., Boettinger, J. L., and Norton, J. M. (1998). Ammonium-loaded clinoptilolite: a slow-release nitrogen fertilizer for sweet corn. *J. Plant Nutr.* 21, 515–530. doi:10.1080/01904169809365421

Pestovsky, Y. S., and Martínez-Antonio, A. (2017). The use of nanoparticles and nanoformulations in agriculture. *J. Nanosci. Nanotechnol.* 17, 8699–8730. doi:10.1166/jnn.2017.15041

Peters, R., Brandhoff, P., Weigel, S., Marvin, H., Bouwmeester, H., Aschberger, K., et al. (2014). *Inventory of Nanotechnology applications in the agricultural, feed and food sector*. Parma, Italy: EFSA Supporting Publications. 11. doi:10.2903/sp.efsa.2014.EN-621

Pijlman, J., Berger, S. J., Lexmond, F., Bloem, J., van Groenigen, J. W., Visser, E. J. W., et al. (2020). Can the presence of plantain (Plantago lanceolataL.) improve nitrogen cycling of dairy grassland systems on peat soils? *New Zealand J. Agric. Res.* 63, 106–122. doi:10.1080/00288233.2019.1698620

Powell, J. M., Gourley, C. J. P., Rotz, C. A., and Weaver, D. M. (2010). Nitrogen use efficiency: a potential performance indicator and policy tool for dairy farms. *Environ. Sci. Pol.* 13, 217–228. doi:10.1016/j.envsci.2010.03.007

Preetha, P. S., and Balakrishnan, N. (2017). A review of nano fertilizers and their use and functions in soil. *Int. J. Curr. Microbiol. App. Sci* 6, 3117–3133. doi:10.20546/ijcmas.2017.612.364

Purnomo, L., Billen, G., Grizzetti, B., Anglade, J., and Garnier, J. (2014). 50 year trends in nitrogen use efficiency of world cropping systems: the relationship between yield and nitrogen input to cropland. *Environ. Res. Lett.* 9, 105011. doi:10.1088/1748-9326/9/10/105011

Raguraj, S., Wijayathunga, W. M. S., Gunaratne, G. P., Amali, R. K. A., Priyadarshana, G., Sandaruwan, C., et al. (2020). Urea-hydroxyapatite nanohybrid as an efficient nutrient source in Camellia sinensis (L.) Kuntze (tea). *J. Plant Nutr.* 43 (15), 2383–2394. doi:10.1080/01904167.2020.1771576

Ramírez-Rodríguez, G. B., Miguel-Rojas, C., Montanha, G. S., Carmona, F. J., Dal Sasso, G., Sillero, J. C., et al. (2020). Reducing nitrogen dosage in Triticum durum plants with urea-doped nanofertilizers. *Nanomaterials* 10, 1043. doi:10.3390/nano10061043

Ramzan, S., Rasool, T., Bhat, R. A., Ahmad, P., Ashraf, I., Rashid, N., et al. (2020). Agricultural soils a trigger to nitrous oxide: a persuasive greenhouse gas and its management. *Environ. Monit. Assess.* 192, 436. doi:10.1007/s10661-020-08410-2

Ribeiro, C., and Carmo, M. (2019). Why nonconventional materials are answers for sustainable agriculture. *MRS Energy Sustain.* 6 (1), E9. doi:10.1557/mre.2019.7

Ruiz-Cañas, M., Quintero, H., Corredor, L., Manrique, E., and Romero Bohórquez, A. (2020). New nanohybrid based on hhydrolyzed polyacrylamide and silica nanoparticles: morphological, structural and thermal properties. *Polymers* 12 (5), 1152–1166. doi:10.3390/polym12051152

Ryle, G. J. A., and Stanley, J. (1992). Effect of elevated CO_2 on stomatal size and distribution in perennial ryegrass. *Ann. Bot.* 69, 563–565. doi:10.1093/oxfordjournals.aob.a088387

Sarkar, S., Datta, S. C., and Biswas, D. R. (2014). Effect of fertilizer loaded nanoclay/superabsorbent polymer composites on nitrogen and phosphorus release in soil. *Proc. Natl. Acad. Sci. India, Sect. B Biol. Sci.* 85, 415. doi:10.1007/s40011-014-0371-2

Schlossberg, M. J., McGraw, B. A., and Sebring, R. L. (2018). Ammonia volatilization from putting greens foliarly fertilized by conventional or stabilized urea. *Agric. Environ. Lett.* 3, 180019. doi:10.2134/ael2018.04.0019

Shang, Y., Hasan, M. K., Ahammed, G. J., Li, M., Yin, H., and Zhou, J. (2019). Applications of nanotechnology in plant growth and crop protection: a review. *Molecules* 24, 2558–2580. doi:10.3390/molecules24142558

Sharif, R., Mujtaba, M., Ur Rahman, M., Shalmani, A., Ahmad, H., Anwar, T., et al. (2018). The multifunctional role of chitosan in horticultural crops; a review. *Molecules* 23, 872. doi:10.3390/molecules23040872

Sharma, L., and Bali, S. (2018). A review of methods to improve nitrogen use efficiency in agriculture. *Sustainability* 10, 51. doi:10.3390/su10010051

Silva, A. G. B., Sequeira, C. H., Sermarini, R. A., and Otto, R. (2017). Urease inhibitor NBPT on ammonia volatilization and crop productivity: a meta-analysis. *Agron. J.* 109, 1–13. doi:10.2134/agronj2016.04.0200

Silva, V. d., Mangrich, A. S., and Wypych, F. (2014). Liberação de nitrato de hidróxidos duplos lamelares como potenciais fertilizantes de liberação lenta. *Rev. Bras. Ciênc. Solo* 38, 821–830. doi:10.1590/S0100-06832014000300013

Snyder, C. S. (2017). Enhanced nitrogen fertiliser technologies support the "4R" concept to optimise crop production and minimise environmental losses. *Soil Res.* 55, 463–472. doi:10.1071/sr16335

Souza, E. F. C., Soratto, R. P., Sandaña, P., Venterea, R. T., and Rosen, C. J. (2020). Split application of stabilized ammonium nitrate improved potato yield and nitrogen-use efficiency with reduced application rate in tropical sandy soils. *Field Crops Res.* 254, 107847. doi:10.1016/10.1016/j.fcr.2020.107847

Stiegler, J. C., Richardson, M. D., and Karcher, D. E. (2011). Foliar nitrogen uptake following urea application to putting green turfgrass species. *Crop Sci.* 51, 1253. doi:10.2135/cropsci2010.06.0377

Tarafder, C., Daizy, M., Alam, M. M., Ali, M. R., Islam, M. J., Islam, R., et al. (2020). Formulation of a hybrid nanofertilizer for slow and sustainable release of micronutrients. *Acs Omega* 5, 23960–23966. doi:10.1021/acsomega.0c03233

Tilman, D., Socolow, R., Foley, J. A., Hill, J., Larson, E., Lynd, L., et al. (2009). Energy. Beneficial biofuels--the food, energy, and environment trilemma. *Science* 325 (5938), 270–271. doi:10.1126/science.1177970

Torres-Dorante, L. O., Lammel, J., and Kuhlmann, H. (2009). Use of a layered double hydroxide (LDH) to buffer nitrate in soil: long-term nitrate exchange properties under cropping and fallow conditions. *Plant Soil* 315, 257–272. doi:10.1007/s11104-008-9748-4

Ureña-Amate, M. D., Boutarbouch, N. D., Socias-Vicianadel, M. d. M. M., and González-Pradas, E. (2011). Controlled release of nitrate from hydrotalcite modified formulations. *Appl. Clay Sci.* 52, 368–373. doi:10.1016/j.clay.2011.03.018

Weeks, J. J., Jr., and Hettiarachchi, G. M. (2019). A review of the latest in phosphorus fertilizer technology: possibilities and pragmatism. *J. Environ. Qual.* 48, 1300–1313. doi:10.2134/jeq2019.02.0067

Weih, M., Asplund, L., and Bergkvist, G. (2011). Assessment of nutrient use in annual and perennial crops: a functional concept for analyzing nitrogen use efficiency. *Plant Soil* 339, 513–520. doi:10.1007/s11104-010-0599-4

Whitehead, D. C. (2000). *Nutrient elements in grassland: soil-plant-animal relationships*. Wallingford, United Kingdom: CABI Publishing.

Xie, H., Huang, Y., Chen, Q., Zhang, Y., and Wu, Q. (2019). Prospects for agricultural sustainable intensification: a review of research. *Land* 8, 157. doi:10.3390/land8110157

Yoon, H. Y., Lee, J. G., Esposti, L. D., Iafisco, M., Kim, P. J., Shin, S. G., et al. (2020). Synergistic release of crop nutrients and stimulants from hydroxyapatite nanoparticles functionalized with humic substances: toward a multifunctional nanofertilizer. *ACS Omega* 5, 6598–6610. doi:10.1021/acsomega.9b04354

Conflict of Interest: The authors declare that the research was conducted in the absence of any commercial or financial relationships that could be construed as a potential conflict of interest.

frontiers in Environmental Science

ORIGINAL RESEARCH
published: 15 April 2021
doi: 10.3389/fenvs.2021.609621

Biochar-Swine Manure Impact on Soil Nutrients and Carbon Under Controlled Leaching Experiment Using a Midwestern Mollisols

Chumki Banik[1], Jacek A. Koziel[1], Mriganka De[2,3], Darcy Bonds[4], Baitong Chen[1], Asheesh Singh[2] and Mark A. Licht[2]*

[1]Department of Agricultural and Biosystems Engineering, Iowa State University, Ames, IA, United States, [2]Department of Agronomy, Iowa State University, Ames, IA, United States, [3]Department of Biological Sciences, Minnesota State University, Mankato, MN, United States, [4]Department of Horticulture, Iowa State University, Ames, IA, United States

Biochar application to the soil can improve soil quality and nutrient leaching loss from swine manure adapted soils. Our working hypothesis was that the biochar-incubated with manure could be a better soil amendment than conventional manure application. The manure-biochar application to the soil would decrease nutrient leaching from manure and increase plant-available nutrients. The study objectives were to 1) assess the physicochemical properties of the manure-biochar mixture after lab incubation and 2) evaluate the impact of biochar-treated swine manure on soil total C, N, and other major and minor nutrients in comparison to conventional manure application to soil. Three biochars 1) neutral pH red-oak (RO), 2) highly alkaline autothermal corn (Zea mays) stover (HAP), and 3) mild acidic Fe-treated autothermal corn stover (HAPE) were incubated with swine manure for a month. The biochar-manure mixture was applied in triplicate to soil columns with an application rate determined by the P_2O_5-P content in manure or manure-biochar mixtures after the incubation. The ammonium (NH_4^+), nitrate (NO_3^-), and reactive P concentrations in soil column leachates were recorded for eight leaching events. Soil properties and plant-available nutrients were compared between treatments and control manure and soil. Manure-(HAP&HAPE) biochar treatments significantly increased soil organic matter (OM), and all biochar-manure mixture increased (numerically) soil total C, N, and improved soil bulk density. Concentrations of NH_4^+ and NO_3^- significantly increased in MHAPE column leachates during this 4-week study and the KCl-extractable NH_4^+ and NO_3^- in the soil at the end of the experiment. A significant reduction in soil Mehlich3 Cu was also observed for the manure-HAPE mixture compared with the manure control. The manure-red oak biochar significantly increased the soil Mn availability than other manure-biochar treatments or manure control. Overall, the manure-biochar incubation enabled biochar to stabilize the C and several nutrients from manure. The subsequent manure-biochar mixture application to soil improved soil quality and plant nutrient availability compared to conventional manure application. This proof-of-the-concept study suggests that biochars could be used to solve both environmental and agronomic challenges and further improve the sustainability of animal and crop production agriculture.

OPEN ACCESS

Edited by:
Muhammad Shaaban, Bahauddin Zakariya University, Pakistan

Reviewed by:
Ronghua Li, South China Agricultural University, China
Eduardo Guimarães Couto, Federal University of Mato Grosso, Brazil

****Correspondence:***
Jacek A. Koziel
koziel@iastate.edu

Specialty section:
This article was submitted to Soil Processes, a section of the journal Frontiers in Environmental Science

Received: *23 September 2020*
Accepted: *18 February 2021*
Published: *15 April 2021*

Citation:
Banik C, Koziel JA, De M, Bonds D, Chen B, Singh A and Licht MA (2021) Biochar-Swine Manure Impact on Soil Nutrients and Carbon Under Controlled Leaching Experiment Using a Midwestern Mollisols. Front. Environ. Sci. 9:609621. doi: 10.3389/fenvs.2021.609621

Keywords: C-mineralization, carbon sequestration, nutrient cycling, sustainability, waste management, animal agriculture, N-immobilization, N-mineralization

INTRODUCTION

Swine manure is a source of valuable nutrients (Chastain et al., 1999), but mismanagement or improper application to soils makes it a potential environmental threat. The application rate of animal manure is often exceeded beyond the plant requirement (Juergens-Gschwind, 1989), and this excessive manure application to the soil can result in an unintended N leaching loss to groundwater (Beckwith et al., 1998). High liquid manure application to soil could also contribute to heavy metals like copper and zinc accumulation to soil and plant systems that generate a risk of contaminating the animal food chain to a threat (Mantovi et al., 2003).

Corn (Zea mays) and soybeans (G. max) crop rotation is a common practice in Midwest United States, and the application of swine manure to fields has been a common practice to both dispose of the stored manure and to provide nutrients for crop growth. Soybean can positively respond to swine manure application as reported by previous studies (Killorn, 1998; Sawyer, 2001). Manure solids, undigested feed, and bedding material in the manure help build soil organic matter, improving soil structure and increasing soil water holding capacity and reducing nutrient leaching loss (Magdoff and Es, 2009). However, the use of liquid swine manure to soil may not increase soil C sequestration; instead, it can increase the native soil C decomposition (Angers et al., 2009), and as a result, leaching loss of macronutrients such as N and sedimental loss of P (Reid et al., 2018) can occur. Furthermore, C and N losses can also occur via greenhouse gas emissions from land-applied swine manure (Maurer et al., 2017a).

Biochar, a product of biomass pyrolysis, heating under low or no O_2 conditions, has attracted much interest as a means of potentially solving soil problems (Laird, 2008). Biochar properties can be useful to address challenges in crop and livestock agriculture (Kalus et al., 2019). Freeze dry manure fertilization to the soil in the presence of biochar has shown a significant decrease in nutrient leaching loss, greater retention of plant nutrients, and improvement in soil C and N compared with control manure-treated soil (Laird et al., 2010a; Laird et al., 2010b). The same study also reported that biochar amendments followed by manure application increase the cation and anion exchange capacity of biochar, enable biochar to both adsorb and release nutrients to/from the soil, hence functioning as both a reservoir and slow-release source of plant nutrients. Biochar properties can be useful to address challenges in crop and livestock agriculture, as recently reviewed elsewhere (Kalus et al., 2019).

The application of alkaline biochar to soil can increase soil pH and reduce problems related to low soil pH, which typically occur after prolonged application of ammonium forms of N fertilizer. Studies have shown that biochar improves soil water holding capacity and is able to reduce soil bulk density (BD) (Rogovska et al., 2014). Unfortunately, most biochars have few positively charged surface sites and hence limited anion exchange capacity and ability to electrostatically adsorb nutrient anions such as PO_4^{3-} and NO_3^- (Lawrinenko and Laird, 2015). There are consistent data in the literature supporting the electrostatic retention of positively charged ammonium (NH_4^+) but not of negatively charged PO_4^{3-} and NO_3^- on biochar surfaces (Yao et al., 2012; Fidel et al., 2018). Iron (Fe) modification of biochar surfaces has been shown to be effective in enhancing PO_4^{3-} adsorption (Wilfert et al., 2015).

In addition to biochar being proposed as a soil amendment, recent studies have shown that surficial application of biochar onto the swine manure can reduce emissions of odorous gases (Meiirkhanuly, 2019) and reduce volatilization loss of ammonia (Maurer et al., 2017b) or in other words biochar addition can improve the N content of manure in storage. Clearly, there is an opportunity to explore the tantalizing question if biochar can be used to address both environmental and crop production challenges in one system. We propose a novel concept of biochar utilization that can simultaneously improve the air quality of the animal production system and the sustainability of crop production agriculture. Biochar can be first used to mitigate gaseous emissions (Chen et al., 2020; Meiirkhanuly et al., 2020a) from stored manure and possibly retain more nutrients in the manure. When the swine manure pits are agitated and cleaned out, the mixture of swine manure and biochar will be pumped out and applied to soils. Environmental and agronomic benefits are expected due to decrease nutrient leaching from manure and increase plant-available nutrients. Biochar pH is important in this regard, and surficial treatment of an alkaline/neutral pH biochar to manure storage can change the manure pH near the manure-air interface within few days of application (Meiirkhanuly et al., 2020b). However, there is a gap in the literature on the use of the biochar-manure mixtures as a soil amendment to replace the conventional use of liquid swine manure. Also, the prospect of functionalizing biochar to improve the environmental sustainability of primary nutrients (e.g., P management with Fe-modified biochar surfaces) can be explored.

The study objectives were to 1) assess the physicochemical properties of the manure-biochar mixture after laboratory incubation and 2) evaluate the impact of biochar-treated swine manure on soil total C, N, and other major and minor nutrients in comparison to conventional manure application to soil. Our working hypothesis was that the biochar-treated manure application to the soil would decrease nutrient leaching from manure, increase plant-available nutrients, and improve soil, irrespective of the biochar feedstock type or the different biochar production process. We also hypothesized that differences among biochars influence soil nutrient availability and leaching. Three biochars 1) neutral pH red-oak (RO), 2) highly alkaline autothermal corn stover (HAP), and 3) mild acidic Fe-treated autothermal corn stover (HAPE) were incubated with swine manure for a month. This was followed by a controlled

column leaching experiment for soils treated with biochar-manure mixtures followed. We characterized some physicochemical properties of the biochar-manure mixtures and investigated the impact of biochar-manure treatments on soil nutrient leachate, soil physicochemical properties (pH, bulk density, total C and N), and plant macronutrients N, P, and K availability. This research also addressed the impact of Fe-modified biochar application on manure to sorb nutrients (P) followed by soil application as an amendment.

MATERIALS AND METHODS

Soil, Biochar, Manure, and Manure-Biochar Incubation

Hanlon (Coarse-loamy, mixed, superactive, mesic Cumulic Hapludolls) soil was collected from the iowa State University Applied Science/Moore research farm. Soybean and corn were mainly grown in rotation in these plots, and no swine manure application history in the last 20 years. Samples of soil surface (0–10 cm) were collected and stored in buckets with lids to keep the moisture at the field level. The buckets were stored at 4°C until analysis started two months after collection. The soil used in the study had a pH of 7.6, containing 2.84% of organic matter, 1.88% of total C and 0.17% of total N, and a TC/TN ratio of 11.1.

Fast pyrolysis (500°C) neutral pH (pH ~7.5) red oak biochar (<2 cm) was obtained from a commercial producer (Avello Bioenergy, Iowa), and a fast pyrolysis high pH (pH~ 9.2) corn stover biochar (HAP) and Fe-modified corn-stover (500°C) biochar (HAPE) with a moderately acidic pH were obtained by autothermal pyrolysis. A detail of the pyrolysis techniques of HAP and HAPE biochar production is given elsewhere (Polin et al., 2019; Rollag et al., 2020). The biochar properties, moisture, volatile matters, fixed C, ash content, total C, and total N were determined by following the method described by Rover et al. (2018).

The swine manure was collected from deep pit storage at an iowa Select Farms facility in the fall of 2019. The manure was stored in a bucket with a lid and stored (at 22–23°C) until incubated with biochar within one month of manure collection. About 250 g biochar (<1 mm) was surface applied on 1,000 g of manure and incubated (at 22–23°C) in an 8.5 L glass container (10 cm i. d. and 27 cm height) for one month at atmospheric condition. After the incubation period, the biochar and manure were mixed thoroughly to homogenize and stored in airtight glass at 4°C until analysis started one month later. A control manure sample was also incubated and mixed thoroughly under the same condition for comparison.

The mixture was analyzed for moisture, total C (TC), total N (TN), mineral content, organic matter (OM), nitrate-N, ammonium-N, P_2O_5-P, and K_2O-K, and the data was provided on a % dry weight basis. Moisture and dry matter in the samples were measured by heating the samples for 16 h at 105–110°C. Organic matter was determined by heating the samples in a muffle furnace at 550°C for 2 h. The total C and N were analyzed by combustion using Elementar Vario Max CN Method 4.01 and 3.3, respectively. Sample nitrate and ammonium-N were measured by KCl extraction and determined on the FIA Lab flow injection autoanalyzer.

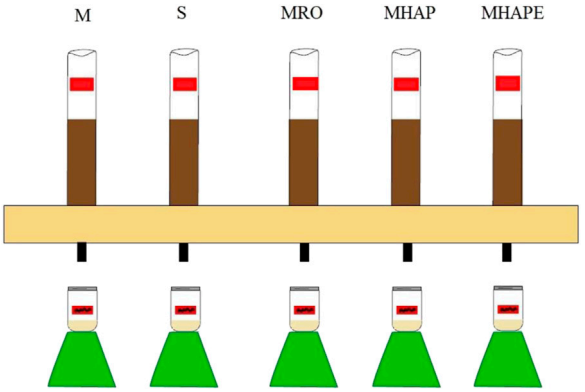

FIGURE 1 | A schematic of the soil column leachate collection apparatus. Each column contains 250 g of soil, treated with one of five treatments. Two of these apparatuses were utilized, resulting in 15 columns; three trials for each of the five treatments. M = manure control; S = soil control; MRO = manure + red oak biochar; MHAP = manure + corn biomass feedstock autothermal alkaline porous biochar; MHAPE = manure + corn biomass feedstock autothermal porous Fe-engineered biochar. **Supplementary Figure S1** for a photograph of the experimental setup.

Soil Column Preparation and Leaching Experiment

The field moist soil was dried, mixed thoroughly to homogenize, sieved (<2 mm), and stored in a bucket with a lid for the column preparation. A total of 15 soil columns (25 cm height and 4.4 cm i. d.) were built from PVC tubes with a PVC male adapter sealed at the bottom using PVC cement. At the base of each column, 4.4 i. d. "air filter pad" was inserted, and then ~2 g of 1 mm glass beads were added on top of that coarse sieve. Each column was filled with 250 g of dried (<2 mm) soil to a length of 15 cm, maintaining an approximate bulk density (BD) of 1.2 g/cm^3. Water was then filled from the bottom of each column to the top of the soil to remove excess air trapped in the soil column and drained the water under gravity (**Figure 1**; **Supplementary Figure S1**) after 24 h. Pore volume was calculated from the weight difference of the before and after saturation of the columns. Based on the pore volume, 50 ml of DI water was added for each leaching event.

De-ionized (DI) water (50 ml) was added from the top of each column, and the leachate was collected from the bottom to collect the baseline soil data two times during one week of column equilibration time. The columns were named depending on the treatments they received, M = manure control (manure added to the soil); S = soil control; MHAP = manure + corn biomass autothermal alkaline porous biochar; MHAPE = manure + corn feedstock autothermal porous Fe-engineered biochar. This study reported the data of a total of 15 columns with five treatments, three replicates for each treatment. The amount of biochar-manure mixture or manure addition was calculated based on the P_2O_5-P content of the mixture to make sure each column gets a recommended rate of P of 135 kg/ha (120 lb/acre) of soil for a

corn-soybean rotational plot (Sawyer and Mallarino, 2016). Treatments were surface applied, and micro tillage was performed with a spatula to mix the treatments with to 3 cm of soil. The same tillage operation was also applied for the control of soil columns. After a week of column equilibration, 50 ml DI water from a beaker was added from the top of each column every three to four days (i.e., every leaching event) over three weeks period.

The leachate was collected overnight in labeled bottles, and the next morning the leachate was transferred to <0°C until analysis. Leachate was collected eight times (eight events) for the total experiment time. Leachates were filtered through a 0.45 µm syringe filter and analyzed for nitrate-N (vanadium III, sulfanilamide and N-(1-naphthyl)-ethylenediamine dihydrochloride), ammonium-N (salicylate and ammonia cyanurate method), and dissolved reactive phosphorus (DRP; malachite green method; D'Angelo et al., 2001) using a Synergy HTX Multi-Mode microplate reader (BioTek Instruments, Inc.) colorimetric method (Doane and Horwáth, 2003; De et al., 2019).

Column Soil Analysis

After the leachate collection was over, the columns were left for a week to drain the excess water from the clogged columns. Once the excess water drained out, the soil from each column was loosened using a long spatula, and soils were collected in Ziploc bags. The soil receiving treatments and control soil was then mixed thoroughly to homogenize, dried, sieved (<2 mm), and analyzed for pH (1:1; soil: water) following the method by McLean (1982) using the glass-electrode meter method. About 2 g soil was weighed, and soil OM was measured by loss on ignition at 360°C by (Schulte and Hopkins, 1996) method; and the total C and N were analyzed by combustion using Elementar Vario Max CN Method 4.01 and 3.3, respectively (Nelson and sommers, 1996). The extractant was prepared by weighing approximately 5 g soil in a 200 ml Nalgene bottle, shaken with KCl at 1:5 ratio for 30 min, and then filtered through Whatman grade 1 filter paper. This extractant was used to measure KCl-extractable soil nitrate-N (vanadium III, sulfanilamide, and N-(1-naphthyl)-ethylenediamine dihydrochloride) and ammonium-N (salicylate and ammonia cyanurate method) (Doane and Horwáth, 2003; De et al., 2019). The Mehlich3 extractable elements (P, K, Ca, Mg, Fe, Mn, Cu, and Zn) were extracted by a modified method of Mehlich (1984) and analyzed by ICP-OES.

Statistical Analysis

The statistical analysis was completed using R. The experiment has three biochar manure mixture, one manure control, and one soil control, with three replicates of each treatment a total of 15 columns. A mixed model was run to analyze the soil column leachate considering time as a factor, then Tukey's pairwise comparison was used to compare treatment effect on total nitrate-N, ammonium-N, and DRP. To report the treatment effects on soil nitrate, ammonium, P, and all Mehlich3 extractable elements, a one-way ANOVA and Tukey's pairwise comparison was performed. A p-value <0.05 was considered statistically significant.

RESULTS

Biochar and Manure Properties Before Mixture Incubation

The swine manure used in this experiment had an alkaline pH of 9.2. Swine manure used in this study contained 37.4% TC and 18.1% of TN, and the TC/TN ratio was 2.1. As recorded, the pH of the autothermal corn stover biochar was mild acidic for HAPE (pH of 5.4) to highly alkaline (9.2) for HAP, and the pH of hardwood RO was 7.5, close to soil pH. The hardwood biochar had 78.5% TC and 0.6% TN by mass and contained 26.4% volatile matters, 15.8% ash, 54.8% fixed C by mass, as indicated by proximate analysis. Whereas the autothermal biochar HAP had 61.4% C and 1.2% TN by mass and contained 16.3% volatile matter, 46.8% ash, 35.0% fixed C by mass, as indicated by proximate analysis. The Fe-pretreated autothermal biochar HAPE had 36.4% TC and 1.2% TN by mass and contained 34.0% volatile matters, 40.0% ash, 24.0% fixed C by mass, as indicated by proximate analysis. The TC/TN ratio ranged between 30 and 130 among the biochars; hardwood RO had the highest carbon content (total and fixed), thus the highest TC/TN ratio. The ash content of RO biochar was the lowest among the three-biochar used in this experiment.

Incubation Effect on Biochar-Manure Physicochemical Parameters

The addition of biochar to the manure changes the physical appearance of manure (**Supplementary Figure S2**). After the one-month incubation, the control manure was liquid slurry with yellow patches on the surface, possibly representing a microbial colony developed during incubation and a persistent manure odor. On the contrary, no such color or odor was observed for any of the biochar samples. During incubation, biochar absorbed the manure moisture, and after mixing to homogenize, its texture resembled loose soil. The moisture content of biochar increased several folds by soaking the manure moisture (**Table 1**). As a result of incubation, the pH increased for all biochar-manure mixtures. An increase in total org-N for the biochar-manure mixture was observed for all biochar mixtures; however, the TC/TN ratio dropped for all biochar-manure mixtures compared with the biochar. The inorganic nutrients N, P, and K contents of all mixtures increased than biochar during incubation with manure (**Table 1**).

The amount of treatment addition was based on the recommended rate of P (135 kg/ha or 120 lb/acre) to soil resulted in an addition of a different amount of all macro and micronutrients to each treatment (**Table 2**). Treatments end up with approximately 3.1 g of manure, 1.8 g of MRO, 4.9 of MHAP, and 3.25 g of MHAPE. The highest (by weight) amount of MHAP amendment added to each column resulted in significantly more N, K, Ca, and Mg addition than any other treatments. The biochar to manure ratio was the same for incubation; additionally, the total N of both HAP and HAPE was 1.2%, but the total N added by the MHAPE treatment was significantly lower than MHAP (**Table 2**). The control manure treatments added significantly more Cu (except for MHAPE) and Zn to soil

TABLE 1 | Physicochemical properties of the different biochar-manure mixtures after incubation. Except for pH, all values were reported on a % dry weight basis.

Properties	Manure (control)	MHAP	MRO	MHAPE
pH	9.2	9.7 ± 0.09	9.9 ± 0.01	7.5 ± 0.01
Moisture (%)	90.8	58.1 ± 0.6	23.6 ± 3.0	49.9 ± 0.9
Mineral matter (%)	43.5	28.7 ± 0.2	45.2 ± 2.8	46.5 ± 0.4
LOI (%)	56.5	71.3 ± 0.2	54.8 ± 2.8	53.5 ± 0.4
Org-N (%)	4.4 ± 0.4	1.9 ± 0.04	1.0 ± 0.02	1.7 ± 0.01
NH_4-N (%)	0.69	0.04 ± 0.01	0.02 ± 0.01	1.0 ± 0.03
NO_3-N (%)	N.D.	N.D.	N.D.	N.D.
P_2O_5-P (%)	5.4 ± 0.06	0.7 ± 0.1	0.8 ± 0.2	0.8 ± 0.02
K_2O-K (%)	16.8 ± 2.6	4.6 ± 0.1	3.8 ± 0.3	5.1 ± 0.1
TC (%)	38.2	51.3 ± 4.5	50.2 ± 3.2	36.3 ± 1.2
TN (%)	5.4 ± 0.1	2.0 ± 0.1	1.0 ± 0.1	2.7 ± 0.04
TC/TN	7.1	26.3 ± 2.6	51.8 ± 4.4	13.3 ± 0.6

N.D. = not detected; ± standard deviation calculated for n = 3; MRO = manure + red oak biochar; MHAP = manure + corn biomass feedstock autothermal alkaline porous biochar; MHAPE = manure + corn biomass feedstock autothermal porous Fe-engineered biochar. LOI = Loss on ignition; TC = total C; TN = total N. Some manure analysis could not be replicated due to insufficient sample amount.

TABLE 2 | Mass of elements added to the columns (mg) by the manure and manure-biochar treatment application. Different letters signify statistical differences between treatments at $p < 0.05$ (column-wise).

Treatment	Total-N	K	Ca	Mg	Fe	Cu	Mn	Zn
M	15.63 ± 0.31b	52.85 ± 0.48d	6.15 ± 0.05d	3.92 ± 0.03d	0.53 ± 0.01c	0.46 ± 0.01a	0.12 ± 0.002c	0.56 ± 0.01a
MRO	10.88 ± 0.45d	66.00 ± 2.78c	8.48 ± 0.36c	4.24 ± 0.18c	0.55 ± 0.02c	0.21 ± 0.01c	0.11 ± 0.004c	0.33 ± 0.0005d
MHAP	18.55 ± 0.03a	93.36 ± 0.15a	32.97 ± 0.05a	13.80 ± 0.02a	4.25 ± 0.01 b	0.33 ± 0.002b	0.29 ± 0.005b	0.47 ± 0.0008b
MHAPE	12.96 ± 0.08c	78.63 ± 0.49b	23.96 ± 0.15b	10.84 ± 0.06b	114.37 ± 0.72a	0.45 ± 0.01a	0.87 ± 0.005a	0.32 ± 0.002c

M = manure, MRO = manure + red oak biochar; MHAP = manure + corn biomass feedstock autothermal alkaline porous biochar; MHAPE = manure + corn biomass feedstock autothermal porous Fe-engineered biochar.

than any manure-biochar treatment, and among all treatments, MRO treatment added the lowest amount of those two elements.

Nutrients in Leached Water

Dissolved inorganic N and P leached out from all columns irrespective of treatments were low during this four-week study. However, the MHAPE treated columns released significantly high total NO_3-N ($p = 0.003$) and NH_4-N ($p = 0.003$) than manure control columns. An upward trend with time was observed for the cumulative NO_3-N and NH_4-N concentration in MHAPE treated column leachate during the last six leaching events (**Figure 2**, **Supplementary Table S1**), whereas control manure-treated columns NO_3-N started to increase in leachate on 7th and 8th leaching events. At the beginning of the column experiment, the MHAPE had about 1% of ammonium (**Table 1**); higher concentrations in comparison to other treatments.

An upward trend with time for the cumulative dissolved P in leachate for all treated columns was observed during the eight events of the leaching study; soil control columns released significantly ($p < 0.05$) higher amount of total DRP. However, no impact of manure or manure-biochar mixture applications to DRP in soil leachates were observed during the course of this study (**Figure 3**, **Supplementary Table S1**).

Treatment Effect on Column Soil Properties

The columns were freely drained for the first four leachings, but the rate of water leaching for the last two events slowed; specifically, in the manure-treated columns. After eight events of leachate collection, the experiment was stopped due to longer leaching time and ponding on column surfaces. Columns with soil and biochar-manure treatments were relatively better drained in comparison to manure columns. Before the treatment application, the starting BD of each column was 1.2. After the treatment application and leaching experiment, the final soil BD ranged from 1.17 to 1.6 g/cm^3, and for manure treated columns ended with higher BD in comparison to biochar-manure mixture receiving columns (**Table 3**). The application of manure and manure-biochar mixtures to the soil columns resulted in an increasing trend in the soil OM content, soil TC, and soil TN relative to control soil columns (**Table 3**).

The TC/TN ratios were between 10.6 and 12.6. Manure-HAP and MHAPE biochar treated columns had significantly ($p < 0.05$) higher OM than manure or soil control columns. There was no significant change in TC and TN observed among manure or manure-biochar treatments. A slight change was observed in soil pH; manure-RO was significantly ($p = 0.04$) higher than manure and among all columns. The pH was mostly got buffered for the manure and manure-biochar treated columns and ranged between 7.3 and 7.6, i.e., close to soil pH. Before application to soil, the pH of all manure and manure-biochar mixtures, except HAPE, were highly alkaline (**Table 1**).

Before application to soil columns, manure had a %TN value of 5.4, the highest among any manure-biochar samples (**Table 1**). Manure-HAPE had 2.7% (1.7% Org-N +1% NH_4-N) of TN before addition to soil columns; the highest %TN among the

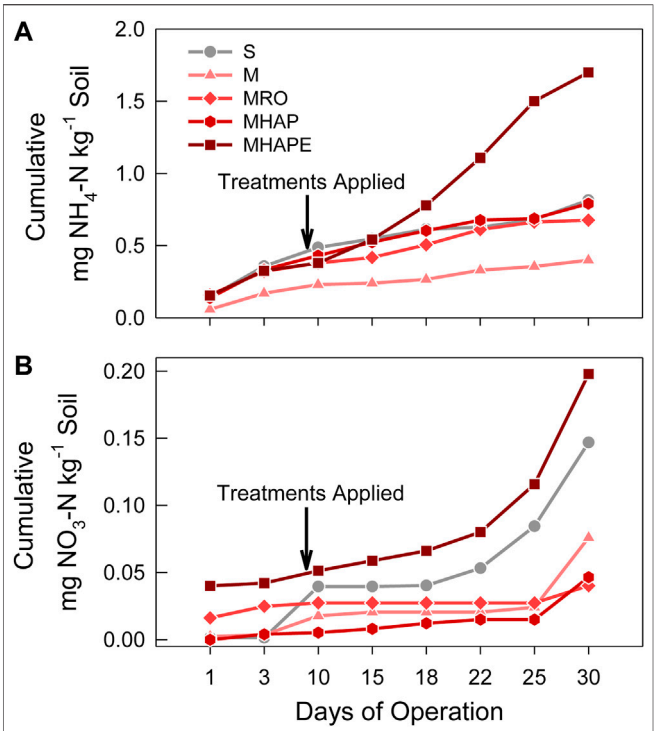

FIGURE 2 | The effect of treatment on leachate cumulative concentrations of soil **(A)** ammonium and **(B)** nitrate. The mean was calculated for a sample of 3 replications. S = soil control; M = manure control; MRO = manure + red oak biochar; MHAP = manure + corn biomass feedstock autothermal alkaline porous biochar; MHAPE = manure + corn biomass feedstock autothermal porous Fe-engineered biochar.

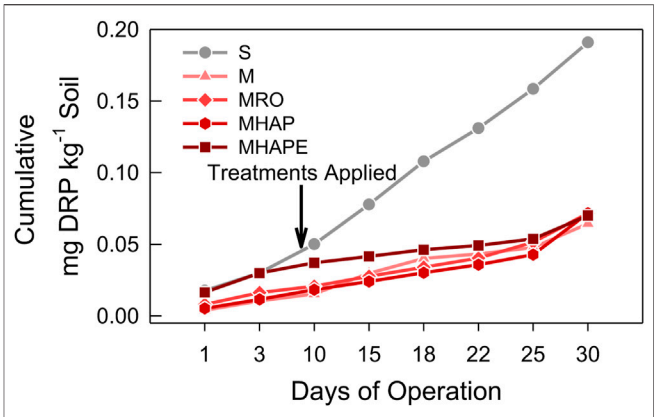

FIGURE 3 | The effect of treatment on cumulative leachate concentrations of soil DRP. The mean was calculated for a sample of 3 replications. S = soil control; M = manure control; MRO = manure + red oak biochar; MHAP = manure + corn biomass feedstock autothermal alkaline porous biochar; MHAPE = manure + corn biomass feedstock autothermal porous Fe-engineered biochar.

manure-biochar mixtures used in this study slightly increased the soil TN. In addition, MHAPE biochar treatment significantly increased soil NO_3-N (p = 0.009) and NH_4-N (p = 0.001) concentration than manure control after the leaching experiment (**Figure 4**). The soil columns not receiving any manure or biochar-manure mixture were not significantly different in NO_3^- and NH_4^+ than the control M, or MRO and MHAP treatments.

Manure addition to soil columns had the highest soil Mehlich3 extractable P (**Figure 5**) and significantly higher ($p < 0.001$) in comparison to other treatments. Among the manure-biochar mixture treated soils, manure-RO ($p < 0.05$) and manure-HAP ($p < 0.05$) significantly increase Mehlich3 soil P and K than control soil. The manure-HAPE treatment did show a small numerical increase in Mehlich3 P (not significant; $p > 0.05$). However, Mehlich3 soil K concentration was highest and significantly higher ($p < 0.001$) than other manure biochar treatments (**Figure 6**) though the manure had a higher concentration of K_2O-K compared with the manure-biochar mixtures.

Biochar-manure mixture addition to soil columns did not impact the soil Mehlich3 extractable Ca and Fe concentrations (**Table 4**). However, MHAPE treatment had a significantly lower concentration of Mehlich3 extractable Mg (p = 0.03) and Cu (p = 0.005) than manure control. All manure-biochar treatments had a significantly ($p < 0.05$) low Mehlich3 extractable Zn compared to the control manure samples, and only MRO treatment had significantly high Mn (p = 0.02) compared to the control manure but not to the control soil column.

DISCUSSION

The high decomposition rate of soil OM can result in low C-sequestration and high loss of C to the atmosphere. Manure with a TC/TN ratio of ~7 after incubation and even lower before incubation (~2) (**Table 1**) supports the notion of N mineralization and volatilization loss to the atmosphere, more likely N loss as NH_3 than C loss as CH_4 or CO_2. Substrate quality is an important deciding factor of its decomposition rate; a low TC/TN ratio means high quality and a readily available substrate to decomposing microbial group (Condron et al., 2010). Incubation of biochar (with a very high C/N ratio) with manure may have resulted in an N immobilization and improved the manure-biochar mixture total C/N ratio.

The treatment MRO had a C to N ratio of 51.8 after incubation, which ended up to 10.6 to the soil after the leaching experiment. Similarly, other manure-biochar mixtures resulted in a total C to N ratio near the soil total C to N ratio (~12) upon application to the soil as an amendment. Also, an increase in OM, total C, and N speculates that the mixture has the capacity to improve C sequestration compared to manure only treatment. The addition of hardwood biochar showed a reduction in the mineralization loss of dairy manure C when biochar and manure were added to the field simultaneously, reported by a study by Lentz and Ippolito (2012). Manure-biochar mixture can alter soil physicochemical properties in a way that improves nutrient leaching loss from manure. This is because biochar application significantly increases the soil-specific surface area, is also capable of holding the plant available moisture considerably, and

TABLE 3 | Column soil physicochemical properties after leaching events were completed, including the pH, bulk density, percentage of organic matter (OM), percentage of total C (TC), percentage of the total N (TN), and the total carbon to nitrogen (C/N) ratio. (Mean +/– standard deviation for n = 3 replicates; values in parentheses represent *p*-values; **Bold** signifies statistical significance for the difference from manure treatment (M) as control).

Soil Treatment	pH	BD g/cm^3	OM (%)	TC (%)	TN (%)	C/N ratio
M	7.43 ± 0.05	1.63 ± 0.5	3.11 ± 0.07	2.18 ± 0.35	0.18 ± 0.01	11.06 ± 1.07
S	7.53 ± 0.05	1.31 ± 0.1	3.08 ± 0.14	1.90 ± 0.11	0.18 ± 0.01	11.84 ± 0.12
MRO	**7.60 ± 0.08 (*p* = 0.045)**	1.26 ± 0.07	3.25 ± 0.01	2.29 ± 0.15	0.19 ± 0.01	10.57 ± 0.44
MHAP	7.57 ± 0.09	1.18 ± 0.01	**3.41 ± 0.02 (*p* = 0.001)**	2.40 ± 0.19	0.19 ± 0.01	11.87 ± 0.53
MHAPE	7.30 ± 0.08	1.17 ± 0.05	**3.37 ± 0.01 (*p* = 0.004)**	2.41 ± 0.11	0.21 ± 0.01	12.63 ± 0.63

S = soil, M = manure, MRO = manure + red oak biochar; MHAP = manure + corn biomass feedstock autothermal alkaline porous biochar; MHAPE = manure + corn biomass feedstock autothermal porous Fe-engineered biochar.

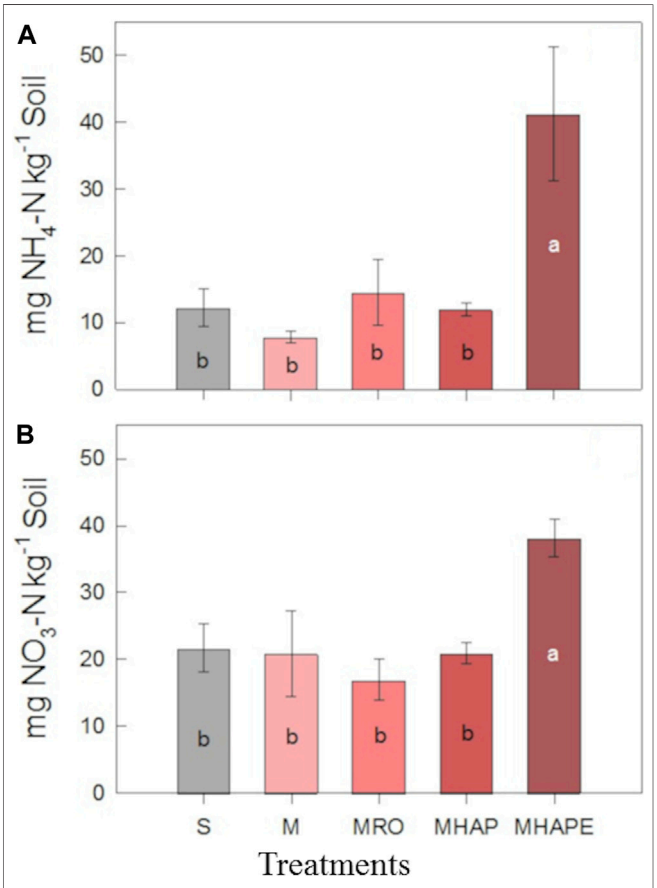

FIGURE 4 | The effect of treatment on concentration of soil **(A)** ammonium and **(B)** nitrate. Soils from each column were homogenized and analyzed after the leaching experiment. Each bar represents an average of the concentrations of three replicates for that group. Error bars show the standard deviation (n = 3). S = soil control; M = manure control; MRO = manure + red oak biochar; MHAP = manure + corn biomass feedstock autothermal alkaline porous biochar; MHAPE = manure + corn biomass feedstock autothermal porous Fe-engineered biochar. Letters mark a significant difference between treatments at $p < 0.05$.

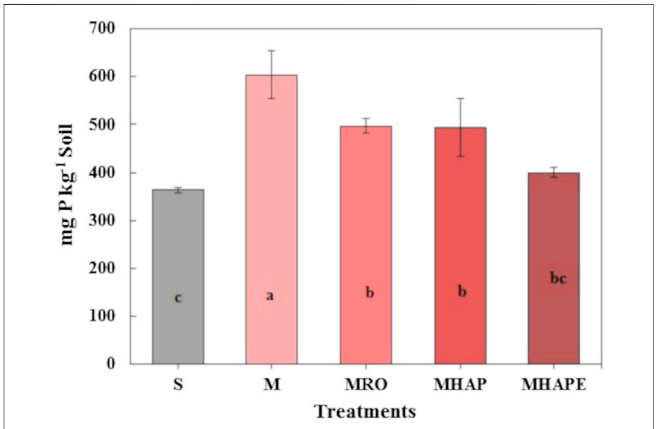

FIGURE 5 | Comparison between treatments of the Mehlich3 extractable soil phosphorus. Soils from each column were homogenized and analyzed after the leaching experiment. Each bar represents an average of the concentrations of three replicates for that group. Error bars show the standard deviation (n = 3). S = soil control; M = manure control; MRO = manure + red oak biochar MHAP = manure + corn biomass feedstock autothermal alkaline porous biochar; MHAPE = manure + corn biomass feedstock autothermal porous Fe-engineered biochar. Letters mark a significant difference between treatments at $p < 0.05$.

improved other plant nutrients availability effectively than soil (Laird et al. 2010b). Our data support the finding of Laird et al. 2010a resulting in a low BD and relatively high OM content in soil with biochar treatments to the manure-biochar soil system.

The soil used in this study was collected right after soybean harvest, and the crop impact may have reflected in soil NO_3^- and NH_4^+ concentrations; only MHAPE treated column had significantly high $NO_3^-$and NH_4^+. Although the total N addition by manure-biochar mixture amendment was lower for MHAPE columns than manure treated column (**Table 2**), the MHAPE treatment resulted in an increase in soil KCl extractable inorganic-N (NO_3^- + NH_4^+) than control manure treatment. This observation suggests that MHAPE treatment may have increased soil microbial activity. The N-mineralization increase with biochar addition is consistent with previous studies that interpret biochar addition is linked with increases in soil microbial respiration (Laird et al., 2010a; Rogovska et al., 2011), which increases soil N mineralization. Application of Fe-modified manure-biochar (MHAPE) treatment to soil resulted in significantly higher NH_4^+ than any other manure-biochar mixture. This observation suggests that the biochar surface modification allows a relatively high H^+ activity than other

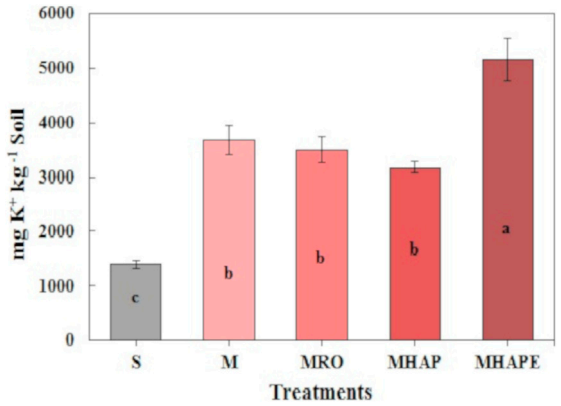

FIGURE 6 | Comparison between treatments of the Mehlich3 extractable soil potassium. Soils from each column were homogenized and analyzed after the leaching experiment. Each bar represents an average of the concentrations of three replicates for that group. Error bars show the standard deviation (n = 3). S = soil control; M = manure control; MRO = manure and red oak biochar; MHAP = manure + corn biomass feedstock autothermal alkaline porous biochar; MHAPE = manure + corn biomass feedstock autothermal porous Fe-engineered biochar. Letters mark a significant difference between treatments at $p < 0.05$.

biochar treatments, capable of stabilizing the NH_4^+, and reducing N volatilization loss. Compared to other manure-biochar or control treatments, the MHAPE column also released significantly more nitrate and ammonium ($p < 0.05$) to the leachate. In plant-soil systems, these inorganic N forms are favorably taken up by plants directly (Tisdale et al., 1985). However, high mobility of nitrate, the N loss in this anion form from the soil in leachate, is well known (Syswerda et al., 2012) and ends up in groundwater contamination. The leaching experiment recorded a 0.4% nitrate-N of the total KCl-extractable soil nitrate that ended in the MHAPE water leachate. In comparison, about 3.5% of the KCl-extractable soil nitrate ended up in manure columns water leachate. This observation suggests that Fe modification to biochar not only increased the N-mineralization but simultaneously it positively impacted nitrate or ammonium sorption onto the biochar surface with less leaching loss than manure control.

All the manure and manure-biochar treated columns received 135 kg/ha (120 lb/acre) P_2O_5-P at the beginning, and only the soil-treated column released significantly high DRP in leachate during the leaching experiment. Sorption of phosphate-P on biochar varies with biochar feedstock and process temperature (Yao et al., 2012), in pure systems and in the absence of competitive ions. The adsorbate's sorption performance depends on the clean adsorbent's surface contact time, and in addition to that, Phosphate-P sorption diminishes with an increase in competitive ions and humic acids in the solution (Chen et al., 2002). Swine manure is a source of competitive ions and humic acids; thus, the phosphate from swine manure sorption on biochar surface is a complex phenomenon. The dissolved reactive P (DRP) concentration was low (<0.05 mg/kg) for manure and manure-biochar treated column, and biochar-manure columns were not significantly different from manure column. This observation contrasts with the study by Laird et al., 2010a showed a significantly more P (mg/column) in manure-treated soil column leachate than biochar + manure treated soil columns with manure addition. Besides, Laird et al., 2010a added 102 mg total P per kg of soil to the swine manure treated columns, which differs from our application rate of 60 mg/kg of soil. At the end of the leaching experiment, the manure treated columns had a significantly ($p < 0.05$) higher amount of Mehlich3-P than manure-biochar treated columns. This observation is different from findings reported by Lentz and Ippolito 2012; this two-year field study reported no difference in soil available P between plots receiving treatments of dairy manure and manure and biochar added simultaneously. In the current study, the difference between manure Mehlich-P and manure-biochar suggests that the applied P in manure-biochar could be associated with the mineral phases of biochar or associated with biochar-OM, not evaluated or reported in this study. The lowest P content of Mehlich3-P in Fe-modified biochar among all manure-biochar treatments suggests a P sorption on oxy-hydroxide phases of Fe-biochar (Bakshi et al., 2019, Bakshi et al., 2021) was not extracted with Mehlich3.

In addition to other major and minor plant nutrients, swine manure is a good source of K (Chastain et al., 1999). A significantly high K ($p < 0.05$) concentration was found in our manure and manure-biochar treated columns compared with control soil columns. All manure-biochar treated columns received significantly more K than manure control through the treatments (**Table 1**). However, soil K in manure-biochar columns, MHAP and MRO, did not statistically differ from the manure-treated soil column. Treatment MHAPE mixture had a significantly ($p < 0.05$) high amount of soil K in comparison to all treatments.

TABLE 4 | Column soil physicochemical properties after leaching events were completed, including the elements, Ca, Mg, Fe, Cu, Mn, and Zn in mg/kg. (Mean ± standard deviation for n = 3 replicates; values in parentheses represent *p*-values; **Bold** signifies significantly different from manure treatment (M) as control).

Treatment	Ca (g/kg)	Mg (g/kg)	Fe (g/kg)	Cu (mg/kg)	Mn (mg/kg)	Zn (mg/kg)
M	19.75 ± 0.14	5.77 ± 0.10	4.77 ± 0.09	3.1 ± 0.2	60.3 ± 5.7	6.3 ± 0.4
S	20.26 ± 1.19	5.84 ± 0.45	4.01 ± 1.2	2.7 ± 0.3	**97.6 ± 12.6 (p = 0.007)**	**4.1 ± 0.7 (p = 0.003)**
MRO	19.68 ± 0.46	5.58 ± 0.19	4.07 ± 0.72	2.5 ± 0.7	**88.6 ± 18.6 (p = 0.02)**	**4.8 ± 0.6 (p = 0.047)**
MHAP	18.82 ± 0.27	5.38 ± 0.10	4.22 ± 0.17	3.1 ± 0.2	79.0 ± 3.7	**4.8 ± 0.6 (p = 0.01)**
MHAPE	18.92 ± 1.07	**5.13 ± 0.22 (p = 0.03)**	4.78 ± 0.02	**1.3 ± 0.1 (p = 0.0005)**	60.0 ± 7.8	**4.5 ± 0.3 (p = 0.003)**

S = soil; M = manure; MRO = manure + red oak biochar; MHAP = manure + corn biomass feedstock autothermal alkaline porous biochar; MHAPE = manure + corn biomass feedstock autothermal porous Fe-engineered biochar.

This result suggests that Fe-modified biochar was capable of stabilizing K better than other biochars used in this study.

The addition of MRO to soil increased the soil Mn availability significantly than manure or other biochar manure treatments. This effect may or may not be related to the significant increase in pH of this manure-wood biochar mixture to soil than other treatments. Lentz and Ippolito, 2012 also reported an increase in the soil Mn availability by adding wood biochar and manure to the soil.

Biochar applications in crop agriculture are often limited by the heavy metal content associated with some types of feedstock and sources (Pulka et al., 2020). Biochar can also be sorbing heavy metals and making them less available to soil exchange sites for the plant to uptake (Zhang et al., 2013). In addition to other nutrients, manure contains several heavy metals. The higher application of manure application to support the recommended macro plant nutrients could also deliver a significantly high concentration of the Cu and Zn like heavy metals, as observed in the study. Copper or Zn toxicity is not an issue in the Midwest United States, but a high concentration of Cu or Zn could be detrimental for soil microbial communities and plants. Bakshi et al. (2014) reported that biochar could immobilize soil Cu and make it less available for the plants to uptake. The MHAPE treatment had a significantly low soil Mehlich3 Cu compared to manure treated column soil, and simultaneously it provided the recommended amount of plant nutrients.

This relatively short control leaching experiment may not be representative of the manure-biochar impact on the soil at the field scale. A more extended soil experiment is essential to carry out to verify the long-term impact of the liquid swine manure-biochar mixture on soil nutrient availability to plants. Also, the slow leachate flow rate of the manure treated control columns made the comparisons challenging for this leaching experiment. Properties of the manure-biochar mixture can vary depending on the manure type, biochar feedstock, biochar production technique, and manure-biochar incubation time, which were not evaluated in this experiment. Microbial biomass was not determined in the study could be one of the limitations of this work; moreover, swine manure from only one representative source and only one soil type was used.

We recommend undertaking socioeconomic analyses for the farm-scale use of biochar treatment to improve the sustainability of the animal and crop production systems. The cost analysis deserves a much broader scope and effort involving analyses for the whole animal and crop production system with consideration of local/regional scales regarding the legal, regulatory, policy, market, labor, soil-water-air quality issues. The cost of biochar treatment will likely decrease if the swine industry adopts biochar as a means to mitigate gaseous emissions from stored manure (e.g., Chen et al., 2020).

CONCLUSION

The results of this short soil leaching experiment suggest that biochar-manure mixture application to agricultural soils significantly improved soil OM compared to the conventional liquid swine manure treatments to the soil, possibly biochar C have stabilized the manure C. In addition, biochar-manure mixture application improved (numerically, without statistical significance) TC, TN, and BD compared to the conventional liquid swine manure treatments to the soil. Biochar-manure mixtures impacted the availability of macro and micronutrients in soil (depending on the biochar type) differently than conventional manure application, as observed by this column leaching experiment. Additionally, the MHAPE treatment to soil significantly increased Mehlich3 K, KCl-extractable NO_3-N, and soil OM content compared with the control soil or manure treated soil. Although the total NO_3-N and NH_4-N concentrations in leachates of MHAPE columns were significantly higher among all treatments, these values were significantly lower (2 vs. 80 mg/kg) than soil NO_3-N and NH_4-N concentrations found at the end of the experiment. A long-term field experiment is warranted to examine the biochar-manure mixture's long-term environmental implication on plant-soil biota.

DATA AVAILABILITY STATEMENT

The original contributions presented in the study are included in the article/**Supplementary Material**, further inquiries can be directed to the corresponding author/s.

AUTHOR CONTRIBUTIONS

Conceptualization, CB, JK; methodology, CB, MD, ML, and AS; software, CB, DB; validation, CB, JK; formal analysis, CB, DB, and MD; investigation, CB and DB; resources, CB, JK, MD, and BC; data curation, CB and JK; writing—original draft preparation, CB and DB; writing—review and editing, CB, DB, JK, AS, and ML; visualization, CB, DB and MD; supervision, CB and JK; project administration, CB and JK; funding acquisition, JK, CB, AS, and ML All authors have read and agreed to the published version of the manuscript.

FUNDING

The authors are thankful to the Leopold Center for Sustainable Agriculture for 'Improving sustainability of iowa agriculture: synergy between improved nutrient recycling, solving livestock odor problems, and crop production' grant #LCSA-AES-Koziel-2020–2. Partial funding came from iowa State University's Freshmen Honors Program (Darcy Bonds) and the iowa Agriculture and Home Economics Experiment Station: project number IOW05556 (Future Challenges in Animal Production Systems: Seeking Solutions through Focused Facilitation, sponsored by Hatch Act and State of iowa funds; JK).

ACKNOWLEDGMENTS

We are thankful to David Laird (Department of Agronomy, ISU) for initial consultations about the experiment and Qinglong Tian (Department of Statistics, ISU) for his help with the statistical model. The authors also thank Wyatt Murphy from the Department of Agricultural and Biosystems Engineering, iowa State University (ABE, ISU) for building the column leachate setup; Peiyang Li and Samuel C. O'Brien (ABE, ISU) for their help with soil sampling, and Zhanibek Meiirkhanuly (ABE, ISU) for the outsourcing of biochar.

SUPPLEMENTARY MATERIAL

The Supplementary Material for this article can be found online at: https://www.frontiersin.org/articles/10.3389/fenvs.2021.609621/full#supplementary-material.

REFERENCES

Angers, D. A., Chantigny, M. H., MacDonald, J. D., Rochette, P., and Côté, D. (2009). Differential retention of carbon, nitrogen and phosphorus in grassland soil profiles with long-term manure application. *Nutr. Cycl. Agroecosys.* 86, 225–229. doi:10.1007/s10705-009-9286-3

Bakshi, S., He, Z. L., and Harris, W. G. (2014). Biochar amendment affects leaching potential of copper and nutrient release behavior in contaminated sandy soils. *J. Environ. Qual.* 43, 1894–1902. doi:10.2134/jeq2014.05.0213

Bakshi, S., Laird, D. A., Smith, R. G., and Brown, R. C. (2021). Capture and release of orthophosphate by Fe-modified biochars: mechanisms and environmental applications. *ACS Sustain. Chem. Eng.* 9 (2), 658. doi:10.1021/acssuschemeng.0c06108

Bakshi, S., Laird, D. A., Smith, R. G., and Brown, R. C. (2019). Phosphate sorption onto modified biochar surface," in The Proceedings of the Biochar and Bioenergy 2019 Conference, Fort Collins, CO, June 30–July 3, 2019.

Beckwith, C. P., Cooper, J., Smith, K. A., and Shepherd, M. A. (1998). Nitrate leaching loss following application of organic manures to sandy soils in arable cropping. i. effects of application time, manure type, overwinter crop cover and nitrification inhibition. *Soil Use Manag.* 14, 123–130. doi:10.1111/j.1475-2743.1998.tb00135.x

Chastain, J. P., Camberato, J. J., Albrecht, J. E., and Adam, J. (1999). *Swine manure production and nutrient content South Carolina confined animal manure managers certification Program*. Clemson, SC: Clemson University, 1–17.

Chen, B., Koziel, J. A., Białowiec, A., Lee, M., Ma, H., Li, P., et al. (2020). The impact of surficial biochar treatment on acute H2S emissions during swine manure agitation before pump-out: proof-of-the-concept. *Catalysts* 10, 940. doi:10.3390/catal10080940

Chen, J. P., Chua, M. L., and Zhang, B. (2002). Effects of competitive ions, humic acid, and pH on removal of ammonium and phosphorous from the synthetic industrial effluent by ion exchange resins. *Waste Manag.* 22 (7), 711–719. doi:10.1016/S0956-053X(02)00051-X

Condron, L., Stark, C., O'Callaghan, M., Clinton, P., and Huang, Z. (2010). "The role of microbial communities in the formation and decomposition of soil organic matter," in *Soil microbiology and sustainable crop production*. Editors G. Dixon and E. Tilston (Dordrecht, Netherlands: Springer).

De, M., Riopel, J. A., Cihacek, L. J., Lawrinenko, M., Baldwin-Kordick, R., Hall, S. J., et al. (2019). Soil health recovery after grassland reestablishment on cropland: the effects of time and topographic position. *Soil Sci. Soc. Am. J.* 84 (2), 568–586. doi:10.1002/saj2.20007

Doane, T. A., and Horwáth, W. R. (2003). Spectrophotometric determination of nitrate with a single reagent. *Anal. Lett.* 36, 2713–2722. doi:10.1081/al-120024647

D'Angelo, E., Crutchfield, J., and Vandiviere, M. (2001). Rapid, sensitive, microscale determination of phosphate in water and soil. *J. Environ. Qual.* 30, 2206–2209. doi:10.2134/jeq2001.2206

Fidel, R. B., Laird, D. A., and Spokas, K. A. (2018). Sorption of ammonium and nitrate to biochars is electrostatic and pH-dependent. *Sci. Rep.* 8, 17627. doi:10.1038/s41598-018-35534-w

Juergens-Gschwind, S. (1989). "Ground water nitrates in other developed countries (Europe)- relationships to land use patterns," in *Nitrogen management and ground water protection*. Editor R. F. Follett (Amsterdam, Netherlands: Elsevier), 75–138.

Kalus, K., Koziel, J., and Opaliński, S. (2019). A review of biochar properties and their utilization in crop agriculture and livestock production. *Appl. Sci.* 9, 3494. doi:10.3390/app9173494

Killorn, R. (1998). Effect of Frequency of swine manure application on the yield of corn and soybean. Swine Research Report 1998 37. Available at: https://www.extension.iastate.edu/Pages/ansci/swinereports/asl-1593.pdfhttps://www.extension.iastate.edu/Pages/ansci/swinereports/asl-1593.pdf (Accessed September 1, 2020).

Laird, D. A, Fleming, P., Wang, B., Horton, R., and Karlen, D. (2010a). Biochar impact on nutrient leaching from a midwestern agricultural soil. *Geoderma* 158, 436–442. doi:10.1016/j.geoderma.2010.05.012

Laird, D. A., Fleming, P., Davis, D. D., Horton, R., Wang, B., and Karlen, D. L. (2010b). Impact of biochar amendments on the quality of a typical Midwestern agricultural soil. *Geoderma* 158, 443–449. doi:10.1016/j.geoderma.2010.05.013

Laird, D. A. (2008). The charcoal vision: a win-win-win scenario for simultaneously producing Bioenergy, permanently sequestering carbon, while improving soil and water quality. *Agron. J.* 100, 178–181. doi:10.2134/agronj2007.0161

Lawrinenko, M., and Laird, D. A. (2015). Anion exchange capacity of biochar. *Green Chem.* 17, 4628–4636. doi:10.1039/c5gc00828j

Lentz, R. D., and Ippolito, J. A. (2012). Biochar and manure affect calcareous soil and corn silage nutrient concentrations and uptake. *J. Environ. Qual.* 41, 1033–1043. doi:10.2134/jeq2011.0126

Magdoff, F., and Es, H. V. (2009). "Animal manures for increasing organic matter and supplying nutrients," in *Building soils for better crops sustainable soil management*. 3rd Edn (Brentwood, MD: USDA SARE), 129–140.

Mantovi, P., Bonazzi, G., Maestri, E., and Marmiroli, N. (2003). Accumulation of copper and zinc from liquid manure in agricultural soils and crop plants. *Plant Soil* 250, 249–257. doi:10.1023/a:1022848131043

Maurer, D., Koziel, J. A., and Bruning, K. (2017a). Field scale measurement of greenhouse gas emissions from land applied swine manure. *Front. Environ. Sci. Eng.* 11 (3), 1. doi:10.1007/s11783-017-0915-9

Maurer, D. L., Koziel, J. A., Kalus, K., Andersen, D., and Opalinski, S. (2017b). Pilot-scale testing of non-activated biochar for swine manure treatment and mitigation of ammonia, hydrogen sulfide, odorous volatile organic compounds (VOCs), and greenhouse gas emissions. *Sustainability* 9 (6), 929. doi:10.3390/su9060929

McLean, E. O. (1982). "Soil pH and lime requirement," in *Methods of soil analysis, part 2*. 2nd Edn. Editor A. L. Page (Madison, WI: Agronomy Monographs), 9, 199–223.

Mehlich, A. (1984). Mehlich 3 soil test extractant: a modification of Mehlich 2 extractant. *Commun. Soil Sci. Plant Anal.* 15, 14091416. doi:10.1080/00103628409367568

Meiirkhanuly, Z., et al. (2019). Evaluation of biochar for mitigation of ammonia, hydrogen sulfide, odorous volatile organic compounds, and greenhouse gases emissions from swine manure. Publisher ProQuest Dissertation publishing. ISBN: 9781088368053.

Meiirkhanuly, Z., Koziel, J. A., Chen, B., Białowiec, A., Lee, M., and Wi, J., et al. (2020a). Mitigation of gaseous emissions from swine manure with the surficial application of biochars. *Atmosphere* 11, 1179. doi:10.3390/atmos11111179

Meiirkhanuly, Z., Koziel, J. A., Bialowiec, A., Banik, C., and Brown, R. C. (2020b). The proof of concept of biochar floating cover influence on swine manure pH, Implications of gaseous emission from area sources. *Front. Chem.* 8, 656. doi:10.3389/fchem.2020.00656

Nelson, D. W., and Sommers, L. E. (1996). "Total carbon, organic carbon, and organic matter," in *Methods of soil analysis: Part 3 Chemical methods*. 3rd Edn, Editors D. L. Sparks, A. L. Page, P. A. Helmke, R. H. Loeppert, P. N. Soltanpour, M. A. Tabatabai, et al. (Madison, WI: SSSA Special Publications), 961–1010.

Polin, J. P., Carr, H. D., Whitmer, L. E., Smith, R. G., and Brown, R. C. (2019). Conventional and autothermal pyrolysis of corn stover: overcoming the processing challenges of high-ash agricultural residues. *J. Anal. Appl. Pyroly.* 143, 104679. doi:10.1016/j.jaap.2019.104679

Pulka, J., Manczarski, P., Stępień, P., Styczyńska, M., Koziel, J. A., and Białowiec, A. (2020). Waste-to-carbon: is the torrefied sewage sludge with high ash content a better fuel or fertilizer? *Materials* 13 (4), 954. doi:10.3390/ma13040954

Reid, K., Schneider, K., and McConkey, B. (2018). Components of phosphorous loss from agricultural landscapes, and how to incorporate them into risk assessment tools. *Front. Earth Sci.* 6, 135. doi:10.3389/feart.2018.00135

Rogovska, N., Laird, D., Cruse, R., Fleming, P., Parkin, T., and Meek, D. (2011). Impact of biochar on manure carbon stabilization and greenhouse gas emissions. *Soil Sci. Soc. Am. J.* 75, 871–879. doi:10.2136/sssaj2010.0270

Rogovska, N., Laird, D. A., Rathke, S. J., and Karlen, D. L. (2014). Biochar impact on midwestern mollisols and maize nutrient availability. *Geoderma* 230-231, 340–347. doi:10.1016/j.geoderma.2014.04.009

Rollag, S. A., Lindstrom, J. K., and Brown, R. C. (2020). Pretreatments for the continuous production of pyrolytic sugar from lignocellulosic biomass. *Chem. Eng. J.* 385, 123889. doi:10.1016/j.cej.2019.123889

Rover, M., Smith, R., and Brown, R. C. (2018). Enabling biomass combustion and co-firing through the use of lignocol. *Fuel* 211, 312–317. doi:10.1016/j.fuel.2017.09.076

Sawyer, J. E., and Mallarino, A. (2016). *Using manure nutrients for crop production. Extension and Outreach*. Ames, IA: Iowa State University.

Sawyer, J. E. (2001). "Nitrogen fertilizer and swine manure application to soybean," in Proceedings of the 13th Annual Integrated Crop Management Conference, Ames, IA, December 6, 2001.

Schulte, E. E., and Hopkins, B. G. (1996). "Estimation of soil organic matter by weight loss-on ignition," in *Soil organic matter: analysis and interpretation*. Editors F. R. Magdoff, M. A. Tabatabai, and E. A. Hanlon (Madison, WI: SSSA Special Publications), 21–32.

Tisdale, S. L., Nelson, W. L., and Beaton, J. D. (1985). *Soil fertility and fertilizers*. 4th Edn. New York, NY: Macmillan.

Wilfert, P., Kumar, P. S., Korving, L., Witkamp, G.-J., and van Loosdrecht, M. C. M. (2015). The relevance of phosphorus and iron chemistry to the recovery of phosphorus from wastewater: a review. *Environ. Sci. Technol.* 49, 9400–9414. doi:10.1021/acs.est.5b00150

Yao, Y., Gao, B., Zhang, M., Inyang, M., and Zimmerman, A. R. (2012). Effect of biochar amendment on sorption and leaching of nitrate, ammonium, and phosphate in a sandy soil. *Chemosphere* 89, 1467–1471. doi:10.1016/j.chemosphere.2012.06.002

Zhang, X., Wang, H., He, L., Lu, K., Sarmah, A., Li, J., et al. (2013). Using biochar for remediation of soils contaminated with heavy metals and organic pollutants. *Environ. Sci. Pollut. Res. Int.* 20, 8472–8483. doi:10.1007/s11356-013-1659-0

Conflict of Interest: The authors declare that the research was conducted in the absence of any commercial or financial relationships that could be construed as a potential conflict of interest.

frontiers in Environmental Science

ORIGINAL RESEARCH
published: 22 April 2021
doi: 10.3389/fenvs.2021.668084

Temporal Patterns of N_2O Fluxes From a Rainfed Maize Field in Northeast China

*Chenxia Su[1], Ronghua Kang[1,2], Wentao Huang[3] and Yunting Fang[1,2]**

[1]CAS Key Laboratory of Forest Ecology and Management, Institute of Applied Ecology, Chinese Academy of Sciences, Shenyang, China, [2]Key Laboratory of Isotope Techniques and Applications, Shenyang, China, [3]College of Land and Environment, Shenyang Agricultural University, Shenyang, China

Rainfed agriculture is one of the most common farming practices in the world and is vulnerable to global climate change. However, only limited studies have been conducted on rainfed agriculture, mainly using low-frequency manual techniques, which caused large uncertainties in estimating annual N_2O emissions. In this study, we used a fully automated system to continuously measure soil N_2O emissions for two years (April 2017 to March 2019) in a typical rainfed maize field in Northeast China. The annual N_2O emissions were 2.8 kg N ha^{-1} in year 1 (April 2017 to March 2018) and 1.8 kg N ha^{-1} in year 2 (April 2018 to March 2019), accounting for 1.9 and 1.2% of the nitrogen fertilizer applied, respectively. The inter-annual variability was mainly due to different weather conditions encountered in years 1 and 2. A severe drought in year 1 reduced plant N uptake, leaving high mineral N in the soil, and the following moderate rainfalls promoted a large amount of N_2O emissions. The seasonal pattern of N_2O fluxes was mainly controlled by soil temperature and soil nitrate concentration. Both soil moisture and the molar ratio of NO/N_2O indicate that N_2O and NO were mainly derived from nitrification, resulting in a significant positive correlation between N_2O and NO flux in the intra-rows (where nitrogen fertilizer was applied). Moreover, we observed that the N_2O emissions during the freeze–thaw periods were negligible in this region for rainfed agriculture. Our long-term and high-resolution measurements of soil N_2O emissions suggest that sampling between LST 9:00 and 10:00 is the best empirical sampling time for the intermittent manual measurements.

Keywords: nitrous oxide, chamber method, rainfed agriculture, drought, nitrification

OPEN ACCESS

Edited by:
Hatano Ryusuke,
Hokkaido University, Japan

Reviewed by:
Yo Toma,
Ehime University, Japan
Zhijian Mu,
Southwest University, China

****Correspondence:***
Yunting Fang
fangyt@iae.ac.cn

Specialty section:
This article was submitted to Soil Processes, a section of the journal Frontiers in Environmental Science

Received: *16 February 2021*
Accepted: *12 April 2021*
Published: *22 April 2021*

Citation:
Su C, Kang R, Huang W and Fang Y (2021) Temporal Patterns of N_2O Fluxes From a Rainfed Maize Field in Northeast China. Front. Environ. Sci. 9:668084. doi: 10.3389/fenvs.2021.668084

INTRODUCTION

Nitrous oxide (N_2O) is a greenhouse gas, with a lifetime of 120 years in the troposphere and a global warming potential approximately 300 times greater than CO_2 over a 100 year scale (Pachauri et al., 2014). N_2O was identified as the dominant ozone-depleting substance throughout the 21st century (Ravishankara et al., 2009). The concentration of N_2O in the atmosphere increased by more than 20% from 270 ppb in 1750 to 331 ppb in 2018 (Tian et al., 2020). Agricultural soils have been recognized as the largest global source of N_2O, accounting for over 50% of the total global N_2O emissions, due to the widespread application of nitrogen fertilizers (Pachauri et al., 2014; Shang et al., 2019).

Both soil nitrification and denitrification can produce N_2O (Firestone and Davidson, 1989), with denitrification often considered the predominant process of N_2O production (Mathieu et al., 2006;

Laville et al., 2011). Using the conceptual hole-in-the-pipe (HIP) model (Firestone and Davidson, 1989; Davidson et al., 2000), nitrification is the aerobic oxidation of ammonium (NH_4^+) via hydroxylamine (NH_2OH) to nitrite (NO_2^-) and nitrate (NO_3^-), and both N_2O and nitric oxide (NO) are byproducts which leak from the pipe; Denitrification is the stepwise anaerobic reduction of NO_3^- to NO_2^-, NO, N_2O, and N_2, which is favored when soils are moist and anaerobic. These microbial processes are strongly affected by natural conditions (e.g., soil available N, temperature, moisture, and soil texture) and agricultural management (Yan et al., 2015; Fentabil et al., 2016; Xia et al., 2017; Zhang et al., 2019). Complex interactions between such factors result in large temporal and spatial variations in N_2O emissions from croplands, and therefore, considerable uncertainties exist in the estimations of regional and global agricultural emissions (Bouwman et al., 2002).

Traditional N_2O measurements are based on manual techniques with low sampling frequencies of once a few days or weeks (Dorich et al., 2020b; Shang et al., 2020). However, with the high daily temporal variations in N_2O emissions (Liu et al., 2010; Laville et al., 2011), low-frequency measurements are unlikely to characterize emissions accurately and lead to uncertainty in the calculations of annual N_2O emissions (Barton et al., 2015). In addition, low-frequency manual sampling will miss some N_2O high emission periods, such as during N fertilization, irrigation, or rain events (Barton et al., 2008, 2013; Wolf et al., 2010). Additionally, most *in-situ* N_2O measurements only monitor soil N_2O emissions during the growing season and ignore the emissions during the non-growing season. Studies have shown that ignoring N_2O emissions in the non-growing season will underestimate annual N_2O emissions by 30% (Shang et al., 2020). Moreover, the freeze–thaw period is a critical emission period of N_2O and may contribute up to 72% of the total annual flux (Wolf et al., 2010; Wagner-Riddle et al., 2017). Therefore, high-frequency and long-term monitoring is crucial for estimating annual N_2O emissions.

Northeast China is one of the most important grain producing regions in China, and over 60% of the arable lands are rainfed (http://www.stats.gov.cn). Maize (*Zea mays L.*) is intensively cultivated in this area (approximately 12 million ha), accounting for over 30% of the national maize planting area in 2019 (data from http://data.stats.gov.cn). The cultivation of maize with its high N requirements (50–374 kg N ha^{-1}) favors microbial activities to produce N_2O. To date, limited studies have focused on N_2O emissions from these rainfed agricultural soils and have reported a wide range of annual N_2O emissions (range from 0.3 to 2.5 kg N ha^{-1} yr^{-1}, Chen et al., 2002, 2014, 2016; Ni et al., 2012; Dong et al., 2018). We observed that all these studies were based on low-frequency manual techniques which may contribute to the large range of annual N_2O emissions. Therefore, using a high-frequency measurement method to understand temporal patterns and major controllers of N_2O fluxes from rainfed agricultural soils is required.

In this study, we used a fully automated system to continuously quantify N_2O fluxes in a rainfed maize field in Northeast China for two years (from April 2017 to March 2019). Our objectives were a) to characterize diurnal, seasonal, and annual patterns of soil N_2O emissions; b) to identify the major drivers of temporal changes in N_2O flux; and c) to quantify the contribution of freezing and thawing periods to annual N_2O emissions.

MATERIALS AND METHODS

Experimental Site

The study was carried out at the National Field Observation and Research Station of Shenyang Agro-ecosystems of the Chinese Academy of Sciences, located in the Liaoning Province, Northeast China (41° 31′ N, 123° 22′ E). The mean annual temperature (MAT) is 7.5°C, and the mean annual precipitation (MAP) is 680 mm, with more than 80% precipitation during the crop-growing season (from May to September, Dong et al., 2018). The soil type is silt loam, with 24.1% clay, 59.6% silt, and 16.3% sand. The soil was acidic (pH 5.6 and 0–10 cm). The soil had a total carbon content of 11.3 g kg^{-1} and total N content of 1.31 g kg^{-1}.

This study was performed over two consecutive years, from April 28, 2017 to March 31, 2019, at a rainfed maize (*Zea mays L.*) field. The soil was plowed on May 5, 2017 (year 1) and April 25, 2018 (year 2), and seeds were planted in the intra-row on May 7, 2017 and April 28, 2018. Maize plants were harvested on October 7, 2017 and September 24, 2018, respectively, and the maize residues were taken away in both years. In year 1, we reseeded on May 24 due to the failure of germination caused by severe drought. The experimental field received a fertilizer mix of urea and diammonium phosphate (at a 2:1 ratio), which was simultaneously applied within 2 cm of seeds on the intra-row (based on local agricultural management), at a rate of 150 kg N ha^{-1}. The same plot was used for both years and received the same fertilizer treatment.

Measurement of Soil N_2O Flux

N_2O concentrations were continuously and automatically measured using a static chamber-based method between April 28, 2017 and March 31, 2019. The system used seven opaque chambers (20 cm diameter × 10 cm height), with three chambers placed in the intra-rows, three placed in the inter-rows, and one reference chamber (gas-tight bottom made of Teflon). During the measurement, each chamber was closed twice to measure NO and N_2O emissions, respectively. For each chamber, first 6 min was for NO analyzing; gas samples were continuously transported at a flow rate of 0.4 L/min, and concentration of NO was measured at 10 s intervals by a chemiluminescence NO-NO_2-NO_x analyzer (42i, Thermo Electron Corporation, Waltham, MA, United States). After the NO analysis was finished, the chamber was opened for evacuation for 5 min, to remove any residual gas within the chamber and tubes. Then the same chamber was programmed to close for 20 min to determine the N_2O flux. The gas was automatically sampled at three time points (i.e., 0, 10, and 20 min after the chamber closure). The N_2O concentration was measured using a gas chromatograph (GC 2014; Shimadzu, Japan) equipped with an electron capture detector. The NO-NO_2-NO_x analyzer and GC were installed in

a temporary cabin next to the study field. Although our automated system simultaneously measured nitric oxide (NO), herein, we only reported N_2O data; NO data was presented in another unpublished manuscript. Both N_2O and NO measurements for each chamber lasted 36 min. Therefore, the seven-chamber device allowed 40 flux measurements per day or 5 to 6 fluxes per day for each of the seven chambers.

The fluxes of N_2O (F_{N2O}, ng N m^{-2} s^{-1}) were calculated using the following equation:

$$F_{N_2O} = \frac{d_C}{d_t}\frac{V}{A}\frac{P}{P_0}\frac{T_0}{T}$$

where d_C/d_t is the rate of N_2O concentration change over time determined by the linear regression, V is the internal chamber volume, and A is the chamber surface area. P_0 (1,013 hPa) and T_0 (273 K) are the atmospheric pressure and absolute temperature under standard conditions, respectively. P and T are the actual air pressure and chamber air temperature, respectively.

Daily fluxes were calculated as the arithmetic means of the 15 or 18 fluxes obtained from the three replicate chambers (5 or 6 fluxes per chamber per day) for the intra-row and inter-row locations. Estimates of field scale daily emissions were calculated using a weighted average of the spatial distribution of intra-row and inter-row areas. Annual cumulative N_2O emissions were calculated using linear interpolation to fill periods with missing data. The ratio of N_2O emissions to the fertilizer amount was calculated by the annual cumulative N_2O emissions directly divided by N fertilizer amount (150 kg N ha^{-1}).

Auxiliary Field Measurements

In addition to the gas-flux measurements, soil temperature (°C) and moisture (%; volumetric water content, VWC) were monitored at 0–6 cm soil depth using six sensors (Campbell Scientific CS650, North Logan, UT, United States): three in the intra-row and three in the inter-row. The VWCs of the intra-row and inter-row soils were converted into water-filled pore space (WFPS), using the respective bulk density (BD) of 1.17 and 1.25 g cm^{-3}, and a theoretical particle density of 2.65 g cm^{-3} ($WFPS = (100 \times VWC)/(1 - BD/2.65)$). Daily precipitation and air temperatures at the study site was monitored by an on-site meteorological station (50 m away).

The mineral N concentrations (ammonium and nitrate) of the topsoil (0–10 cm) were separately sampled from intra-row and inter-row soils once a week after fertilization last one month, and bi-weekly to monthly during the remaining sample period. The soil was sieved (2 mm mesh), and 10 g of sieved soil was extracted with 50 ml of 2 M KCl solution. Extracts were frozen at −18°C and later analyzed by a discrete chemistry analyzer (Smartchem 200, Westco Scientific Instruments, Inc., Italy). The obtained values (mg N L^{-1}) were converted to soil dry weight basis (mg N kg^{-1} soil).

Data Analysis

Statistical analyses were implemented using R, version 3.6.3 (R Core Team, 2019) and RStudio (version February 1, 5033). Graphics were implemented using both RStudio and Origin 9. The differences in the soil temperature, moisture, temperature and mineral N concentration between inter-rows and intra-rows were tested using a one-way ANOVA. A nonlinear or linear regression analysis was used to explore the relationship between soil N_2O fluxes and environmental factors (e.g., soil temperature, moisture, and mineral N concentration). A significance level of $P < 0.05$ was used for all data analyses.

RESULTS

Environmental Parameters

The annual precipitation was 439 and 642 mm in the first and second measurement years, respectively. This difference was largely due to the rainfall in the first 30 days following fertilization, with 13 mm in year 1 and 150 mm in year 2 (**Figure 1A**). The mean WFPS in the intra-rows during the growing season was 28 ± 12% WFPS in year 1, significantly lower than that in year 2 (31 ± 15% WFPS). The temporal pattern of soil moisture in the inter-rows was similar to the intra-rows but was significantly wetter (**Figure 1B**). The mean annual soil temperatures for the intra-rows were 9.7°C in year 1 and 9.1°C in year 2. There was no significant temperature difference between the rows and inter-rows (**Figure 1C**).

Soil NH_4^+–N concentration in the intra-row increased markedly following fertilization on May 7, 2017 and April 28, 2018 (**Figure 1D**). In year 1, the NH_4^+–N concentration increased to 333 mg N kg^{-1} immediately following fertilizer application and remained at that level for approximately a month. After precipitation in early June, the NH_4^+–N concentration started to decrease, but still averaged 232 and 113 mg N kg^{-1} in June and July, respectively. In year 2, the NH_4^+–N concentration also increased following fertilization but reached a considerably lower level (120 mg N kg^{-1}) compared to year 1. Then, it decreased gradually to only 2 mg N kg^{-1} in mid-July and remained at that level in the remaining months (**Figure 1D**). The NO_3^-–N concentration increased following the decrease in NH_4^+–N (**Figure 1D–E**). The peak concentration of NO_3^-–N concentration in both years was significantly lower than NH_4^+–N concentrations (234 mg N kg^{-1} on July 5, 2017 and 80 mg N kg^{-1} on May 24, 2018). In the inter-row, where no fertilizer had been applied, the mineral N concentrations were considerably lower than those in the intra-rows. In year 1, the mineral N concentrations showed a small pulse following fertilization, with NH_4^+–N concentration increasing to 25 mg N kg^{-1} and NO_3^-–N concentration increasing to 70 mg N kg^{-1} in the inter-row soils before immediately decreasing below 10 mg N kg^{-1} (**Figure 1D–E**).

Temporal Patterns of N_2O Fluxes

We observed pronounced seasonal variations in N_2O emissions during both measurement years (**Figure 2**), being highest after fertilizer application in summer and lowest in winter. Daily N_2O fluxes from the intra-rows also exhibited large interannual variation (**Figure 2**), despite the application of the same amount of fertilizer. Mean daily N_2O fluxes (ng N m^{-2} s^{-1}) ranged from 1.4 to 122.1 (averaged 23.8 ± 3.2) in year 1, and

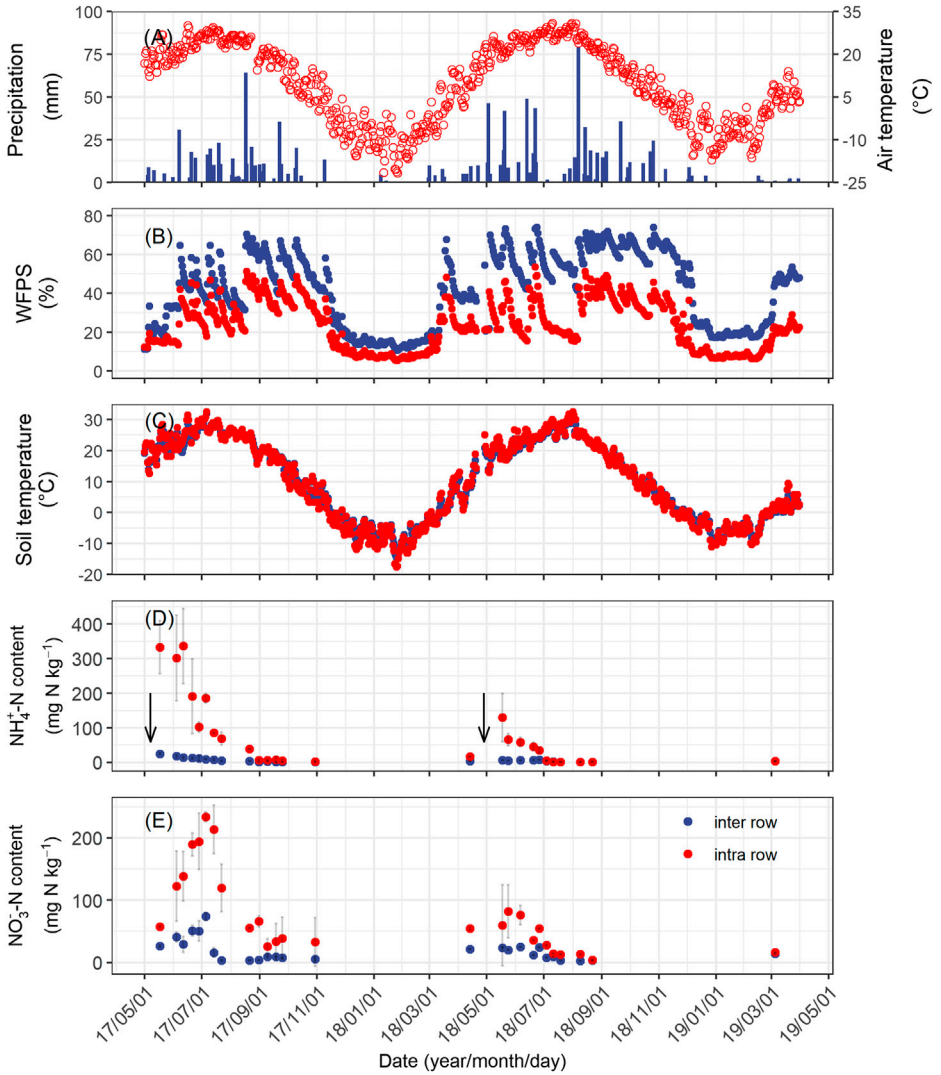

FIGURE 1 | Seasonal changes in mean daily air temperature and daily precipitation (**A**), daily mean soil temperature (**B**), and moisture (**C**) at a depth of 5 cm; concentration of ammonium (**D**), and nitrate (**E**) at a depth of 0–10 cm soil of the intra-row and inter-row soils from April 2017 to March 2019. Error bars indicate standard errors. The downward arrows represent the time of fertilization.

−3.8 to 53.1 (averaged 10.0 ± 1.6) in year 2. In year 1, the peak N_2O emission in the intra-row (122.1 ng N m^{-2} s^{-1}, **Figure 2**) occurred on July 16, approximately two months following the fertilization, and the highest flux (35 ng N m^{-2} s^{-1}) in year 2 appeared on May 30, approximately one month following fertilization (**Figure 2**). The high emission period in the intra-row following N application lasted approximately three months (from June to August) in year 1 and two months (May to June) in year 2. The average N_2O fluxes from the inter-rows were 10.5 ± 1.6 ng N m^{-2} s^{-1} in year 1 and 7.3 ± 1.1 ng N m^{-2} s^{-1} in year 2; both were significantly lower than those from the intra-rows. In both years, we found no increase in N_2O fluxes during the spring freeze–thaw period (**Supplementary Figure S1**).

The cumulative annual N_2O emissions in year 1 were 2.8 kg N ha^{-1}, which was approximately 1.6 times higher than that in year 2 (1.8 kg N ha^{-1}), accounting for 1.9 and 1.2% of the applied N fertilizer (150 kg N ha^{-1} yr^{-1}). Approximately 70% of the difference in annual N_2O emissions can be attributed to the different accumulated emissions from July and August (**Supplementary Figure S2**), when soils produced 1.5 kg N ha^{-1} in year 1 and 0.8 kg N ha^{-1} in year 2. N_2O emissions during the non-growing season (November to March) contributed to 23.2% of the annual N_2O emissions in year 1 and 9.7% in year 2.

For the diurnal cycles of N_2O flux, we only observed clear diurnal patterns from intra-rows during the growing season, which correlated well with the changes in soil temperature (**Figure 3**). We found that sampling at LST (local standard time) 9:00–10:00 or 18:00–19:00 best represented the daily average N_2O emissions in this area.

We simultaneously measured NO flux; detailed analysis is provided in another unpublished manuscript; however, herein, we only present the daily molar ratio of NO and N_2O fluxes

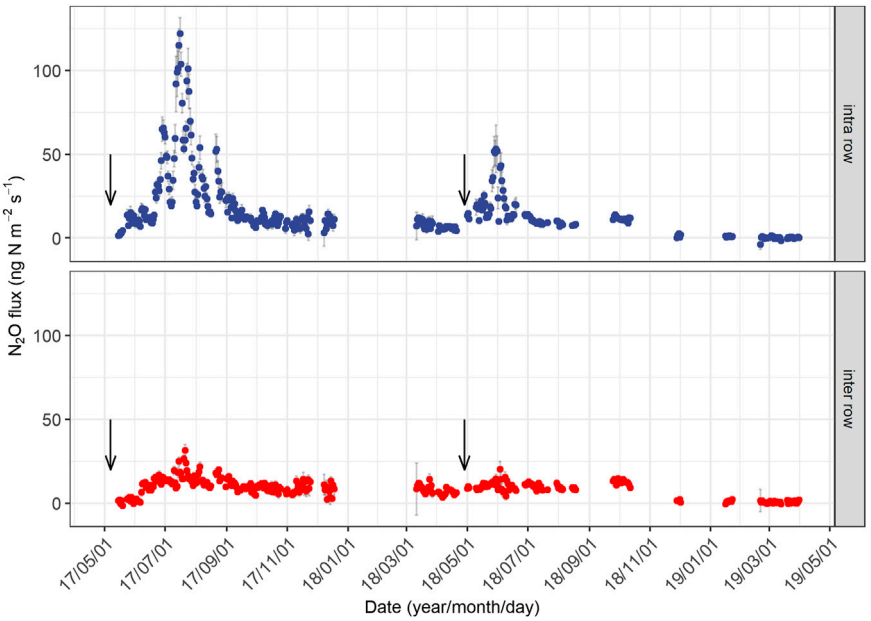

FIGURE 2 | Seasonal changes in daily mean N_2O fluxes from the intra-row and inter-row soils in two years. The downward arrows represent the time of fertilization. The period without data is because of equipment failure. Error bars indicate standard errors.

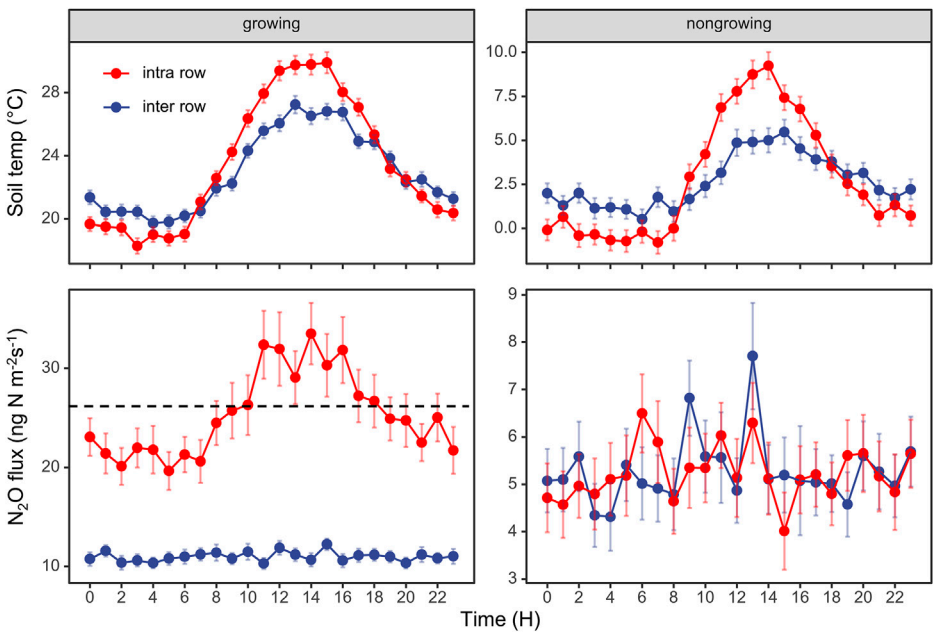

FIGURE 3 | Diurnal variations in N_2O fluxes and soil temperature at 5 cm depth. The data are average values aggregated for different times of the day, using the entire dataset from the intra-row and inter-row locations in growing season and nongrowing season. The dashed line represents the daily average of soil N_2O fluxes. Error bars indicate standard errors.

(**Figure 4**). In the intra-rows (with high mineral N concentration and low soil moisture), the NO/N_2O ratio >1 prevailed for 97 and 56% of the measured fluxes during the growing season in year 1 and year 2, respectively, (**Figure 4**). The NO emission was over 10 times greater than N_2O emissions during the peak emission period, especially in year 1 (May to August), and the ratio began to decline when the NH_4^+–N concentration approached 0 mg N kg^{-1}. The ratios in the inter-rows (with high soil

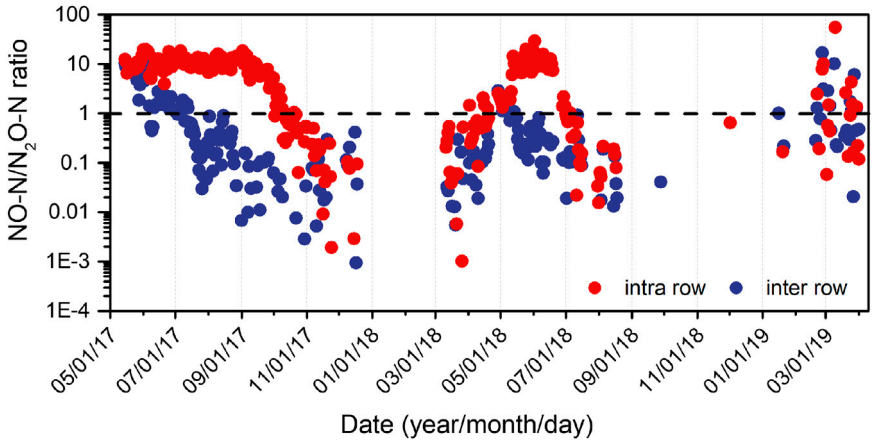

FIGURE 4 | Seasonal changes in the molar ratio between NO to N_2O fluxes from intra-row and inter-row soils in two years.

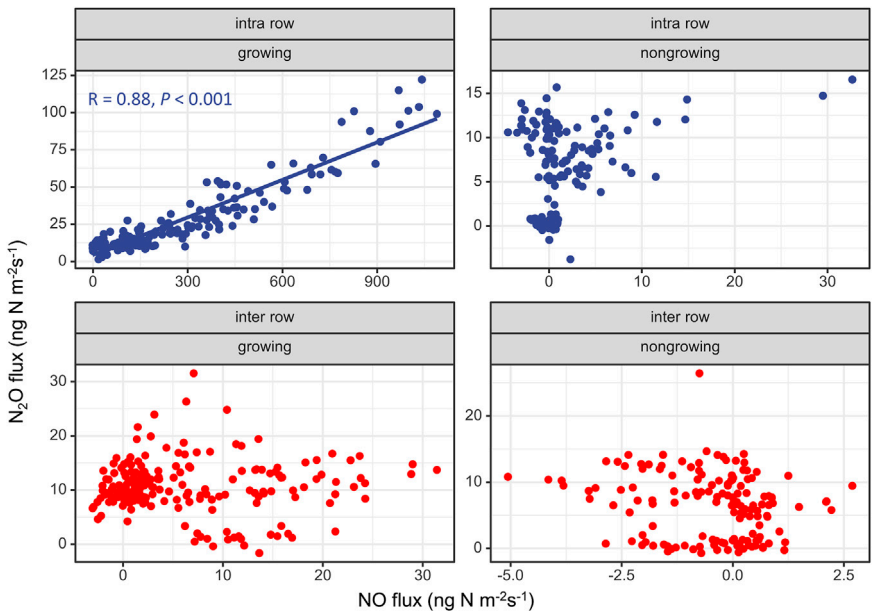

FIGURE 5 | Correlations between N_2O and NO fluxes.

moisture and low mineral N concentration) were usually less than one (**Figure 4**), with $NO/N_2O < 1$ accounting for 60% of the measurements in year 1 and 84% in year 2. However, from April 28 to mid-June in year 1, when the inter-row soil moisture was very low (from 15 to 30% WFPS), the NO/N_2O ratios were >1 (**Figure 4**).

Figure 5 shows the relationship between N_2O and NO fluxes from intra-rows and inter-rows during the growing and non-growing seasons. We found that there was a significant linear correlation between N_2O and NO fluxes from intra-rows during the growing season, and the R^2 reached 0.88. No significant relationships were found in the non-growing season (**Figure 5**).

Relationship of N_2O Fluxes with Temperature, Soil Mineral N Concentration, and Moisture.

In this study, we divided the entire observation period into three periods: the growing season (May to September), non-growing season (October to February), and freeze–thaw period (March), to analyze the correlation between soil N_2O flux and soil temperature or moisture (**Figure 6**, **Supplementary Figure S3**). The results showed that for the intra-rows, soil N_2O fluxes were significantly and exponentially correlated with soil temperature during the growing seasons in both years and during the non-growing season in year 2 (**Figure 6**). For the inter-rows,

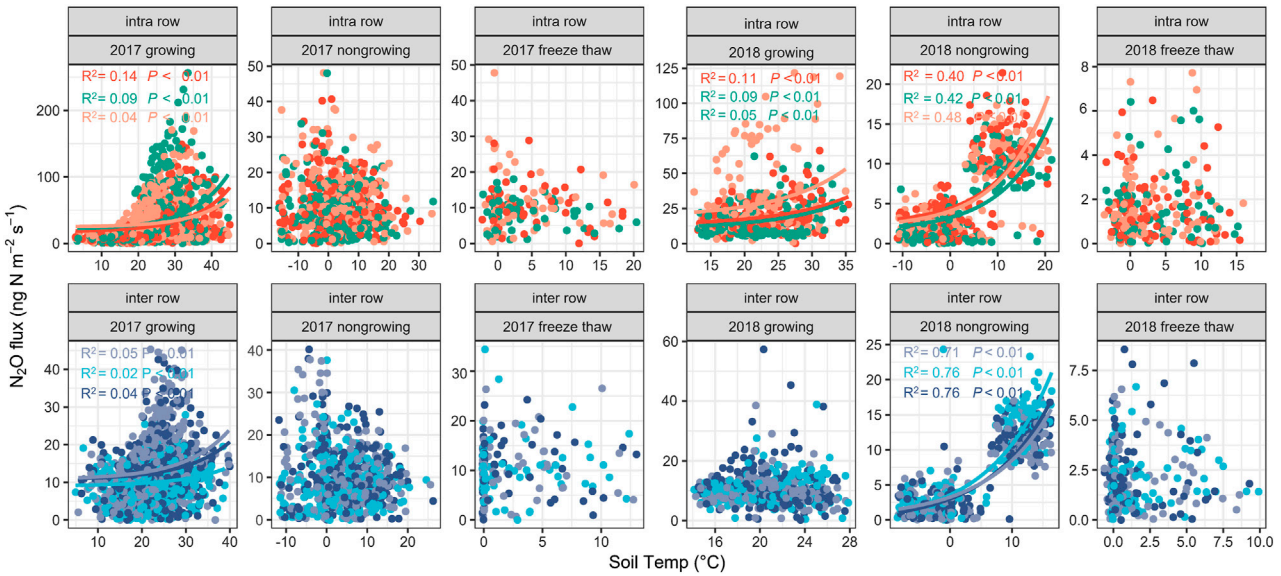

FIGURE 6 | Correlations of N_2O fluxes with soil temperature at 5 cm depth. Different dot colors indicate N_2O fluxes from different chambers.

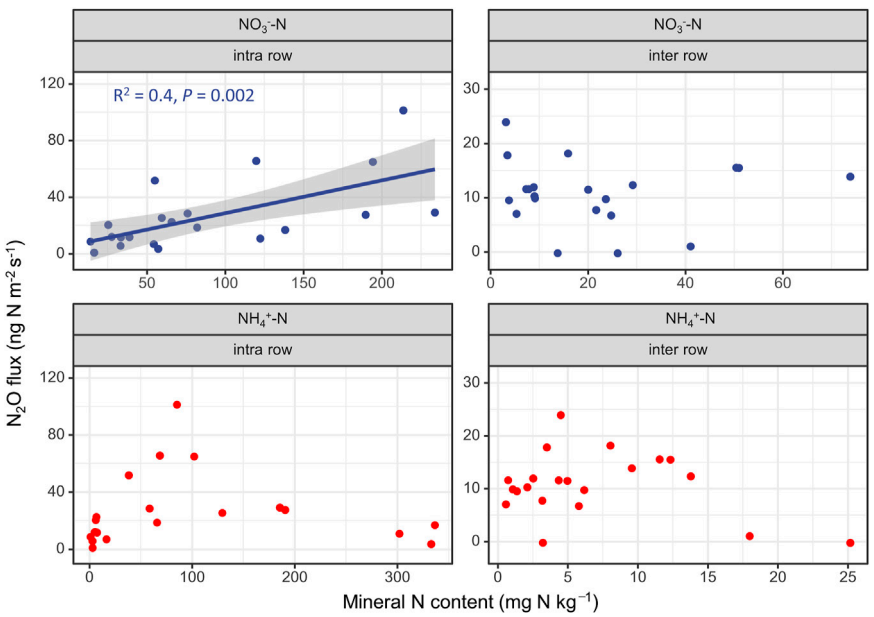

FIGURE 7 | Correlations between N_2O fluxes and mineral N content (NH_4^+–N and NO_3^-–N).

the N_2O fluxes are significantly correlated with the soil temperature during the growing season in year 1 and the non-growing season in year 2 (**Figure 6**). There were no significant relationships between N_2O fluxes and soil temperature during the two-year freeze–thaw periods. No significant correlation between N_2O flux and soil moisture were observed (**Supplementary Figure S3**), and the optimum moistures for N_2O production were 25–30% WFPS in the intra-rows and 50–60% WFPS in the inter-rows during growing season in both measurement years (**Supplementary Figure S3**).

For soil available N, a positive and significant linear relationship with N_2O fluxes was only found against NO_3^-–N in the intra-rows, and no significant correlation was found with NH_4^+–N for both intra-rows and inter-rows (**Figure 7**).

DISCUSSION

Annual N_2O Emissions

We monitored soil N_2O fluxes based on an automatic and continuous method over two years for a rainfed maize field in Northeast China. The cumulative N_2O emission in year 1 and year 2 was 2.8 and 1.8 kg N ha^{-1}, respectively, which were comparable to another multiyear measurement obtained at the same field station (ranging from 0.3 to 2.5 kg N ha^{-1}, Dong et al., 2018). However, it is higher than the N_2O emission (0.1–0.6 kg N ha^{-1}) reported by Ni et al. (2012) from another maize field in Northeast China, which may be attributed to their short-term monitoring (only measured the growing season). Shang et al. (2020) summarized more than 20 studies which monitored N_2O emissions *in-situ* and found that ignoring N_2O emissions in the non-growing season would lead to an underestimation of annual N_2O emissions by 10–30%. Therefore, the measurement of N_2O emissions over an entire year is essential to accurately estimate annual N_2O emissions. In addition, our annual N_2O emissions were considerably lower than those in the report of Gagnon et al. (2011), from a maize field in Canada (ranging from 4.6 to 22.8 kg N ha^{-1}), which used the same type and amount of nitrogen fertilizer as in this study. Notably, the soil in Gagnon's report was poorly drained, and the soil organic matter (SOC = 4.6%) was significantly higher than that in our study (1.1%), which may easily form an anaerobic environment and provide sufficient carbon to promote denitrification and produce more N_2O (Stehfest and Bouwman, 2006; Dong et al., 2018).

The N_2O emission factors (EF, in %) is defined as the N_2O emission from fertilized treatment minus the emission from unfertilized control treatment expressed as a percentage of the N applied (Eggleston et al., 2006). However, our study had no unfertilized control treatments, neglecting background N_2O emissions, the annual N_2O emissions accounted for 1.9 and 1.2% of the fertilizer amount (150 kg N ha^{-1}) in years 1 and 2, respectively. We assume that the N_2O emissions from inter-rows (without fertilization) can be used as background N_2O emissions, and their annual emissions for the two years were 1.9 and 0.9 kg N ha^{-1}, respectively. Thus, the estimated EF–N_2O for both years was 0.6%, which corresponds with other studies from rainfed maize fields in Northeast China (0.3–1.1%, Ni et al., 2012; Guo et al., 2013; Chen et al., 2014; Dong et al., 2018). However, this estimation might be conservative, due to the relatively high soil moisture of the inter-rows. The EF–N_2O values of these rainfed agricultural soils were lower than those of irrigated agricultural soils. For example, McSwiney and Robertson (2005) monitored N_2O emissions from irrigated maize fields for three years, and the EF–N_2O values ranged from 2 to 7%. Liu et al. (2011) also reported an EF–N_2O value of 2% from an irrigated maize field. A review by Aguilera et al. (2013) found that N_2O emissions from rainfed agriculture were one order of magnitude lower than those from conventional irrigated fields in the Mediterranean climate cropping system. One of the main reasons is that the low precipitation and soil moisture in rainfed agricultural soil suppresses N_2O production (Ni et al., 2012; Dong et al., 2018).

The cumulative annual N_2O emission in year 1 (2.8 kg N ha^{-1}) was considerably higher than in year 2 (1.8 kg N ha^{-1}). Although the precipitation in the second year (634 mm) was more than that in the first year (439 mm). However, the severe drought before and after fertilization in the first year reduced the plants N uptake (maize emergence and extension was notably delayed in year 1), resulting in substantial levels of nitrogen remaining in soil, and the soil mineral N concentration (NH_4^+–N + NO_3^-–N) reached 460 mg N kg^{-1} in mid-May to early June in year 1, approximately three times higher than the highest soil N concentration in year 2 (**Figures 1D–E**). After the precipitation in early June, the mineral N concentration started to decrease but remained above 30 mg N kg^{-1} until late September. An extended period of high soil N concentrations in year 1 extended the window of N_2O emissions (**Figure 2**), resulting in higher N_2O emissions in year 1 than in year 2.

Microbial Processes Responsible for N_2O Productions

We suggest that N_2O emissions from the intra-rows were mainly attributed to nitrification, and the inter-row process was more complicated. First, the soil moisture of intra-rows was lower than 60% WFPS during the growing season (averaged 30 ± 10%, range from 12 to 53% WFPS), suggesting that nitrification would be dominant (Davidson, 1993; Bateman and Baggs, 2005; Pilegaard, 2013); the soil moisture of the inter-rows exhibited a wide range (from 10 to 75% WFPS), suggesting that both nitrification and denitrification processes may occur. Second, the molar ratio of NO/N_2O has been used as a useful indicator for evaluating the contribution of nitrification (NO/N_2O > 1) and denitrification (NO/N_2O < 1; Anderson and Levine, 1986; Skiba et al., 1993; Davidson et al., 2000; Zhang et al., 2011). In the intra-rows, during the high emission period in year 1 (June to September) and year 2 (May to June), over 90% of the NO/N_2O ratios were higher than one (**Figure 4**), suggesting that nitrification was dominant, and the soil NO/N_2O ratio of the inter-rows was mostly less than 1 (80%), indicating that denitrification was dominant (**Figure 4**).

Surprisingly, we found a significant positive correlation between the NO and N_2O emission rates from the intra-rows during the growing season (**Figure 5**), indicating that NO and N_2O were produced by similar processes and controlled by similar environmental factors. In other words, when nitrification dominated NO and N_2O production, their fluxes were significantly positively correlated. Similar results were also revealed by Ding et al. (2007) from a lab incubation experiment. This finding will aid building models to predict NO emissions (which is a reactive nitrogen gas and less *in-situ* measurements) based on N_2O *in-situ* measurements (Dorich et al., 2020a). For the inter-rows, both nitrification and denitrification can occur, and there was no significant linear relationship between NO and N_2O emissions.

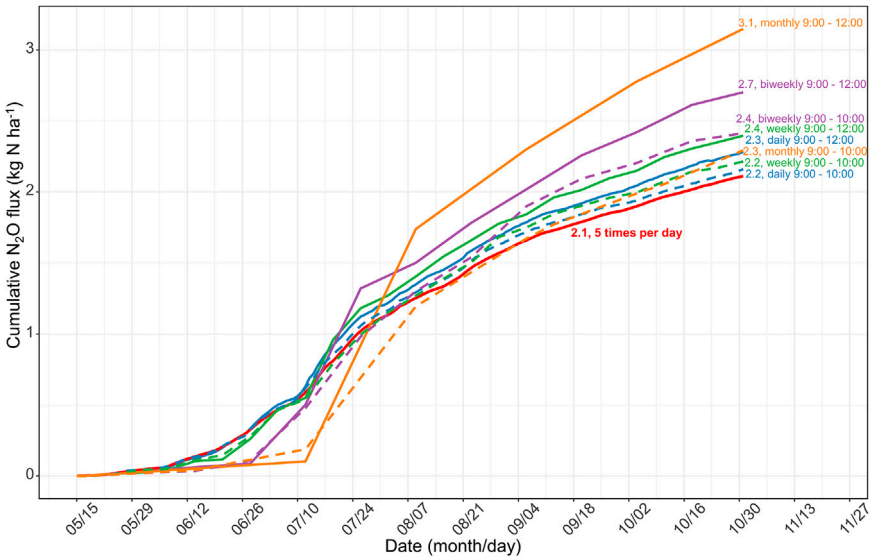

FIGURE 8 | Difference in the estimated N_2O emission during growing season (May to October) in 2017, due to different sample frequency (daily, weekly, biweekly, and monthly intervals presented in different colors) at the different sampling time (LST 09:00 to 12:00 presented in solid lines and LST 09:00 to 10:00 in dashed lines). The solid line in red represents the scenario with 5 measurements per day as mentioned in the present study. The numbers indicate the amounts of cumulative N_2O emissions.

N_2O Emissions During the Freeze–Thaw Period

Many studies reported that soil freeze–thaw cycles promote N_2O emissions, contributing 17–85% of the annual N_2O emissions (Yanai et al., 2011; Abalos et al., 2016; Wagner-Riddle et al., 2017; Gao et al., 2018). Several hypotheses may explain the increase in N_2O emissions during this period: 1) enhanced available C and N substrates due to the physical cracking of soil aggregates and the nutrients from the microbial community that died during winter freeze (de et al., 2009; Wolf et al., 2010); 2) increased soil moisture which formed an anaerobic environment and increased denitrifier activities (Priemé and Christensen, 2001; Teepe et al., 2001; Congreves et al., 2018). Several studies have observed that clay soil with high organic carbon content more easily produces high N_2O emissions during the freeze–thaw period (Van et al., 2000; Müller et al., 2003; Groenevelt and Grant, 2013; Wang et al., 2014). Dong et al. (2018) found that the N_2O pulses during freeze–thaw cycles are also related to the precipitation and depth of snow cover during the non-growing season. However, in our study, we found that there was no significant increase in N_2O emissions during the freeze–thaw period in both years. The main reasons were 1) our study located in a temperate semi-humid continental monsoon climate with little snowfall episode in winter, leading to insufficient anaerobic conditions during the freeze-thaw period, which inhibits denitrification to occur; 2) the SOC is low (1.1 g C kg^{-1}) in our study site and cannot provide sufficient carbon substrate for denitrification; and 3) the soil clay content is low (24.1%). Chen et al. (2014) also found that the contribution of the soil freeze–thaw period to annual N_2O emissions from rainfed agriculture in Northeast China is negligible.

Impacts of Sampling Frequency and Time on Estimating Cumulative N_2O Emissions

Most *in-situ* N_2O measurements are still carried out by manual sampling, repeated usually in the intervals of days to weeks, and are in turn integrated across time to calculate annual losses. Such low-frequency measurements over or underestimate annual emission budgets (Liu et al., 2010). Barton et al. (2015) suggested that automated chambers should be continuously used to build guidelines for manual sampling. Here, we assume that the temporal coverage of manual flux measurements is daily, weekly, biweekly, and monthly, to analyze the influence of sampling frequency on calculating cumulative N_2O emissions from May to October in 2017. The subset is the N_2O flux between 09:00 and 12:00 extracted from our hourly measurements (similar to previous studies, e.g., Zhao et al., 2015; Guardia et al., 2017; Dong et al., 2018, 2018; Yao et al., 2019). **Figure 8** shows that, compared with the high-resolution continuous measurements (5 times a day), low sampling frequencies can overestimate N_2O emissions by 8–49% (**Figure 8**). Therefore, sampling between 09:00 and 12:00 with low-frequency manual measurements can lead to considerable uncertainties in quantifying annual emissions.

Previous studies reported that sampling at LST 08:15 (Laville et al., 2011) or 09:00 (Liu et al., 2010) best represented the daily average of N_2O emissions; however, the best sampling time requires investigation across a broader range of land uses and climates (Smith and Dobbie, 2001; Barton et al., 2015). Here, we intended to reveal the best sampling time during the day for rainfed agriculture in our study region of Northeast China. After aggregating the entire dataset, **Figure 3** shows that sampling at LST 9:00 to 10:00 am or 18:00 to 17:00 pm best represents the daily mean N_2O flux. We then calculated the cumulative N_2O emission sampling from 9:00 to 10:

00 at daily, weekly, biweekly, and monthly intervals. We found that the deviations ranged from +2% to +9% ("+" indicated overestimations), which was considerably smaller than the deviation when sampling was performed between 9:00 and 12:00 (**Figure 8**). Therefore, we suggest that sampling between 9:00 and 10:00 is the best empirical sampling time for the intermittent manual measurements of N_2O emissions in our study region. High-frequency flux measurements enabled us to identify the diurnal pattern and highlight the effect of sampling frequency and sampling time on N_2O flux balance and provide guidance for low-frequency manual sampling.

DATA AVAILABILITY STATEMENT

The original contributions presented in the study are included in the article/**Supplementary Material**, further inquiries can be directed to the corresponding author.

AUTHOR CONTRIBUTIONS

CS, YF, and WH contributed to the conception and design of the study. CS, RK, and YF organized the database. CS wrote the first draft of the manuscript. All authors contributed to manuscript revision, read, and approved the submitted version.

FUNDING

This research was financially supported by the National Key Research and Development Program of China (grant no. 2017YFC0212700, grant no. 2016YFA0600802), the Key Research Program of Frontier Sciences of Chinese Academy of Sciences (grant no. QYZDB-SSWDQC002), the National Natural Science Foundation of China (grant no. 41773094).

ACKNOWLEDGMENTS

We are grateful to Xin Chen, Yi Shi and Caiyan Lu for their helpful comments and suggestions during the field measurements. We are grateful to the Shenyang Ecological Experimental Station, Chinese Academy of Sciences, for providing the experimental field and the meteorological data.

SUPPLEMENTARY MATERIAL

The Supplementary Material for this article can be found online at: https://www.frontiersin.org/articles/10.3389/fenvs.2021.668084/full#supplementary-material.

REFERENCES

Abalos, D., Brown, S. E., Vanderzaag, A. C., Gordon, R. J., Dunfield, K. E., and Wagner-Riddle, C. (2016). Micrometeorological Measurements over 3 Years Reveal Differences in N2O Emissions between Annual and Perennial Crops. *Glob. Change Biol.* 22, 1244–1255. doi:10.1111/gcb.13137

Aguilera, E., Lassaletta, L., Sanz-Cobena, A., Garnier, J., and Vallejo, A. (2013). The Potential of Organic Fertilizers and Water Management to Reduce N2O Emissions in Mediterranean Climate Cropping Systems. A Review. *Agric. Ecosyst. Environ.* 164, 32–52. doi:10.1016/j.agee.2012.09.006

Anderson, I. C., and Levine, J. S. (1986). Relative Rates of Nitric Oxide and Nitrous Oxide Production by Nitrifiers, Denitrifiers, and Nitrate Respirers. *Appl. Environ. Microbiol.* 51, 938–945. doi:10.1128/aem.51.5.938-945.1986

Barton, L., Gleeson, D. B., Maccarone, L. D., Zúñiga, L. P., and Murphy, D. V. (2013). Is Liming Soil a Strategy for Mitigating Nitrous Oxide Emissions from Semi-arid Soils?. *Soil Biol. Biochem.* 62, 28–35. doi:10.1016/j.soilbio.2013.02.014

Barton, L., Kiese, R., Gatter, D., Butterbach-bahl, K., Buck, R., Hinz, C., et al. (2008). Nitrous Oxide Emissions from a Cropped Soil in a Semi-arid Climate. *Glob. Change Biol.* 14, 177–192. doi:10.1111/j.1365-2486.2007.01474.x

Barton, L., Wolf, B., Rowlings, D., Scheer, C., Kiese, R., Grace, P., et al. (2015). Sampling Frequency Affects Estimates of Annual Nitrous Oxide Fluxes. *Scientific Rep.* 5, 15912. doi:10.1038/srep15912

Bateman, E. J., and Baggs, E. M. (2005). Contributions of Nitrification and Denitrification to N2O Emissions from Soils at Different Water-Filled Pore Space. *Biol. Fertil. Soils* 41, 379–388. doi:10.1007/s00374-005-0858-3

Bouwman, A. F., Boumans, L. J. M., and Batjes, N. H. (2002). Modeling Global Annual N2O and NO Emissions from Fertilized Fields. *Glob. Biogeochem. Cycles* 16, 1080. doi:10.1029/2001gb001812

Chen, X., Cabrera, M. L., Zhang, L., Wu, J., Shi, Y., Yu, W. T., et al. (2002). Nitrous Oxide Emission from Upland Crops and Crop-Soil Systems in Northeastern China. *Nutrient Cycling in Agroecosystems* 62, 241–247. doi:10.1023/A:1021202114354

Chen, Z., Ding, W., Luo, Y., Yu, H., Xu, Y., Müller, C., et al. (2014). Nitrous Oxide Emissions from Cultivated Black Soil: A Case Study in Northeast China and Global Estimates Using Empirical Model. *Glob. Biogeochem. Cycles* 28, 1311–1326. doi:10.1002/2014gb004871

Chen, Z., Ding, W., Xu, Y., Müller, C., Yu, H., and Fan, J. (2016). Increased N2O Emissions during Soil Drying after Waterlogging and Spring Thaw in a Record Wet Year. *Soil Biol. Biochem.* 101, 152–164. doi:10.1016/j.soilbio.2016.07.016

Congreves, K. A., Wagner-Riddle, C., Si, B. C., and Clough, T. J. (2018). Nitrous Oxide Emissions and Biogeochemical Responses to Soil Freezing-Thawing and Drying-Wetting. *Soil Biol. Biochem.* 117, 5–15. doi:10.1016/j.soilbio.2017.10.040

Davidson, E. A., Keller, M., Erickson, H. E., Verchot, L. V., and Veldkamp, E. (2000). Testing a Conceptual Model of Soil Emissions of Nitrous and Nitric Oxides. *BioScience* 50, 667–680. doi:10.1641/0006-3568(2000)050[0667:tacmos]2.0.co;2

Davidson, E. A. (1993). "Soil Water Content and the Ratio of Nitrous Oxide to Nitric Oxide Emitted from Soil," Biogeochemistry of Global Change: Radiatively Active Trace Gases Selected Papers from the Tenth International Symposium on Environmental Biogeochemistry, San Francisco, August 19–24, 1991. Editor R. S. Oremland (Boston, MA: Springer US), 369–386. doi:10.1007/978-1-4615-2812-8_20

de, B. A, Butterbach-Bahl, K., Blagodatsky, S., and Grote, R. (2009). Model evaluation of different mechanisms driving freeze–thaw N_2O emissions. *Agric. Ecosyst. & Environ.* 133, 196–207. doi:10.1016/j.agee.2009.04.023

Ding, W., Yagi, K., Akiyama, H., Sudo, S., and Nishimura, S. (2007). Time-lagged Induction of N2O Emission and its Trade-Off with NO Emission from a Nitrogen Fertilized Andisol. *Soil Sci. Plant Nutr.* 53, 362–372. doi:10.1111/j.1747-0765.2007.00152.x

Dong, D., Kou, Y., Yang, W., Chen, G., and Xu, H. (2018). Effects of Urease and Nitrification Inhibitors on Nitrous Oxide Emissions and Nitrifying/denitrifying Microbial Communities in a Rainfed Maize Soil: A 6-year Field Observation. *Soil Tillage Res.* 180, 82–90. doi:10.1016/j.still.2018.02.010

Dorich, C. D., Conant, R. T., Albanito, F., Butterbach-Bahl, K., Grace, P., Scheer, C., et al. (2020a). Improving N2O Emission Estimates with the Global N2O

Database. *Curr. Opin. Environ. Sustainability* 47, 13–20. doi:10.1016/j.cosust.2020.04.006

Dorich, C. D., De Rosa, D., Barton, L., Grace, P., Rowlings, D., Migliorati, M. D. A., et al. (2020b). Global Research Alliance N 2 O Chamber Methodology Guidelines: Guidelines for Gap-filling Missing Measurements. *J. Environ. Qual.* 49, 1186–1202. doi:10.1002/jeq2.20138

Eggleston, H. S., Buendia, L., Miwa, K., Ngara, T., and Tanabe, K. (2006). 2006 IPCC Guidelines for National Greenhouse Gas Inventories. (Kanagawa, Japan: IGES). Available at: https://www.osti.gov/etdeweb/biblio/20880391.

Fentabil, M. M., Nichol, C. F., Neilsen, G. H., Hannam, K. D., Neilsen, D., Forge, T. A., et al. (2016). Effect of Micro-irrigation Type, N-Source and Mulching on Nitrous Oxide Emissions in a Semi-arid Climate: An Assessment across Two Years in a Merlot Grape Vineyard. *Agric. Water Management* 171, 49–62. doi:10.1016/j.agwat.2016.02.021

Firestone, M. K., and Davidson, E. A. (1989). Microbiological Basis of NO and N_2O Production and Consumption in Soil. *Exchange Trace Gases between terrestrial Ecosyst. Atmosphere* 47, 7–21.

Gagnon, B., Ziadi, N., Rochette, P., Chantigny, M. H., and Angers, D. A. (2011). Fertilizer Source Influenced Nitrous Oxide Emissions from a Clay Soil under Corn. *Soil Sci. Soc. Am. J.* 75, 595–604. doi:10.2136/sssaj2010.0212

Gao, D., Zhang, L., Liu, J., Peng, B., Fan, Z., Dai, W., et al. (2018). Responses of Terrestrial Nitrogen Pools and Dynamics to Different Patterns of Freeze-Thaw Cycle: A Meta-Analysis. *Glob. Change Biol.* 24, 2377–2389. doi:10.1111/gcb.14010

Groenevelt, P. H., and Grant, C. D. (2013). Heave and Heaving Pressure in Freezing Soils: A Unifying Theory. *Vadose Zone J.* 12. doi:10.2136/vzj2012.0051

Guardia, G., Cangani, M. T., Andreu, G., Sanz-Cobena, A., García-Marco, S., Álvarez, J. M., et al. (2017). Effect of Inhibitors and Fertigation Strategies on GHG Emissions, NO Fluxes and Yield in Irrigated Maize. *Field Crops Res.* 204, 135–145. doi:10.1016/j.fcr.2017.01.009

Guo, Y., Luo, L., Chen, G., Kou, Y., and Xu, H. (2013). Mitigating Nitrous Oxide Emissions from a Maize-Cropping Black Soil in Northeast China by a Combination of Reducing Chemical N Fertilizer Application and Applying Manure in Autumn. *Soil Sci. Plant Nutr.* 59, 392–402. doi:10.1080/00380768.2013.775006

Laville, P., Lehuger, S., Loubet, B., Chaumartin, F., and Cellier, P. (2011). Effect of Management, Climate and Soil Conditions on N2O and NO Emissions from an Arable Crop Rotation Using High Temporal Resolution Measurements. *Agric. For. Meteorology* 151, 228–240. doi:10.1016/j.agrformet.2010.10.008

Liu, C., Wang, K., Meng, S., Zheng, X., Zhou, Z., Han, S., et al. (2011). Effects of Irrigation, Fertilization and Crop Straw Management on Nitrous Oxide and Nitric Oxide Emissions from a Wheat-Maize Rotation Field in Northern China. *Agric. Ecosyst. Environ.* 140, 226–233. doi:10.1016/j.agee.2010.12.009

Liu, C., Zheng, X., Zhou, Z., Han, S., Wang, Y., Wang, K., et al. (2010). Nitrous Oxide and Nitric Oxide Emissions from an Irrigated Cotton Field in Northern China. *Plant Soil* 332, 123–134. doi:10.1007/s11104-009-0278-5

Mathieu, O., Hénault, C., Lévêque, J., Baujard, E., Milloux, M.-J., and Andreux, F. (2006). Quantifying the Contribution of Nitrification and Denitrification to the Nitrous Oxide Flux Using 15N Tracers. *Environ. Pollut.* 144, 933–940. doi:10.1016/j.envpol.2006.02.005

McSwiney, C. P., and Robertson, G. P. (2005). Nonlinear Response of N2O Flux to Incremental Fertilizer Addition in a Continuous Maize (Zea mays L.) Cropping System. *Glob. Change Biol.* 11, 1712–1719. doi:10.1111/j.1365-2486.2005.01040.x

Müller, C., Kammann, C., Ottow, J. C. G., and Jäger, H.-J. (2003). Nitrous Oxide Emission from Frozen Grassland Soil and during Thawing Periods. *J. Plant Nutr. Soil Sci.* 166, 46–53. doi:10.1002/jpln.200390011

Ni, K., Ding, W., Zaman, M., Cai, Z., Wang, Y., Zhang, X., et al. (2012). Nitrous Oxide Emissions from a Rainfed-Cultivated Black Soil in Northeast China: Effect of Fertilization and Maize Crop. *Biol. Fertil. Soils* 48, 973–979. doi:10.1007/s00374-012-0709-y

Pachauri, R. K., Allen, M. R., Barros, V. R., Broome, J., Cramer, W., Christ, R., et al. (2014). "Climate Change 2014: Synthesis Report," in *Contribution of Working Groups I, II and III to the Fifth Assessment Report of the Intergovernmental Panel on Climate Change*. Editors R. K. Pachauri and L. Meyer, Available at: https://epic.awi.de/id/eprint/37530/.

Pilegaard, K. (2013). Processes Regulating Nitric Oxide Emissions from Soils. *Phil. Trans. R. Soc. B* 368, 20130126. doi:10.1098/rstb.2013.0126

Priemé, A., and Christensen, S. (2001). Natural Perturbations, Drying-Wetting and Freezing-Thawing Cycles, and the Emission of Nitrous Oxide, Carbon Dioxide and Methane from Farmed Organic Soils. *Soil Biol. Biochem.* 33, 2083–2091. doi:10.1016/s0038-0717(01)00140-7

Ravishankara, Daniel., Daniel, J. S., and Portmann, J. S. (2009). Nitrous Oxide (N2O): The Dominant Ozone-Depleting Substance Emitted in the 21st Century. 326, 4.doi:10.1126/science.1176985

Shang, Z., Abdalla, M., Kuhnert, M., Albanito, F., Zhou, F., Xia, L., et al. (2020). Measurement of N2O Emissions over the Whole Year Is Necessary for Estimating Reliable Emission Factors. *Environ. Pollut.* 259, 113864. doi:10.1016/j.envpol.2019.113864

Shang, Z., Zhou, F., Smith, P., Saikawa, E., Ciais, P., Chang, J., et al. (2019). Weakened Growth of cropland-N 2 O Emissions in China Associated with Nationwide Policy Interventions. *Glob. Change Biol.* 25, 3706–3719. doi:10.1111/gcb.14741

Skiba, U., Smith, K. A., and fowler, D. (1993). Nitrification and Denitrification as Sources of Nitric Oxide and Nitrous Oxide in a Sandy Loam Soil. *Soil Biol. Biochem.* 25, 1527–1536. doi:10.1016/0038-0717(93)90007-x

Smith, K. A., and Dobbie, K. E. (2001). The Impact of Sampling Frequency and Sampling Times on Chamber-Based Measurements of N2 O Emissions from Fertilized Soils. *Glob. Change Biol.* 7, 933–945. doi:10.1046/j.1354-1013.2001.00450.x

Stehfest, E., and Bouwman, L. (2006). N2O and NO Emission from Agricultural Fields and Soils under Natural Vegetation: Summarizing Available Measurement Data and Modeling of Global Annual Emissions. *Nutr. Cycl Agroecosyst* 74, 207–228. doi:10.1007/s10705-006-9000-7

Teepe, R., Brumme, R., and Beese, F. (2001). Nitrous Oxide Emissions from Soil during Freezing and Thawing Periods. *Soil Biol. Biochem.* 33, 1269–1275. doi:10.1016/s0038-0717(01)00084-0

Tian, H., Xu, R., Canadell, J. G., Thompson, R. L., Winiwarter, W., Suntharalingam, P., et al. (2020). A Comprehensive Quantification of Global Nitrous Oxide Sources and Sinks. *Nature* 586, 248–256. doi:10.1038/s41586-020-2780-0

Van, B. E., Prévost, D., and Pelletier, F. (2000). Effects of Freeze–Thaw and Soil Structure on Nitrous Oxide Produced in a Clay Soil. *Soil Sci. Soc. America J.* 64, 1638–1643. doi:10.2136/sssaj2000.6451638x

Wagner-Riddle, C., Congreves, K. A., Abalos, D., Berg, A. A., Brown, S. E., Ambadan, J. T., et al. (2017). Globally Important Nitrous Oxide Emissions from Croplands Induced by Freeze-Thaw Cycles. *Nat. Geosci.* 10, 279–283. doi:10.1038/ngeo2907

Wang, J., Song, C., Hou, A., Miao, Y., Yang, G., and Zhang, J. (2014). Effects of Freezing-Thawing Cycle on Peatland Active Organic Carbon Fractions and Enzyme Activities in the Da Xing'anling Mountains, Northeast China. *Environ. Earth Sci.* 72, 1853–1860. doi:10.1007/s12665-014-3094-z

Wolf, B., Zheng, X., Brüggemann, N., Chen, W., Dannenmann, M., Han, X., et al. (2010). Grazing-induced Reduction of Natural Nitrous Oxide Release from Continental Steppe. *Nature* 464, 881–884. doi:10.1038/nature08931

Xia, L., Lam, S. K., Chen, D., Wang, J., Tang, Q., and Yan, X. (2017). Can Knowledge-Based N Management Produce More Staple Grain with Lower Greenhouse Gas Emission and Reactive Nitrogen Pollution? A Meta-Analysis. *Glob. Change Biol.* 23, 1917–1925. doi:10.1111/gcb.13455

Yan, G., Yao, Z., Zheng, X., and Liu, C. (2015). Characteristics of Annual Nitrous and Nitric Oxide Emissions from Major Cereal Crops in the North China Plain under Alternative Fertilizer Management. *Agric. Ecosyst. Environ.* 207, 67–78. doi:10.1016/j.agee.2015.03.030

Yanai, Y., Hirota, T., Iwata, Y., Nemoto, M., Nagata, O., and Koga, N. (2011). Accumulation of Nitrous Oxide and Depletion of Oxygen in Seasonally Frozen Soils in Northern Japan - Snow Cover Manipulation Experiments. *Soil Biol. Biochem.* 43, 1779–1786. doi:10.1016/j.soilbio.2010.06.009

Yao, Z., Yan, G., Wang, R., Zheng, X., Liu, C., and Butterbach-Bahl, K. (2019). Drip Irrigation or Reduced N-Fertilizer Rate Can Mitigate the High Annual N2O+NO Fluxes from Chinese Intensive Greenhouse Vegetable Systems. *Atmos. Environ.* 212, 183–193. doi:10.1016/j.atmosenv.2019.05.056

Zhang, X., Meng, F., Li, H., Wang, L., Wu, S., Xiao, G., et al. (2019). Optimized Fertigation Maintains High Yield and Mitigates N2O and NO Emissions in an Intensified Wheat-Maize Cropping System. *Agric. Water Management* 211, 26–36. doi:10.1016/j.agwat.2018.09.045

Zhang, Y., Liu, J., Mu, Y., Pei, S., Lun, X., and Chai, F. (2011). Emissions of Nitrous Oxide, Nitrogen Oxides and Ammonia from a Maize Field in the North China Plain. *Atmos. Environ.* 45, 2956–2961. doi:10.1016/j.atmosenv.2010.10.052

Zhao, M., Tian, Y., Ma, Y., Zhang, M., Yao, Y., Xiong, Z., et al. (2015). Mitigating Gaseous Nitrogen Emissions Intensity from a Chinese Rice Cropping System through an Improved Management Practice Aimed to Close the Yield Gap. *Agric. Ecosyst. Environ.* 203, 36–45. doi:10.1016/j.agee.2015.01.014

Conflict of Interest: The authors declare that the research was conducted in the absence of any commercial or financial relationships that could be construed as a potential conflict of interest.

frontiers in Environmental Science

REVIEW
published: 17 May 2021
doi: 10.3389/fenvs.2021.660055

Microbial Small RNAs – The Missing Link in the Nitrogen Cycle?

*Sophie Moeller[1], Gloria Payá[2], María-José Bonete[2], Andrew J. Gates[1], David J. Richardson[1], Julia Esclapez[2] and Gary Rowley[1]**

[1]School of Biological Sciences, University of East Anglia, Norwich Research Park, Norwich, United Kingdom, [2]Agrochemistry and Biochemistry Department, Biochemistry and Molecular Biology Division, Faculty of Science, University of Alicante, Alicante, Spain

Non-coding small RNAs (sRNAs) regulate a wide range of physiological processes in microorganisms that allow them to rapidly respond to changes in environmental conditions. sRNAs have predominantly been studied in a few model organisms, however it is becoming increasingly clear that sRNAs play a crucial role in environmentally relevant pathways. Several sRNAs have been shown to control important enzymatic processes within the nitrogen cycle and many more have been identified in model nitrogen cycling organisms that remain to be characterized. Alongside these studies meta-transcriptomic data indicates both known and putative sRNA are expressed in microbial communities and are potentially linked to changes in environmental processes in these habitats. This review describes the current picture of the function of regulatory sRNAs in the nitrogen cycle. Anthropogenic influences have led to a shift in the nitrogen cycle resulting in an increase in microbial emissions of the potent greenhouse gas nitrous oxide (N_2O) into the atmosphere. As the genetic, physiological, and environmental factors regulating the microbial processes responsible for the production and consumption of N_2O are not fully understood, this represents a critical knowledge gap in the development of future mitigation strategies.

Keywords: denitrification, biogeochemical cycles & processes, *Paracoccus denitrificans*, sRNA, nitrous oxide, nitrogen cycle

OPEN ACCESS

Edited by:
Yupeng Wu,
Huazhong Agricultural University, China

Reviewed by:
Patrick Sorensen,
Lawrence Berkeley National Laboratory, United States
Britt Dianne Hall,
University of Regina, Canada

****Correspondence:***
Gary Rowley
g.rowley@uea.ac.uk

Specialty section:
This article was submitted to Biogeochemical Dynamics, a section of the journal Frontiers in Environmental Science

Received: *28 January 2021*
Accepted: *28 April 2021*
Published: *17 May 2021*

Citation:
Moeller S, Payá G, Bonete M-Jé, Gates AJ, Richardson DJ, Esclapez J and Rowley G (2021) Microbial Small RNAs – The Missing Link in the Nitrogen Cycle? Front. Environ. Sci. 9:660055. doi: 10.3389/fenvs.2021.660055

INTRODUCTION

Microorganisms are required to sense, respond to and recover from changes in their external environment such as fluctuations in nutrient availability. To thrive under stressful conditions, complex transcriptional regulatory networks fine tune the expression of a variety of genes. Besides transcriptional regulators and the use of alternative sigma factors, gene regulation also involves short regulatory RNAs (sRNAs). These sRNAs are heterogenous in length, sequence composition and secondary structures and modulate a vast range of regulatory circuits required for the cellular response to spatio-temporal changes. The abundance of sequenced bacterial and archaeal genomes alongside the availability of improved sequencing and computational tools has led to a boost in the discovery of sRNAs, making it a fast and exciting area of research. Many of the discovered sRNAs regulate major biological processes such as stress responses by binding to target regions, called seed regions, in the mRNA. This can result in either the activation or the repression of gene expression at the posttranscriptional level (**Figure 1**) (Wassarman, 2002; Dutta and Srivastava, 2018). sRNAs can originate from within a gene of interest or be processed from the 5′ or 3′ untranslated regions (Bossi and Figuera-Bossi, 2016). Many are then further processed by RNase E to produce sRNA fragments. This can be observed in the processing of RoxS in *Bacillus subtilis* resulting in an expanded repertoire

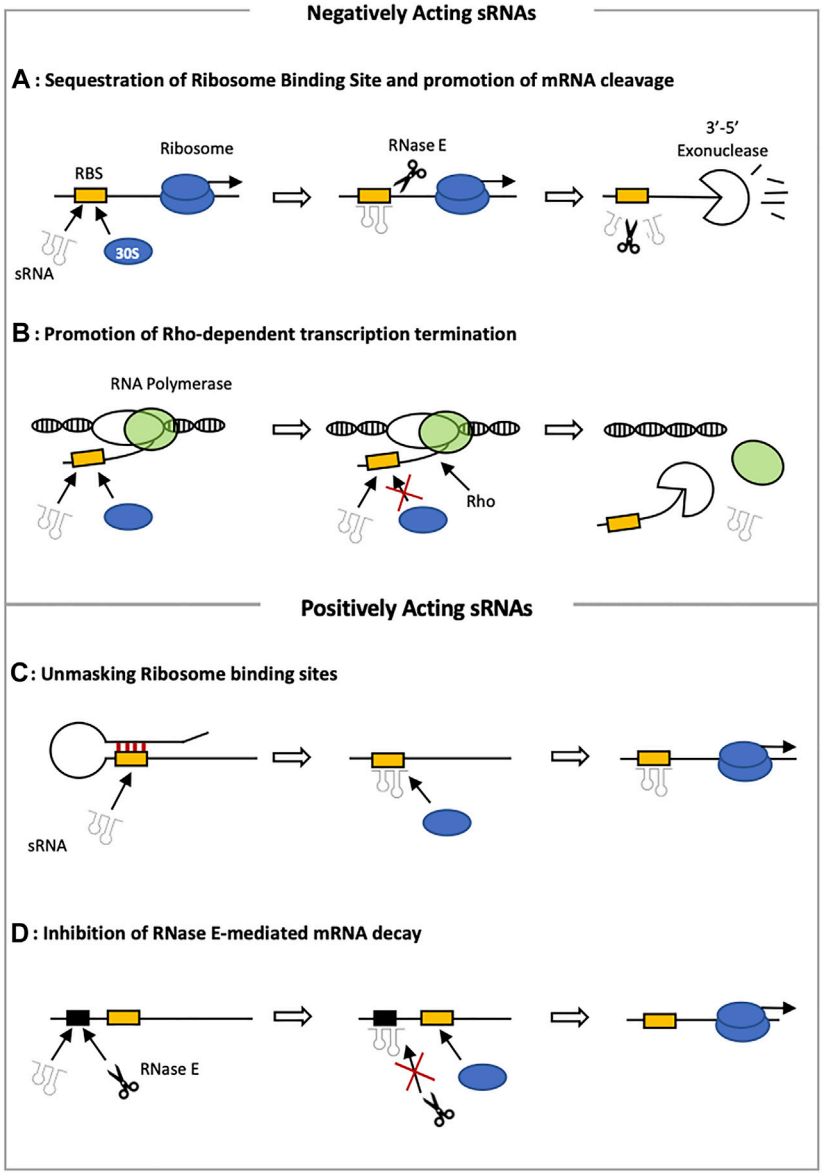

FIGURE 1 | Mechanisms of sRNA induced gene repression and activation. **(A)** When the sRNA target sequence overlaps with the ribosome binding site (RBS) translation initiation is blocked. This leaves the RNA more susceptible to RNase-mediated decay. **(B)** Alternatively, sRNAs can enhance Rho-binding and subsequently cause premature termination of transcription. **(C)** Positively acting sRNAs can bind to hairpin-like structures in their target, causing conformational changes to expose a previously inaccessible RBS and stimulate translation initiation. **(D)** Lastly, sRNAs are able to mask RNase E sites to stabilize their target and activate expression.

of target mRNAs (Durand et al., 2015). This review will present the regulatory circuits controlling the nitrogen cycle, discuss the emerging role of sRNAs in these regulatory networks and point towards the potential applications of sRNAs in the field.

Interactions of sRNAs and their targets rely on base-pairings between complementary sequences (Georg et al., 2019). There are two classes of sRNAs–*cis*-encoded and *trans*-encoded sRNAs. *Cis*-encoded sRNAs are transcribed from the DNA strand complementary to the one from which the target mRNA is transcribed resulting in high levels of complementarity. *Trans*-encoded sRNAs however, are transcribed from regions unrelated to those of their target genes often resulting in reduced complementarity (Gottesman, 2005; Bossi and Figuera-Bossi, 2016; Dutta and Srivastava, 2018). Due to a lower level of complementarity, *trans* encoded sRNAs can form base pairing with multiple target mRNAs and result in a global regulation of a physiological response. sRNA base-pairing with the target is initiated through fast, high affinity binding of a few exposed nucleotides in the stem loop of the sRNA. This initial interaction promotes pairing of additional nucleotides, which frequently

results in alterations to the RNA secondary structure (Otaka et al., 2011; Dutta and Srivastava, 2018). Structure-driven pairing of sRNAs and their targets in which the sRNA recognizes C-rich stretches within accessible loops of the mRNA has also been demonstrated (Storz et al., 2011). Often, *trans*-encoded sRNAs require the presence of an RNA chaperone to facilitate binding to their target mRNA as their sequences are unrelated (Wagner, 2013). In enteric pathogenic bacteria, such as *E. coli* and *Salmonella,* sRNAs have already been particularly well studied and many are associated with pathogenicity (Bossi and Figuera-Bossi, 2016).

The Role of RNA Chaperones in sRNA-mRNA Interactions

The RNA chaperone Hfq is an Sm-like (Lsm) protein in the shape of a homohexameric ring, which can bind both sRNA and mRNA. Lsm proteins play key roles in RNA metabolism in Eukaryotes, Bacteria and Archaea. Hfq was first identified in *E. coli*, in which it acts as a host factor for the replication of the bacteriophage Qβ (Franze de Fernandez et al., 1968). Binding of Hfq acts to protect free sRNA from degradation by the cellular degradosome and increases local mRNA and sRNA concentrations, but Hfq can also recruit the degradosome to induce accelerated decay of the sRNA-mRNA complex (Georg et al., 2019). Most *trans*-encoded sRNAs contain a 3′-stem loop, which allows anchoring of the sRNA to Hfq *via* interactions of poly (U) to the inner rim of the Hfq homohexamer (Otaka et al., 2011). The molecular mechanism of Hfq action has been explained in detail for its role in positive regulation of *rpoS* mRNA by the sRNA DsrA in *E. coli* (McCullen et al., 2010). Multilateral interactions between Hfq and the mRNA are formed distorting the mRNA structure to a more compact form, which facilitates binding of the sRNA (McCullen et al., 2010; DeLay and Gottesman, 2011). The binding of the RNA chaperone to a sequence motif in *rpoS* mRNA results in correct positioning of Hfq and is therefore essential for the pairing of this sRNA to its target mRNA. It is also hypothesized that Hfq increases the local concentration of RNAs, increasing the likelihood of sRNA-mRNA pairing (De Lay et al., 2013).

In addition to Hfq, recent studies have revealed the existence of a second RNA chaperone, ProQ, that can be found additionally to Hfq in *Salmonella* Typhimurium and *E. coli.* ProQ has been shown to facilitate binding of sRNAs and their targets, the molecular mechanism for this is however unknown (Smirnov et al., 2016; Smirnov et al., 2017; Westermann et al., 2019). In *Salmonella,* a loss of this chaperone results in a loss of virulence, as ProQ controls the expression of genes involved in motility, chemotaxis as well as SPI-1 transcripts (Westermann et al., 2019). The FinO domain of ProQ as well as other chromosomally encoded proteins containing a FinO domain are equally grouped as an additional class of bacterial RNA chaperones (Oleiniczak and Storz, 2017).

Interactions between Lsm proteins and sRNAs have also been observed in Archaea. Some, including halophilic archaea, encode a single Lsm protein (Lsm1), while others encode two Lsm proteins (Lsm1 and Lsm2) (Fischer et al., 2010). Lsm1 proteins form heptamers capable of binding DNA. Lsm2 proteins have been shown to associate to hexameric or heptameric complexes in *Archaeoglobus fulgidus* (Kilic et al., 2006). Crenarchaeota contain a third Lsm3 protein which forms 14-mer complexes. Interestingly the archaeon *Methanocaldococcus jannaschii* lacks an archaeal Lsm gene and instead contains an Hfq-like protein (Sauter et al., 2003; Nielsen et al., 2007; Vogel and Luisi, 2011). Lsm crystal structures obtained from *Archaeoglobus fulgidus* and *Pyrococcus abyssi* show that they are able to bind U-rich RNA in a similar way to Hfq (Töro et al., 2001; Törö et al., 2002; Thore et al., 2003). Binding of Lsm proteins to U-rich stretches was also observed in the crenarchaeum *Sulfolobus solfataricus* (Märtens et al., 2017), However, despite *in vivo* confirmation of the interaction of FLAG-tagged archaeal Lsm protein and sRNAs, the physiological functions remain poorly understood (Fischer et al., 2010; Märtens et al., 2015).

Mechanisms of Gene Repression by sRNA

Regulatory sRNAs can directly or indirectly affect the expression of single or multiple genes. In numerous examples, sRNA binding results in blocking of the ribosome binding site (RBS), subsequent inhibition of translation initiation as well as mRNA cleavage *via* RNAse E and Rho-dependent transcription termination (Storz et al., 2004; **Figures 1A,B**). Binding of an sRNA within the physical boundary of the RBS of the target mRNA prevents entry of the 30S ribosomal subunit and therefore blocks translation initiation (**Figure 1A**) (Udekwu et al., 2005; Morita et al., 2006; Bouvier et al., 2008). Many sRNAs repress their targets by masking the Shine Dalgarno (SD) sequence or the AUG start codon. This mechanism is utilized by the sRNA RhyB found in *E. coli*. RhyB downregulates Fe-storage and non-essential Fe-binding proteins when iron availability is limited (Masse and Gottesman, 2002; Dutta and Srivastava, 2018). Absence of iron increases RhyB expression, which interferes with the binding of the 30S subunit to the RBS of the target mRNAs. An interaction of RhyB with Hfq can also result in the repression of the enzyme methionine sulfoxide reductase by binding to two sites on *msrB* mRNA. Binding to the first site stops ribosome entry at the RBS whereas binding to the second site results in a recruitment of RNase E (Bos et al., 2013; Dutta and Srivastava, 2018). Other sRNAs, such as OxyS, however can bind as far downstream as the 5th codon, without any interaction with the SD or the start codon (Bouvier et al., 2008). When ribosome entry sites are blocked, it is possible for the 30S subunit to bind to 'Standby regions', which are located 100 nucleotides upstream of the translation initiation site (Darfeuille et al., 2007). This mechanism is followed by the *cis*-acting sRNA Isr-1 in *E. coli* and does not require the presence of an Hfq chaperone (Darfeuille et al., 2007).

In addition to the blocking of ribosome entry sites, base pairing of an sRNA and its target at either the 5′UTR region or at downstream coding sequences can also lead to recruitment of ribonucleases such as RNase E. In prokaryotes, RNase E is a crucial ribonuclease responsible for the turnover of sRNAs and mRNAs (Chao et al., 2017). In some cases, Hfq can act as a protective layer against RNase E degradation by stabilizing the sRNA and promoting base-pairing with the target. It has also

been shown that Hfq has the capacity to directly bind to an unstructured C-terminal domain within RNase E forming a ribonucleoprotein with the sRNA that induces mRNA decay (Morita et al., 2005). The involvement of RNase E in sRNA induced gene repression has been confirmed for a large number of sRNAs such as RhyB and SgrS in *E. coli*.

Attenuation of transcription is a final mechanism of sRNA-induced gene repression. An example of this is the repression of the virulence gene *icsA* by the sRNA, RnaG, in *Shigella flexneri* (Giangrossi et al., 2010). The promoter of both the RnaG sRNA and the *icsA* virulence gene are convergent and lie less than 120bp apart. Hetero-duplex formation of the sRNA and its target gene results in a conformational change generating an intrinsic terminator that blocks the movement of RNA polymerase and thus attenuating *icsA* transcription.

Mechanisms of sRNA-Induced Gene Activation

sRNAs are also able to mediate activation of genes involved in a wide array of physiological processes (Frohlich and Vogel, 2009; Dutta and Srivastava, 2018). One mechanism of gene activation is the stabilization of target mRNAs by protecting them from degradation by cellular RNases (**Figure 1D**). This has been observed for the glucose phosphate stress induced sRNA SgrS found in *E. coli* and *Salmonella* (Vanderpool and Gottesman, 2007). Binding of SgrS to its target mRNA *pldB-yigL* masks an RNase E site within the *pldB* open reading frame and facilitates production of the YigL phosphatase (Papenfort et al., 2013). Often, the secondary structure of mRNAs sequesters the ribosome binding site, which can be liberated for protein synthesis through pairing with an sRNA (**Figure 1C**). This process is also referred to as 'anti-antisense' mechanism. This activation of the 5′ UTR was first discovered for the sRNA, RNAIII, in *Staphylococcus aureus* (Morfeldt et al., 1995). RNAIII is regulated by cell density through quorum sensing and activates the *hla* gene, which encodes an α-Toxin (Novick and Geisinger, 2008; Papenfort and Vanderpool, 2015). Activation is achieved through an interaction of the 5′-end of the sRNA and the SD-sequence of the target, preventing the formation of a translation-inhibitory structure formation. This 'anti-antisense' mechanism can also be observed in the activation of the sigma factor σ^S in *E. coli*. As the 5′ UTR of the σ^S-mRNA (*rpoS*) is unusually long, it forms a complex hairpin structure, making it inaccessible for ribosomal entry (Battesti et al., 2011). Several sRNAs (DsrA, RprA, ArcZ) are able to bind to specific sections within the 5′ UTR to rearrange the structure and enhancing the rate of σ^S translation (Bossi and Figuera-Bossi, 2016).

In addition to the anti-antisense mechanism observed in *rpoS* activation, a unique transcription anti-termination system has been discovered to play a crucial role in inhibiting Rho-dependent transcription termination in the 5′ UTR of *rpoS* (Sedlyarova et al., 2016). Rho is a hexameric helicase protein and together with its cofactor NusG it acts as a global transcription termination factor in prokaryotes (Boudvillain et al., 2013). Rho binds to a stretch of C-rich unstructured RNA that is around 80 nucleotides in length and is located near the transcription terminator. After mRNA binding, Rho atpase activity is stimulated. Under specific circumstances, Rho also appears to be active in the 5′ UTR, which induces premature termination of transcription. Within *rpoS,* one of these Rho loading sites can be found in the leader sequence. Binding of an sRNA close to this Rho-loading site blocks binding of Rho and enhances transcription and protects from cleavage induced by RNase E (**Figure 1D**) (McCullen et al., 2010). Hfq further increases the stability of the sRNA-*rpoS* interaction.

In some cases, sRNA can positively regulate expression of an open reading frame (ORF) through interactions with its 5′ UTR that can result in a subsequent upregulation of a different cistron of the mRNA which is translationally coupled to the ORF (Dutta and Srivastava, 2018). In *Pseudomonas aruginosa,* the oxygen-responsive sRNA PhrS activates the *ufo-pqsR* operon in the absence of oxygen (Sonnleitner et al., 2011). The transcriptional regulator PqsR controls the expression of several virulence genes in *P. aeruginosa* including the toxic pigment pyocyanin (PYO) and the quorum sensing and biofilm formation signal PQS. PhrS binds to the 5′ region of *ufo* which results in conformational change liberating the RBS. As *ufo* is translationally coupled to *pqsR,* the presence of sRNA PhrS eventually results in enhanced translation of PqsR and increased levels of PYO and PQS (Sonnleitner et al., 2011).

sRNA Induced Protein Sequestration

Certain sRNAs have the ability to directly sequester RNA-binding proteins inhibiting them from carrying out their functions or bind enzymatic proteins to inhibit or modify their enzymatic activity. Therefore, these sRNAs can indirectly regulate the expression of many genes related to this protein. The RNA-binding protein CsrA is a post-transcriptional regulator that has multiple targets, which include several genes involved in carbon flux pathways (Babitzke and Romeo, 2007). The presence of sRNAs such as CsrB results in an inactivation of CsrA activity as CsrB acts as a direct competitor for the CsrA target mRNAs in the cell removing its function and changing the expression level of a large number of genes. Inhibition of a protein's enzymatic activity can be observed for sRNA 6S which binds to RNA polymerase in bacteria interfering with σ^{70}-induced transcription (Wassarman and Storz, 2000). Production of 6S is maximized during stationary phase and as a result the expression of several genes is reprogrammed to allow the cell to adapt to the given environmental conditions. The RNase BN/Z facilitates 6S RNA decay (Chen et al., 2016).

The Role of sRNAs in Physiological Responses

As sRNAs are significantly smaller than mRNAs and do not require translation into a protein, they have a potential energetic advantage over the production of protein transcription factors (Beisel and Storz, 2010). sRNA copy number within the cell can also be very high while their turnover time is short, resulting in a sharp deterioration of sRNA numbers once they have exerted their rapid and effective function in response to an environmental signal. This suggests that sRNA could be crucial in the rapid

adaptation to dramatic shocks such as sudden nutrient change that challenge the survival of the microorganism. As more advances are made in sRNA research, the more mechanisms are discovered that demonstrate the diverse mechanisms of action of sRNAs and their association with a large variety of physiological processes.

It is becoming more and more clear that cell communication during quorum sensing and biofilm formation is regulated by sRNAs. To react to changes in cell density *V. cholerae* possesses two-component membrane-bound sensor kinases. At low cell density, the response regulator LuxO is phosphorylated and activates the expression of five sRNAs that regulate the expression of genes involved in virulence and biofilm formation (Bardill et al., 2011; Michaux et al., 2014). In pathogenesis, sRNAs often modulate expression levels of outer membrane proteins which are targets for the immune system, as well as other responses required for the survival within the host. Members of the CsrB family of sRNAs in *Salmonella, Yersinia, Vibrio* and other pathogenic bacteria have already proven to alter infection by antagonizing global regulators of virulence genes (Waters and Storz, 2009). Other sRNAs are involved in the adaptation to nutrient availability. Switches between nutrient availability and starvation trigger major changes in gene expression and require a coordination of regulatory networks. In *E. coli*, the sRNA SgrR modulates the response to an accumulation of glucose 6-phosphate which is toxic when present at high concentrations (Vanderpool and Gottesman, 2004). Besides biofilm formation and pathogenesis, many of the known sRNAs are involved in stress responses such as oxidative stress, osmotic stress and the switch between aerobic and anaerobic metabolism.

THE GLOBAL NITROGEN CYCLE

Although the focus of sRNA studies has predominantly been on key model bacteria, with a particular focus on stress responses and pathogenesis, it is becoming clear that sRNAs also play a crucial role in environmentally relevant pathways. Biogeochemical cycles are critical to all forms of life on earth. They describe the dynamic transformation of energy and matter from different reservoirs including the atmosphere, the oceans, the terrestrial biosphere and the geosphere into usable forms that support the optimal function of all ecosystems. The major biotic drivers of these transformations are plants and microorganisms. Most of the naturally occurring organic compounds required for the existence of life contain the life sustaining elements carbon (C), hydrogen (H) and one or more of the elements: nitrogen (N), oxygen (O), phosphorus (P) and sulfur (S) (Brusseau, 2019). Cycling of these key elements through the different reservoirs is interconnected *via* anabolic and catabolic processes including photosynthesis, assimilation, respiration and decomposition (Brusseau, 2019). An example of this strong interconnection of the cycles is the use of reduced carbon forms in anoxic habitats which can be oxidized, creating an electron flow eventually utilized by microbes in respiration to reduce, for example, nitrate to atmospheric N_2 (denitrification), to reduce sulfate to sulfite (sulfate reduction) or to reduce carbon dioxide (CO_2) to methane (methanogenesis) (Madsen, 2011). Mineral metal oxide respiration such as Fe(III) and Mn(IV) are major drivers in organic carbon oxidation and therefore also influence nitrogen and sulfur cycles (Richardson et al., 2012). Perturbations to a single biogeochemical cycle can therefore have detrimental effects on all other cycles leading to changes in the health and function of ecosystems. Anthropogenic influences such as the combustion of fossil fuels and the use of synthetic fertilisers have already caused significant imbalance to the global P and N cycles. An understanding of the structure, function and regulation of the biogeochemical processes in a changing climate is crucial to determine future mitigation strategies.

The nitrogen cycle has already experienced a global scale perturbation. Nitrogen gas (N_2) constitutes 78% of the Earth's atmosphere. However, the gaseous form of nitrogen cannot be accessed by the majority of living organisms. Atmospheric N_2 is only accessible to microorganisms, the N_2-fixing Bacteria and Archaea, which are estimated to biologically fix approximately 0.1% of the N_2 pool (Vitousek and Howarth, 1991). Once fixed by these microorganisms, nitrogen becomes available to plants and animals. With the discovery of the Haber-Bosch process at the beginning of the 20th century it became possible to industrially fix the atmospheric nitrogen converting N_2 into reactive N-forms (Chen et al., 2019). Most of the industrially fixed nitrogen is utilized to produce nitrogen rich fertilizers used in agriculture to feed the ever-growing world population. It was estimated that in 2002, over half of the world's population consumed food produced with N fixed *via* the Haber-Bosch process (Smil, 2002). Despite their importance, the application of these fertilizers can cause huge environmental concerns and major changes to the balance of the biogeochemical nitrogen cycle (Richardson et al., 2009). Large quantities of reactive nitrogen from fertilisers are lost to the environment due to runoff, or as gaseous products, which can cause soil acidification as well as increased emissions of the greenhouse gas nitrous oxide (N_2O). N_2O has a global warming potential almost 300 times higher than CO_2 (Galloway and Cowling, 2002). Since the beginning of industrialization, the atmospheric loading of N_2O has increased by over 20% and subsequently it has been listed as one of six gases subjected to restriction in the Kyoto protocol (Richardson et al., 2009; Smith et al., 2012; Prinn et al., 2018). The Intergovernmental Panel on Climate Change (IPCC) estimates that one third of the total global N_2O emissions are a result of anthropogenic activities, with agriculture accounting for the largest fraction (Stocker et al., 2013). The economic costs as a result of nitrogen pollution across Europe are estimated to range from 70 to 320 billion euros a year, mainly due to reduced air and water quality (Sutton et al., 2011).

The nitrification pathway is responsible for the conversion of ammonium to nitrite. Nitrates and nitrites are a natural component of plant material, however an increase in nitrite from fertilisers can lead to accumulation of nitrate in vegetable tissue (Renseigne et al., 2007). High levels of nitrate in food are responsible for methemoglobinemia (blue baby syndrome) in young children (Chan, 2011). Additionally, increased conversion of ammonium can lead to a loss of soil nitrogen through leaching

which results in a wastage of fertiliser and water pollution through eutrophication of rivers and lakes (Robertson and Vitousek, 2009; Sutton et al., 2011). In freshwater ecosystems, the levels of nitrite are continuously increasing due to industrial effluents from industries producing metals, dyes, sewage aquaculture and runoff from agricultural soils supplemented with nitrogen fertilisers (Van Maanen et al., 1996; Jensen 2003). As nitrite is rapidly oxidized to nitrate (NO_3^-), NO_3^- is often the predominant N-form found in ground- and surface waters. Elevated levels of nitrite in both sea and fresh-water environments have detrimental effects on aquatic animals by interfering with multiple physiological functions such as ion regulation, respiration and the cardiovascular system (Jensen et al., 2003). Biological removal of both nitrate and nitrite from aquatic environments can be achieved aerobically through the processes of nitrate or nitrite assimilation or anaerobically *via* denitrification. Microorganisms and plants are responsible for the transformation of more than 10^4 megatons of inorganic nitrogen per year *via* the process of assimilatory nitrate reduction (Guerrero et al., 1981).

The production of N_2O in the soil is primarily attributed to the microbial processes of nitrification and denitrification, although under certain environmental conditions such as nitrate-sufficiency and nitrite accumulation, dissimilatory nitrate and nitrite reduction to ammonium may well significantly contribute to N_2O production (Rowley et al., 2012; Stremińska et al., 2012). However, the denitrification process is the only known biological process physiologically capable of the consumption of this greenhouse gas (Bernhard, 2010), putting aside the non-physiological reduction of N_2O by nitrogenase (Hoch et al., 1960). Complete denitrification is a sequential four-step reduction of soluble nitrogen oxides nitrate and nitrite to the gaseous nitrogen oxides nitric oxide, nitrous oxide and dinitrogen, which takes place in the absence of oxygen (Zumft and Kroneck, 2007). The enzymes catalyzing these reactions are nitrate reductase, nitrite reductase, nitric oxide reductase and the periplasmic nitrous oxide reductase respectively. As the denitrification process is a modular pathway, some organisms are capable of completely reducing NO_3^- to nitrogen gas while others may lack one or several of the enzymes required for the other steps involved in the reduction cascade (Philippot et al., 2002). The nitrous oxide reductase (NosZ) protein phylogeny has two distinct groups – clade I, and the recently discovered clade II (Jones et al., 2013; Hallin et al., 2018)). The two clades differ not only in protein phylogeny but also in the *nos* gene cluster organization, the NosZ translocation pathway as well as the frequency of co-occurrence with other denitrification genes. Clade I organisms are complete denitrifiers which also possess *nirS* or *nirK* genes encoding for nitrite reductase (Jones et al., 2013; Conthe et al., 2018). The majority of the clade II organisms lack complete denitrification machinery and appear to be non-denitifying N_2O reducers capable of consuming N_2O without contributing to its production, making these organisms of significant interest as they may be potential N_2O sinks in the

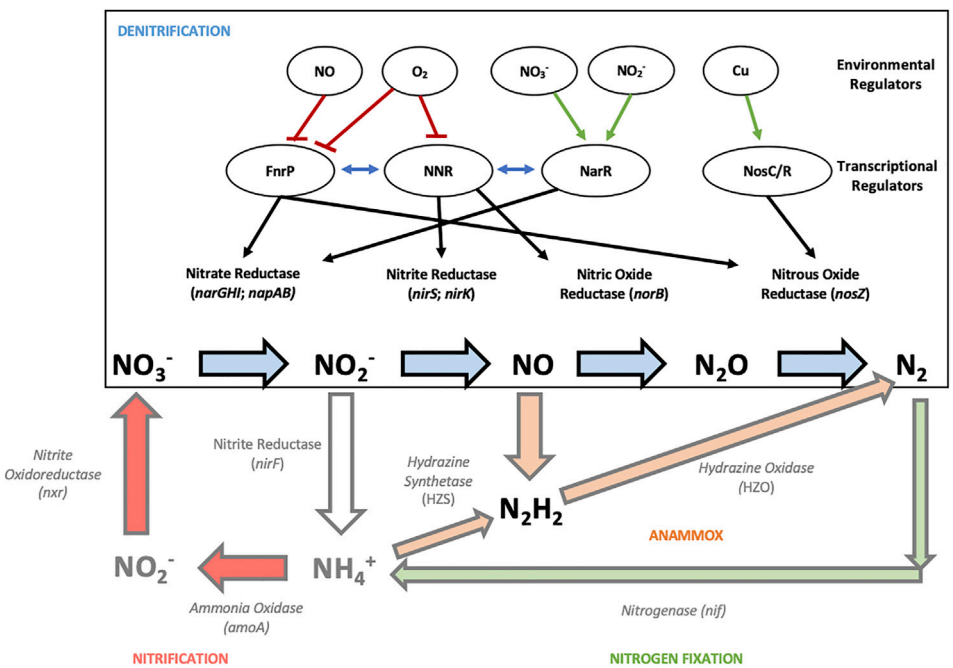

FIGURE 2 | An overview of the known transcriptional and environmental regulators of the denitrification pathway in the model denitrifying bacterium *Paracoccus denitrificans*. The black and red arrows between the upper layer of the environmental regulatory signals and the layer of the regulatory proteins indicate signaling events (red indicates an inhibitory effect while green indicates activation), while the arrows between the regulatory proteins and the denitrification enzymes indicate regulation of gene expression. The blue arrows between the transcriptional regulators indicate the cross-talk between the regulators which compete with each other to bind upstream of their targets.

environment. Despite the pressing need to develop mitigation strategies to combat the ever-increasing N_2O emissions, we still do not fully understand the regulatory network underlying the microbial reaction pathways responsible for the production and consumption of this greenhouse gas. An enhanced understanding of the ecology of the *nosZ* clade II organisms as well as the conditions under which their activity is favored is needed (Domeignoz-Horta et al., 2016). This includes an increased knowledge regarding sRNA content and activity in these organisms.

An Overview of Transcriptional Regulation of the Nitrogen Cycle

Bacteria and Archaea have developed a range of strategies allowing the uptake and utilization of various nitrogen sources from their environment. These processes are tightly regulated in response to environmental conditions to ensure the correct temporo-spatial control of the pathways and minimize any inappropriate energetic costs as well as maximize the competitive growth advantage. Biological nitrogen fixation is a crucial process providing an input of fixed nitrogen into soils and therefore directly affecting natural ecosystem productivity (Dixon and Kahn, 2004). Nitrogen fixing Bacteria and Archaea are found in a wide variety of habitats including soil and marine environments. The enzyme required for the fixation of nitrogen, nitrogenase (*nif*), is ATP-dependent as well as highly oxygen sensitive and is therefore tightly regulated in response to fixed nitrogen, carbon, energy and extracellular oxygen levels (Dixon and Kahn, 2004). Thus, in the model *K. pneumoniae* the transcription of the *nif* genes is under the regulation of the global two-component system *ntrBC* (Dixon et al., 1986). In the absence of nitrogen NtrB phosphorylates NtrC which subsequently activates the transcription of *nifA* which then modulates the expression of numerous other *nif* genes. The *nifA* gene is co-transcribed with *nifL* which encodes a nitrogen-responsive flavoprotein acting as a negative regulator of NifA. This co-transcription adds an additional level of nitrogenase regulation in response to changing oxygen levels and nitrogen fixation (Halbleib and Ludden, 2000). Variations of this core regulatory mechanism are found in many nitrogen fixing microorganisms. In response to changing levels of oxygen in diazotrophic *Proteobacteria*, the transcription of *nif* genes depends on the alternative sigma factor σ^{54} whose activation requires NifA, an enhancer binding protein. NifA transcription is directly oxygen-responsive in these bacteria. In other diazotrophs, NifA is not directly regulated by oxygen levels and instead its activity is regulated by the flavoprotein NifL (Martinez-Argudo et al., 2004). Another protein shown to be involved in the regulation of *nif* genes is the histidine kinase RegB which can respond to the cellular redox status through an active cysteine. RegB is found in *Rhodobacter capsulatus* in which it binds to the *nifA2* promoter providing an additional layer of redox control (Elsen et al., 2004) Little is known about regulation of nitrogen fixation in archaea. The best studied examples of regulation in nitrogen fixing archaea are the methanogenic models *Methanococcus maripaludis* and *Methanosarzina mazei*. Under nitrogen sufficient conditions in these methanoarchaea, the global regulator NrpR regulates target gene expression by binding to the corresponding operator and blocking the recruitment of the RNA polymerase. Depletion of extracellular nitrogen levels result in an increased production of intracellular 2-oxoglutarate which binds to NrpR causing it to release its target promoters. Homologues of this regulator have been found across many other archaeal species (Dixon and Kahn, 2004).

The bacterial assimilation of nitrogen sources such as ammonia or amino acids is also under tight control by several transcriptional regulators (Prasse and Schmitz, 2018). Nitrate assimilation is widespread across proteobacteria and is often controlled at a transcriptional level by extracellular concentrations of nitrate and nitrite as well as ammonium (Luque-Almagro et al., 2017). In the presence of ammonium in *cyanobacteria*, the transcriptional regulator NtcA represses the nitrate reduction machinery. Once this nitrogen source is depleted the nitrate reductase genes are activated. In *proteobacteria*, the two-component system NtrB/NtrC regulates the activation of σ^{54} promoters and therefore controls central nitrogen metabolism (Herrero et al., 2001; Muro-Pastor et al., 2005). The sensor histidine kinase NtrB senses low nitrogen conditions and subsequently autophosphorylates and transfers a phosphoryl group to the NtrC response regulator protein. NtrC then acts as a transcriptional activator (Sanders et al., 1992). Another two-component system with a proposed role in nitrogen assimilation and similarities to NtrBC is the NtrYX system found in diazotrophs. In *Azorhizobium caulinodans* it has been suggested to interact with the NtrBC system to respond to changing levels of nitrate (Pawlowsky et al., 1991). In the model denitrifier *Paracoccus denitrificans*, NtrBC is mainly required for nitrate regulation and NtrYX only has a minor contribution. It has been proposed that nitrate assimilation is regulated at three levels in *P. denitrificans* (Luque-Almagro et al., 2017). Firstly, NtrC activates the expression of the assimilatory nitrate reductase (Nas) in the absence of ammonium. Level two consists of regulation *via* the NasTS system, which controls expression of the *nas* operon by transcription antitermination in response to nitrate levels. In the absence of nitrate, the positively acting RNA-binding transcription antitermination regulator NasT is held inactive in inhibitory complex with the nitrate sensor NasS. When NasS binds nitrate, dissociation of the NasTS complex is triggered which leads to increased levels of free and active NasT. NasT then may activate expression at the level of mRNA synthesis and translation. This novel regulatory mechanism involving NasTS is similar to that present in *Klebsiella oxytoca* mediated by NasR and could be of importance in a wide number of other bacteria (Chai and Stewart, 1999; Luque-Almagro et al., 2011; Luque-Almagro et al., 2017). The crystal structure of both NasT and NasR has shown that both possess an ANTAR domain crucial for specific binding to a leader mRNA (Boudes et al., 2012). Recent work on the soybean endosymbiont *Bradyrhizobium japonicum* has provided evidence of a cross talk between N-assimilation and N-respiration at an RNA-level (Sánchez et al., 2014). The study suggested that the

nasTS genes regulate respiratory nitrous oxide and periplasmic nitrate reductases. In cyanobacteria, regulation of N-assimilation is taken over by NtcA which forms dimers capable of binding promoters in response to the given levels of nitrogen available. As ammonium can be directly incorporated into glutamate it is often the preferred source of nitrogen for many organisms. However, the enzyme responsible for this conversion, glutamate dehydrogenase, has a low ammonium binding affinity. Therefore, a combination of the high ammonium-affinity enzyme glutamine synthetase and a glutamine oxoglutarate aminotransferase are responsible for the assimilation of ammonium under nitrogen limitation. This regulation is sensed and regulated by PII-like sensor proteins.

Little is known about the transcriptional regulation of nitrification. Nitrification is carried out in two steps: the conversion of ammonia to nitrite carried out by ammonia oxidisers such as *Nitrosomonas* and *Nitrosospira* and secondly the conversion of nitrite to nitrate which is carried out by nitrite oxidisers such as *Nitrobacter* and *Nitrospira* (Prosser, 2007; Norton and Stark, 2011). The rate of nitrification largely depends on environmental conditions such as temperature, soil moisture and pH (Norton and Stark, 2011). Heavy metals such as Ni (II), Zn (II), Cd (II) and Pb (II) have been shown to strongly impact the levels of nitrification. In *Nitrosomonas europaea*, exposure to Cd (II) caused a significant decrease in the production of ammonia monooxygenase (*amoA*), while exposure to Zn (II) resulted in an upregulation of *amoA* (Kapoor et al., 2015). Transcription levels of *amoA* have also been investigated in response to changes in water availability. Wetting of dry soil to model rainfall after a period of drought resulted in a rapid increase in *amoA* transcripts demonstrating a tight coupling of transcription levels of nitrification genes to the soil environment (Placella and Firestone, 2013; Norton and Ouyang, 2019).

In comparison to nitrification, transcriptional regulation in denitrification has been extensively studied, particularly in recent years (Gaimster et al., 2018). The expression of the denitrification enzymes Nar, Nir, Nor and Nos in *P. denitrificans* is regulated by environmental signals including availability of oxygen, nitrate, nitrite, nitric oxide and copper (**Figure 2**) (Gaimster et al., 2018).

When oxygen levels become limiting, denitrifiers are forced to activate the expression of the denitrification enzymes to avoid entrapment in anoxic conditions without energy. Recent evidence has shown that *P. denitrificans* displays a bet hedging strategy, a phenomenon that has been observed across a variety of prokaryotes which accept energetic penalties for a fraction of the population to achieve a long-term fitness advantage (Lycus et al., 2018). In the model denitrifier *P. denitrificans* this strategy involves the production of Nos in all cells, while Nir is only synthesized in a small number of cells.

Transcriptional regulation in the model denitrifier *P. denitrificans* is partly controlled by the regulators FnrP (fumarate and nitrate reduction protein), NNR (nitrite reductase and nitric oxide reductase regulator) and NarR (nitrate reductase regulator). Both FnrP and NNR are sensitive to oxygen and NO and are therefore involved in the switch between aerobic and anaerobic respiration to achieve maximum energy yields for the given environmental conditions (Van Spanning et al., 1995; Gaimster et al., 2018). To further fine-tune the denitrification network, the three transcriptional regulators FnrP, NnrR and NarR may serve as repressors of each other by competing for the binding upstream of their targets (**Figure 2**) (Giannopoulos et al., 2017). FnrP acts as an activator of the *nar* and *nos* operons and recognizes FNR-binding sequences (TTGAGAATTGTCAA and TTGACCTAAGTCAA) in the promoter region of the genes (Bouchal et al., 2010). Interaction of the FnrP 4Fe-4S cluster with O_2 leads to a separation of the transcriptionally active FnrP dimer into monomers (Crack et al., 2016). Hence, denitrification is switched off in the presence of oxygen as O_2 respiration provides significantly higher ATP yields. Additionally, it has been shown that the FnrP 4Fe-4S cluster interacts with multiple NO molecules leading to a dissociation of the transcriptional regulator into monomers. The transcriptional regulator NNR is homologous to FnrP and activates expression of the genes encoding nitrite (Nir) and nitric oxide reductases (Nor) (Van Spanning et al., 1995). Homologs of these transcriptional regulators have been identified in various other bacterial denitrifiers such as *Pseudomonas* species, *P. stutzeri* and *Rhodobacter* (Tosques et al., 1996; Elsen et al., 2004; Schreiber et al., 2007; Torres et al., 2017).

In *Pseudomonas* species the regulation of the denitrification machinery is equally dominated by members of the FNR superfamily such as the FnrP equivalent ANR (anaerobic regulator of arginine deaminase and nitrite reductase) (Schreiber et al., 2007). This transcription factor activates transcription of genes encoding for a nitrite transporter and a nitrite reductase if oxygen is limited. *P. stutzeri* encodes four FNR-type proteins which lack the cysteine residues required for the formation of a 4Fe-4S cluster (Vollack et al., 1999; Gaimster et al., 2018). NNR homologs have also been identified in a wide range of denitrifiers including *Rhodobacter sphaeroides* (Tosques et al., 1996). In *R. sphaeroides*, the regulator NnrR activates nitrite reductase and nitric oxide reductase. Outside of *P. denitrificans,* other transcriptional regulators have also been shown to be involved in the regulation of denitrification. These include the RegB/RegA two-component system. First discovered in *Rhodobacter capsulatus*, this system has been shown to regulate a large number of biological processes (Elsen et al., 2004). By controlling the expression of nitrite reductase, the RegB/RegA system in *R spaeroides* acts in concert with the regulator NnrR and therefore plays an important role in the denitrification cascade. In *B. diazoefficiens*, the denitrification machinery is regulated by two interconnected regulatory cascades, FixLJ-$FixK_2$-NnrR and RegSR-NifA that detect low levels of oxygen outside of the cell (Torres et al., 2017).

The transcriptional regulators, FNR, NNR and NarR underpin the ability of bacteria to sense and respond to oxygen and the denitrification intermediates. However, there are other critical external factors that must be detected and integrated into the regulatory network of the cell. Copper has long been recognized as an important factor in the regulation of NosZ activity (**Figure 2**) (Sullivan et al., 2013). Around 20% of Europe's arable lands are biologically copper deficient and as NosZ requires the unique multi-copper-sulphide centres, Cu_Z and Cu_A to bind and activate N_2O, it places a high Cu demand on the bacterium (Sinclair and Edwards, 2008; Pauleta and Moura,

2017). Other enzymes in bacterial enzymes require Cu for activity, such as haem Cu-oxidases or superoxide dismutases but for all of these enzymes there are non-Cu alternatives that can perform the same function in the absence of Cu (Zumft, 2005). This is however not the case for NosZ. As a result, in Cu deficient conditions, the final reduction step cannot be carried out leading to truncated denitrification and emission of N_2O. Studies carried out in 2012 demonstrated that copper-limited environments indeed lead to a downregulation of *nosZ* expression and an increased net N_2O emission without a significant effect on the biomass of the culture (Felgate et al., 2012; Sullivan et al., 2013). A down-regulation of *nosZ* expression in copper limited medium additionally influences expression of genes controlled by vitamin B_{12} riboswitches as accumulation of N_2O inactivates vitamin B_{12} (Sullivan et al., 2013). This work also showed that the accessory proteins NosC and NosR play an important role in copper-dependent expression of the *nos*-operon. Copper levels can therefore be manipulated in laboratory studies to create N_2O or N_2 genic conditions and induce global changes in gene expression, a useful tool to further understand the underlying regulatory and biochemical pathways (Felgate et al., 2012).

Other environmental factors such as zinc and pH have also been linked to transcriptional regulation of denitrification enzymes (Bergaust et al., 2010; Gaimster et al., 2018). Zinc depletion has been shown to upregulate the expression of nitric oxide reductase and nitrite reductase as well as *nosC*, which was upregulated nearly 10-fold (Neupane et al., 2017). Low soil pH increases the N_2O:N_2 ratio which has been linked to lowered levels of NosZ protein synthesis and assembly as transcription rates were unaffected by changes in pH (Bergaust et al., 2010). Denitrification in heterotrophs is highly dependent on carbon sources and therefore, increasing levels of organic carbon in the soil enhance denitrification rates as well as N_2O emissions (Saggar et al., 2013). Both environmental factors and transcriptional regulators strongly influence when denitrification is switched on and once switched on affect the denitrification rate. Numerous studies have analyzed their influence in both a laboratory environment as well as in an agricultural background. Nevertheless, many variables involved in the switch between N_2O emission and N_2O consumption remain unknown.

BEYOND DNA BINDING PROTEINS - sRNAs REGULATING THE NITROGEN CYCLE

sRNAs Indirectly Involved in Nitrogen Metabolism

Diazotrophs in the soil and the ocean are capable of using molecular nitrogen as the sole nitrogen source, preventing a loss of N from the biosphere and providing sources of fixed nitrogen. The key enzymes of nitrogen fixation, dinitrogenase and dinitrogenase reductase are energy driven and are therefore costly for the cell. Therefore, the nitrogen fixation process is tightly regulated at both the transcriptional and posttranscriptional level (Prasse and Schmitz, 2018). With increasing research into the regulatory role of sRNAs it is predicted that large numbers of these influence nitrogen cycle associated metabolism across many microorganisms (**Figure 3**). Direct involvement of sRNAs in the response to N-fluctuations in the environment or in the regulation of N_2-fixation has not been identified until recently. Indirect participation of sRNAs in N-metabolism however has been reported previously. In cyanobacteria for instance, NsiR1 controls the formation of heterocysts as well as the switch to nitrogen fixation (Ionescu et al., 2010). This *trans*-encoded sRNA is conserved across many heterocyst-forming cyanobacteria and is dependent on the regulatory protein HetR which is required for cell differentiation in *Anabaena*. Similar to NsiR1, sRNAs NsiR2, NsiR8 and NsiR9 have been shown to be co-expressed with heterocyst-specific genes. However, to date no specific function has been assigned to these three sRNAs. Furthermore, ArrF of *Azotobacter vinelandii* is involved in the regulation of FeSII (DeLay and Gottesman, 2009), which plays a key role in the protection of the nitrogenase (N_2-fixing) enzyme under oxidative conditions (Jung and Kwon, 2008). sRNAs indirectly involved in nitrogen assimilation include CyaR, GcvB and MmgR. CyaR, present in *E. coli*, inhibits the translation of an ammonium dependent NAD-synthethase responsible for the catalysis of NAD synthesis from either NH_3 or glutamine as well as the nicotinic acid adenine dinucleotide (De Lay and Gottesman, 2009). The sRNA GcvB is one of the most highly conserved Hfq associated sRNAs in Gram-negative bacteria. It inhibits the expression of a number of ABC transporters responsible for transporting amino acids in *E. coli* and *Salmonella* Typhimurium (Sharma et al., 2007). In *Sinorhizobium meliloti*, hundreds of sRNAs have been identified, with the focus on the sRNA MmgR which shows expression patterns highly dependent on the available nitrogen source (Ceizel Borella et al., 2016). Further work is required to elucidate its exact role.

sRNAs Regulating Nitrogen Fixation

An sRNA found to be directly involved in N-metabolism, NfiS, was identified in the root associated bacterium *P. stutzeri* A1501. *Via* a stem loop in the sRNAs secondary structure it is predicted to bind to the 5′ region of *nifK* mRNA which encodes a subunit of the nitrogenase enzyme. This interaction increases mRNA half-life and thus increases the translation efficiency of *nifK* optimizing N-fixation (Zhan et al., 2016). The stability of NfiS appears to be strongly affected by the presence of Hfq, as the transcript is hardly detectable in an *hfq* deletion strain. A complete knockout of NfiS results in decreased nitrogenase activity, while an overexpression of this sRNA can lead to an increase of up to 150% activity. Although NfiS is highly conserved in *P. stutzeri*, it cannot be found in other bacterial species.

Many mechanistic features of the cellular transcription and translation machinery in archaea are more closely related to the eukaryotic counterparts, however characterisations of archaeal sRNAs have suggested similar mechanisms as observed in bacteria. The best-known examples of sRNA regulation of nitrogen fixation in Archaea are the methanoarchaea *M. mazei* and *M. maripaludis*. Both strains contain the global N-repressor NrpR which is known to transcriptionally regulate a variety of target genes in response to changes in N-levels. An RNA-seq study in *M. mazei* Gö1 under conditions of varied nitrogen availabilities lead to the identification of 242 putative sRNAs

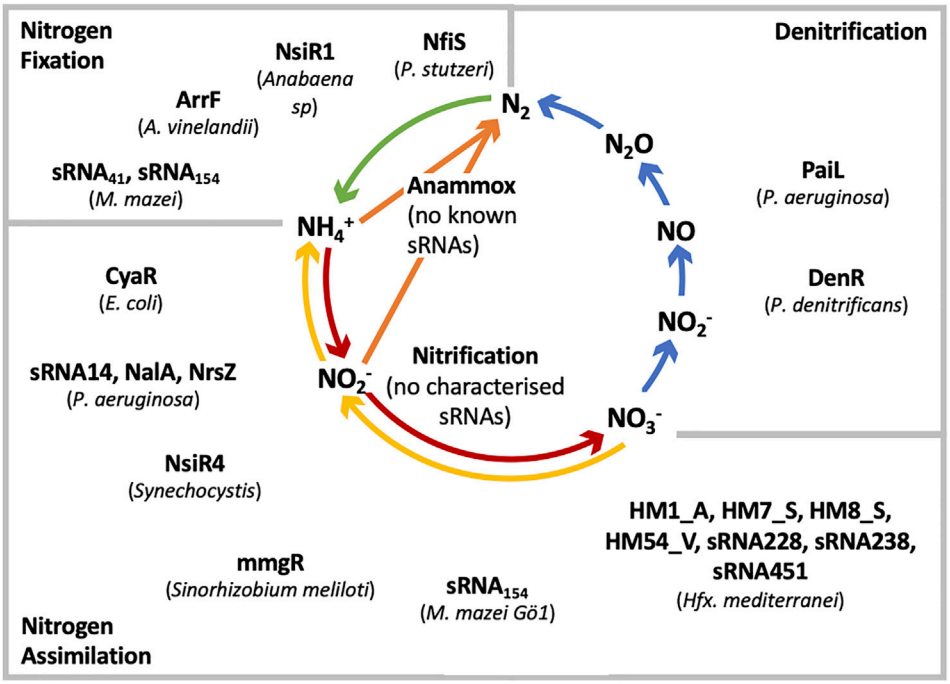

FIGURE 3 | Microorganisms and known sRNAs that regulate the nitrogen cycle. The sRNAs are grouped into the processes of nitrogen fixation, assimilatory nitrate reduction and denitrification.

(Jäger et al., 2009; Jäger et al., 2012). The discovery of $sRNA_{41}$ in *M. mazei* Gö1 introduced a sRNA in Archaea with a regulatory impact on the metabolic cycles of both carbon and nitrogen (Buddeweg et al., 2018). The sRNA is induced 100-fold in a N-rich environment compared to N-limitation and interacts with the mRNA encoding for an acetyl-coenzyme a decarbonylase/synthase (ACDS) complex (Buddeweg et al., 2018). In the absence of nitrogen, reduced amounts of $sRNA_{41}$ result in the upregulation of the ACDS complex and a subsequent production of amino acids for the synthesis of nitrogenase. A further sRNA found in *M* mazei, $sRNA_{154}$, was found to be exclusively present under nitrogen-limited conditions (Ehlers et al., 2011). A computational analysis of the transcriptional regulation network in *M. acetivorans* has shown that 5% of genes in this methanoarchaeon are regulated under nitrogen limitation. Two sRNAs, $sRNA_{154}$ and $sRNA_{159}$ were identified which include Nrp binding sites suggesting an involvement in gene regulation under N-limitation (Peterson et al., 2014). The first confirmed directly acting sRNA in *M. mazei*, $sRNA_{154}$, is under direct control of the global N-repressor NrpR (Weidenbach et al., 2008; Weidenbach et al., 2010). By stabilizing the polycistronic mRNA encoding for the nitrogenase enzyme as well as stabilizing the transcription of the regulatory protein NrpA it enhances expression of the N-fixing machinery (Prasse et al., 2017). The sequence and structure of this sRNA is highly conserved across members of the *Methanosarcinales*.

Despite nitrification being an important part of the nitrogen cycle, few sRNAs have been shown to be involved in the regulation of this pathway due to a lack of studies around this topic. In the ammonia oxidizing archaea *Nitrosopumilus maritimus* six candidates for sRNAs have been identified and it is highly likely that there many more with a potential involvement in the nitrification process (Walker et al., 2010).

sRNAs Controlling Nitrogen Assimilation

A differential RNA-seq analysis of the cyanobacteria *Anabaena sp.* PCC7120 in response to N-availability identified over 600 transcriptional start sites indicating an abundance of *cis*- and *trans*-encoded sRNAs involved in the regulation of N-assimilation. Cyanobacteria are of importance in both aquatic and terrestrial ecosystems and are important links between the C- and the N- cycle. A cyanobacterial small RNA directly involved in the regulation of N-assimilation, NsiR4, was first reported by Klähn et al. in 2015. NsiR4 expression in cyanobacteria is stimulated during nitrogen limiting conditions *via* the transcriptional regulator NtcA which is known to regulate a variety of genes involved in nitrogen metabolism. It is predicted to interact with the 5′ UTR of *gifA* mRNA, encoding for the glutamine synthetase inactivating factor (IF)7. By affecting IF7 expression, the sRNA also alters the activity of glutamine synthetase, a key enzyme in biological nitrogen assimilation (Klähn et al., 2015).

In *Pseudomonas aeruginosa*, the putative sRNA NalA is encoded upstream of the nitrate assimilation operon *nirBD*–PA1779–*cobA*. The transcription of this sRNA is σ^{54} and NtrC-dependent (Romeo et al., 2012). A deletion mutant of NalA was unable to grow in presence of nitrate as the sole

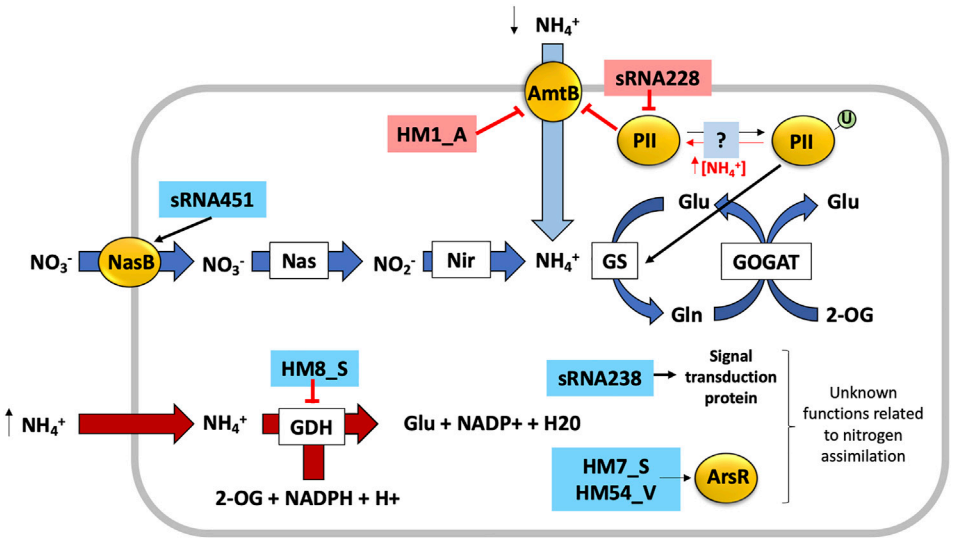

FIGURE 4 | Proposed regulation of nitrogen assimilation by sRNAs in *H. mediterranei.* The sRNAs highlighted in red correspond to sRNAs expressed in presence of ammonium, while sRNAs shaded blue correspond to those expressed in the presence of nitrate as a source of nitrogen. The red arrows indicate negative regulation and the black arrows indicate positive regulation of their respective target genes.

nitrogen source, instead it grew similarly to the parental strain in presence of ammonium. The results showed that NalA sRNA and nitrate are required for transcription of the nitrate assimilation operon, being an essential sRNA for the assimilation of nitrate (Romeo et al., 2012). Further studies performed in *P. aeruginosa* allowed the identification of sRNAs related to detoxification of industrial cyanide-containing wastewaters. For this purpose, a differential expression study was carried out by RNA-seq from cells cultured with a cyanide-containing wastewater, sodium cyanide or ammonium chloride as the sole nitrogen source. Among the sRNAs identified, $sRNA_{14}$ (overexpressed in the presence of ammonium) stood out, as its putative target genes include the nitrilase NitC, essential for cyanide assimilation, the FAD-dependent oxidoreductase NitH; and the glutamine synthetase, related to ammonia assimilation. Moreover, $sRNA_{14}$ showed a high conservation among enterobacterial species (Olaya-Abril et al., 2019).

In the archaeon *Haloferax* mediterranei, sRNAs have been studied to elucidate their possible role in the regulation of nitrogen assimilation in Haloarchaea (Payá et al., 2018; Payá et al., 2020). The initial identification of sRNAs in *H. mediterranei* was performed using a library of sRNAs identified in other archaeal species which resulted in the discovery of 295 putative sRNAs genes (hot spots) in the genome of *H. mediterranei*. *Via* bioinformatic and RNomic approaches, 88 sRNAs were identified. The differential expression analysis of these 88 sRNAs showed 16 sRNAs with different expression patterns according to the nitrogen source. The expression of their predicted target genes also depends strongly on the nitrogen source. Three regulatory mechanisms mediated by sRNAs were proposed in this study (**Figure 4**). The sRNA HM8_S which is overexpressed in presence of nitrate is predicted to target glutamate dehydrogenase, under expressed in presence of nitrate. Therefore, this sRNA could negatively regulate the expression of glutamate dehydrogenase. Both HM7_S and HM54_V sRNAs, overexpressed in presence of nitrate, are predicted to target transcriptional regulators belonging to the ArsR family, whose expression depends on the nitrogen source. Finally, the putative target of HM1_A (overexpressed in the presence of ammonium) is an ammonium transporter (expressed in the presence of nitrate or under nitrogen starvation) and therefore this sRNA could be involved in the regulation of ammonium uptake from the extracellular medium. However, more work is needed to confirm these regulatory mechanisms (Payá et al., 2018).

The second step in the identification of sRNAs in *H. mediterranei* results in the identification of the complete sRNAome in presence of ammonium or nitrate as the sole nitrogen source. 460 sRNAs were present in both conditions, 102 of which showed differences in their transcriptional patterns. Specifically, sRNAs with potential target genes related to nitrogen metabolism, such as *nosL, glnK1, gdh, glnA2, nasB, ilvB3, ilvE2, ilvAm, rrfh1, tyrA, gst2, gabT, gaD2, argD, gltp, purL, argB, gatD, nadE, fdx, exsB, gcvP1* and *pyrF* also presented differences in their transcriptional expression patterns according to the nitrogen source. From these findings, three potential regulatory mechanisms of nitrogen metabolism pathways mediated by sRNAs were proposed (**Figure 4**): 1) sRNA228 could be involved in the repression of nitrogen regulatory protein PII (*glnK1*) in the presence of ammonium, potentially through the posttranscriptional degradation of *glnK1* mRNA preventing its transcription and therefore the activation of the GS/GOGAT pathway; 2) the sRNA451 could be involved in the positive regulation of the nitrate/nitrite transporter (nasB) expression

in presence of nitrate as nitrogen source, by transcriptional stabilization of the *nasB* mRNA, increasing nitrate uptake under these conditions; and 3) sRNA238 could be involved in the transcriptional stabilization of the *HFX_RS05100* gene (both overexpressed in presence of nitrate). Although *HFX_RS05100* encodes a signal transduction protein of unknown function, the results of this work suggest that it may be involved in nitrogen metabolism (Payá et al., 2020).

sRNAs Controlling Denitrification

The importance of sRNA regulation in denitrifiers is a relatively recent discovery. However, 167 putative sRNAs across the *P. denitrificans* genome have now been identified when cultured under denitrifying conditions (Gaimster et al., 2016). Over one third of these sRNAs were differentially expressed between N_2 and N_2O emitting cultures suggesting a role of these sRNAs in production or consumption of the greenhouse gas. Several of these sRNAs showed sequence homology and conservation across other species in the α-proteobacteria. Interestingly, one particular sRNA, intergenic 28, showed sequence homology to members of the β-proteobacteria, including members of the *Bordetella* genus which include strains of human host-restricted pathogens as well as free-living environmental strains isolated from both aquatic and soil environments. Commonly predicted targets of sRNAs were transcriptional regulators such as Xre, Fis and TetR- Family regulators, which may act globally. This is consistent with other studies in which global regulators in other bacterial species have been shown to be subject to regulation by multiple Hfq-dependent sRNAs. *P. denitrificans* is predicted to encode an Hfq protein, Pden_4124, that has 95% sequence identity to Hfq found in *R. sphaeroides* and 54% sequence identity to *P. aeruginosa* Hfq. Many sRNAs found in both these bacteria are Hfq-dependent suggesting the same may be the case in *P. denitrificans* (Gamister et al., 2016). Additional predicted targets for sRNAs in *P. denitrificans* are transport proteins, also the most commonly predicted sRNA target in the marine denitrifier *R. pomeroyi* (Rivers et al., 2016).

Mechanistic studies carried out by Gaimster et al. then went on to report a novel regulatory pathway controlling denitrification *via* a single sRNA, sRNA29 (DenR) (Gaimster et al., 2019). DenR is suggested to stabilize the expression of a previously unknown GntR-type transcriptional regulator, NirR, which in turn represses the denitrification rate through repressing NirS, resulting in reduced N_2O emissions. The predicted region of interaction is a 7bp-seed region located within the CDS of *nirR*, and the underlying mechanism is currently being resolved. GntR-type regulators have been identified across many bacterial species in which they play crucial roles in the regulation of intracellular processes. They are named after the gluconate-operon repressor in *Bacillus subtilis* and they consist of a conserved N-terminal helix-turn-helix DNA-binding domain, which is linked to a C-terminal signaling domain. The overexpression of DenR also results in altered expression levels of 53 other genes that are mostly genes of either unknown function, genes involved in energy metabolism or transport as well as genes involved in carbohydrate metabolism. Interestingly, DenR has been found to be conserved across several denitrifying bacterial species in the *Rhodobacteraceae* genus. This includes the closely related species *Paracoccus aminophilus* but also the more distantly related marine denitrifier *Ruegeria pomeroyi*. All these species encode a transcriptional regulator with homology to NirR, suggesting a similar, conserved mode of action. Mechanistic studies for other sRNA that are differentially regulated between N_2 and N_2O genic cultures are currently underway. Although there are limited findings in other denitrifiers, for the opportunistic pathogen *P. aeruginosa*, the anaerobically induced sRNA Pail is known to be required for efficient denitrification by affecting the conversion of nitrite to nitric oxide (Tata et al., 2017).

THE ROLE OF sRNAs IN OTHER MAJOR ENVIRONMENTAL CYCLES

As marine dissolved organic matter contains equal concentrations of carbon as the Earth's atmosphere it represents a crucial component of the global carbon cycle. Despite microorganisms being important drivers if the carbon cycle, the microbial activities that regulate the turnover of dissolved organic matter still remain largely unsolved (McCarren et al., 2010). Studies focussing on marine cyanobacteria have identified key sRNAs involved in the regulation of the photosystem which is involved in photosynthesis. Several sRNAs have been found to play an important role in the response to light stress including six sRNAs in the marine bacterium *Synechococcus* that could have a regulatory effect on the light harvesting apparatus, a major driver of biogeochemical cycles through carbon fixation (Gierga et al., 2012). The sRNA PsrR1 in the cyanobacteria *Synechocystis 6803* was established to downregulate the expression of several photosynthesis-related genes in response to high light intensity by targeting several photosynthesis related genes including photosystem I-related proteins, cytochrome c553 and subunit N of the light-independent protochlorophyllide reductase (Gierga et al., 2012; Kopf and Hess, 2015; Pei et al., 2017, Hu and Wang, 2018). The sRNA appears to be regulated by the RpaB protein which is responsible for an increase in the expression of several genes under low light.

Equally, the discovery of 99 putative sRNAs under carbon and nitrogen limitation in the model marine bacterium *Ruegeria pomeroyi* is of great interest, as this bacterium is suggested to scavenge for alternate sources of organic C, influencing the ratios of major biomolecules in C-limited conditions (McCarren et al., 2010; Rivers et al., 2016). Fourteen of these sRNAs were differentially expressed under C- and N- nutrient limited cultures and their predicted targets include genes involved in transport, cell-cell interactions and nitrogen metabolism. Interestingly, one sRNA showed homology to 6S RNA which is of importance in *E. coli* and many other bacteria and has been found to downregulate multiple genes under environmentally stressful conditions, including nutrient limitation (Cavanagh and Wassarman, 2014). In *R. pomeroyi*, 6S was upregulated under C- and N- limited conditions and also showed interesting expression patterns in the context of sulfur metabolism.

Carbon and sulfur cycling in the biosphere are tightly interwoven through various biological processes carried out by marine microorganisms. Dimethylsulfoniopropionate (DMSP) represents not only a major carbon source, but also a source of reduced sulfur in the ocean. It is produced by phytoplankton and is metabolized by bacteria *via* two separate pathways, the demethylation pathway or the cleavage pathway, that result either in the formation methanethiol (MeSH) or dimethyl sulfide (DMS) respectively (Reisch et al., 2013). MeSH is a major source of reduced carbon and sulfur utilized by marine microbes as an important food source while the production of DMS accounts for a significant flux of sulfur from the ocean (Burns et al., 2016). DMS emissions have been linked to cloud albedo and climate and it has also been shown that DMS emissions influence the level of ocean carbon uptake underlining the close link of carbon and sulfur cycle. The genes involved in both pathways have been extensively studied, however there is little knowledge on the underlying regulatory processes controlling the pathways (Williams and Todd, 2019). It has however been shown that increased light intensity and nitrogen starvation influence levels of DMSP production (Kettles et al., 2014). The enzyme DsyB was recently identified to catalyze a key step in the DMSP production pathway in phytoplankton. In the diatom *F. cylindrus* both DMSP production and *DSYB* transcription are increased when nitrogen becomes limiting (Curson et al., 2018). The discovery of 182 potential sRNAs with putative targets including a wide range of regulatory, transport and signaling molecules in *R. pomeroyi* when grown on DMSP, DMSP intermediates or methionine suggested a potential involvement of sRNAs in posttranscriptional regulation of both DMSP metabolic pathways. Indeed, a knockout of sRNA129 showed significant alterations in the release of DMS and MeSH compared to the wild type *R. pomeroyi* strain (Burns et al., 2016). Further sRNAs such as sRNA42 and sRNA53, suggested to play a metabolic role *via* the demethylation pathway, have been predicted to target DMSP lyase *dddQ* mRNA raising a possibility of post-transcriptional regulation of *dddQ*. Uncovering the roles of these and other sRNAs found in marine bacteria will enhance the understanding of the cycling of sulfur and other elements in the ocean which is of major importance (Burns et al., 2016).

Human activities have significantly increased the availability of phosphorus in marine habitats leading to eutrophication and increasing primary production of cyanobacterial blooms. A study by Teikari et al., examined the transcriptomic landscape of the cyanobacterium *Anabaena* sp., one of the most common bloom-forming bacteria, in response to P limitation to increase the understanding of how the changing levels of P affect these diazotrophs. Indeed, they identified differentially expressed intergenic regions which could give rise to sRNAs crucial in the functioning of the cell in response to changing P-levels (Teikari et al., 2015).

Evidence suggests that the archaeal $sRNA_{162}$ plays a crucial role in the adaptation to different carbon sources, such as when cells switch from methanol to trimethylamine metabolism in the methanoarchaeon *Methanosarcina mazei* (Jäger et al., 2012). Overexpression of $sRNA_{162}$ results in a reduced production of its *trans*-encoded target, the ArsR-type transcriptional regulator MM2441, which affects the transcription level of a number of soluble methyltransferase genes. These genes are recognized as the most highly regulated genes in methanoarchaea and are involved in the degradation of methanol and methylamines (Veit et al., 2005; Bose et al., 2008; Krätzer et al., 2009). The sRNA is suggested to be constitutively expressed during exponential growth phase with methanol as a carbon source, repressing MM2441 by blocking the translation initiation region (Jäger et al., 2012). A fast turnover of $sRNA_{162}$ however ensures that low MM2441 protein levels are maintained that are still sufficient to repress the *mtm*B_2C_2 operon encoding for a methyltransferase and a cognate corrinoid protein. In stationary phase, the turnover time of $sRNA_{162}$ is reinforced leading to full translational repression of MM2441 and subsequent expression of the *mtm*B_2C_2 operon. Additional to the *trans*-encoded target MM2441, $sRNA_{162}$ also represents a *cis* acting RNA, interacting with the 5′-UTR of MM2442, encoding a conserved protein of unknown function.

HOW TO ADVANCE THE FIELD OF sRNA RESEARCH IN ENVIRONMENTAL CYCLES

Although sRNAs regulate a wide range of important biological processes, our current understanding of their role is far from complete, particularly with respect to the microbial ecology of diverse environments. A manipulation of only a handful of these sRNAs in the lab can lead to drastic changes in the response of the lab organism to an experimental condition. For instance, overexpression of DenR in *P. denitrificans* leads to a drastic decrease in the levels of N_2O emitted from the bacterial culture (Gaimster et al., 2019). This suggests that much larger networks of currently completely unknown sRNAs must be involved in an entire environmental response. Uncovering these networks would contribute largely to our understanding of the environmental stimuli that result in the switch from complete denitrification to incomplete denitrification and N_2O emissions as well as other processes driving our major biogeochemical cycles.

The use of high-throughput RNA-seq has led to significant advances in the identification of sRNAs. However, the majority of available information for sRNAs associated with biogeochemical cycles is restricted to a few model organisms, and even in these only a few selected sRNAs and their targets have been characterized in detail. Traditionally, coding genes were annotated using automated pipelines, while non-coding regions were overlooked (**Figure 5A**). The diverse characteristics of sRNAs such as their variation in length and secondary structures as well as a lack of sRNA conservation across distantly related genomes have made their computational discovery a difficult task. Advances in computational biology such as comparative genomics, RNA structure and thermodynamic stability-based approaches as well as transcriptional signal-based sRNA identification have contributed to the identification of a plethora of sRNAs

(Sridhar and Gunasekaran, 2013). Though the majority of sRNAs have been identified using comparative genomics, transcriptional signal-based approaches are promising in the discovery of novel intergenic sRNAs (Rajendran et al., 2020). The breadth of bacterial and archaeal species with fully sequenced genomes and pre-existing whole transcriptome studies may well also contribute to the identification of novel sRNA. In *Salmonella* Typhimurium SL1344 novel and refined sRNA identification methodologies have led to the discovery of large numbers of novel sRNA, suggesting that sRNA genes may even outnumber protein coding genes (Houserova et al., 2021).

Once an sRNA has been identified, the critical bottleneck in the functional characterization is the detection of sRNA targets. By identifying sRNA targets it is possible to integrate this regulatory RNA into the existing models of regulatory networks that fine-tune all microbial processes. This is a crucial step in the development of future mitigation strategies to counter anthropogenically induced shifts in the natural biogeochemical cycles. Experimental target identification *via* genetic screens, knockouts and sRNA overexpression often followed by proteomics and microarray analysis or qRT-PCR are time-consuming and laborious (Backofen and Hess, 2010; Georg et al., 2019). Therefore, efficient computational target prediction tools are highly desirable (**Figure 5B**). Existing tools predict sRNA targets based on sequence, thermodynamic scoring of mRNA-sRNA mixed duplexes and RNA secondary structure. However, the accuracy of these tools is highly variable, and their use is complex (Kumar et al., 2020). Therefore, we can assume that many sRNAs remain undiscovered, especially in organisms that are less studied. It will be a major challenge to adapt these methods to gain an idea of the sRNA-targets interactions in complex ecological environments. A more user-friendly approach is necessary to make sRNA identification and characterization more accessible in the future.

To increase our understanding of sRNAs outside of lab model organisms, it is crucial to extend the study of sRNAs in single organisms to a metagenomic scale. In our natural environment, microorganisms do not live by themselves. Instead, they are found in communities which often work together in the response to environmental stresses. Integrative omics approaches can give insights into genes, RNA, proteins and metabolites present in the entire microbial community with a particular function in the environment (**Figure 5C**). Novel sequencing methods based on sRNAs in a variety of human samples can generate complete metagenomic profiles giving insights into the bacterial communities present in patient samples which is a promising tool for the analysis of both the entire sRNA content and the microbial profile of a sample (Mjelle et al., 2020). Microbial metatransciptomic data sets from the ocean have already revealed the abundance of sRNA in microbial communities and their importance in processes such as carbon metabolism and nutrient acquisition (Shi et al., 2009). Many of these sRNAs were identified as part of pyrosequencing of the total RNA extracted from microbial communities extracted from the Hawaiian ocean. A large fraction of the sequences that shared no homology with known proteins were found to be comprised of known as well as novel, uncharacterized sRNAs (Shi et al., 2009). Another study identified an abundance of diverse sRNAs from an extremophilic microbial community in the Atacama Desert (Gelsinger et al., 2020). Putative targets of these sRNA are involved in osmotic adjustments to major rain events as well as nutrient acquisition which underpins the importance of sRNAs in the community stress response in the natural environment. Community studies like these are

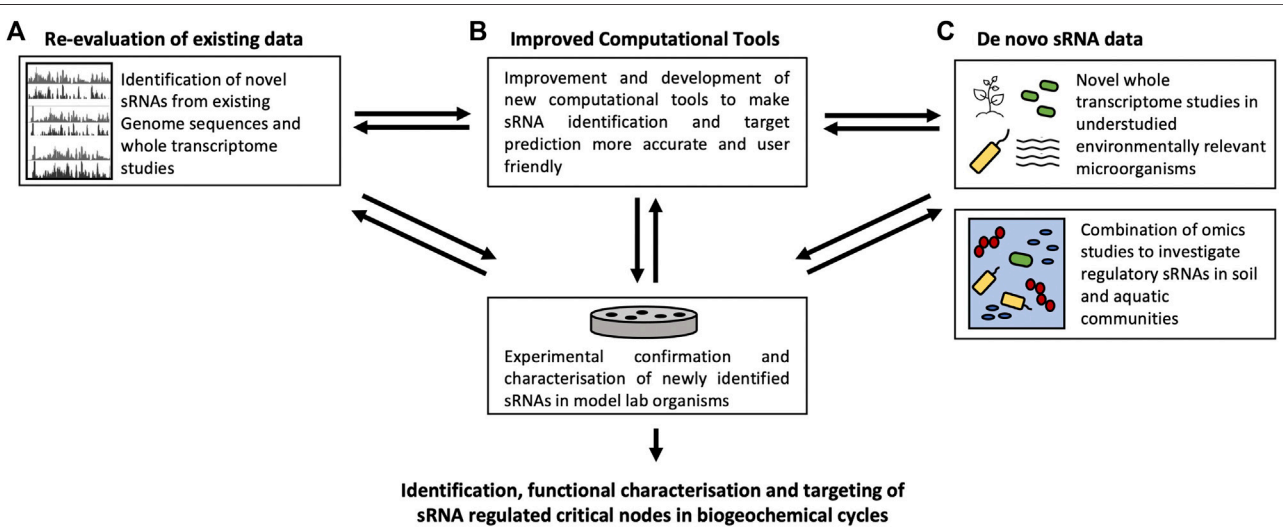

FIGURE 5 | Roadmap for the progression of sRNA research in environmental cycles includes **(A)** the Re-evaluation of existing data, **(B)** the development of improved computational tools and **(C)** the generation of de-novo sRNA data.

important contributors to uncover large numbers of sRNAs *in situ* that are of environmental importance which can then be further characterized *in vitro* (Gierga et al., 2012).

sRNA Applications

Recent work has demonstrated that integrated analyses of the microbiome and the bacterial as well as human small noncoding RNAs could be key in the development of novel diagnostic tools (Tarallo et al., 2019; Mjelle et al., 2020; Vogel et al., 2020). For instance, host-microbiome dysbiosis in colorectal cancer patients results in an altered sRNA profile in the human stool compared to that observed in healthy patient samples (Tarallo et al., 2019). Pathogenic bacteria such as *Mycobacterium tuberculosis* are able to secrete sRNAs which can subsequently be detected in the patient plasma. In both examples, sRNAs could potentially act as biomarkers for diseases. A pathogen often associated with colorectal cancer is *Fusarium nucleatum* (Brennan and Garrett, 2019). It has been suggested that selective depletion of this pathogen in the colon by administrating a short antisense sRNA targeting the mRNA of an essential gene could provide crucial insights into the link of *F. nucleatum* to disease (Vogel, 2020). Despite a lack of knowledge around the transcriptome structure and cell envelope of some of these potential target organisms, programmable RNA 'antibiotics' are a promising approach to target antibiotic resistant bacteria in the future.

These findings could also be applied in non-host microbiomes. Having established the importance of singular sRNAs in a physiological response, an analysis of the entirety of sRNA present in an environmental sample could provide valuable insights into the specific responses of each microbe present in the sample. Presence of known sRNAs could provide information about the nature of an environmental response. Similar to the potential use of sRNA biomarkers in infection, they could act as biomarkers or 'ecomarkers' to identify, for example, whether the microbial communities in an agricultural soil are contributing to the production or consumption of N_2O. The idea of RNA 'antibiotics' could also be translated to a non-host environment. For example, sRNAs could be engineered to target key microbes or key enzymes in the denitrification cascade, known to be involved in switching on or off N_2O production *in situ*. These could then be added to fertilizers, giving us a chance to control greenhouse gas emissions from the agriculture industry.

CONCLUSION

Microbial sRNAs have already proven to modulate a range of microbial responses. Meta analyses of communities in conjunction with mechanistic data obtained computationally and experimentally from model organisms as well as advancements in the computational sRNA and sRNA-target prediction tools, will are vital and needed to resolve the complex sRNA regulatory networks underpinning biogeochemical cycles such as the nitrogen cycle in the environment. A broader understanding of all sRNAs involved in the switch between N_2O production and N_2O consumption could contribute to the development of mitigation strategies and sRNAs could be applied to counter the rising levels of the greenhouse gas while maintaining global food security.

AUTHOR CONTRIBUTIONS

SM and GP reviewed the literature, co-wrote the manuscript, and prepared the figures. M-JB, AG, DR, JE and GR conceived the idea and co-edited the drafts.

FUNDING

This work was funded by the Biotechnology and Biological Sciences Research Council (United Kingdom) (BB/L022796/1, BB/M00256X/1, BB/S008942/1) and a University of East Anglia studentship as well as a Generalitat Valenciana (Spain) studentship (grant ACIF/2018/200), "Programa Propio para el Formento de la I+D+I del Vicerrectorado de Investigación y Transferencia de Conociemiento (GRE20-02-C)" University of Alicante.

REFERENCES

Babitzke, P., and Romeo, T. (2007). CsrB sRNA Family: Sequestration of RNA-Binding Regulatory Proteins. *Curr. Opin. Microbiol.* 10, 156–163. doi:10.1016/j.mib.2007.03.007

Backofen, R., and Hess, W. R. (2010). Computational Prediction of sRNAs and Their Targets in Bacteria. *RNA Biol.* 7 (1), 33–42. doi:10.4161/rna.7.1.10655

Bardill, J. P., Zhao, X., and Hammer, B. K. (2011). The *Vibrio cholerae* Quorum Sensing Response Is Mediated by Hfq-dependent sRNA/mRNA Base Pairing Interactions. *Mol. Microbiol.* 80, 1381–1394. doi:10.1111/j.1365-2958.2011.07655.x

Battesti, A., Majdalani, N., and Gottesman, S. (2011). The RpoS-Mediated General Stress Response inEscherichia Coli. *Annu. Rev. Microbiol.* 65 (1), 189–213. doi:10.1146/annurev-micro-090110-102946

Beisel, C. L., and Storz, G. (2010). Base Pairing Small RNAs and Their Roles in Global Regulatory Networks. *FEMS Microbiol. Rev.* 34 (5), 866–882. doi:10.1111/j.1574-6976.2010.00241.x

Bergaust, L., Mao, Y., Bakken, L. R., and Frostegård, A. (2010). Denitrification Response Patterns during the Transition to Anoxic Respiration and Posttranscriptional Effects of Suboptimal pH on Nitrogen Oxide Reductase in Paracoccus Denitrificans. *Appl Environ Microbiol.* 76, 6387–6396. doi:10.1128/AEM.00608-10

Bernhard, A. (2010). The Nitrogen Cycle: Processes, Players and Human Impact. *Nat. Educ. Knowledge Project* 3 (10), 25

Bos, J., Duverger, Y., Thouvenot, B., Chiaruttini, C., Branlant, C., Springer, M., et al. (2013). The sRNA RyhB Regulates the Synthesis of the *Escherichia coli* Methionine Sulfoxide Reductase MsrB but Not MsrA. *PLoS One.* 8 (5), e63647. doi:10.1371/journal.pone.0063647

Bose, A., Pritchett, M. A., and Metcalf, W. W. (2008). Genetic Analysis of the Methanol- and Methylamine-specific Methyltransferase 2 Genes of *Methanosarcina Acetivorans* C2A. *J Bacteriol.* 190, 4017–4026. doi:10.1128/JB.00117-08

Bossi, L., and Figueroa-Bossi, N. (2016). Competing Endogenous RNAs: a Target-Centric View of Small RNA Regulation in Bacteria. *Nat. Rev. Microbiol.* 14 (12), 775–784. doi:10.1038/nrmicro.2016.129

Bouchal, P., Struhárová, I., Budinská, E., Šedo, O., Vyhlídalová, T., Zdráhal, Z., et al. (2010). Unraveling an FNR Based Regulatory Circuit in Paracoccus Denitrificans Using a Proteomics-Based Approach. *Biochim. Biophys. Acta*. 1804, 1350–1358. doi:10.1016/j.bbapap.2010.01.016

Boudes, M., Lazar, N., Graille, M., Durand, D., Gaidenko, T. A., Stewart, V., et al. (2012). The Structure of the NasR Transcription Antiterminator Reveals a One-Component System with a NIT Nitrate Receptor Coupled to an ANTAR RNA-Binding Effector. *Mol. Microbiol.* 85, 431–444. doi:10.1111/j.1365-2958.2012.08111.x

Boudvillain, M., Figueroa-Bossi, N., and Bossi, L. (2013). Terminator Still Moving Forward: Expanding Roles for Rho Factor. *Curr. Opin. Microbiol.* 16, 118–124. doi:10.1016/j.mib.2012.12.003

Bouvier, M., Sharma, C. M., Mika, F., Nierhaus, K. H., and Vogel, J. (2008). Small RNA Binding to 5′ mRNA Coding Region Inhibits Translational Initiation. *Mol. Cel.* 32 (6), 827–837. doi:10.1016/j.molcel.2008.10.027

Brennan, C. A., and Garrett, W. S. (2019). Fusobacterium Nucleatum - Symbiont, Opportunist and Oncobacterium. *Nat. Rev. Microbiol.* 17, 156–166. doi:10.1038/s41579-018-0129-6

Brusseau, M. L. (2019). *Ecosystems and Ecosystem Services. Environmental and Pollution Science*. Third Edition. Acad Press, 89–102. doi:10.1016/b978-0-12-814719-1.00006-9

Buddeweg, A., Sharma, K., Urlaub, H., and Schmitz, R. A. (2018). sRNA41affects Ribosome Binding Sites within Polycistronic mRNAs inMethanosarcina mazeiGö1. *Mol. Microbiol.* 107, 595–609. doi:10.1111/mmi.13900

Burns, A. S., Bullock, H. A., Smith, C., Huang, Q., Whitman, W. B., and Moran, M. A. (2016). Small RNAs Expressed during Dimethylsulfoniopropionate Degradation by a Model Marine Bacterium. *Environ. Microbiol. Rep.* 8 (5), 763–773. doi:10.1111/1758-2229.12437

Cavanagh, A. T., and Wassarman, K. M. (2014). 6S RNA, a Global Regulator of Transcription inEscherichia Coli,Bacillus Subtilis, and beyond. *Annu. Rev. Microbiol.* 68, 45–60. doi:10.1146/annurev-micro-092611-150135

Ceizel Borella, G., Lagares, A., and Valverde, C. (2016). Expression of theSinorhizobium Melilotismall RNA genemmgRis Controlled by the Nitrogen Source. *FEMS Microbiol. Lett.* 363, fnw069. doi:10.1093/femsle/fnw069

Chai, W., and Stewart, V. (1999). RNA Sequence Requirements for NasR-Mediated, Nitrate-Responsive Transcription Antitermination of the Klebsiella Oxytoca M5al nasF Operon Leader 1 1Edited by M. Gottesman. *J. Mol. Biol.* 292, 203–216. doi:10.1006/jmbi.1999.3084

Chan, T. Y. K. (2011). Vegetable-borne Nitrate and Nitrite and the Risk of Methaemoglobinaemia. *Toxicol. Lett.* 200, 107–108. doi:10.1016/j.toxlet.2010.11.002

Chao, Y., Li, L., Girodat, D., Förstner, K. U., Said, N., Corcoran, C., et al. (2017). *In Vivo* Cleavage Map Illuminates the Central Role of RNase E in Coding and Non-coding RNA Pathways. *Mol. Cel.* 65, 39–51. doi:10.1016/j.molcel.2016.11.002

Chen, H., Dutta, T., and Deutscher, M. P. (2016). Growth Phase-dependent Variation of RNase BN/Z Affects Small RNAs. *J. Biol. Chem.* 291, 26435–26442. doi:10.1074/jbc.M116.757450

Chen, S., Perathoner, S., Ampelli, C., and Centi, G. (2019). "Electrochemical Dinitrogen Activation: To Find a Sustainable Way to Produce Ammonia," in *"Electrochemical Dinitrogen Activation: To Find a Sustainable Way to Produce Ammonia" Studies in Surface Science and Catalysis* (Elsevier), Vol. 178, 31–46. doi:10.1016/b978-0-444-64127-4.00002-1

Conthe, M., Wittorf, L., Kuenen, J. G., Kleerebezem, R., Hallin, S., and Van Loosdrecht, M. C. M. (2018). Growth Yield and Selection of nosZ Clade II Types in a Continuous Enrichment Culture of N2 O Respiring Bacteria. *Environ. Microbiol. Rep.* 10 (3), 239–244. doi:10.1111/1758-2229.12630

Crack, J. C., Hutchings, M. I., Thomson, A. J., and Le Brun, N. E. (2016). Biochemical Properties of *Paracoccus Denitrificans* FnrP: Reactions with Molecular Oxygen and Nitric Oxide. *J. Biol. Inorg. Chem.* 21 (1), 71–82. doi:10.1007/s00775-015-1326-7

Curson, A. R. J., Williams, B. T., Pinchbeck, B. J., Sims, L. P., Martínez, A. B., Rivera, P. P. L., et al. (2018). DSYB Catalyses the Key Step of Dimethylsulfoniopropionate Biosynthesis in Many Phytoplankton. *Nat. Microbiol.* 3, 430–439. doi:10.1038/s41564-018-0119-5

Darfeuille, F., Unoson, C., Vogel, J., and Wagner, E. G. H. (2007). An Antisense RNA Inhibits Translation by Competing with Standby Ribosomes. *Mol. Cel.* 26, 381–392. doi:10.1016/j.molcel.2007.04.003

De Lay, N., and Gottesman, S. (2009). The Crp-Activated Small Noncoding Regulatory RNA CyaR (RyeE) Links Nutritional Status to Group Behavior. *J Bacteriol.* 191, 461–476. doi:10.1128/JB.01157-08

De Lay, N., and Gottesman, S. (2011). Role of Polynucleotide Phosphorylase in sRNA Function in *Escherichia coli*. *RNA*. 17 (6), 1172–1189. doi:10.1261/rna.2531211

De Lay, N., Schu, D., and Gottesman, S. (2013). Bacterial Small RNA-based Negative Regulation: Hfq and its Accomplices. *J. Biol. Chem.* 288 (12), 7669–8003. doi:10.1074/jbc.R112.441386

Dixon, R., and Kahn, D. (2004). Genetic Regulation of Biological Nitrogen Fixation. *Nat. Rev. Microbiol.* 2 (8), 621–631. doi:10.1038/nrmicro954

Dixon, R. A., Buck, M., Drummond, M., Hawkes, T., Khan, H., MacFarlane, S., et al. (1986). Regulation of the Nitrogen Fixation Genes inKlebsiella Pneumoniae: Implications for Genetic Manipulation. *Plant Soil.* 90, 225–233. doi:10.1007/BF02277399

Domeignoz-Horta, L. A., Putz, M., Spor, A., Bru, D., Breuil, M. C., Hallin, S., et al. (2016). Non-denitrifying Nitrous Oxide-Reducing Bacteria - an Effective N2O Sink in Soil. *Soil Biol. Biochem.* 103, 376–379. doi:10.1016/j.soilbio.2016.09.010

Durand, S., Tomasini, A., Braun, F., Condon, C., and Romby, P. (2015). sRNA and mRNA Turnover in Gram-Positive Bacteria. *FEMS. Microbiol. Rev.* 39 (3), 316–330. doi:10.1093/femsre/fuv007

Dutta, T., and Srivastava, S. (2018). Small RNA-Mediated Regulation in Bacteria: A Growing Palette of Diverse Mechanisms. *Gene*. 656 (656), 60–72. doi:10.1016/j.gene.2018.02.068

Ehlers, C., Jäger, D., and Schmitz, R. A. (2011). Establishing a Markerless Genetic Exchange System forMethanosarcina mazeiStrain Gö1 for Constructing Chromosomal Mutants of Small RNA Genes. *Archaea*. 2011, 1–7. doi:10.1155/2011/439608

Elsen, S., Swem, L. R., Swem, D. L., and Bauer, C. E. (2004). RegB/RegA, a Highly Conserved Redox-Responding Global Two-Component Regulatory System. *Microbiol Mol Biol Rev.* 68 (2), 263–279. doi:10.1128/MMBR.68.2.263-279.2004

Felgate, H., Giannopoulos, G., Sullivan, M. J., Gates, A. J., Clarke, T. A., Baggs, E., et al. (2012). The Impact of Copper, Nitrate and Carbon Status on the Emission of Nitrous Oxide by Two Species of Bacteria with Biochemically Distinct Denitrification Pathways. *Environ. Microbiol.* 14 (7), 1788–1800. doi:10.1111/j.1462-2920.2012.02789.x

Fischer, S., Benz, J., Späth, B., Maier, L.-K., Straub, J., Granzow, M., et al. (2010). The Archaeal Lsm Protein Binds to Small RNAs. *J. Biol. Chem.* 285 (45), 34429–34438. doi:10.1074/jbc.M110.118950

Franze de Fernandez, M. T., Eoyang, L., and August, J. T. (1968). Factor Fraction Required for the Synthesis of Bacteriophage Qβ-RNA. *Nature*. 219 (5154), 588–590. doi:10.1038/219588a0

Fröhlich, K. S., and Vogel, J. (2009). Activation of Gene Expression by Small RNA. *Curr. Opin. Microbiol.* 12, 674–682. doi:10.1016/j.mib.2009.09.009

Gaimster, H., Chalklen, L., Alston, M., Munnoch, J. T., Richardson, D. J., Gates, A. J., et al. (2016). Genome-wide Discovery of Putative sRNAs in *Paracoccus Denitrificans* Expressed under Nitrous Oxide Emitting Conditions. *Front. Microbiol.* 7 (7), 1806. doi:10.3389/fmicb.2016.01806

Gaimster, H., Alston, M., Richardson, D. J., Gates, A. J., and Rowley, G. (2018). Transcriptional and Environmental Control of Bacterial Denitrification and N2O Emissions. *FEMS. Microbiol. Lett.* 365, 5. doi:10.1093/femsle/fnx277

Gaimster, H., Hews, C. L., Griffiths, R., Soriano-Laguna, M. J., Alston, M., Richardson, D. J., et al. (2019). A Central Small RNA Regulatory Circuit Controlling Bacterial Denitrification and N2O Emissions. *mBio*. 10 (4), e01165–19. doi:10.1128/mBio.01165-19

Galloway, J. N., and Cowling, E. B. (2002). Reactive Nitrogen and the World: 200 Years of Change. *AMBIO: A J. Hum. Environ.* 31 (2), 64–71. doi:10.1579/0044-7447-31.2.64

Gelsinger, D. R., Uritskiy, G., Reddy, R., Munn, A., Farney, K., and DiRuggiero, J. (2020). Regulatory Noncoding Small RNAs Are Diverse and Abundant in an Extremophilic Microbial Community. *mSystems*. 5, e00584. doi:10.1128/mSystems.00584-19

Georg, J., Lalaouna, D., Hou, S., Lott, S. C., Caldelari, I., Marzi, S., et al. (2019). The Power of Cooperation: Experimental and Computational Approaches in the Functional Characterization of Bacterial sRNAs. *Mol. Microbiol.* 113 (3), 603–612. doi:10.1111/mmi.14420

Giangrossi, M., Prosseda, G., Tran, C. N., Brandi, A., Colonna, B., and Falconi, M. (2010). A Novel Antisense RNA Regulates at Transcriptional Level the Virulence Gene icsA of *Shigella Flexneri*. *Nucleic Acids Res.* 38 (10), 3362–3375. doi:10.1093/nar/gkq025

Giannopoulos, G., Sullivan, M. J., Hartop, K. R., Rowley, G., Gates, A. J., Watmough, N. J., et al. (2017). Tuning the modularParacoccus Denitrificansrespirome to Adapt from Aerobic Respiration to Anaerobic Denitrification. *Environ. Microbiol.* 19, 4953–4964. doi:10.1111/1462-2920.13974

Gierga, G., Voss, B., and Hess, W. R. (2012). Non-coding RNAs in Marine *Synechococcus* and Their Regulation under Environmentally Relevant Stress Conditions. *ISME. J.* 6 (8), 1544–1557. doi:10.1038/ismej.2011.215

Gottesman, S. (2005). Micros for Microbes: Non-coding Regulatory RNAs in Bacteria. *Trends Genet.* 21 (7), 399–404. doi:10.1016/j.tig.2005.05.008

Guerrero, M. G., Vega, J. M., and Losada, M. (1981). The Assimilatory Nitrate-Reducing System and its Regulation. *Annu. Rev. Plant Physiol.* 32, 169–204. doi:10.1146/annurev.pp.32.060181.001125

Halbleib, C. M., and Ludden, P. W. (2000). Regulation of Biological Nitrogen Fixation. *J. Nutr.* 130 (5), 1081–1084. doi:10.1093/jn/130.5.1081

Hallin, S., Philippot, L., Löffler, F. E., Sanford, R. A., and Jones, C. M. (2018). Genomics and Ecology of Novel N2O-Reducing Microorganisms. *Trends Microbiol.* 26, 43–55. doi:10.1016/j.tim.2017.07.003

Herrero, A., Muro-pastor, A. M., and Flores, E. (2001). Nitrogen Control in Cyanobacteria. *J. Bacteriol.* 183 (2), 411–425. doi:10.1128/jb.183.2.411-425.2001

Hoch, G. E., Schneider, K. C., and Burris, R. H. (1960). Hydrogen Evolution and Exchange, and Conversion of N2O to N2 by Soybean Root Nodules. *Biochim. Biophys. Acta*. 37 (2), 273–279. doi:10.1016/0006-3002(60)90234-1

Houserova, D. M., Dahmer, D. J., Amin, S. V., King, V. M., Barnhill, E. C., Huang, Y., et al. (2021). Characterization of 475 Novel, Putative Small RNAs (sRNAs) in Carbon-Starved *Salmonella enterica* Serovar Typhimurium. *Biorxiv. Preprint*. 10, 305. doi:10.1101/2021.01.11.426214

Hu, J., and Wang, Q. (2018). Regulatory sRNAs in Cyanobacteria. *Front. Microbiol.* 9, 2399. doi:10.3389/fmicb.2018.02399

Ionescu, D., Voss, B., Oren, A., Hess, W. R., and Muro-Pastor, A. M. (2010). Heterocyst-Specific Transcription of NsiR1, a Non-coding RNA Encoded in a Tandem Array of Direct Repeats in Cyanobacteria. *J. Mol. Biol.* 398 (2), 177–188. doi:10.1016/j.jmb.2010.03.010

Jäger, D., Sharma, C. M., Thomsen, J., Ehlers, C., Vogel, J., and Schmitz, R. A. (2009). Deep Sequencing Analysis of the Methanosarcina Mazei Go1 Transcriptome in Response to Nitrogen Availability. *Proc. Natl. Acad. Sci.* 106 (51), 21878–21882. doi:10.1073/pnas.0909051106

Jäger, D., Pernitzsch, S. R., Richter, A. S., Backofen, R., Sharma, C. M., and Schmitz, R. A. (2012). An Archaeal sRNA Targeting Cis - and Trans -encoded mRNAs via Two Distinct Domains. *Nucleic Acids Res.* 40 (21), 10964–10979. doi:10.1093/nar/gks847

Jensen, F. B. (2003). Nitrite Disrupts Multiple Physiological Functions in Aquatic Animals. *Comp. Biochem. Physiol. A: Mol. Integr. Physiol.* 135, 9–24. doi:10.1016/s1095-6433(02)00323-9

Jones, C. M., Graf, D. R., Bru, D., Philippot, L., and Hallin, S. (2013). The Unaccounted yet Abundant Nitrous Oxide-Reducing Microbial Community: a Potential Nitrous Oxide Sink. *Isme J.* 7, 417–426. doi:10.1038/ismej.2012.125

Jung, Y.-S., and Kwon, Y.-M. (2008). Small RNA ArrF Regulates the Expression of sodB and feSII Genes in Azotobacter vinelandiisodB and feSII Genes in Azotobacter Vinelandii. *Curr. Microbiol.* 57, 593–597. doi:10.1007/s00284-008-9248-z

Kapoor, V., Li, X., Elk, M., Chandran, K., Impellitteri, C. A., and Santo Domingo, J. W. (2015). Impact of Heavy Metals on Transcriptional and Physiological Activity of Nitrifying Bacteria. *Environ. Sci. Technol.* 49, 13454–13462. doi:10.1021/acs.est.5b02748

Kettles, N. L., Kopriva, S., and Malin, G. (2014). Insights into the Regulation of DMSP Synthesis in the Diatom Thalassiosira Pseudonana through APR Activity, Proteomics and Gene Expression Analyses on Cells Acclimating to Changes in Salinity, Light and Nitrogen. *PLoS One.* 9, e94795. doi:10.1371/journal.pone.0094795

Kilic, T., Sanglier, S., Van Dorsselaer, A., and Suck, D. (2006). Oligomerization Behavior of the Archaeal Sm2-type Protein fromArchaeoglobus Fulgidus. *Protein Sci.* 15 (10), 2310–2317. doi:10.1110/ps.06219150910.1110/ps.062191506

Klähn, S., Schaal, C., Georg, J., Baumgartner, D., Knippen, G., Hagemann, M., et al. (2015). The sRNA NsiR4 Is Involved in Nitrogen Assimilation Control in Cyanobacteria by Targeting Glutamine Synthetase Inactivating Factor IF7. *Proc. Natl. Acad. Sci. USA.* 112 (45), E6243–E6252. doi:10.1073/pnas.1508412112

Kopf, M., and Hess, W. R. (2015). Regulatory RNAs in Photosynthetic Cyanobacteria. *FEMS. Microbiol. Rev.* 39 (3), 301–315. doi:10.1093/femsre/fuv017

Krätzer, C., Carini, P., Hovey, R., and Deppenmeier, U. (2009). Transcriptional Profiling of Methyltransferase Genes during Growth of *Methanosarcina Mazei* on Trimethylamine. *J. Bacteriol.* 191, 5108–5115. doi:10.1128/JB.00420-09

Kumar, K., Chakraborty, A., and Chakrabarti, S. (2020). PresRAT: A Server for Identification of Bacterial Small-RNA Sequences and Their Targets with Probable Binding Region. *RNA Biol.*, 1–8. doi:10.1080/15476286.2020.1836455

Luque-Almagro, V. M., Gates, A. J., Moreno-Vivián, C., Ferguson, S. J., Richardson, D. J., and Roldán, M. D. (2011). Bacterial Nitrate Assimilation: Gene Distribution and Regulation. *Biochem. Soc. Trans.* 39 (6), 1838–1843. doi:10.1042/BST20110688

Luque-Almagro, V. M., Manso, I., Sullivan, M. J., Rowley, G., Ferguson, S. J., Moreno-Vivián, C., et al. (2017). Transcriptional and Translational Adaptation to Aerobic Nitrate Anabolism in the Denitrifier *Paracoccus Denitrificans*. *Biochem. J.* 474 (11), 1769–1787. doi:10.1042/BCJ20170115

Lycus, P., Soriano-Laguna, M. J., Kjos, M., Richardson, D. J., Gates, A. J., Milligan, D. A., et al. (2018). A Bet-Hedging Strategy for Denitrifying Bacteria Curtails Their Release of N2O. *Proc. Natl. Acad. Sci. USA.* 115 (46), 11820–11825. doi:10.1073/pnas.1805000115

Märtens, B., Sharma, K., Urlaub, H., and Bläsi, U. (2017). The SmAP2 RNA Binding Motif in the 3′UTR Affects mRNA Stability in the Crenarchaeum *Sulfolobus solfataricus*. *Nucleid Acids Res.* 45 (15), 8957–8967. doi:10.1093/nar/gkx581

Madsen, E. L. (2011). Microorganisms and Their Roles in Fundamental Biogeochemical Cycles. *Curr. Opin. Biotechnol.* 22 (3), 456–464. doi:10.1016/j.copbio.2011.01.008

Märtens, B., Bezerra, G., Kreuter, M., Grishkovskaya, I., Manica, A., Arkhipova, V., et al. (2015). The Heptameric SmAP1 and SmAP2 Proteins of the Crenarchaeon *Sulfolobus Solfataricus* Bind to Common and Distinct RNA Targets. *Life (Basel).* 5, 1264–1281. doi:10.3390/life5021264

Martinez-Argudo, I., Little, R., Shearer, N., Johnson, P., and Dixon, R. (2004). The NifL-NifA System: a Multidomain Transcriptional Regulatory Complex that Integrates Environmental Signals. *J Bacteriol.* 186, 601–610. doi:10.1128/jb.186.3.601-610.2004

Masse, E., and Gottesman, S. (2002). A Small RNA Regulates the Expression of Genes Involved in Iron Metabolism in *Escherichia coli*. *Proc. Natl. Acad. Sci.* 99 (7), 4620–4625. doi:10.1073/pnas.032066599

McCarren, J., Becker, J. W., Repeta, D. J., Shi, Y., Young, C. R., Malmstrom, R. R., et al. (2010). Microbial Community Transcriptomes Reveal Microbes and Metabolic Pathways Associated with Dissolved Organic Matter Turnover in the Sea. *Proc. Natl. Acad. Sci.* 107 (38), 16420–16427. doi:10.1073/pnas.1010732107

McCullen, C. A., Benhammou, J. N., Majdalani, N., and Gottesman, S. (2010). Mechanism of Positive Regulation by DsrA and RprA Small Noncoding RNAs: Pairing Increases Translation and Protects rpoS mRNA from Degradation. *J Bacteriol.* 192 (21), 5559–5571. doi:10.1128/JB.00464-10

Michaux, C., Verneuil, N., Hartke, A., and Giard, J.-C. (2014). Physiological Roles of Small RNA Molecules. *Microbiol.* 160 (6), 1007–1019. doi:10.1099/mic.0.076208-0

Mjelle, R., Aass, K., Sjursen, W., Hofsli, E., and Saetrom, P. (2020). sMETAseq: Combined Profiling of Microbiota and Host Small RNAs. *iScience*. 23, 5. doi:10.1016/j.sci.2020.10113110.1016/j.isci.2020.101131

Morfeldt, E., Taylor, D., von Gabain, A., and Arvidson, S. (1995). Activation of Alpha-Toxin Translation in *Staphylococcus aureus* by the Trans-encoded Antisense RNA, RNAIII. *EMBO J.* 14, 4569–4577. doi:10.1002/j.1460-2075.1995.tb00136.x

Morita, T., Maki, K., and Aiba, H. (2005). RNase E-Based Ribonucleoprotein Complexes: Mechanical Basis of mRNA Destabilization Mediated by Bacterial

Noncoding RNAs. *Genes Development*. 19, 2176–2186. doi:10.1101/gad.1330405

Morita, T., Mochizuki, Y., and Aiba, H. (2006). Translational Repression Is Sufficient for Gene Silencing by Bacterial Small Noncoding RNAs in the Absence of mRNA Destruction. *Proc. Natl. Acad. Sci.* 103 (13), 4858–4863. doi:10.1073/pnas.0509638103

Muro-Pastor, M. I., Reyes, J. C., and Florencio, F. J. (2005). Ammonium Assimilation in Cyanobacteria. *Photosynth. Res.* 83, 135–150. doi:10.1007/s1120-004-2082-710.1007/s11120-004-2082-7

Neupane, D. P., Jacquez, B., Sundararajan, A., Ramaraj, T., Schilkey, F. D., and Yukl, E. T. (2017). Zinc-dependent Transcriptional Regulation in *Paracoccus Denitrificans*. *Front. Microbiol.* 8, 569. doi:10.3389/fmicb.2017.00569

Nielsen, J. S., Boggild, A., Andersen, C. B. F., Nielsen, G., Boysen, A., Brodersen, D. E., et al. (2007). An Hfq-like Protein in Archaea: Crystal Structure and Functional Characterization of the Sm Protein from *Methanococcus Jannaschii*. *RNA*. 13, 2213–2223. doi:10.1261/rna.689007

Norton, J., and Ouyang, Y. (2019). Controls and Adaptive Management of Nitrification in Agricultural Soils. *Front. Microbiol.* 10. doi:10.3389/fmicb.2019.01931

Norton, J. M., and Stark, J. M. (2011). Regulation and Measurement of Nitrification in Terrestrial Systems. *Methods Enzymol.* 486, 343–368. doi:10.1016/B978-0-12-381294-0.00015-8

Novick, R. P., and Geisinger, E. (2008). Quorum sensing in *Staphylococci*. *Annu. Rev. Genet.* 42, 541–564. doi:10.1146/annurev.genet.42.110807.091640

Olaya-Abril, A., Luque-Almagro, V. M., Pérez, M. D., López, C. M., Amil, F., Cabello, P., et al. (2019). Putative Small RNAs Controlling Detoxification of Industrial Cyanide-Containing Wastewaters by *Pseudomonas pseudoalcaligenes* CECT5344. *Plos. One.* 14 (2), e0212032. doi:10.1371/journal.pone.0212032

Oleijniczak, M., and Storz, G. (2017). ProQ/FinO-domain Protein: Another Ubiquitous Family of RNA Matchmakers?. *Mol. Microbiol.* 104 (6), 905–915. doi:10.1111/mmi.13679

Otaka, H., Ishikawa, H., Morita, T., and Aiba, H. (2011). PolyU Tail of Rho-independent Terminator of Bacterial Small RNAs Is Essential for Hfq Action. *Proc. Natl. Acad. Sci. USA*. 108, 13059–13064. doi:10.1073/pnas.1107050108

Papenfort, K., and Vanderpool, C. K. (2015). Target Activation by Regulatory RNAs in Bacteria. *FEMS Microbiol. Rev.* 39, 362–378. doi:10.1093/femsre/fuv016

Papenfort, K., Sun, Y., Miyakoshi, M., Vanderpool, C. K., and Vogel, J. (2013). Small RNA-Mediated Activation of Sugar Phosphatase mRNA Regulates Glucose Homeostasis. *Cell.* 153, 426–437. doi:10.1016/j.cell.2013.03.003

Pauleta, S. R., and Moura, I. (2017). Assembly of CuZ and CuA in Nitrous Oxide Reductase. *Encycl Inorg. Bioinorg Chem.*, 1–11. doi:10.1002/9781119951438.eibc2477

Pawlowsky, K., Klosse, U., and the Brujin, F. (1991). Characterization of a Novel *Azorhizobium Caulinodans* ORS571 Two-Component Regulatory System, NtrY/NtrX, Involved in Nitrogen Fixation Metabolism. *Mol. Gen. Genet.* 231 (1), 124–138. doi:10.1007/BF00293830

Payá, G., Bautista, V., Camacho, M., Castejón-Fernández, N., Alcaraz, L., Bonete, M.-J., et al. (2018). Small RNAs of *Haloferax Mediterranei:* Identification and Potential Involvement in Nitrogen Metabolism. *Genes*. 9 (2), 83. doi:10.3390/genes9020083

Payá, G., Bautista, V., Camacho, M., Bonete, M.-J., and Esclapez, J. (2020). New Proposal of Nitrogen Metabolism Regulation by Small RNAs in the Extreme Halophilic Archaeon *Haloferax Mediterranei*. *Mol. Genet. Genomics.* 295 (3), 775–785. doi:10.1007/s00438-020-01659-9

Pei, G., Sun, T., Chen, S., Chen, L., and Zhang, W. (2017). Systematic and Functional Identification of Small Non-coding RNAs Associated with Exogenous Biofuel Stress in Cyanobacterium *Synechocystis* Sp. PCC 6803. *Biotechnol. Biofuels.* 10, 57. doi:10.1186/s13068-017-0743-y

Peterson, J. R., Labhsetwar, P., Ellermeier, J. R., Kohler, P. R. A., Jain, A., Ha, T., et al. (2014). Towards a Computational Model of a Methane Producing Archaeum. *Archaea*. 2014, 1–18. doi:10.1155/2014/898453

Philippot, L., Piutti, S., Martin-Laurent, F., Hallet, S., and Germon, J. C. (2002). Molecular Analysis of the Nitrate-Reducing Community from Unplanted and Maize-Planted Soils. *Appl Environ Microbiol.* 68 (12), 6121–6128. doi:10.1128/aem.68.12.6121-6128.2002

Placella, S. A., and Firestone, M. K. (2013). Transcriptional Response of Nitrifying Communities to Wetting of Dry Soil. *Appl. Environ. Microbiol.* 79 (10), 3294–3302. doi:10.1128/AEM.00404-13

Prasse, D., and Schmitz, R. A. (2018). Small RNAs Involved in Regulation of Nitrogen Metabolism. *Microbiol. Spectr.* 6, 4. doi:10.1128/microbiolspec.RWR-0018-2018

Prasse, D., Förstner, K. U., Jäger, D., Backofen, R., and Schmitz, R. A. (2017). sRNA154 a Newly Identified Regulator of Nitrogen Fixation in Methanosarcina Mazei Strain Gö1. *RNA Biol.* 14 (11), 1544–1558. doi:10.1080/15476286.2017.1306170

Prinn, R. G., Weiss, R. F., Arduini, J., Arnold, T., DeWitt, H. L., Fraser, P. J., et al. (2018). History of Chemically and Radiatively Important Atmospheric Gases from the Advanced Global Atmospheric Gases Experiment (AGAGE). *Earth Syst. Sci. Data* 10, 985–1018. doi:10.5194/essd-10-985-2018

Prosser, J. I. (2007). The Ecology of Nitrifying Bacteria. *Biol. nitrogen Cycle*, 223–243. doi:10.1016/B978-04445285710.1016/b978-044452857-5.50016-3

Rajendran, K., Kumar, V., Raja, I., Kumariah, M., and Tennyson, J. (2020). Identification of Small Non-coding RNAs from *Rhizobium Etli* by Integrated Genome-wide and Transcriptome-Based Methods. *ExRNA*. 2, 14. doi:10.1186/s41544-020-00054-1

Reisch, C. R., Crabb, W. M., Gifford, S. M., Teng, Q., Stoudemayer, M. J., Moran, M. A., et al. (2013). Metabolism of Dimethylsulphoniopropionate byRuegeria Pomeroyi DSS-3. *Mol. Microbiol.* 89, 774–791. doi:10.1111/mmi.12314

Renseigne, N., Umar, S., and Iqbal, M. (2007). Nitrate Accumulation in Plants, Factors Affecting the Process, and Human Health Implication. *A. Review. Agron. Sustain. Dev. Springer/edp Sciences/inra.* 27 (1), 45–57. doi:10.1051/agro:2006021

Richardson, D., Felgate, H., Watmough, N., Thomson, A., and Baggs, E. (2009). Mitigating Release of the Potent Greenhouse Gas N2O from the Nitrogen Cycle - Could Enzymic Regulation Hold the Key?. *Trends Biotechnol.* 27 (7), 388–397. doi:10.1016/j.tibtech.2009.03.009

Richardson, D. J., Edwards, M. J., White, G. F., Baiden, N., Hartshorne, R. S., Fredrickson, J., et al. (2012). Exploring the Biochemistry at the Extracellular Redox Frontier of Bacterial Mineral Fe(III) Respiration. *Biochem. Soc. Trans.* 40, 493–500. doi:10.1042/BST20120018

Rivers, A. R., Burns, A. S., Chan, L.-K., and Moran, M. A. (2016). Experimental Identification of Small Non-coding RNAs in the Model Marine Bacterium *Ruegeria Pomeroyi* DSS-3. *Front. Microbiol.* 7 (7), 380. doi:10.3389/fmicb.2016.00380

Robertson, G. P., and Vitousek, P. M. (2009). Nitrogen in Agriculture: Balancing the Cost of an Essential Resource. *Annu. Rev. Environ. Resour.* 34 (1), 97–125. doi:10.1146/annurev.environ.032108.105046

Romeo, A., Sonnleitner, E., Sorger-Domenigg, T., Nakano, M., Eisenhaber, B., and Bläsi, U. (2012). Transcriptional Regulation of Nitrate Assimilation in *Pseudomonas aeruginosa* Occurs via Transcriptional Antitermination within the nirBD-PA1779-cobA Operon. *Microbiol.* 158, 1543–1552. doi:10.1099/mic.0.053850-0

Rowley, G., Hensen, D., Felgate, H., Arkenberg, A., Appia-Ayme, C., Prior, K., et al. (2012). Resolving the Contributions of the Membrane-Bound and Periplasmic Nitrate Reductase Systems to Nitric Oxide and Nitrous Oxide Production in *Salmonella enterica* Serovar Typhimurium. *Biochem. J.* 441, 755–762. doi:10.1042/BJ20110971

Sánchez, C., Itakura, M., Okubo, T., Matsumoto, T., Yoshikawa, H., Gotoh, A., et al. (2014). The Nitrate-Sensing NasST System Regulates Nitrous Oxide Reductase and Periplasmic Nitrate Reductase inBradyrhizobium Japonicum. *Environ. Microbiol.* 16, 3263–3274. doi:10.1111/1462-2920.12546

Saggar, S., Jha, N., Deslippe, J., Bolan, N. S., Luo, J., Giltrap, D. L., et al. (2013). Denitrification and N2O:N2 Production in Temperate Grasslands: Processes, Measurements, Modelling and Mitigating Negative Impacts. *Sci. Total Environ.* 465, 173–195. doi:10.1016/j.scitotenv.2012.11.050

Sanders, D. A., Gillece-Castro, B. L., Burlingame, A. L., and Koshland, D. E. (1992). Phosphorylation Site of NtrC, a Protein Phosphatase Whose Covalent Intermediate Activates Transcription. *J. Bacteriol.* 174, 5117–5122. doi:10.1128/jb.174.15.5117-5122.1992

Sauter, C., Basquin, J., and Suck, D. (2003). Sm-like Proteins in Eubacteria: the Crystal Structure of the Hfq Protein from *Escherichia coli*. *Nucleic Acids Res.* 31, 4091–4098. doi:10.1093/nar/gkg480

Schreiber, K., Krieger, R., Benkert, B., Eschbach, M., Eschbach, M., Arai, H., et al. (2007). The Anaerobic Regulatory Network Required for *Pseudomonas*

aeruginosa Nitrate Respiration. *J Bacteriol*. 189 (11), 4310–4314. doi:10.1128/JB.00240-07

Sedlyarova, N., Shamovsky, I., Bharati, B. K., Epshtein, V., Chen, J., Gottesman, S., et al. (2016). sRNA-mediated Control of Transcription Termination in *E. coli*. *Cell*. 167, 111–121. doi:10.1016/j.cell.2016.09.004

Sharma, C. M., Darfeuille, F., Plantinga, T. H., and Vogel, J. (2007). A Small RNA Regulates Multiple ABC Transporter mRNAs by Targeting C/A-rich Elements inside and Upstream of Ribosome-Binding Sites. *Genes Development*. 21 (21), 2804–2817. doi:10.1101/gad.447207

Shi, Y., Tyson, G. W., and DeLong, E. F. (2009). Metatranscriptomics Reveals Unique Microbial Small RNAs in the Ocean's Water Column. *Nature*. 459, 266–269. doi:10.1038/nature08055

Sinclair, A. H., and Edwards, A. C. (2008). *Micronutrient Deficiency Problems in Agricultural Crops in Europe. Micronutrient Deficiencies in Global Crop Production*. Dordrecht: Springer, 225–244. doi:10.1007/978-1-4020-6860-7_9

Smil, V. (2002). Nitrogen and Food Production: Proteins for Human Diets. *AMBIO: A J. Hum. Environ.* 31, 126–131. doi:10.1579/0044-7447-31.2.126

Smirnov, A., Förstner, K. U., Holmqvist, E., Otto, A., Günster, R., Becher, D., et al. (2016). Grad-seq Guides the Discovery of ProQ as a Major Small RNA-Binding Protein. *Proc. Natl. Acad. Sci. USA*. 113, 11591–11596. doi:10.1073/pnas.1609981113

Smirnov, A., Wang, C., Drewry, L. L., and Vogel, J. (2017). Molecular Mechanism of mRNA Repression in Trans by a ProQ-dependent Small RNA. *EMBO. J.* 36, 1029–1045. doi:10.15252/embj.201696127

Smith, K. A., Mosier, A. R., Crutzen, P. J., and Winiwarter, W. (2012). The Role of N 2 O Derived from Crop-Based Biofuels, and from Agriculture in General, in Earth's Climate. *Phil. Trans. R. Soc. B.* 367, 1169–1174. doi:10.1098/rstb.2011.0313

Sonnleitner, E., Gonzalez, N., Sorger-Domenigg, T., Heeb, S., Richter, A. S., Backofen, R., et al. (2011). The Small RNA PhrS Stimulates Synthesis of the *Pseudomonas aeruginosa* Quinolone Signal. *Mol. Micobiol.* 80, 868–885. doi:10.1111/j.1365-2958.2011.07620.x

Sridhar, J., and Gunasekaran, P. (2013). Computational Small RNA Prediction in Bacteria. *Bioinform. Biol. Insights.* 7, BBI.S11213–95. doi:10.4137/BBI.S11213

Stocker, T., Qin, D., Plattner, G., Tignor, M., Allen, S., Boschung, J., et al. (2013). *IPCC (2013) Climate Change 2013: The Physical Science Basis. Contribution of Working Group I to the Fifth Assessment Report of the Intergovernmental Panel on Climate Change*. Cambridge, United Kingdom and New York. NY. USA: Cambridge University Press, 1535

Storz, G., Opdyke, J. A., and Zhang, A. (2004). Controlling mRNA Stability and Translation with Small, Noncoding RNAs. *Curr. Opin. Microbiol.* 7 (2), 140–144. doi:10.1016/j.mib.2004.02.015

Storz, G., Vogel, J., and Wassarman, K. M. (2011). Regulation by Small RNAs in Bacteria: Expanding Frontiers. *Mol. Cel* 43 (6), 880–891. doi:10.1016/j.molcel.2011.08.022

Stremińska, M. A., Felgate, H., Rowley, G., Richardson, D. J., and Baggs, E. M. (2012). Nitrous Oxide Production in Soil Isolates of Nitrate-Ammonifying Bacteria. *Environ. Microbiol. Rep.* 4, 66–71. doi:10.1111/j.1758-2229.2011.00302.x

Sullivan, M. J., Gates, A. J., Appia-Ayme, C., Rowley, G., and Richardson, D. J. (2013). Copper Control of Bacterial Nitrous Oxide Emission and its Impact on Vitamin B12-dependent Metabolism. *Proc. Natl. Acad. Sci.* 110 (49), 19926–19931. doi:10.1073/pnas.1314529110

Sutton, M., Howard, C., Erisman, J., Billen, G., Bleeker, A., van Grinsven, H., et al. (2011). *The European Nitrogen Assessment: Sources, Effects and Policy Perspectives*. Cambridge: Cambridge University Press. ISBN 9781107006126

Tarallo, S., Ferrero, G., Gallo, G., Francavilla, A., and Clerico, G. (2019). Altered Fecal Small RNA Profiles in Colorectal Cancer Reflect Gut Microbiome Composition in Stool Samples. *mSystems*. 4 (5), e00289–19. doi:10.1128/mSystems.00289-19

Tata, M., Amman, F., Pawar, V., Wolfinger, M. T., Weiss, S., Häussler, S., et al. (2017). The Anaerobically Induced sRNA PaiI Affects Denitrification in *Pseudomonas aeruginosa* PA14. *Front. Microbiol.* 8, 2312. doi:10.3389/fmicb.2017.02312

Teikari, J., Österholm, J., Kopf, M., Battchikova, N., Wahlsten, M., Aro, E.-M., et al. (2015). Transcriptomic and Proteomic Profiling of *Anabaena Sp.* Strain 90 under Inorganic Phosphorus Stress. *Appl. Environ. Microbiol.* 81 (15), 5212–5222. doi:10.1128/AEM.01062-15

Thore, S., Mayer, C., Sauter, C., Weeks, S., and Suck, D. (2003). Crystal Structures of the Pyrococcus Abyssi Sm Core and its Complex with RNA. *J. Biol. Chem.* 278, 1239–1247. doi:10.1074/jbc.M207685200

Törö, I., Thore, S., Mayer, C., Basquin, J., Séraphin, B., and Suck, D. (2001). RNA Binding in an Sm Core Domain: X-Ray Structure and Functional Analysis of an Archaeal Sm Protein Complex. *EMBO. J.* 20, 2293–2303. doi:10.1093/emboj/20.9.2293

Törö, I., Basquin, J., Teo-Dreher, H., and Suck, D. (2002). Archaeal Sm Proteins Form Heptameric and Hexameric Complexes: Crystal Structures of the Sm1 and Sm2 Proteins from the Hyperthermophile *Archaeoglobus Fulgidus*. *J. Mol. Biol.* 320, 129–142. doi:10.1016/S0022-2836(02)00406-0

Torres, M. J., Bueno, E., Jiménez-Leiva, A., Cabrera, J. J., Bedmar, E. J., Mesa, S., et al. (2017). FixK2 Is the Main Transcriptional Activator of *Bradyrhizobium Diazoefficiens nosRZDYFLX* Genes in Response to Low Oxygen. *Front. Microbiol.* 8, 1621. doi:10.3389/fmicb.2017.01621

Tosques, I. E., Shi, J., and Shapleigh, J. P. (1996). Cloning and Characterization of nnrR, Whose Product Is Required for the Expression of Proteins Involved in Nitric Oxide Metabolism in Rhodobacter Sphaeroides 2.4.3. *J. Bacteriol.* 178, 4958–4964. doi:10.1128/jb.178.16.4958-4964.1996

Udekwu, K. I., Darfeuille, F., Vogel, J., Reimegard, J., Holmqvist, E., and Wagner, E. (2005). Hfq-dependent Regulation of OmpA Synthesis Is Mediated by an Antisense RNA. *Genes Development* 19 (19), 2355–2366. doi:10.1101/gad.354405

Van Maanen, J. M., Welle, I. J., Hageman, G., Dallinga, J. W., Mertens, P. L., and Kleinjans, J. C. (1996). Nitrate Contamination of Drinking Water: Relationship with HPRT Variant Frequency in Lymphocyte DNA and Urinary Excretion of N-Nitrosamines. *Environ. Health Perspect.* 104, 522–528. doi:10.1289/ehp.96104522

Van Spanning, R. J. M., De Boer, A. P. N., Reijnders, W. N. M., Spiro, S., Westerhoff, H. V., Stouthamer, A. H., et al. (1995). Nitrite and Nitric Oxide Reduction in *Paracoccus Denitrificans* Is under the Control of NNR, a Regulatory Protein that Belongs to the FNR Family of Transcriptional Activators. *FEBS. Lett.* 360 (2), 151–154. doi:10.1016/0014-5793(95)00091-m

Vanderpool, C., and Gottesman, S. (2007). A Dual Function for a Bacterial Small RNA: SgrS Performs Base Pairing-dependent Regulation and Encodes a Functional Polypeptide. *PNAS*. 104 (51), 20454–20459. doi:10.1073/pnas.0708102104

Vanderpool, C. K., and Gottesman, S. (2004). Involvement of a Novel Transcriptional Activator and Small RNA in Post-transcriptional Regulation of the Glucose Phosphoenolpyruvate Phosphotransferase System. *Mol.r Microbiol.* 54 (4), 1076–1089. doi:10.1111/j.1365-2958.2004.04348.x

Veit, K., Ehlers, C., and Schmitz, R. A. (2005). Effects of Nitrogen and Carbon Sources on Transcription of Soluble Methyltransferases in Methanosarcina Mazei Strain Gö1. *J Bacteriol*. 187, 6147–6154. doi:10.1128/JB.187.17.6147-6154.2005

Vitousek, P., and Howarth, R. (1991). Nitrogen Limitation on Land and in the Sea: How Can it Occur?. *Biogeochemistry*. 13, 87–115. doi:10.1007/BF00002772

Vogel, J., and Luisi, B. F. (2011). Hfq and its Constellation of RNA. *Nat. Rev. Microbiol.* 9, 578–589. doi:10.1038/nrmicro2615

Vogel, J. (2020). An RNA Biology Perspective on Species-specific Programmable RNA Antibiotics. *Mol. Microbiol.* 113 (3), 550–559. doi:10.1111/mmi.14476

Vollack, K.-U., Härtig, E., Körner, H., and Zumft, W. G. (1999). Multiple Transcription Factors of the FNR Family in Denitrifying Pseudomonas Stutzeri : Characterization of Four Fnr-like Genes, Regulatory Responses and Cognate Metabolic Processes. *Mol. Microbiol.* 31 (6), 1681–1694. doi:10.1046/j.1365-2958.1999.01302.x

Wagner, E. G. H. (2013). Cycling of RNAs on Hfq. *RNA Biol.* 10, 619–626. doi:10.4161/rna.24044

Walker, C. B., de la Torre, J. R., Klotz, M. G., Urakawa, H., Pinel, N., Arp, D. J., et al. (2010). *Nitrosopumilus Maritimus* Genome Reveals Unique Mechanisms for Nitrification and Autotrophy in Globally Distributed Marine Crenarchaea. *Proc. Natl. Acad. Sci.* 107 (19), 8818–8823. doi:10.1073/pnas.0913533107

Wassarman, K. M., and Storz, G. (2000). 6S RNA Regulates *E. coli* RNA Polymerase Activity. *Cell*. 101, 613–623. doi:10.1016/s0092-8674(00)80873-9

Wassarman, K. M. (2002). Small RNAs in Bacteria. *Cell*. 109 (2), 141–144. doi:10.1016/S0092-8674(02)00717-1

Waters, L. S., and Storz, G. (2009). Regulatory RNAs in Bacteria. *Cell*. 136 (4), 615–628. doi:10.1016/j.cell.2009.01.043

Weidenbach, K., Ehlers, C., Kock, J., Ehrenreich, A., and Schmitz, R. A. (2008). Insights into the NrpR Regulon in Methanosarcina Mazei Gö1. *Arch. Microbiol.* 190, 319–332. doi:10.1007/s00203-008-0369-3

Weidenbach, K., Ehlers, C., Kock, J., and Schmitz, R. A. (2010). NrpRII Mediates Contacts between NrpRI and General Transcription Factors in the Archaeon Methanosarcina Mazei Gö1. *FEBS. J.* 277, 4398–4411. doi:10.1111/j.1742-4658.2010.07821.x

Westermann, A. J., Venturini, E., Sellin, M. E., Förstner, K. U., Hardt, W.-D., and Vogel, J. (2019). The Major RNA-Binding Protein ProQ Impacts Virulence Gene Expression inSalmonella entericaSerovar Typhimurium. *mBIO*. 10 (1), e02504–18. doi:10.1128/mBio.02504-18

Williams, B. T., and Todd, J. D. (2019). A Day in the Life of Marine Sulfonates. *Nat. Microbiol.* 4 (10), 1610–1611. doi:10.1038/s41564-019-0576-5

Zhan, Y., Yan, Y., Deng, Z., Chen, M., Lu, W., Lu, C., et al. (2016). The Novel Regulatory ncRNA, NfiS, Optimizes Nitrogen Fixation via Base Pairing with the Nitrogenase Gene nifK mRNA in Pseudomonas Stutzeri A1501. *Proc. Natl. Acad. Sci. USA*. 113 (30), E4348–E4356. doi:10.1073/pnas.1604514113

Zumft, W. G., and Kroneck, P. M. (2007). Respiratory Transformation of Nitrous Oxide (N2O) to Dinitrogen by Bacteria and Archaea. *Adv. Microb. Physiol.* 52, 107–227. doi:10.1016/S0065-2911(06)52003-X

Zumft, W. (2005). Nitric Oxide Reductases of Prokaryotes with Emphasis on the Respiratory, Heme?copper Oxidase Type. *J. Inorg. Biochem.* 99 (1), 194–215. doi:10.1016/j.jinorgbio.2004.09.024

Conflict of Interest: The authors declare that the research was conducted in the absence of any commercial or financial relationships that could be construed as a potential conflict of interest.

frontiers in Environmental Science

METHODS
published: 31 May 2021
doi: 10.3389/fenvs.2021.658779

Experimental Design and Interpretation of Terrestrial Ecosystem Studies Using ^{15}N Tracers: Practical and Statistical Considerations

Patrick Schleppi[1]* *and Wim W. Wessel*[2]

[1]Forest Soils and Biogeochemistry, Swiss Federal Institute for Forest, Snow and Landscape Research, Birmensdorf, Switzerland, [2]Department of Ecosystem and Landscape Dynamics, Institute for Biodiversity and Ecosystem Dynamics, University of Amsterdam, Amsterdam, Netherlands

The stable isotope ^{15}N is an extremely useful tool for studying the nitrogen (N) cycle of terrestrial ecosystems. The affordability of isotope-ratio mass spectrometry has increased in the last decades and routine measurements of $\delta^{15}N$ with an accuracy better than 1‰ are now easily achieved. Except perhaps for wood, which has a very high C/N ratio, isotope analysis of samples is, thus, no longer the main challenge in measuring the partitioning of ^{15}N used as tracer in ecosystem studies. The central aim of such experiments is to quantitatively determine the fate of N after it enters an ecosystem, mainly as fertilizer, as atmospheric deposition or as plant litter. By measuring how much of this incoming N goes into different ecosystem pools, inferences can be made about the entire N cycle. Sample collection and preparation can be tedious work. Optimizing sampling schemes is thus an important aspect in the application of ^{15}N in ecosystem research and can be helpful for obtaining a high precision of the results with the available manpower and budget. In this contribution, we combine statistical and practical considerations and give recommendations for the design of labeling experiments and also for assessments of natural ^{15}N abundance. In particular, we discuss soil, vegetation and water sampling. We additionally address the most common questions arising during the calculation of tracer partitioning, and we provide some examples of the interpretation of experimental results.

Keywords: nitrogen, isotopes, nitrogen-15, tracer, recovery, experimental design

OPEN ACCESS

Edited by:
Muhammad Shaaban, Bahauddin Zakariya University, Pakistan

Reviewed by:
Patrick Höhener, Aix Marseille Université, France
Yu Liu, Northwest A and F University, China

***Correspondence:**
Patrick Schleppi
patrick.schleppi@wsl.ch

Specialty section:
This article was submitted to Biogeochemical Dynamics, a section of the journal Frontiers in Environmental Science

Received: *26 January 2021*
Accepted: *10 May 2021*
Published: *31 May 2021*

Citation:
Schleppi P and Wessel WW (2021) Experimental Design and Interpretation of Terrestrial Ecosystem Studies Using ^{15}N Tracers: Practical and Statistical Considerations. Front. Environ. Sci. 9:658779. doi: 10.3389/fenvs.2021.658779

INTRODUCTION

System ecology and biogeochemistry focus on the dynamics of substances or energy in ecosystems. To monitor the flows of elements through the different pools of an ecosystem, tracers can be an extremely useful tool (Fry, 2006). Nitrogen (N) consists mainly of the stable isotope ^{14}N, with the heavier stable isotope ^{15}N making up a small proportion (0.3663% of the atoms in atmospheric N_2). N compounds with a non-natural ^{15}N content can thus be used as a tracer. As such, they make it possible to study the dynamics of N in ecosystems, especially the double role of this element as an essential but also potentially harmful element. N is indeed an essential component of all organisms

and plays a role in practically all biological processes. On the other hand, since the beginning of the 20th century, humans have enormously increased its availability in the environment by converting N_2 into biologically reactive forms of N. This occurs partly on purpose, through the production of N fertilizers and partly as oxidation byproducts in combustion processes. In many cases this increase has led to eutrophication, acidification and a decrease in the biodiversity of ecosystems (Erisman et al., 2011).

According to Hauck and Bremner (1976), the use of ^{15}N in biological research started around 1940, not long after it became possible to produce substances enriched in this isotope. The first applications were in investigations of plant N uptake from decomposing plant material or from fertilizers. In the following decades, there were hundreds of publications on agricultural research involving ^{15}N. Around 1970, N isotope ratios could only be determined with a precision that was in the same order of magnitude as variations observed in different natural sources (Hauck et al., 1972). At that time, ^{15}N started to be used in large-scale field research, still mostly in agricultural systems [Hauck and Bremner, 1976; Nadelhoffer and Fry, 1994; see also a synthesis by; Gardner and Drinkwater (2009)]. One of the oldest experiments in a forest was conducted in Sweden in the 1960s (Nömmik, 1966; Björkman et al., 1967). A tracer experiment in an alpine grassland in Austria was started in the 1970s and was resampled 27 years later (Gerzabek et al., 2004). According to Nadelhoffer and Fry (1994), large-scale ^{15}N tracer experiments were still a relatively new development in the 1990s. At that time, the analytical precision had improved and became sufficient to even measure variations in ^{15}N natural abundance. For ^{15}N tracer studies, this meant that measurements had become possible even in large ecosystem pools in which the tracer would be strongly diluted. Currently, routine measurements by isotope-ratio mass spectrometry (IRMS) have an accuracy better than one thousandth of the natural abundance, which corresponds to approximately 1 out of 300,000 N atoms in a sample. As an example, it is possible to apply just 1 g or even less of a highly enriched nitrate salt (e.g. KNO_3 with 99% ^{15}N) to the soil under a large conifer tree (500 kg biomass), and to quantitatively measure how much of this tracer is recovered in the foliage one year later. And this can be achieved by analyzing a sample weighing less than a single needle of the tree.

Because of improvements in the techniques and a reduction of costs, field studies using ^{15}N as a tracer have increased considerably in popularity. Based on knowledge gained from our own experiments, during counseling activities and through discussions with other researchers (in particular Templer et al., 2012), we want here to summarize methodological aspects of such studies. We will focus on terrestrial ecosystems, mainly on unfertilized ones. We will discuss the setup of experiments, the application of the tracer, the sampling of the various parts of the ecosystem, and the calculation of the tracer recoveries. Finally, we will discuss some examples of how results can be interpreted. Of course, each experiment has its own questions and hypotheses, which affect the choice of methods, but the overall aim of tracer field experiments is to determine the fate of the labeled compounds and to infer about process rates. In this respect, a number of general principles deserve consideration. The goal of the present contribution is, thus, to help researchers in planning, conducting and interpreting ^{15}N tracer field experiments.

EXPERIMENTAL DESIGN

Field experiments with labeled N have the advantage that they can be run for a long time, even years, without disturbing the natural conditions of the system. Due to the complexity of the N cycle in an ecosystem, especially in the soil, field tracer studies usually do not have the aim of quantifying a specific process like N mineralization or nitrification. Using ^{15}N to measure such processes generally requires bringing soil samples to the laboratory and mixing the tracer with the soil, thus disturbing its natural structure. Relatively short incubation periods are then applied, in the order of magnitude of one day (e.g. Wessel and Tietema, 1992; Schleppi et al., 2019). Instead, the aim of field studies is to describe the overall fate of the applied tracer. In this approach, the interpretation of recovery rates is relatively straight forward, especially if the tracer is added to a preexisting N flux into or within the ecosystem. The best examples are ^{15}N added to fertilizer, applied as simulated atmospheric deposition, or applied as labeled plant litter. In many cases, however, single (net or gross) process rates are difficult to estimate from such experiments because pathways of N within the system are multiple and partly bidirectional. Two complementary techniques can help: repeated analyses over time and modeling (Currie, 2007; Krause et al., 2012). With repeated analyses, it is possible to unravel processes that occur on different time scales, for example fast uptake of N by microbes including mycorrhiza (e.g. Zhang et al., 2019) and slower uptake by plants, followed by very slow mineralization of dead plant material and humus. For example, in an experiment with small plots, Providoli et al. (2006) carried out eight sampling events with increasing time intervals, from 1 h up to one year after tracer application. Additional insight can be obtained by analyzing individual N compounds for their concentration and ^{15}N abundance. See "Specific Ecosystem Pools and Fluxes" section for some examples.

With these considerations in mind, we propose a scheme of aspects to consider when setting up ^{15}N tracer experiments in the field (**Table 1**). This scheme partly reflects well-known statistical knowledge, especially for the difference between true replications and replicated measurements within experimental units. The variability of the ecosystem depends, of course, on the type of system studied and its characteristics. In the case of a forest with adult trees, a much larger study area is required if N fluxes in the trees are considered than if only the soil is studied. In order to obtain measurable ^{15}N abundances in all relevant pools and fluxes, these values may be estimated in advance using recovery rates obtained in previous studies with similar characteristics (e.g. Templer et al., 2012) and various amounts of tracer. A more sophisticated approach is to run an ecosystem model (Van Dam and Van Breemen, 1995; Currie et al., 2004) to simulate the fate of the tracer before applying it. This method was applied, for example, within the European NITREX project

TABLE 1 | Decision scheme for whole ecosystem ^{15}N tracer studies.

Parameter	Decision criteria
Plot (experimental unit) size	Large enough to be representative of small-scale variability Small enough that tracer costs are reasonable
Amount of tracer applied per area	Large enough to achieve labeling of large, dilute pools and fluxes Small enough to avoid unwanted fertilization/eutrophication Small enough that tracer costs are reasonable
Number of replications	Important to achieve precise, testable results Small enough that work load and analytical costs are reasonable
Number of samples per plot	Useful to improve the level of precision Small enough that work load is reasonable Samples can be pooled for analysis without really compromising statistics
Number of analyses per sample	Multiple analyses are marginally useful for improving precision
Sampling frequency	Should match the time scale of relevant N transformation processes

(Wright and Dise, 1992). In the last few decades, many ^{15}N tracer studies have been conducted in natural ecosystems and, more generally, in ecosystems that do not receive fertilizers (e.g. Schlesinger, 2009; Templer et al., 2012). In such ecosystems, the amount of tracer has to be kept low in order to avoid inducing a fertilization or eutrophication effect, i.e. to keep the system in its original trophic state. In agriculture, the amount of tracer applied may be higher, but its cost also has to be taken into account, especially if larger areas need to be labeled. In amounts typically needed for larger field studies (1 mol or more), the tracer itself currently costs around 2,000–3,000 USD per mole.

TRACER APPLICATION

Besides the amount of tracer to apply, addressed in the previous section, there are several other practical aspects connected to the application of the tracer. These are mainly: the method of application, the chemical form of the tracer and the timing. Their optimization always depends on the questions asked in these studies. In experiments with mineral fertilizers, tracers can be chosen in the same chemical form and applied mixed into the fertilizer. More questions arise in experiments with the aim of assessing the fate of atmospheric N deposition. In their meta-analysis, Templer et al. (2012) distinguish between three chemical forms ($^{15}NH_4{}^{15}NO_3$, $^{15}NH_4{}^+$ or $^{15}NO_3{}^-$) and between two application methods (to the canopy or to the soil). The choice of the chemical form depends on the local composition of the deposition that researchers want to trace. If it is possible to do so, applying $^{15}NH_4{}^+$ and $^{15}NO_3{}^-$ to separate plots leads to a better understanding of their respective short-term plant uptake and immobilization processes. Ammonium is retained much better in the soil than nitrate, by adsorption on clay and humus, and both ions also differ in their uptake by plants (Providoli et al., 2006; Feng et al., 2008; Liu et al., 2017). The preference of plants for these ions appears to be related to their mycorrhizal association (Goodale, 2017). Organic forms of N like glycine have mainly been tested in cold ecosystems where they may play a greater role in plant uptake (Sorensen et al., 2008; Dawes et al., 2017).

As long as the goal is to understand the fate of N from atmospheric deposition, applying the tracer over the canopy is the most representative method. In forests, this has been successfully done by helicopter (Dail et al., 2009). Due to the cost of this method (especially if the application has to be repeated over time), most studies are done by applying the tracer under the tree canopy, over the ground vegetation (Templer et al., 2012). This obviously does not allow for tracer uptake by tree foliage, a mechanism found for both broadleaves and needles, especially in young trees (Wilson and Tiley, 1998; Sparks, 2009; Nair et al., 2016). In contrast, application directly on or into the soil can be used to study plant uptake only via the roots.

The timing of tracer application is also a factor to be considered, as it is well known from agricultural crops that N availability should coincide with plant demand to maximize uptake. Atmospheric deposition, in contrast, has its own seasonality. In order to quantify the fate of N deposition over a year, it is thus advisable to follow a similar seasonality with the tracer, applying it in multiple small amounts. This was done, for example, in small headwater catchments by Providoli et al. (2005). They even noticed that applying the tracer at time of rain events led to more tracer appearing in leached nitrate than when the tracer was applied independent of the weather. This finding can be explained by preferential water flow through the soil during rain events, which hinders nitrate uptake. In experiments with roofs, deposition with a manipulated chemical composition was applied using automated sprinkler systems that simulated the actual rain events (Boxman et al., 1995; Lamersdorf and Borken, 2004; Feng et al., 2008). A single-dose tracer application, as sometimes performed, has the disadvantage that the obtained tracer partitioning is not representative of the actual seasonal dynamics.

A different approach is to follow the recycling of N within the ecosystem using labeled plant litter (Blumfield et al., 2004; Tonon et al., 2007; Hatton et al., 2012). For such experiments, labeled litter is first produced, typically by cultivating plants in pots with a ^{15}N-enriched fertilizer. This prior step may be a reason why the application of ^{15}N *via* plant litter is chosen relatively seldomly, despite its importance for understanding the release of N from decomposing plant litter and its incorporation into older soil organic matter.

SAMPLING AND CALCULATIONS

Three Components to Determine Tracer Recovery

To calculate the tracer recovery in an ecosystem pool or flux, it is necessary to measure three variables: the tracer fraction, the element concentration and the total mass of the pool or flux.

The **tracer fraction** in a pool or flux, also called specific labeling, is calculated from an N mass balance. Without tracer, all N pools and fluxes already contain ^{15}N at a natural abundance level. This means that measured ^{15}N is partly native and partly stems from the tracer (see equations below). Three ^{15}N fractional abundances thus enter the calculation: the abundance in the tracer itself, the natural (native) abundance in the pool or flux and the abundance coming from the tracer. These abundances can be measured by isotope-ratio mass spectrometry (IRMS). For a bulk analysis, the IRMS is usually coupled to an element analyzer in which the samples are completely oxidized. In this case, it can easily be combined with the analysis of ^{13}C, but other configurations are possible according to the chemical compounds of interest (see some details in "Specific Ecosystem Pools and Fluxes" section).

Abundances can be quantified with a relative precision that deteriorates with increasing natural and experimental variability. Because the natural abundance is relatively constant through space and time, it requires few samples and analyses to achieve a sufficient precision. In the labeled pools and fluxes, in contrast, the ^{15}N abundance varies because of inhomogeneity both in the tracer application (experimental imprecision) and in the N cycling processes (natural variability). To compensate for this variability, the labeled pools and fluxes should be sampled and analyzed with a higher intensity than the controls used for the determination of natural abundances. This is especially true in short-term studies, where N pools and fluxes are analyzed at a frequency of hours or days: at this time scale, the natural abundances usually do not show any measurable changes. If the ^{15}N abundance in the pool remains much higher than its natural abundance, the latter may even be ignored in the calculation (see **Eq. 4** below).

The **N concentration** in the pools or fluxes is usually measured in the same samples used to determine their ^{15}N abundance, most of the time in the same mass spectrometry analysis. Because the mass spectrometer is optimized for measuring the ^{15}N abundance and not necessarily the N concentration, a separate analysis may improve the precision and also make it possible to measure other chemical elements like carbon and sulfur.

The **pool sizes or fluxes** are often measured independently from the N and ^{15}N analyses. The measurement techniques vary according to the nature of these pools or fluxes (e. g. soil, plants, water) and will, thus, be discussed in the following sections.

Calculation of Tracer Recovery

Methods for calculating tracer recovery have been described in many publications, but often with diverging or even mathematically improper notations. Equations (Providoli et al., 2005) are therefore recalled and completed here, using SI units and thus avoiding unnecessary conversion factors. Abundances of stable isotopes in samples are routinely expressed in the δ notation in relation to a standard (**Eq. 1**):

$$\delta^{15}\mathrm{N} = \mathrm{R}_{\mathrm{sample}} \big/ \mathrm{R}_{\mathrm{standard}} - 1 \tag{1}$$

where R is defined as the molar fraction of the heavier to the lighter isotope, i.e. ^{15}N/^{14}N. δ values are essentially dimensionless and mostly expressed in ‰. For ^{15}N, the standard is atmospheric N_2, with $R_{standard}$ = 0.0036765. R_{sample} can be calculated by inverting **Eq. 1** to **Eq. 2**:

$$\mathrm{R}_{\mathrm{sample}} = \left(\delta^{15}\mathrm{N}_{\mathrm{sample}} + 1\right) \cdot \mathrm{R}_{\mathrm{standard}} = {}^{15}\mathrm{N}_{\mathrm{sample}} \big/ {}^{14}\mathrm{N}_{\mathrm{sample}} \tag{2}$$

For further calculations, we use the molar ratio to calculate the fractional abundance (**Eq. 3**):

$$\mathrm{F} = \mathrm{R} / (\mathrm{R} + 1) = {}^{15}\mathrm{N} / \left({}^{14}\mathrm{N} + {}^{15}\mathrm{N}\right) \tag{3}$$

Equation 3 is given without subscripts because it applies to samples as well as to standard and reference material. Unfortunately, there are actually two definitions of δ coexisting in scientific publications. The second has the same form as **Eq. 1** but with F instead of R, and thus uses $F_{standard}$ = 0.003663. To avoid unnecessary confusion, we do not give this second equation explicitly. The F-based δ would actually be preferable because it makes calculations a bit easier, but IRMS laboratories typically use the R-based definition and report results in this form. Therefore, **Eq. 2** and **Eq. 3** should normally be used in calculations based on δ values from an IRMS laboratory. Double-checking this is still advisable.

In a next step (**Eq. 4**), fractional abundances are used to calculate the tracer fraction X_{sample}, defined as the molar ratio of tracer N to total N in a sample:

$$\mathrm{X}_{\mathrm{sample}} = \left(\mathrm{F}_{\mathrm{sample}} - \mathrm{F}_{\mathrm{reference}}\right) \big/ \left(\mathrm{F}_{\mathrm{tracer}} - \mathrm{F}_{\mathrm{reference}}\right) \tag{4}$$

where $F_{reference}$ is the fractional abundance in unlabeled samples and F_{tracer} is the abundance in the applied tracer (typically given as atom % by the producer). All equations so far are based on the number of atoms and not on their mass. For further calculations, we need amounts of N, which are typically obtained as masses (g) from IRMS laboratories. It is therefore necessary to convert these masses to moles (**Eq. 5**):

$$\mathrm{n} = \mathrm{m}/\mathrm{M} \tag{5}$$

where n is the molar quantity, m the mass and M the molar mass. Because of the different masses of the isotopes, the molar mass itself is not constant but needs to be calculated from the isotope fraction F (**Eq. 6**):

$$\begin{aligned} \mathrm{M} &= 14.003074 \cdot (1 - \mathrm{F}) + 15.000109 \cdot \mathrm{F} \\ &= 14.003074 + 0.997035 \cdot \mathrm{F} \end{aligned} \tag{6}$$

Note that coefficients in **Eq. 6** (in g mol^{-1}) are often rounded to the unit, i.e. to 14, 15 and 1, which affects the results only from the fifth significant digit onwards. Finally, the tracer recovery Z (tracer recovered in a pool or flux relative to the tracer applied) can be calculated (**Eq. 7**):

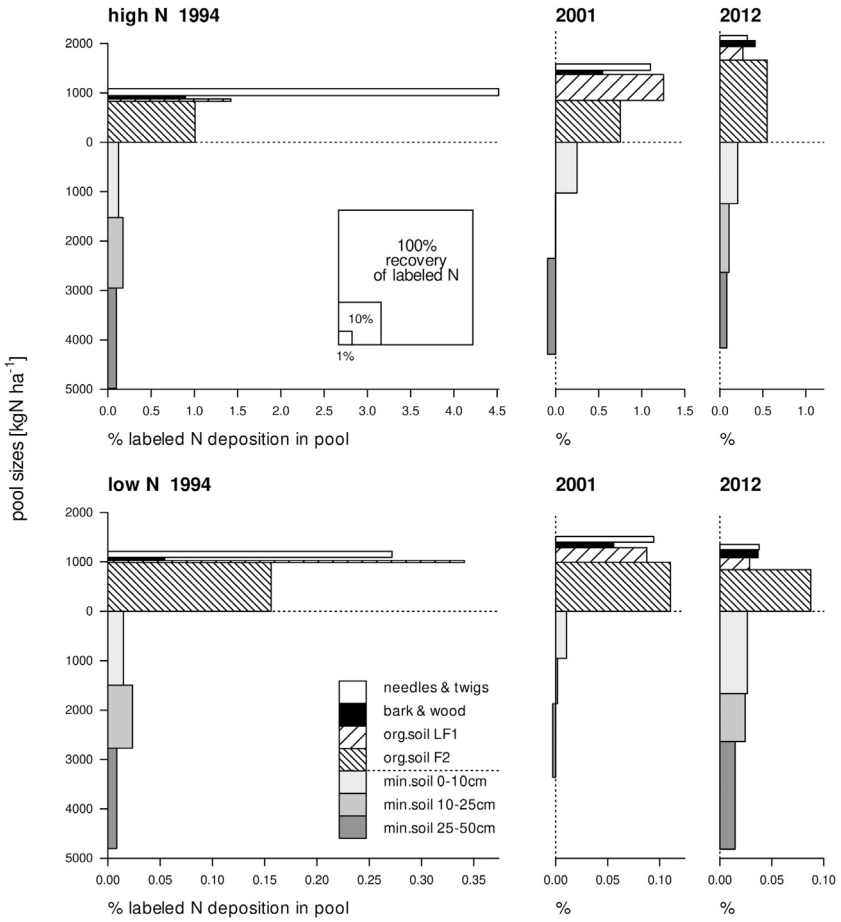

FIGURE 1 | Size of each N pool against the presence of tracer in the pool in high and low N deposition plots in a Scots pine forest, one, eight and nineteen years after labeling. The area of each rectangle represents the recovery of ^{15}N in that pool (expressed as the proportion of applied label, see legend in upper left panel). Please note that the *x*-axes for the high and the low N deposition treatments have different scales. Redrawn from Wessel et al. (2021).

$$Z_{pool} = X_{sample} \cdot n_{pool}/n_{tracer} \quad (7)$$

where n_{pool} and n_{tracer} are the total amounts of *N* (in mol) in the pool and in the tracer, respectively. These amounts of *N* can be expressed per experimental unit (plot) or per area, but both should obviously be on the same basis. The tracer recovery Z_{pool} is usually expressed in %, but this is again only a transformation of units and thus not included in the SI-based equation.

In some studies, *N* masses were not transformed into molar quantities, i.e. N masses were used in **Eq. 7** instead of N amounts in mol (Hauck and Bremner, 1976; Nadelhoffer and Fry, 1994). The resulting difference in terms of tracer recovery can be quantified. Substituting **Eq. 5** and **Eq. 6** into **Eq. 7** gives:

$$Z_{pool} = X_{sample} \cdot m_{pool}/m_{tracer} \cdot \left(14 + F_{tracer}\right)/\left(14 + F_{pool}\right) \quad (8)$$

So if tracer recovery is calculated using masses (m) instead of molar quantities (n), the resulting Z_{pool} differs from the true value by a factor $(14 + F_{tracer})/(14 + F_{pool})$. In case of a highly enriched tracer ($F_{tracer} \approx 1$) and small sample enrichments ($F_{pool} << 1$), this factor equals 15/14. This means that tracer recoveries are underestimated by about 7%.

Graphical Representation of ^{15}N Recovery

In a tracer experiment, recovery in an N pool (Z in the above calculations) is proportional to the pool's size (n_{pool}) times its tracer fraction (X). This is illustrated graphically in **Figure 1**, which shows the results of two tracer experiments in a forest with experimental low and high N deposition (Wessel et al., 2021). The area of each rectangle represents the recovery in an N pool, with the vertical dimension indicating the size of the N pool and the horizontal dimension the tracer fraction. As the tracer application amounts differed between N deposition treatments, the *x*-axis scale differs among panels. In the figure it is apparent that some pools contributed considerably to the total tracer recovery because they were large, such as the mineral soil pools. Other pools, such as the aboveground vegetation and the LF1 layer, only made a small contribution to the total ^{15}N recovery despite their relatively large tracer fraction because their N pool sizes were small.

TABLE 2 | Calculation of tracer recovery by averaging the recovery of single samples (replications) vs. the calculation based on average N concentrations and δ^{15}N.

	Pool mass (g/m^2)	N concentration (mg/g)	δ^{15}N (‰)	N pool (mol/m^2)	^{15}N ratio R	^{15}N fraction F	Tracer fraction X	Tracer recovery Z
Tracer applied				0.00889		0.99		
Reference	6,956	10.93	–3.11	5.43	0.0036651	0.0036517		
Replication 1	4,120	19.10	46.51	5.62	0.0038475	0.0038327	0.0001836	0.1160
Replication 2	13,091	10.82	15.61	10.11	0.0037339	0.0037200	0.0000693	0.0788
Replication 3	9,463	11.91	55.73	8.05	0.0038814	0.0038664	0.0002177	0.1971
Replication 4	6,975	10.51	108.17	5.23	0.0040742	0.0040577	0.0004116	0.2424
Average recovery								0.1586
Average-based calculation	8,412	13.09	56.51	7.25	0.0038842	0.0038692	0.0002206	0.1950

Data from the organic soil layer in a forest, one year after spraying a $^{15}NH_4Cl$ tracer (Providoli et al., 2006). The overestimation of tracer recovery by the second calculation method can be explained by negative correlations, in this case –0.73 between soil dry mass and N concentration and -0.21 between N concentration and δ^{15}N.

SPECIFIC ECOSYSTEM POOLS AND FLUXES

Soil

Much of the applied ^{15}N tracer is typically recovered in the soil (Templer et al., 2012), and the accuracy of the total recovery thus largely depends on the accuracy of the soil analysis. Soil cores are typically taken according to sampling schemes similar to those used for other chemical analyses. These cores are then analyzed individually or combined to form composite samples. If present, undecomposed plant litter can be taken from the same cores and separated from the decomposing organic soil horizon. After this, the soil cores have to be cut according to their horizons. This step is crucial because it determines how well the obtained results will be comparable across plots, treatments, sampling times or even between different experiments and soil types. Cutting horizons by depth or along horizon borders is a matter of choice, as is the case of soil analyses in general. Working with horizons can facilitate interpretation of the results, but working with depths can be more reproducible across soil types. Apparent soil densities may show large spatial and temporal variations within a layer or horizon. For this reason, it is always advisable to measure the dry mass of each horizon in each sample. Relying on an average density can lead to gross errors, especially when this density is low and the soil tends to be compressed during coring.

If the mass, the N concentration and the tracer fraction are all measured from the same sample (corresponding to one or several cores), then the N recovery can also be calculated per sample before being averaged. This is better than calculating averages of the mass, N concentration and tracer fraction for two reasons. First, it allows a direct calculation of statistical parameters (standard deviation, standard error, confidence intervals) of the recovery. Second, it is not biased if the three variables are somehow correlated. For example, a sample having a higher N content (higher mass and/or higher N concentration) can be expected to have a lower tracer fraction due to dilution by the native N. In this case, averaging the tracer fractions would lead to an overestimation compared with averaging the tracer recoveries (**Table 2**). This leads to the following general advice: calculate averages of amounts, not of abundances or concentrations. If, for any reason, the mass, N concentration and tracer fraction are not measured in the same samples, then error propagation laws have to be used to estimate the standard error of the tracer recovery. In most such cases, correlations between the three components of the recovery are not known, and this prevents a proper calculation of error propagation. However, because pool mass, N concentration and tracer fraction are more likely to be negatively than positively correlated, a calculation without accounting for these correlations can be considered conservative.

Soil Components

N is present in many different bio-physico-chemical forms in the soil. Besides calculating total tracer recovery in soil horizons, it is often interesting to determine in greater detail the forms in which the applied tracer is present. The most frequent goal of these analyses is to separate more or less stable fractions, which can store and release the tracer at different time scales. Typical methods are extraction (e.g. Providoli et al., 2006), hydrolysis (e.g. Morier et al., 2010) and density fractionation (e.g. Hatton et al., 2012; Kramer et al., 2017, on natural ^{15}N abundance). The fumigation-extraction method (Brookes et al., 1985) plays a specific role as it allows the estimation of tracer recovery in soil microorganisms. It is not our goal here to examine the advantages and limitations of these methods, which are not directly related to isotopes. The analysis of aqueous solutions obtained from extractions will be treated in "*Water*" section, along with the analysis of natural water samples.

In the context of ^{15}N tracer experiments, the recovery rate of extraction or separation methods always plays a central role, as it also affects the recovery rate of the tracer. Correction factors are often applied, for example to estimate microbial N from the fumigation-extraction method. Applying the same factor to the tracer is always questionable and should in any case be interpreted with caution. Further, one of the greatest challenges is certainly to relate fractions empirically obtained by analyses to pools defined conceptually or implemented practically in ecosystem models.

Roots

Fine roots (<2 mm as the standard definition) are usually taken from the same soil cores as used for soil analysis. Depending on the morphology of the roots and on the soil structure, this task can be very time consuming. This is especially the case for dense

root systems of Gramineae. In some cases, it is easier to work with separate cores and to wash the roots free of soil with water, subsequently calculating tracer recovery in the root-free soil as a difference.

Coarse roots, especially coarse tree-roots, can rarely be sampled quantitatively by soil coring. A separate estimation of their dry mass can improve the results, but the accuracy is essentially limited by the difficulty in accessing root systems. Systematic sampling often requires a considerable amount of digging, i.e. more destructive sampling. If available, allometric estimations based on aboveground parameters may be sufficient to estimate the dry mass of coarse roots. As the tracer fraction and pool size are not estimated from the same samples, the accuracy of the tracer recovery has to be estimated by error propagation laws, and, as a consequence, possible correlations between the two remain unnoticed. Another consequence of using allometric relationships is that the spatial variation in the dry mass is practically impossible to determine, and is generally ignored in calculations and statistical tests.

Ground Vegetation

The ground vegetation comprises mosses and aboveground parts of herbaceous vegetation and of shrubs. Except for taller shrubs, ground vegetation is best analyzed by quantitatively harvesting patches. The number and size of the patches must be chosen according to the homogeneity of the vegetation cover. In ecosystems with only a few plant species, the individual species can be weighed and analyzed separately. In species-rich systems, functional groups may be considered, for example separating mosses, monocotyledons and dicotyledons. If a species or a functional group is absent from a sample, then its tracer fraction and N concentration are missing data. Its tracer recovery, however, is not missing data but rather zero. Treating it as missing data would mean overestimating the average recovery by systematically removing all zero values. Again, to avoid bias in the recovery calculation, the same rule as for the soil (see above) should be applied: amounts can be averaged, whereas abundances and concentrations should not.

Trees

The aboveground parts of large shrubs and trees can rarely be harvested quantitatively to analyze their tracer recovery. Just as in the case of coarse roots, the biomass of their different parts has to be estimated by allometric relationships: foliage, branches and trunks (bark, wood). The corresponding pools are sampled and analyzed separately. Wood is often difficult to analyze because of its high C/N ratio (Savard et al., 2020), meaning that its combustion for mass spectrometry produces much CO_2 but little N. Wood must be finely ground before analysis because the combustion of even tiny wood chips is not fast enough. In some species, it has been observed that tracer N also enters older wood (Tomlinson et al., 2014). It is thus important to take wood cores that go deep enough into the trunks. In spruce trees, for example, tree rings from at least the last 30 years should be analyzed, but rings can be grouped (Schleppi et al., 1999). Analyzing wood from different heights above the ground has also been tested but does not appear to be necessary (Nadelhoffer et al., 2004). The wood mass of each ring or ring group is then calculated from the ring widths and wood densities, and from the size of the trees. A model for the shape of the tree species is therefore necessary (for example a simple conical shape). For the diagnostic of nutrient status, tree foliage is typically taken from the top, sunlight-exposed part of the crowns, which enables comparisons between trees and between stands. For a mass balance, however, it is essential to remember that shade foliage can be very different from sunlit foliage. This is true for its chemical composition but also especially for its morphological parameters, with shade foliage having a lower specific mass (less dry matter per area). The specific leaf mass is required in the calculation of the total mass of foliage based on indirect measurements of the leaf area index (leaf area per ground area). It is thus advisable to sample foliage from different heights within a forest canopy.

Water

For the analysis of soluble N compounds in water samples or soil extracts, it is necessary to separate them from the water, which is often time consuming. For the combined analysis of ^{15}N and ^{18}O in nitrate, we refer to the extensive publication by Kendall et al. (2007). As long as no other isotope has to be measured (e.g. ^{18}O in nitrate), the method of ammonia diffusion is well established, giving good recovery rates and sufficient precision (Schleppi et al., 2006a). With this method, it is possible to determine the isotope fraction in inorganic N. This is achieved directly for ammonium and for nitrate after its reduction to ammonium. Total dissolved ^{15}N can be measured by first lyophilizing the water samples, then analyzing the residue by IRMS. The ^{15}N fraction in dissolved organic N (DON) can be calculated as the difference between total N and inorganic N (e.g. Providoli et al., 2006). If there is much more tracer in inorganic N than in DON, however, this calculation becomes too inaccurate.

In contrast to soil or plant pools, water can be highly mobile in an ecosystem, in which case its fluxes must be considered. This requires more frequent sampling and appropriate methods to integrate element fluxes based on discrete analyses (Schleppi et al., 2006b). In hydrologically defined catchments, dissolved N compounds leaving the ecosystem can be determined by quantifying and sampling the runoff. For vertical movements of water-dissolved N in the soil, water fluxes need to be modeled (Koopmans et al., 1996; Gundersen, 1998; Feng et al., 2008). The application and constraints of such an approach are not different than for dissolved compounds in general and thus will not be detailed here (Tiktak and Van Grinsven, 1995).

LONGITUDINAL STUDIES AND MODELING

Longitudinal studies involve the repeated sampling and analysis of pools and fluxes over several years or even decades. Compared with short-term studies with a time scale of days, long-term studies pose some specific challenges and opportunities. The long-term fate of ^{15}N tracers is especially useful to assess the effect of slow changes, as brought about by atmospheric deposition (Veerman et al., 2020; Wessel et al., 2021) or

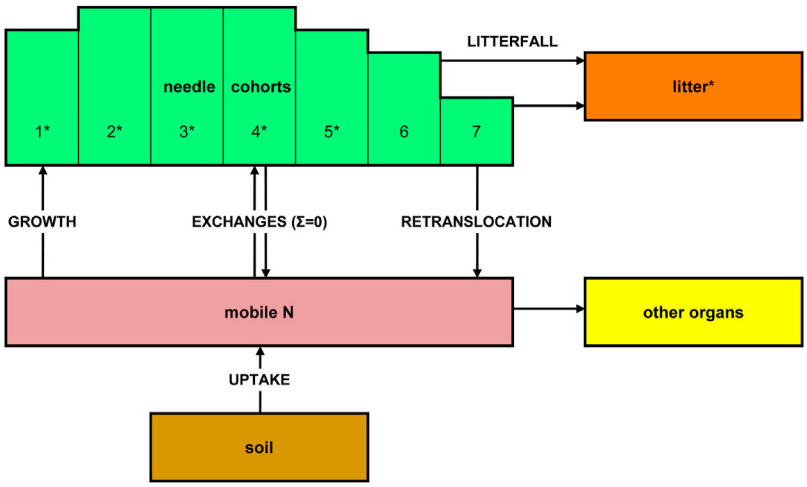

FIGURE 2 | Simple model used to describe the translocation of ^{15}N tracer in coniferous trees with several needle age classes (cohorts). Measured N pool and ^{15}N abundances are indicated by stars.

climate change (Cheng et al., 2019). Interpretation of long-term tracer experiments can be a challenge, but can be improved by the use of models (Currie, 2007). These vary from simple mixing models to derive the N dynamics of one tracer experiment (Gerzabek et al., 2004) to complete ecosystem models (Van Dam and Van Breemen, 1995; Currie et al., 2004). The latter are complex models, including many ecosystem processes such as photosynthesis, substrate allocation, litter production, soil organic carbon transformations, and water and solute flow. Such models, however, have only been applied to field experiments in a few cases (Koopmans and Van Dam, 1998; Currie et al., 2004; Krause et al., 2012), as all the different processes in the model have to be parameterized and calibrated before the model can be put to use. An alternative to these models is the approach used by Rastetter et al. (2005), in which an already existing model is used for the simulation of the N dynamics, after which a second model just adds the ^{15}N dynamics to the total N simulation results from the first model. As the ^{15}N does not affect the N transformations or any other process in the ecosystem, its dynamics can be calculated afterward. Another approach is to mimic ^{15}N dynamics in models by running such a model twice, adding a small amount of additional N into the N deposition input stream representing the tracer during the second model run (Thomas et al., 2013; Cheng et al., 2019). As these models have a broader application than just for the modeling of ^{15}N tracer, the effort needed to get them to produce meaningful output may be less.

As an example of a simple model application, we show here how the analysis of ^{15}N in tree needles and litter can help to understand the plant uptake of N brought about by atmospheric deposition. The data (**Figure 2**) are from a long-term NH_4NO_3 addition to a subalpine coniferous forest where the treatment was labeled on both ions ($^{15}NH_4{}^{15}NO_3$) during the first year (Schleppi et al., 1999). Needles of conifers can be separated according to their age. Here, we sampled five cohorts and repeated the measurements for nine years. Litter was also collected, with

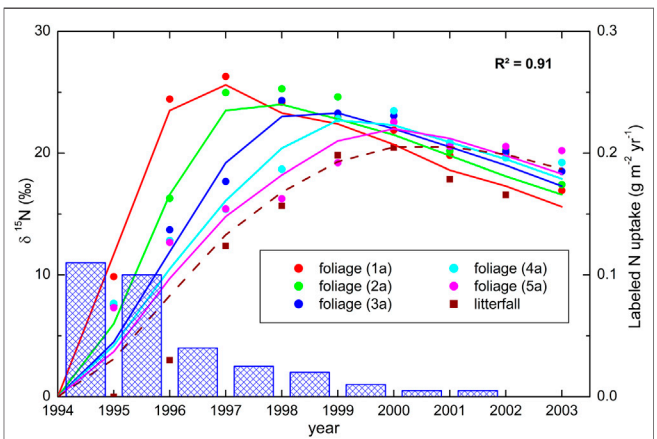

FIGURE 3 | ^{15}N abundances in Norway spruce needle cohorts and in litterfall in an N addition experiment in which a $^{15}NH_4{}^{15}NO_3$ tracer was applied during the initial year (Schleppi et al., 1999). Dots represent measurements and lines are modeled δ^{15}N values. The modeled tracer uptake by the trees is shown as bars.

about two thirds of this material being old needles. The N translocation model used with these data is based on three plant pools (**Figure 2**): the needles (divided into seven age classes), a mobile N pool in woody tissues and bark, and the N immobilized in such tissues. The uptake from the soil, translocation within the plant and N loss by litterfall were the considered fluxes, with rates calibrated by fitting the model to the available data. These rates are all depicted in **Figure 3**. The best fit explained R^2 = 91% of the variance in the δ^{15}N measurements. Besides the incorporation of new N into growing needles (cohort 1, marginally also cohort 2) and retranslocation out of senescing needles (cohorts 4–7), relatively large exchanges between the different cohorts via the mobile N pool had to be taken into account in order to achieve the observed partitioning of tracer

across the different needle age classes. The modeled tracer N uptake by the trees is shown as bars in **Figure 3**. This time-course contrasts very much with the rapid disappearance of ^{15}N in nitrate leached from this forest (Providoli et al., 2005; Schleppi et al., 2017). On the other hand, ^{15}N available to trees decreases markedly from year to year while tracer in the bulk soil remains quite stable for decades, as observed in this experiment as well as in three other experimental forests across Europe (Veerman et al., 2020). This clearly shows that different N pools with different turnover times are involved. A simple model like the one considered here obviously cannot unravel the different processes taking place in the soil itself, but it shows the potential value of combining longitudinal tracer studies with ecosystem models.

CHALLENGES AND OPPORTUNITIES

According to Templer et al. (2012), most ^{15}N studies in terrestrial ecosystems show a total tracer recovery well below 100%. Grasslands show even less recovery than forests in spite of the fact that an herbaceous vegetation is much easier to sample quantitatively. Some fluxes often remain unaccounted for in such studies, especially volatilization immediately after application, denitrification, grazing and lateral fluxes out of the plots. N leaching (mainly as nitrate but also as DON) is usually not directly measured but calculated by multiplying concentrations in soil water under the rooting zone by water infiltration at this level. This approach neglects preferential flow and may thus lead to an underestimation of the leaching flux. While lateral fluxes can be minimized by labeling also borders around the sampled plots (mainly above the plot if it is on a slope), all other processes are relatively difficult to capture and thus remain a challenge for future studies.

^{15}N tracer studies in terrestrial ecosystems, especially in forests, have been used to constrain global climate models (Nadelhoffer et al., 1999; Cheng et al., 2019). This kind of application has been criticized because N uptake by tree canopies is not taken into account when ^{15}N tracer is applied under tree crowns (Sievering, 1999; Nair et al., 2016). While the uptake of sprayed tracer by foliage of small trees has been well documented (Sparks, 2009), the magnitude of this process is still not really quantified for trees in their forest environment, especially considering the difficulty of reproducing experimentally the N deposition brought by natural rain events. Towers built in forests for research purposes may give opportunities to conduct realistic tracer experiments where ^{15}N could be sprayed over trees specifically during rain events.

DATA AVAILABILITY STATEMENT

The model and dataset presented in this study are available upon request from the corresponding author.

AUTHOR CONTRIBUTIONS

PS planned and wrote large parts of the manuscript. WWW wrote other parts. Both authors edited the manuscript.

ACKNOWLEDGMENTS

The European Science Foundation funded a visit by W. W. Wessel to the Swiss Federal Institute for Forest, Snow and Landscape Research (ClimMani Exchange Grant 2012). We thank Dr M. Dawes for language editing of the manuscript.

REFERENCES

Björkman, E., Lundeberg, G., and Nömmik, H. (1967). Distribution and Balance of N^{15} Labeled Fertilizer Nitrogen Applied to Young Pine Trees (*Pinus silvestris* L.). *Stud. For. Suec.* 48, 5–23.

Blumfield, T. J., Xu, Z., Mathers, N. J., and Saffigna, P. G. (2004). Decomposition of Nitrogen-15 Labeled Hoop Pine Harvest Residues in Subtropical Australia. *Soil Sci. Soc. Am. J.* 68, 1751–1761. doi:10.2136/sssaj2004.1751

Boxman, A. W., Van Dam, D., Van Dijk, H. F. G., Hogervorst, R., and Koopmans, C. J. (1995). Ecosystem Responses to Reduced Nitrogen and Sulphur Inputs into Two Coniferous Forest Stands in the Netherlands. *For. Ecol. Manage.* 71, 7–29. doi:10.1016/0378-1127(94)06081-S

Brookes, P. C., Kragt, J. F., Powlson, D. S., and Jenkinson, D. S. (1985). Chloroform Fumigation and the Release of Soil Nitrogen: The Effects of Fumigation Time and Temperature. *Soil Biol. Biochem.* 17, 831–835. doi:10.1016/0038-0717(85)90143-9

Cheng, S. J., Hess, P. G., Wieder, W. R., Thomas, R. Q., Nadelhoffer, K. J., Vira, J., et al. (2019). Decadal Fates and Impacts of Nitrogen Additions on Temperate Forest Carbon Storage: a Data-Model Comparison. *Biogeosciences* 16, 2771–2793. doi:10.5194/bg-16-2771-2019

Currie, W. S., Nadelhoffer, K. J., and Aber, J. D. (2004). Redistributions of ^{15}N Highlight Turnover and Replenishment of Mineral Soil Organic N as a Long-Term Control on Forest C Balance. *For. Ecol. Manage.* 196, 109–127. doi:10.1016/j.foreco.2004.03.015

Currie, W. S. (2007). "Modeling the Dynamics of Stable-Isotope Ratios for Ecosystem Biogeochemistry," in *Stable Isotopes in Ecology and Environmental Science*. Editors R. Michener and K. Lajtha. 2nd ed. (Malden, MA, USA: Blackwell), 450–479. doi:10.1002/9780470691854.ch13

Dail, D. B., Hollinger, D. Y., Davidson, E. A., Fernandez, I., Sievering, H. C., Scott, N. A., et al. (2009). Distribution of Nitrogen-15 Tracers Applied to the Canopy of a Mature Spruce-Hemlock Stand, Howland, Maine, USA. *Oecologia* 160, 589–599. doi:10.1007/s00442-009-1325-x

Dawes, M. A., Schleppi, P., and Hagedorn, F. (2017). The Fate of Nitrogen Inputs in a Warmer Alpine Treeline Ecosystem: a ^{15}N Labelling Study. *J. Ecol.* 105, 1723–1737. doi:10.1111/1365-2745.12780

Erisman, J. W., van Grinsven, H., Grizzetti, B., Bouraoui, F., Powlson, D., Sutton, M. A., et al. (2011). "The European Nitrogen Problem in a Global Perspective," in *The European Nitrogen Assessment: Sources, Effects and Policy Perspectives*. Editors M. A. Sutton, C. M. Howard, J. W. Erisman, G. Billen, A. Bleeker, et al. (Cambridge: Cambridge University Press), 9–31. url: http://www.nine-esf.org/files/ena_doc/ENA_pdfs/ENA_c2.pdf

Feng, Z., Brumme, R., Xu, Y.-J., and Lamersdorf, N. (2008). Tracing the Fate of Mineral N Compounds Under High Ambient N Deposition in a Norway Spruce Forest at Solling/Germany. *For. Ecol. Manage.* 255, 2061–2073. doi:10.1016/j.foreco.2007.12.049

Fry, B. (2006). *Stable Isotope Ecology*. New York: Springer. doi:10.1007/0-387-33745-8

Gardner, J. B., and Drinkwater, L. E. (2009). The Fate of Nitrogen in Grain Cropping Systems: a Meta-Analysis of ^{15}N Field Experiments. *Ecol. Appl.* 19, 2167–2184. doi:10.1890/08-1122.1

Gerzabek, M. H., Haberhauer, G., Stemmer, M., Klepsch, S., and Haunold, E. (2004). Long-Term Behaviour of ^{15}N in an Alpine Grassland Ecosystem. *Biogeochem.* 70, 59–69. doi:10.1023/B:BIOG.0000049336.84556.62

Goodale, C. L. (2017). Multiyear Fate of a ^{15}N Tracer in a Mixed Deciduous Forest: Retention, Redistribution, and Differences by Mycorrhizal Association. *Glob. Change Biol.* 23, 867–880. doi:10.1111/gcb.13483

Gundersen, P. (1998). Effects of Enhanced Nitrogen Deposition in a Spruce Forest at Klosterhede, Denmark, Examined by Moderate NH_4NO_3 Addition. *For. Ecol. Manage.* 101, 251–268. doi:10.1016/S0378-1127(97)00141-2

Hatton, P.-J., Kleber, M., Zeller, B., Moni, C., Plante, A. F., Townsend, K., et al. (2012). Transfer of Litter-Derived N to Soil Mineral-Organic Associations: Evidence from Decadal ^{15}N Tracer Experiments. *Org. Geochem.* 42, 1489–1501. doi:10.1016/j.orggeochem.2011.05.002

Hauck, R. D., and Bremner, J. M. (1976). Use of Tracers for Soil and Fertilizer Nitrogen Research. *Adv. Agron.* 28, 219–266. doi:10.1016/S0065-2113(08)60556-8

Hauck, R. D., Bartholomew, W. V., Bremner, J. M., Broadbent, F. E., Cheng, H. H., Edwards, A. P., et al. (1972). Use of Variations in Natural Nitrogen Isotope Abundance for Environmental Studies: a Questionable Approach. *Science* 177, 453–456. doi:10.1126/science.177.4047.453

Kendall, C., Elliott, E. M., and Wankel, S. D. (2007). "Tracing Anthropogenic Inputs of Nitrogen to Ecosystems," in *Stable Isotopes in Ecology and Environmental Science*. Editors R. Michener and K. Lajtha. 2nd Edn. (Malden, MA: Blackwell), 375–449. doi:10.1002/9780470691854.ch12

Koopmans, C. J., and Van Dam, D. (1998). Modelling the Impact of Lowered Atmospheric Nitrogen Deposition on a Nitrogen Saturated Forest Ecosystem. *Water Air Soil Pollut.* 104, 181–203. doi:10.1023/A:1004992614988

Koopmans, C. J., Tietema, A., and Boxman, A. W. (1996). The Fate of ^{15}N Enriched Throughfall in Two Coniferous Forest Stands at Different Nitrogen Deposition Levels. *Biogeochem.* 34, 19–44. doi:10.1007/BF02182953

Kramer, M. G., Lajtha, K., and Aufdenkampe, A. K. (2017). Depth Trends of Soil Organic Matter C:N and ^{15}N Natural Abundance Controlled by Association with Minerals. *Biogeochem.* 136, 237–248. doi:10.1007/s10533-017-0378-x

Krause, K., Providoli, I., Currie, W. S., Bugmann, H., and Schleppi, P. (2012). Long-Term Tracing of Whole Catchment ^{15}N Additions in a Mountain Spruce Forest: Measurements and Simulations with the TRACE Model. *Trees* 26, 1683–1702. doi:10.1007/s00468-012-0737-0

Lamersdorf, N. P., and Borken, W. (2004). Clean Rain Promotes Fine Root Growth and Soil Respiration in a Norway Spruce Forest. *Glob. Change Biol.* 10, 1351–1362. doi:10.1111/j.1365-2486.2004.00811.x

Liu, J., Peng, B., Xia, Z., Sun, J., Gao, D., Dai, W., et al. (2017). Different Fates of Deposited NH_4^+ and NO_3^- in a Temperate Forest in Northeast China: a ^{15}N Tracer Study. *Glob. Change Biol.* 23, 2441–2449. doi:10.1111/gcb.13533

Morier, I., Schleppi, P., Saurer, M., Providoli, I., and Guenat, C. (2010). Retention and Hydrolysable Fraction of Atmospherically Deposited Nitrogen in Two Contrasting Forest Soils in Switzerland. *Eur. J. Soil Sci.* 61, 197–206. doi:10.1111/j.1365-2389.2010.01226.x

Nadelhoffer, K. J., and Fry, B. (1994). "Nitrogen Isotope Studies in Forest Ecosystems," in *Stable Isotopes in Ecology and Environmental Science*. Editors K. Lajtha and R. H. Michener (Oxford: Blackwell), 22–44.

Nadelhoffer, K. J., Emmett, B. A., Gundersen, P., Kjønaas, O. J., Koopmans, C. J., Schleppi, P., et al. (1999). Nitrogen Deposition Makes a Minor Contribution to Carbon Sequestration in Temperate Forests. *Nature* 398, 145–148. doi:10.1038/18205

Nadelhoffer, K. J., Colman, B. P., Currie, W. S., Magill, A., and Aber, J. D. (2004). Decadal-Scale Fates of Tracers Added to Oak and Pine Stands Under Ambient and Elevated N Inputs at the Harvard Forest (USA). *For. Ecol. Manage.* 196, 89–107. doi:10.1016/j.foreco.2004.03.014

Nair, R. K. F., Perks, M. P., Weatherall, A., Baggs, E. M., and Mencuccini, M. (2016). Does Canopy Nitrogen Uptake Enhance Carbon Sequestration by Trees? *Glob. Change Biol.* 22, 875–888. doi:10.1111/gcb.13096

Nömmik, H. (1966). The Uptake and Translocation of Fertilizer N^{15} in Young Trees of Scots Pine and Norway Spruce. *Stud. For. Suec.* 35, 1–18.

Providoli, I., Bugmann, H., Siegwolf, R., Buchmann, N., and Schleppi, P. (2005). Flow of Deposited Inorganic N in Two Gleysol-Dominated Mountain Catchments Traced with $^{15}NO_3^-$ and $^{15}NH_4^+$. *Biogeochem.* 76, 453–475. doi:10.1007/s10533-005-8124-1

Providoli, I., Bugmann, H., Siegwolf, R., Buchmann, N., and Schleppi, P. (2006). Pathways and Dynamics of $^{15}NO_3^-$ and $^{15}NH_4^+$ Applied in a Mountain *Picea abies* forest and in a Nearby Meadow in Central Switzerland. *Soil Biol. Biochem.* 38, 1645–1657. doi:10.1016/j.soilbio.2005.11.019

Rastetter, E. B., Kwiatkowski, B. L., and McKane, R. B. (2005). A Stable Isotope Simulator that Can Be Coupled to Existing Mass Balance Models. *Ecol. Appl.* 15, 1772–1782. doi:10.1890/04-0643

Savard, M. M., Marion, J., and Bégin, C. (2020). Nitrogen Isotopes of Individual Tree-Ring Series - The Validity of Middle- to Long-Term Trends. *Dendrochronologia* 62, 125726. doi:10.1016/j.dendro.2020.125726

Schleppi, P., Bucher-Wallin, L., Siegwolf, R., Saurer, M., Muller, N., and Bucher, J. B. (1999). Simulation of Increased Nitrogen Deposition to a Montane Forest Ecosystem: Partitioning of the Added ^{15}N. *Water Air Soil Pollut.* 116, 129–134. doi:10.1023/A:1005206927764

Schleppi, P., Bucher-Wallin, I., Saurer, M., Jäggi, M., and Landolt, W. (2006a). Citric Acid Traps to Replace Sulphuric Acid in the Ammonia Diffusion of Dilute Water Samples for ^{15}N Analysis. *Rapid Commun. Mass. Spectrom.* 20, 629–634. doi:10.1002/rcm.2351

Schleppi, P., Curtaz, F., and Krause, K. (2017). Nitrate Leaching From a Sub-Alpine Coniferous Forest Subjected to Experimentally Increased N Deposition for 20 Years, and Effects of Tree Girdling and Felling. *Biogeochem.* 134, 319–335. doi:10.1007/s10533-017-0364-3

Schleppi, P., Waldner, P. A., and Fritschi, B. (2006b). Accuracy and Precision of Different Sampling Strategies and Flux Integration Methods for Runoff Water: Comparisons Based on Measurements of the Electrical Conductivity. *Hydrol. Process.* 20, 395–410. doi:10.1002/hyp.6057

Schleppi, P., Körner, C., and Klein, T. (2019). Increased Nitrogen Availability in the Soil Under Mature *Picea abies* Trees Exposed to Elevated CO_2 Concentrations. *Front. For. Glob. Change* 2, 59. doi:10.3389/ffgc.2019.00059

Schlesinger, W. H. (2009). On the Fate of Anthropogenic Nitrogen. *Proc. Natl. Acad. Sci. USA* 106, 203–208. doi:10.1073/pnas.0810193105

Sievering, H. (1999). Nitrogen Deposition and Carbon Sequestration. *Nature* 400, 629–630. doi:10.1038/23176

Sorensen, P. L., Michelsen, A., and Jonasson, S. (2008). Ecosystem Partitioning of ^{15}N-Glycine After Long-Term Climate and Nutrient Manipulations, Plant Clipping and Addition of Labile Carbon in a Subarctic Heath Tundra. *Soil Biol. Biochem.* 40, 2344–2350. doi:10.1016/j.soilbio.2008.05.013

Sparks, J. P. (2009). Ecological Ramifications of the Direct Foliar Uptake of Nitrogen. *Oecologia* 159, 1–13. doi:10.1007/s00442-008-1188-6

Templer, P. H., Mack, M. C., Iii, F. S. C., III, Christenson, L. M., Compton, J. E., Crook, H. D., et al. (2012). Sinks for Nitrogen Inputs in Terrestrial Ecosystems: a Meta-Analysis of ^{15}N Tracer Field Studies. *Ecology* 93, 1816–1829. doi:10.1890/11-1146.1

Thomas, R. Q., Zaehle, S., Templer, P. H., and Goodale, C. L. (2013). Global Patterns of Nitrogen Limitation: Confronting Two Global Biogeochemical Models with Observations. *Glob. Change Biol.* 19, 2986–2998. doi:10.1111/gcb.12281

Tiktak, A., and Van Grinsven, H. J. M. (1995). Review of Sixteen Forest-Soil-Atmosphere Models. *Ecol. Model.* 83, 35–53. doi:10.1016/0304-3800(95)00081-6

Tomlinson, G., Siegwolf, R. T. W., Buchmann, N., Schleppi, P., Waldner, P., and Weber, P. (2014). The Mobility of Nitrogen Across Tree-Rings of Norway Spruce (*Picea abies* L.) and the Effect of Extraction Method on Tree-Ring δ^{15}N and δ^{13}C Values. *Rapid Commun. Mass. Spectrom.* 28, 1258–1264. doi:10.1002/rcm.6897

Tonon, G., Ciavatta, C., Solimando, D., Gioacchini, P., and Tagliavini, M. (2007). Fate of ^{15}N Derived from Soil Decomposition of Abscised Leaves and Pruning Wood From Apple (*Malus domestica*) Trees. *Soil Sci. Plant Nutr.* 53, 78–85. doi:10.1111/j.1747-0765.2007.00112.x

Van Dam, D., and Van Breemen, N. (1995). NICCCE: a Model for Cycling of Nitrogen and Carbon Isotopes in Coniferous Forest Ecosystems. *Ecol. Model.* 79, 255–275. doi:10.1016/0304-3800(94)00184-J

Veerman, L., Kalbitz, K., Gundersen, P., Kjønaas, J., Moldan, F., Schleppi, P., et al. (2020). The Long-Term Fate of Deposited Nitrogen in Temperate Forest Soils. *Biogeochem.* 150, 1–15. doi:10.1007/s10533-020-00683-6

Wessel, W. W., and Tietema, A. (1992). Calculating Gross N Transformation Rates of ^{15}N Pool Dilution Experiments With Acid Forest Litter: Analytical and

Numerical Approaches. *Soil Biol. Biochem.* 24, 931–942. doi:10.1016/0038-0717(92)90020-X

Wessel, W. W., Boxman, A. W., Cerli, C., van Loon, E. E., and Tietema, A. (2021). Long-Term Stabilization of ^{15}N-Labeled Experimental NH_4^+ Deposition in a Temperate Forest Under High N Deposition. *Sci. Total Environ.* 768, 144356. doi:10.1016/j.scitotenv.2020.144356

Wilson, E. J., and Tiley, C. (1998). Foliar Uptake of Wet-Deposited Nitrogen by Norway Spruce. *Atmos. Environ.* 32, 513–518. doi:10.1016/S1352-2310(97)00042-3

Wright, R. F., and Dise, N. B. (1992). The NITREX Project (Nitrogen Saturation Experiments). *Ecosyst. Res. Rep.* 2. Brussels: Commission of the European Communities. url: https://op.europa.eu/en/publication-detail/-/publication/53885773-40dc-47d8-87d7-a28dc793153a/language-en

Zhang, Z., Yuan, Y., Liu, Q., and Yin, H. (2019). Plant Nitrogen Acquisition From Inorganic and Organic Sources Via Root and Mycelia Pathways in Ectomycorrhizal Alpine Forests. *Soil Biol. Biochem.* 136, 107517. doi:10.1016/j.soilbio.2019.06.013

Conflict of Interest: The authors declare that the research was conducted in the absence of any commercial or financial relationships that could be construed as a potential conflict of interest.

frontiers in Environmental Science

ORIGINAL RESEARCH
published: 05 July 2021
doi: 10.3389/fenvs.2021.660133

Comparison of N_2O Emissions From Cold Waterlogged and Normal Paddy Fields

Xiangyu Xu[1,2,3†], *Minmin Zhang*[1,2,3†], *Yousheng Xiong*[1,2,3], *Muhammad Shaaban*[4,5], *Jiafu Yuan*[1,2,3*] *and Ronggui Hu*[6]

[1]Institute of Plant Protection and Soil Fertilizer, Hubei Academy of Agricultural Sciences, Wuhan, China, [2]Key Laboratory of Fertilization from Agricultural Wastes, Ministry of Agriculture, Wuhan, China, [3]Qianjiang Scientific Observing and Experimental Station of Agro-Environment and Arable Land Conservation, Ministry of Agriculture, Qianjiang, China, [4]Institute of Mountain Hazards and Environment, Chinese Academy of Sciences, Chengdu, China, [5]Department of Soil Science, Faculty of Agricultural Sciences and Technology, Bahauddin Zakariya University, Multan, Pakistan, [6]College of Resources and Environment, Huazhong Agricultural University, Wuhan, China

Paddy fields are major sources of atmospheric N_2O. Soil temperature and moisture strongly affect N_2O emissions from rice fields. However, N_2O emissions from cold-waterlogged paddy fields (CW), an important kind of paddy soil in China, are not well studied so far. It is unclear whether the N_2O emissions from cold-waterlogged paddy fields are the same as normal paddy fields (NW). We investigated the N_2O emission characteristics from the CW and NW paddy fields under with (R_1) and without (R_0) rice in Tuku Village, Baisha Town, Yangxin County (YX site, monitoring in 2013) and Huandiqiao Town, Daye City (DY site, monitoring in 2014); compared the difference and influencing factors between the CW and NW paddy fields at two sites in South China. The results showed that the N_2O emissions from NWR_0 were 13.4 times higher than from CWR_0, and from NWR_1 were 10.3 times higher than from CWR_1 in the YX site. The N_2O emissions from NWR_0 were 2.4 times higher than from CWR_0, and from NWR_1 were 17.3 times higher than from CWR_1 in the DY site. The structural equation models (SEMs) showed that the N_2O emissions are mainly driven by rice planting and soil moisture in the NW fields at the annual scale, while soil temperature in the CW fields. Overall, N_2O emissions from cold waterlogged paddy fields are significantly lower than those of normal paddy fields due to the low temperature and higher water content; however, there are dinitrogen emissions from cold waterlogged paddy fields denitrification should be further examined.

Keywords: cold-waterlogged paddy field, N_2O, soil temperature, nitrate, ammonium

OPEN ACCESS

Edited by:
Fereidoun Rezanezhad, University of Waterloo, Canada

Reviewed by:
Alison E. King, Colorado State University, United States
S. M. Mofijul Islam, Bangladesh Rice Research Institute, Bangladesh

***Correspondence:**
Jiafu Yuan
fu1682@sina.com

†These authors have contributed equally to this work

Specialty section:
This article was submitted to Biogeochemical Dynamics, a section of the journal Frontiers in Environmental Science

Received: *28 January 2021*
Accepted: *18 June 2021*
Published: *05 July 2021*

Citation:
Xu X, Zhang M, Xiong Y, Shaaban M, Yuan J and Hu R (2021) Comparison of N_2O Emissions From Cold Waterlogged and Normal Paddy Fields. Front. Environ. Sci. 9:660133. doi: 10.3389/fenvs.2021.660133

INTRODUCTION

Nitrous oxide (N_2O) is the third-largest long-lived greenhouse gas following CO_2 and CH_4. The lifetime of N_2O in the atmosphere is about 121 years, and its greenhouse effect is 265 times that of CO_2 on a hundred-year scale (IPCC, 2014). Farmland ecosystems are the primary anthropogenic source of N_2O emissions.

The nitrification and denitrification of the soil's nitrogen cycle can lead to N_2O emissions (Spott et al., 2011; Butterbach-Bahl et al., 2013; Hu et al., 2015a). Soil water change, soil aggregate

fragmentation, organic matter degradation, and organic nitrogen mineralization regulate N_2O emissions (Čuhel et al., 2010; Sheng et al., 2013; Wissing et al., 2013; Zhu et al., 2013; Wang et al., 2014; Weller et al., 2016).

Rice is a staple food and feeds nearly 50% of the global population (Alexandratos and Bruinsma, 2012). Paddy fields are an important source of N_2O emissions, and 8–11% of China's agricultural N_2O emissions were estimated from rice fields (Zou et al., 2009). A cold-waterlogged paddy field is a major type of low-yield paddy soil in China, accounting for 15.2% of the total paddy fields in this country (Xie et al., 2015). Its main characteristics are higher groundwater levels and lower soil temperature than normal paddy fields (Qiu et al., 2013; Liu et al., 2016). Those environments make strong anaerobic conditions, poor soil structure, high organic matter contents, and low rates of N mineralization (Xie et al., 2015). Those properties of CW fields result in significantly lower rice biomass yields and higher methane emissions than normal paddy fields (NW fields) (Xu et al., 2020).

Soil water content has a decisive influence on the process of nitrification and denitrification (Davidson and Verchot, 2000). Soil water-saturated areas or flooding conditions hinder gas diffusion and form an anaerobic soil environment (Zhu et al., 2013). Alternating wet and dry, the most common water management measures in normal rice fields, causes repeated nitrification and denitrification and results in a large amount of N_2O production and emission Hofstra and Bouwman (2005), Hu et al. (2015b), Patrick and Wyatt (1964), Fierer and Schimel (2002), Gaihre et al. (2017), Islam et al. (2018), and N_2O emissions from lowland rice fields showed significant spatial and seasonal variations from lowland rice fields (Gaihre et al., 2017). However, due to the high groundwater level, the effects of alternating dry and wet measures in cold-waterlogged paddy fields are far inferior to normal rice fields.

As mentioned above, there are considerable differences in soil water content, soil temperature, soil organic matter content, rice yield, and methane emissions between CW fields and NW field. However, N_2O fluxes characteristics, total N_2O emissions, and influencing factors of cold-waterlogged paddy fields have not been explored. We hypothesized that the cold-waterlogged paddy fields have lower N_2O emissions than normal rice fields. The impact of rice planting on nitrous oxide emissions and the significant effect of nitrous oxide emissions should differ from normal rice fields. Therefore, this study intends to systematically monitor the cold-waterlogged paddy field's N_2O emissions characteristics on an annual scale in two representative regions and analyze the main controlling factors that affect N_2O emissions. It's significant to understand rice fields' total greenhouse effect, accurately assessing the N_2O emissions of China's rice field system, and reasonably formulate the emission reduction measures of this type of rice field.

MATERIALS AND METHODS

Study Site and Experimental Design

The study was conducted at two sites with different climate zones in Huangshi, Hubei Province, China. One belongs to a subtropical climate zone in Tuku Village, Baisha Town, Yangxin County (YX site, 2013), and soil-derived from acid aplite. Another is Huandiqiao Town, Daye City (DY site, 2014), a northern subtropical monsoon climate zone and soil derived from carbonatite. Soil physical and chemical properties of the surface layer soil (0–20 cm) are listed in **Table 1**. We conducted eight treatments, including NW planted with (NWR_1) or without (NWR_0) rice and CW planted with (CWR_1) or without (CWR_0) rice in both sites. The area of each plot with rice was 100 m^2 (10 m × 10 m), and the subplot without rice was 3 m^2 (1.5 m × 2 m). Each treatment had three replicates. Urea, calcium superphosphate, and potassium chloride were applied as nitrogen, phosphorous, and potassium fertilizers, respectively (N: P_2O_5: K_2O = 180: 90: 120 kg hm^{-2}) at both sites. Specifically, 50% nitrogen, 100% potassium, and 100% phosphorus were applied as basal fertilizer. The remaining 30% nitrogen applied at the jointing stage, and another 20% nitrogen applied ~15 days after full heading.

Gas Collection and Analysis

N_2O fluxes were measured using a static chamber technique, as reported previously (Xu et al., 2020). Each static chamber consisted of three parts: a bottom base, a middle chamber, and a top chamber. The chambers were wrapped with a layer of thermal insulation material. The base's four walls were drilled at 10 cm from the top with two rows of 2-cm-diameter holes to facilitate water and fertilizer flow. The base (42 cm long × 42 cm wide × 20 cm high), with a groove around the top edge, was inserted 20 cm into the soil and remained *in situ* except for tillage. The middle chambers with a groove around the top edge and top chambers (42 cm long × 42 cm wide × 50 cm high) covered the base (with a volume equal to the sum of middle and top chambers).

At transplanting, we transplanted four rice plants (at the same density as outside of the chamber) in the base. The gas samples are sampled every 7–10 days in the non-rice season. During the rice planting period, gases were collected for five consecutive days; thereafter, the gases were periodically collected at 7-days intervals. For each sampling, the gas within the chamber was collected four times from 8:00–10:00 a.m., using a 30-ml gas-tight syringe at 0, 5, 10, 15, and 20 min. The samples were transported to the laboratory and analyzed within 24 h. Meanwhile, soil temperature at a depth of 5 cm was recorded using an electronic digital thermometer.

The concentrations of N_2O in gas samples were analyzed by gas chromatography (Agilent 7890A, United States) equipped with an electron capture (ECD) for N_2O concentration analyses at 350°C, and the carrier gas was purified N_2. We calculate the N_2O fluxes by making a linear regression of the gas concentration.

The N_2O fluxes was calculated using the following formula:

$$F = \rho \times \frac{V}{S} \times \frac{dC}{dt} \times \frac{273}{273 + T}$$

Where F is the N_2O flux (ug $m^{-2}h^{-1}$); ρ is the N_2O density in the standard state (kg m^{-3}); V is the effective volume of the closed chamber (m^3), S is the base area (m^2); dC/dt is the change of N_2O concentration in the sealed chamber per unit time, and T is the average temperature in the closed section.

TABLE 1 | Soil physical and chemical properties (mean ± SD, n = 3) in paddy fields at the two experimental sites in Hubei Province, China.

Site	Type	OM (g kg^{-1})	TN (g kg^{-1})	AN (mg kg^{-1})	TP (g kg^{-1})	AP (mg kg^{-1})	TK (g kg^{-1})	AK (mg kg^{-1})	pH	MST (°C)
YX	CW	25.58 ± 0.58b	2.01 ± 0.12a	185.5 ± 22.2a	0.65 ± 0.05b	3.72 ± 0.11b	17.12 ± 0.31b	32.20 ± 2.36b	6.19 ± 0.01a	26.99 ± 2.31a
	NW	21.74 ± 0.37c	1.62 ± 0.11b	189.7 ± 19.5a	0.81 ± 0.07a	7.86 ± 0.56a	19.50 ± 0.89b	36.14 ± 3.56b	6.16 ± 0.01a	27.36 ± 2.58a
DY	CW	33.05 ± 0.66a	1.55 ± 0.06b	157.2 ± 16.3b	0.24 ± 0.02c	4.26 ± 0.32b	25.6 ± 1.58a	58.14 ± 6.56a	5.19 ± 0.01b	23.76 ± 2.12b
	NW	32.51 ± 0.41a	1.48 ± 0.09b	162.2 ± 11.0b	0.24 ± 0.01c	6.74 ± 0.15 ab	24.3 ± 1.25a	61.16 ± 5.89a	5.06 ± 0.02b	23.83 ± 2.68b

Note: OM, TN, AN, TP, AP, TK, AK, and MST indicate organic matter, total nitrogen, available nitrogen, total phosphorus, available phosphorus, total potassium, available potassium, and mean soil temperature. YX and DY mean Yangxin site and Daye site. CW and NW mean cold-waterlogged paddy fields and normal paddy fields. Different lowercase letters within a single column indicate statistically significant differences at p < 0.05 *between treatments. MST is mean temperature of 5 cm soil layer during rice planting.*

The N_2O cumulative gas emissions was calculated by interpolation using the following formula (Iqbal et al., 2008):

$$Ec = \sum_{i=1}^{n} \frac{(F_i + F_{i+1})}{2} \times t_{i+1} - t_i \times 24/1000$$

where Ec is the cumulative emissions (mg m^{-2}), n is the number of observations, F_i (ug $m^{-2}h^{-1}$), and F_{i+1} (ug m^{-2} h^{-1}) are the fluxes of the i and i+1 sampling, and t_i and t_{i+1} are the i and i+1 sampling date.

Soil Variable Measurements

Soil temperature near the base frames was measured at a depth of 5 cm in each plot and subplot using an E278 probe-type digital thermometer (Minggao Electronics Ltd., Shenzhen, China). Topsoil samples (0–20 cm) were collected randomly from five points per plot (including the plot and subplot) using a gauge auger (3-cm inner diameter) and transported immediately to the laboratory, and then homogenized and divided into two parts. One part was dried at 105°C for 24 h to determine soil water content by gravimetric. The other part was extracted with 0.5 M K_2SO_4 solution (soil: water = 1:5) for 1 h shaking and then filtrated to determine soil mineral N (NH_4^+-N and NO_3^--N) and dissolved organic carbon (DOC). The NH_4^+-N and NO_3^--N were analyzed using a flow-injection auto-analyzer. The DOC was measured with a TOC analyzer (Wu et al., 2017).

Statistical Analysis

N_2O accumulation emissions are expressed as the mean ± standard deviation (SD) from three replicates. Statistical analysis was conducted using SPSS 24 (IBM SPSS, Somers, United States). The relationship between N_2O fluxes and environmental factors was performed in R (v3.6.1) using the "basicTrendline" packages with a single environmental factor as the independent variable and N_2O flux as the dependent variable. The model parameter is used to select the fitting function, and the p-value and R^2 value are used to determine the final regression model. Finally, SEMs were used to analyse the direct and indirect relationships between environmental factors and the N_2O fluxes. The first step in an SEM requires establishing an a priori model based on the known effects and the relationships among the driving variables. The piecewiseSEM package (version 2.1.0) was used to analyze SEMs. We used non-significant (p > 0.05) Fisher's C values to indicate a good fit (Ochoa-Hueso et al., 2020).

RESULTS

Characteristic of Environmental Factors

Regardless of rice planting, the mean soil water content of CW fields was significantly higher than that of NW fields during the monitoring period (**Figure 1**, p < 0.01), and rice planting has no difference at both types of fields at two sites. The average concentration of DOC for the CWR_0 and CWR_1 was significantly higher than those of the NWR_0 and the NWR_1 at the DY site (**Figure 1**, p < 0.01), but no difference at the YX site. The average concentration of NO_3^--N for the CWR_0 was significantly higher than that for the NWR_0 at the DY site (**Figure 1**, p < 0.01), and the average concentration of NH_4^+-N of the CWR_1 was significantly higher than that of the NWR_1 at the DY site (**Figure 1**, p < 0.01). In the same site, the CW fields' mean soil temperature was lower than that of the NW fields' during the entire monitoring period, and the differences were not statistically significant (p > 0.05). However, from July 1, 2013, to September 1, 2013, the average soil temperature of the CW fields (28.45 ± 1.98°C) was significantly lower (p < 0.001) than the NW fields (29.87 ± 1.98°C) (**Figure 1** A3), and from July 1, 2014, to September 1, 2014, the average soil temperature of the CW fields (29.97 ± 1.20°C) was significantly lower (p < 0.001) than the NW fields (31.52 ± 1.74°C) (**Figure 1** A3).

Characteristic of N_2O Fluxes and Cumulative Emissions

The N_2O emissions characteristics of CW paddy fields and NW paddy fields are shown in **Figure 2**. The N_2O fluxes at the YX site are between −32.93 −778.98 μg m^{-2} h^{-1}, and the DY site is between −11.82 −93.42 μg m^{-2} h^{-1}. The NW rice field of the YX site has three obvious emission peaks without rice. The other three treatments have no emission peaks. All the treatment emission peaks of the DY site are significantly lower than the YX site under the same treatment.

The annual mean N_2O fluxes of NWR_0 treatment are 35.29 ± 16.17 μg m^{-2} h^{-1}, and 8.91 ± 3.03 μg m^{-2} h^{-1} at YX and DY sites, respectively, and of CWR_0 treatment are 4.26 ± 1.72 and 2.10 ± 1.31 μg m^{-2} h^{-1} at YX and DY sites, respectively. The mean N_2O fluxes from CWR_0 treatment was12.1% of that of NWR_0 treatment at the YX site and was 23.6% at the DY site, respectively. The mean N_2O fluxes of NWR_1 treatment was 12.78 ± 2.91 μg m^{-2} h^{-1} at the YX site and was 36.00 ± 26.48 μg m^{-2} h^{-1} at the DY site,

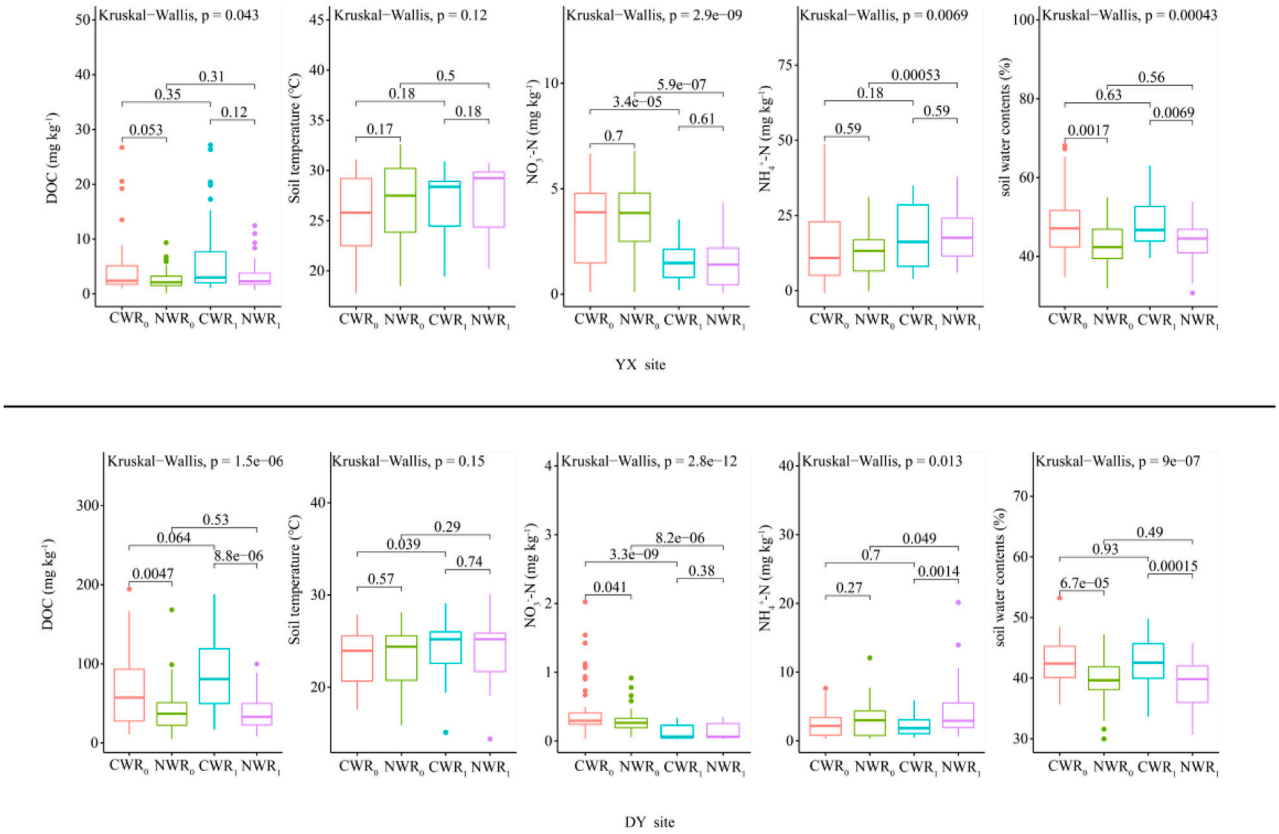

FIGURE 1 | The difference of environmental factors between YX site and DY site (adapted from Xu et al., 2020). Note: CWR_0 and CWR_1 are cold-waterlogged paddy field without and with rice planting, respectively; NWR_0 and NWR_1 are normal paddy field without and with rice planting, respectively. The number on the horizontal line indicates the significance of the difference. The points outside the box plot indicate outliers.

respectively. The mean N_2O fluxes of CWR_1 treatment was 3.82 ± 2.07 μg m^{-2} h^{-1} at the YX site and was 0.43 ± 1.43 μg m^{-2} h^{-1} at the DY site, respectively, and mean N_2O fluxes from CWR_1 treatment was 29.89% of that from NWR_1 treatment at the YX site and was 1.20% at DY site, respectively.

The cumulative N_2O emissions were calculated by interpolation (**Table 2**). The results showed that the N_2O cumulative emissions from the CWR_1 treatment were the lowest at both sites. The highest N_2O cumulative emissions were observed in NWR_0 treatment at the YX site and in NWR_1 treatment at the DY site. Regardless of rice planting, N_2O cumulative emissions of the NW fields were significantly higher than that in the CW fields (**Table 2**, $p < 0.05$) at both sites. Rice planting significantly reduced the cumulative N_2O emissions from the NW field at the YX site but increased dramatically at the DY site. However, rice planting had no significant effect on the cumulative N_2O emissions from CW fields at both sites (**Table 2**).

Relationships between Environmental Factors and N_2O Emissions

For the YX site, the N_2O fluxes decrease first and then rise with the increase of the soil temperature in the NWR_0 treatment ($p < 0.001$, **Figure 3** A_3). The N_2O fluxes decrease first and then rise with the rise of the soil water content ($p < 0.001$, **Figure 3** B_3), and the N_2O fluxes decrease first and then rise with the increase of the NH_4^+-N concentration ($p < 0.001$, **Figure 3** D_3) in the NWR_1 treatment. For the DY site, the N_2O fluxes decrease first and then rise with the increase of the soil DOC concentration ($p < 0.05$, **Figure 4** C_1) in the CWR_0 treatment. The N_2O fluxes decrease first and then rise with the increase of the soil temperature ($p < 0.001$, **Figure 4** B_1) in the CWR_1 treatment. The N_2O fluxes present a trend of first decreasing and then increasing with the increase of the soil temperature ($p < 0.05$, **Figure 4** A_4), and N_2O fluxed increases with the soil NO_3^--N concentration ($p < 0.05$, **Figure 4** E_4) in the NWR_1 treatment. Other indicators at both sites have no significant relationship with N_2O fluxes (**Figure 3** and **Figure 4**).

The structural equation model showed that both fields' N_2O fluxes are significantly different between the experiment sites ($p < 0.05$, **Figure 5**). Soil temperature directly positively affects N_2O fluxes in the CW field (**Figure 5** CW). In contrast, other factors, such as soil water content, DOC, NO_3^--N, NH_4^+-N, and rice planting, had no direct effect on N_2O fluxes. Rice planting directly affects ($p < 0.05$, **Figure 5** NW) on N_2O fluxes at the NW fields. Simultaneously, the soil water content and rice planting directly affected N_2O fluxes in the NW fields. Other factors, such as DOC content, NO_3^--N content, and NH_4^+-N, have no direct effects on N_2O fluxes in both sites. The DOC

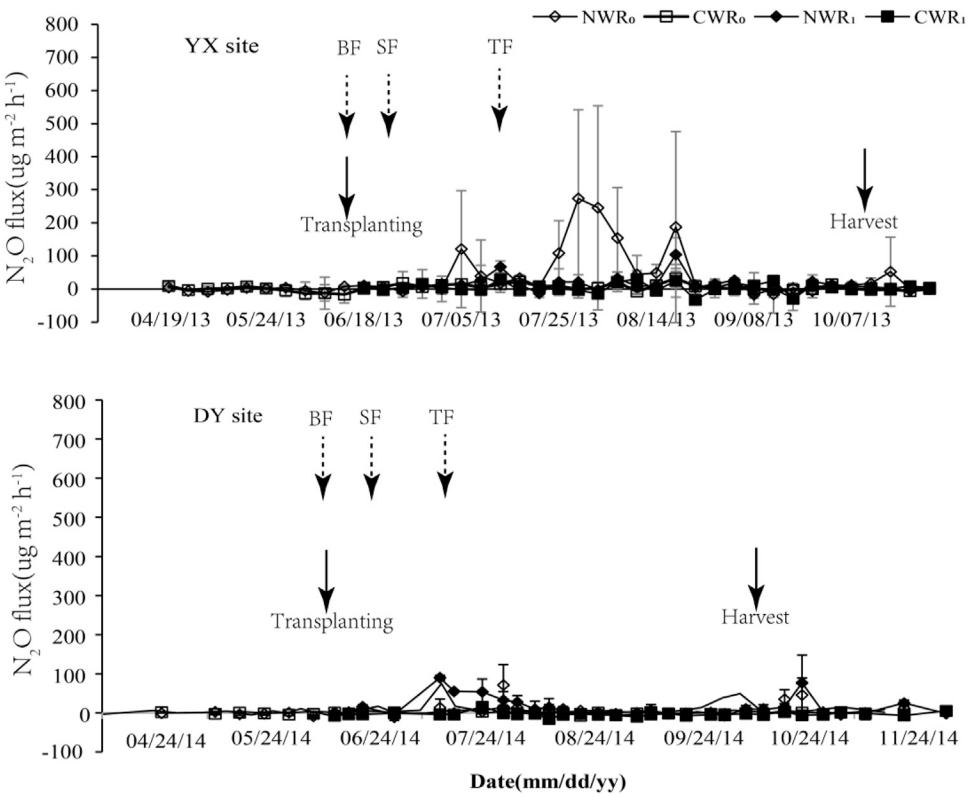

FIGURE 2 | Annual N_2O emissions from the CW and the NW paddy fields under different treatments. Note: CWR_0 and CWR_1 are cold-waterlogged paddy field without and with rice planting, respectively; NWR0 and NWR1 are normal paddy field without and with rice planting, respectively. The values are means ± SD ($n = 3$). BF, SF, and TF are base fertilization, seedling fertilization, and tillering fertilization.

TABLE 2 | N_2O cumulative emissions and ratio at different stages during the monitoring period.

Site	Month. Date	Cumulative emissions (mg N_2O m^{-2})			
		NWR_0	**NWR_1**	**CWR_0**	**CWR_1**
YX	4.19–6.17 (60 days, BT stage)	−2.7 ± 10.2 (−1.83%)	−2.7 ± 10.2 (−6.30%)	−2.8 ± 7.8 (−15.19%)	−2.8 ± 7.8 (−30.25%)
	6.18–7.25 (38 days, FI stage)	40.1 ± 30.6 (27.49%)	15.0 ± 8.2 (35.33%)	10.8 ± 4.2 (58.33%)	4.6 ± 6.2 (49.67%)
	7.26–8.9 (15 days, Dr. stage)	56.4 ± 59.9 (38.69%)	4.4 ± 4.3 (10.46%)	2.0 ± 2.9 (11.02%)	1.6 ± 3.7 (17.34%)
	8.10–10.7 (52 days, Mo stage)	40.9 ± 34.9 (28.08)	24.0 ± 7.2 (56.63%)	10.0 ± 6.0 (54.11%)	3.6 ± 6.4 (38.92%)
	10.8–11.4 (27 days, AH stage)	11.1 ± 12.9 (7.58%)	1.6 ± 2.7 (3.88%)	−1.5 ± 3.6 (−8.26%)	2.3 ± 1.9 (24.30%)
	4.19–11.4 (192 days, full monitoring)	145.7 ± 53.7a (100%)	42.4 ± 19.5b (100%)	18.5 ± 8.8c (100%)	9.3 ± 8.8c (100%)
DY	4.24–6.10 (48 days, BT stage)	1.4 ± 4.8 (3.21%)	1.4 ± 4.8 (0.95%)	1.3 ± 1.2 (12.04%)	1.3 ± 1.2 (31.69%)
	6.11–7.23 (43 days, FI stage)	9.4 ± 6.1 (21.45%)	57.8 ± 15.3 (36.43%)	3.3 ± 2.4 (29.97%)	3.2 ± 2.3 (77.87%)
	7.24–8.14 (22 days, Dr. stage)	8.4 ± 6.9 (19.25%)	10.1 ± 2.7 (6.37%)	1.0 ± 1.3 (9.15%)	−0.6 ± 1.5 (−13.70%)
	8.15–10.5 (51 days, Mo stage)	4.8 ± 1.1 (11.01%)	3.3 ± 3.1 (2.08%)	1.6 ± 2.4 (15.04%)	−1.7 ± 1.9 (−41.80%)
	10.6–12.2 (58 days, AH stage)	19.7 ± 13.1 (45.08%)	86.0 ± 93.8 (54.17%)	3.7 ± 4.1 (33.83%)	1.9 ± 0.6 (46.00%)
	4.24–12.2 (222 days, full monitoring)	43.7 ± 13.9b (100%)	158.7 ± 101.7a (100%)	10.9 ± 6.9c (100%)	4.1 ± 6.0c (100%)

Note: BT, FI, Dr., Mo, AH indicate before transplanting, flooding, drainage, moisture, after harvest, respectively. Different letters in a row indicate significant differences in the same treatment between different sites (p < 0.05).

concentrations, NO_3^--N, and NH_4^+-N of both type fields were significantly different in both sites ($p < 0.005$, in Fig. 6CW and **Figure 5** NW).

For NW paddy fields, rice planting has a significant direct positive effect on NO_3^--N ($p < 0.005$, **Figure 5** NW) and on NH_4^+-N ($p < 0.005$, **Figure 5** NW), and a negative effect on DOC ($p < 0.005$, **Figure 5** NW). Simultaneously, soil temperature has a significant direct negative effect on DOC ($p < 0.005$, **Figure 5** NW) and a positive effect on NH_4^+-N ($p < 0.005$, Figure 6 NW). For CW paddy fields, rice planting and soil water content have a

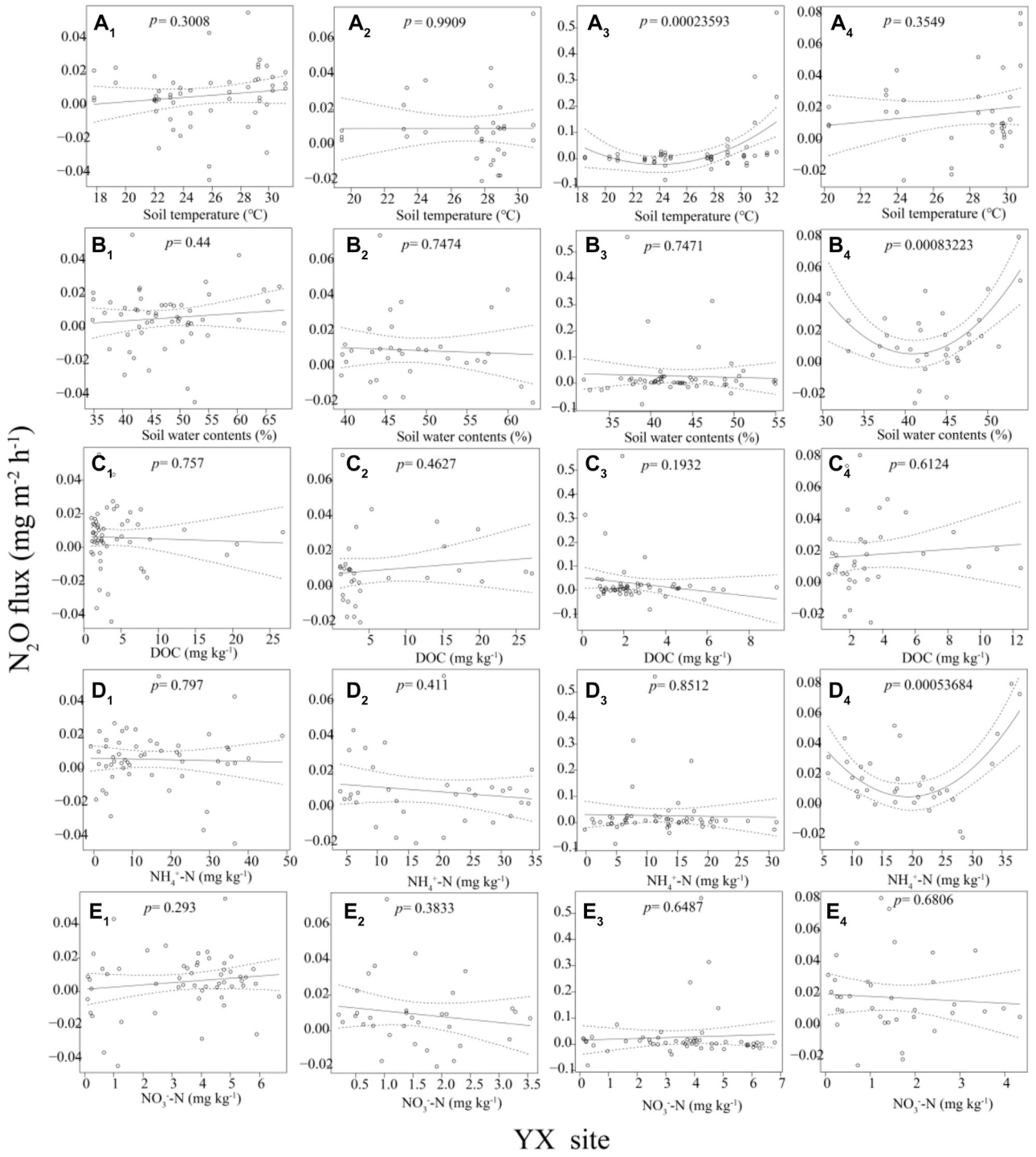

FIGURE 3 | A_1, B_1, C_1, D_1, and E_1 means the relationships between N_2O fluxes and soil temperature, soil water content, DOC contents, NH_4^+-N contents, and NO_3^--N contents in the CWR_0, respectively. A_2, B_2, C_2, D_2, and E_1 means the relationships between N_2O fluxes and soil temperature, soil water content, DOC contents, NH_4^+-N contents, and NO_3^--N contents in the CWR_1, respectively. A_3, B_3, C_3, D_3, and E_3 means the relationships between N_2O fluxes and soil temperature, soil water content, DOC contents, NH_4^+-N contents, and NO_3^--N contents in the NWR_0, respectively. A_4, B_4, C_4, D_4, and E_4 means the relationships between N_2O fluxes and soil temperature, soil water content, DOC contents, NH_4^+-N contents, and NO_3^--N contents in the NWR_1, respectively.

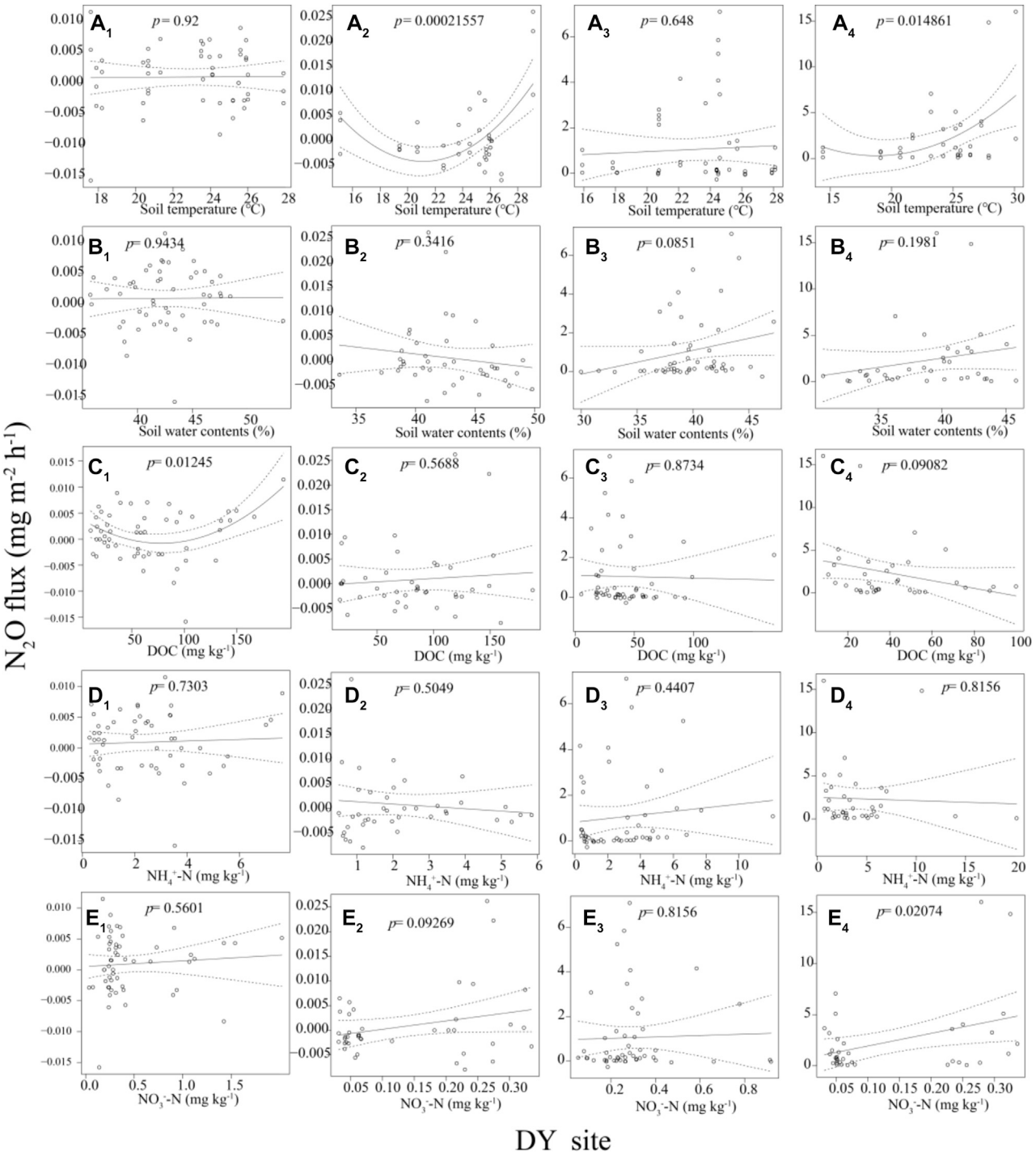

FIGURE 4 | A_1, B_1, C_1, D_1, and E_1 means the relationships between N_2O fluxes and soil temperature, soil water content, DOC contents, NH_4^+-N contents, and NO_3^--N contents in the CWR_0, respectively. A_2, B_2, C_2, D_2, and E_1 means the relationships between N_2O fluxes and soil temperature, soil water content, DOC contents, NH_4^+-N contents, and NO_3^--N contents in the CWR_1, respectively. A_3, B_3, C_3, D_3, and E_3 means the relationships between N_2O fluxes and soil temperature, soil water content, DOC contents, NH_4^+-N contents, and NO_3^--N contents in the NWR_0, respectively. A_4, B_4, C_4, D_4, and E_4 means the relationships between N_2O fluxes and soil temperature, soil water content, DOC contents, NH_4^+-N contents, and NO_3^--N contents in the NWR_1, respectively.

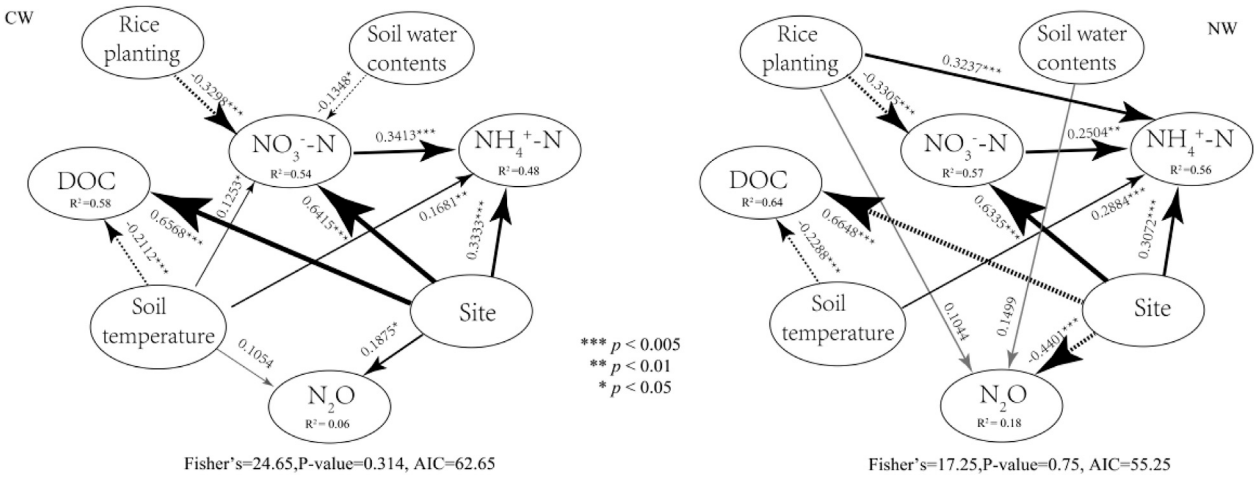

FIGURE 5 | Structural equation model. SEMs assessed direct and indirect associations between soil temperature (ST), soil water content (SWC), ammonium nitrogen (NH_4^+-N), nitrate-nitrogen (NO_3^--N), and dissolved organic carbon (DOC) and N_2O fluxes. Numbers adjacent to the arrows are standardized path coefficients, analogous to relative regression weights, and indicate the relationship's effect size. Double-headed arrows indicate covariance between variables; single-headed arrows indicate a one way directed relationship. Solid lines indicate positive associations. Dashed lines indicate a negative association. The width of the arrow is proportional Line width is proportional to the strength of path coefficients. The proportion of variance explained (conditional R^2) appears below every response variable in the model.

significant direct negative effect on NO_3^--N ($p < 0.005$, **Figure 5** CW), and soil temperature have a significant direct positive effect on NO_3^--N ($p < 0.05$, **Figure 5** CW), NH_4^+-N ($p < 0.01$, **Figure 5** CW), and a significant direct negative effect on DOC ($p < 0.005$, **Figure 5** CW). NO_3^--N directly affects NH_4^+-N ($p < 0.01$, **Figure 5** NW and **Figure 5** CW) at both type fields.

DISCUSSION

Our results demonstrated that the N_2O emissions from the CW fields are significantly lower than that of the NW fields, regardless of rice planting ($p < 0.05$, **Table 2**). In this study, the soil temperature of the CW fields is significantly lower than that of the NW rice fields during the high air temperature (**Figure 6** A3 and B3). However, there is no significant difference on an annual scale. The relationship between soil temperature and N_2O emissions is not uniform (Zhou et al., 2018; Wang et al., 2019); this difference is mainly affected by soil moisture (Wu et al., 2013). N_2O emissions from soil are affected by the interaction of multiple environmental factors under natural conditions, and the relationship between temperature and water content determines whether to promote N_2O emissions. This may be why the relationship between a single factor and N_2O is not consistent in our study.

The N_2O annual cumulative emissions from the NW fields are consistent with the results of Lan et al. (2020) but smaller than those reported by Huang et al. (2019), and the CW fields' N_2O annual emissions are lower than previous studies (Huang et al., 2019; Lan et al., 2020). The possible reason is that the soil water content in Huang's research is lower than that of the NW fields and the CW fields in this study. In this study, the soil water content of the CW fields is significantly higher than that of NW fields on the annual scale (**Figure 1**). Soil moisture determines the soil's redox state (Mei et al., 2011; Blagodatskaya et al., 2014). Previous research had shown that it might reduce 30–80% of N_2O in the deep soil layer (anaerobic layer) to N_2 before being released into the atmosphere (Clough et al., 2005). The N_2 emissions from soil denitrification are considered to be a major gaseous N loss pathway, particularly in flooded paddy fields, where the strictly anaerobic environment promotes the complete reduction of nitrate or nitrite to N_2 through the intermediates of N_2O and NO (Davidson and Verchot, 2000; Butterbach-Bahl et al., 2013). In our study, the CW rice field has been saturated for a long time and under a strictly anaerobic state (Xu et al., 2020). The strong reduction state may lead to the complete reduction of N_2O to N_2 (Parton et al., 1996; Zhu et al., 2014). Simultaneously, the rice biomass accumulation is lower in the CW field than in the NW fields, and lower biomass accumulation means less N_2O emissions (Xu et al., 2020). The above two points may lead to significantly lower N_2O emissions from CW fields.

Rice planting may provide channels for N_2O emissions, contributing more than 70% of soil N_2O emissions during flooding but less than 20% after drainage (Yu et al., 1997; Yan et al., 2000). In this study, rice planting promoted the N_2O accumulative emissions in the NW field at the DY site. However, the N_2O emissions from NWR_1 were significantly lower than that of NWR_0 at the YX site, which may be related to more weeds in the treatment, and weeds (especially Monochoria vaginalis) could lead to a large amount of N_2O production and emission. At the same time, it may also be the N_2O emissions from NWR_0 at the YX site were significantly

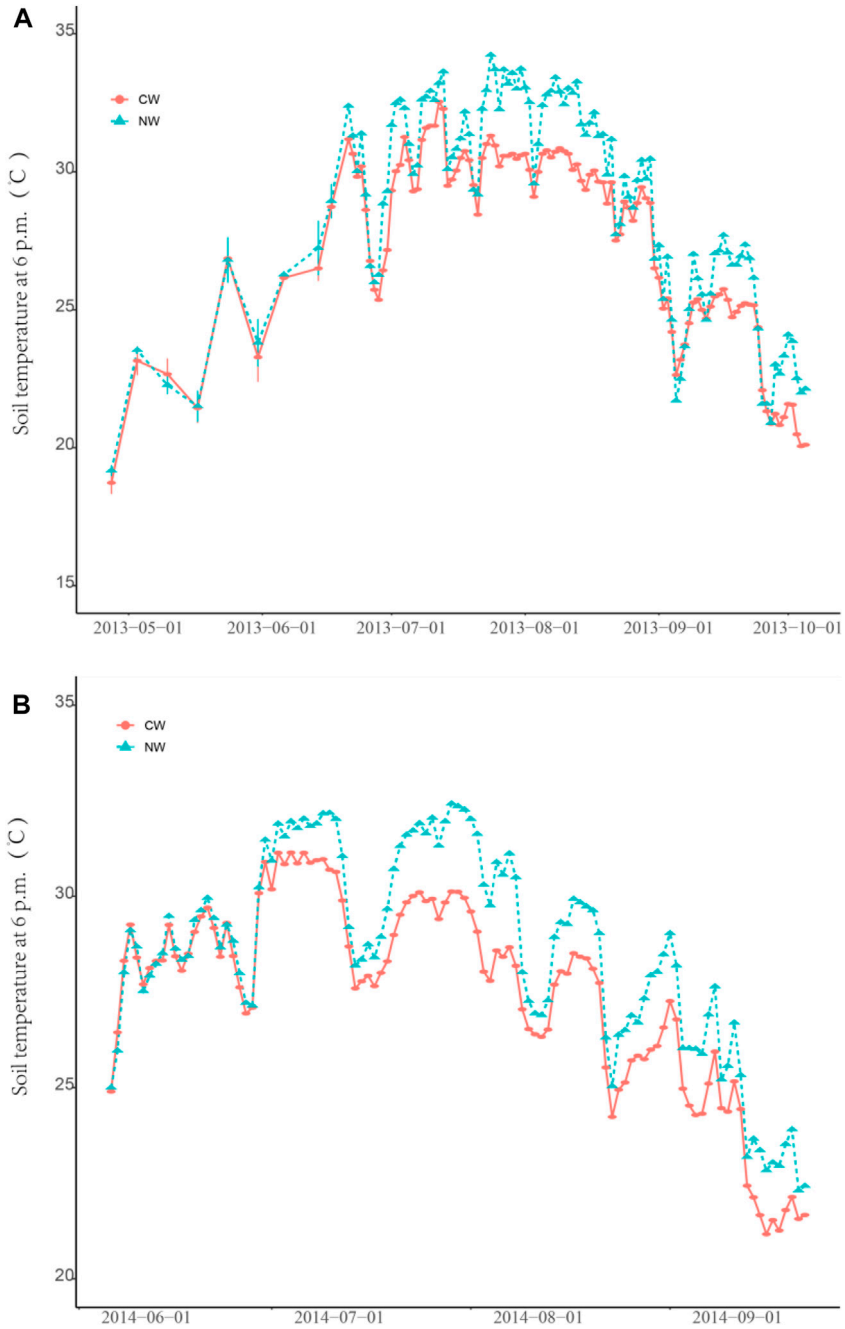

FIGURE 6 | Annual variation trend of soil temperature and temperature difference during high temperature period. Note: Buried three temperature recorders in each field. **(A)** and **(B)** are the annual variation trend of 5 cm soil temperature during the monitoring period in YX site and DY site, respectively.

higher than that of the DY site, which has no weeds. N_2O emissions from NWR_1 treatments at the DY site were significantly higher than that of the YX site, and this may be related to the lower rice biomass (15,957 kg hm^{-2} at the DY site and 15,021 kg hm^{-2} at the YX site) Xu et al. (2020) and the higher soil pH (**Table 1**), due to the N_2O emissions from low-pH soils are significantly higher than those with high-pH soils (Wang et al., 2017).

N_2O emissions from paddy fields are affected by various environmental factors (Schaufler et al., 2010; Hu et al., 2015a). Pärn et al. (2018) reported that soil NO_3^--N and soil volumetric water content together determine the geographic differentiation of global organic soil N_2O emissions (n = 58, R^2 = 0.72, p < 0.001), and the relationship between soil temperature and N_2O emissions is affected by region (Pärn et al., 2018). In the present study, the structural equation model

showed that the N_2O emissions of the same type of rice fields are significantly different between the different sites. At the same time, environmental factors have no significant direct effects on N_2O emissions. However, there are significant direct or indirect effects between soil environmental factors in each type of paddy field, confirming the cover-up effect of regional differences on environmental factors (Pärn et al., 2018).

CONCLUSION

The CW fields' annual N_2O cumulative emissions were significantly lower than that of the NW fields under the same climatic conditions and planting systems. N_2O emissions from the CW fields are mainly in the flooding period after transplanting, while the NW fields are primarily in the drainage period after flooding. N_2O emissions from the CW fields are mainly affected by soil temperature; however, they are mainly affected by rice planting and soil moisture from the NW fields. The CW fields have very low N_2O emissions and may have gaseous nitrogen emissions by denitrification. We suggest that follow-up research should study and evaluate the gaseous nitrogen emissions, and this has certain enlightenment for the governance of environmental nitrogen pollution.

DATA AVAILABILITY STATEMENT

The original contributions presented in the study are included in the article/**Supplementary Materials**, further inquiries can be directed to the corresponding author/s.

AUTHOR CONTRIBUTIONS

XX and JY conceived the idea, XX, MZ, and YX conducted experiment analyzed data, XX, MZ, and MS wrote the manuscript, RH, JY, and MS. reviewed, revised and improved the manuscript.

FUNDING

This study was financially supported by the National Natural Science Foundation of China (No. 41301306), the Scientific and Technological Achievements Cultivation Project of Hubei Academy of Agricultural Sciences, China (2017CGPY01), and the Integration and Demonstration of Key Technologies of Crop Straw Returning in Hubei Province, China.

REFERENCES

Alexandratos, N., and Bruinsma, J. (2012). *World Agriculture towards 2030/2050: The 2012 Revision*. Rome: FAO, ESA Working paper.

Blagodatskaya, E., Zheng, X., Blagodatsky, S., Wiegl, R., Dannenmann, M., and Butterbach-Bahl, K. (2014). Oxygen and Substrate Availability Interactively Control the Temperature Sensitivity of CO2 and N2O Emission from Soil. *Biol. Fertil. Soils* 50, 775–783. doi:10.1007/s00374-014-0899-6

Butterbach-Bahl, K., Baggs, E. M., Dannenmann, M., Kiese, R., and Zechmeister-Boltenstern, S. (2013). Nitrous Oxide Emissions from Soils: How Well Do We Understand the Processes and Their Controls?. *Philosophical Trans. R. Soc. B* 368, 1–13. doi:10.1098/rstb.2013.0122

Clough, T. J., Sherlock, R. R., and Rolston, D. E. (2005). A Review of the Movement and Fate of N2O in the Subsoil. *Nutr. Cycl Agroecosyst* 72, 3–11. doi:10.1007/s10705-004-7349-z

Čuhel, J., Šimek, M., Laughlin, R. J., Bru, D., Chèneby, D., Watson, C. J., et al. (2010). Insights into the Effect of Soil pH on N_2O and N_2 Emissions and Denitrifier Community Size and Activity. *Appl. Environ. Microbiol.* 76, 1870–1878.

Davidson, E. A., and Verchot, L. V. (2000). Testing the Hole-In-The-Pipe Model of Nitric and Nitrous Oxide Emissions from Soils Using the TRAGNET Database. *Glob. Biogeochem. Cycles* 14, 1035–1043. doi:10.1029/1999gb001223

Fierer, N., and Schimel, J. P. (2002). Effects of Drying-Rewetting Frequency on Soil Carbon and Nitrogen Transformations. *Soil Biol. Biochem.* 34, 777–787. doi:10.1016/s0038-0717(02)00007-x

Gaihre, Y. K., Singh, U., Islam, S. M. M., Huda, A., Islam, M. R., Sanabria, J., et al. (2017). Nitrous Oxide and Nitric Oxide Emissions and Nitrogen Use Efficiency as Affected by Nitrogen Placement in lowland rice fields. *Nutr. Cycl Agroecosyst* 110, 277–291. doi:10.1007/s10705-017-9897-z

Hofstra, N., and Bouwman, A. F. (2005). Denitrification in Agricultural Soils: Summarizing Published Data and Estimating Global Annual Rates. *Nutr. Cycl Agroecosyst* 72, 267–278. doi:10.1007/s10705-005-3109-y

Hu, H.-W., Chen, D., He, J.-Z., and van der Meer, J. R. (2015a). Microbial Regulation of Terrestrial Nitrous Oxide Formation: Understanding the Biological Pathways for Prediction of Emission Rates. *FEMS Microbiol. Rev.* 39, 729–749. doi:10.1093/femsre/fuv021

Hu, H.-W., Macdonald, C. A., Trivedi, P., Holmes, B., Bodrossy, L., He, J.-Z., et al. (2015b). Water Addition Regulates the Metabolic Activity of Ammonia Oxidizers Responding to Environmental Perturbations in Dry Subhumid Ecosystems. *Environ. Microbiol.* 17, 444–461. doi:10.1111/1462-2920.12481

Huang, R., Wang, Y., Liu, J., Li, J., Xu, G., Luo, M., et al. (2019). Variation in N2O Emission and N2O Related Microbial Functional Genes in Straw- and Biochar-Amended and Non-amended Soils. *Appl. Soil Ecol.* 137, 57–68. doi:10.1016/j.apsoil.2019.01.010

IPCC (2014). "Summary for Policymakers. Climate Change. Mitigation of Climate Change," in *Contribution of Working Group III to the Fifth Assessment Report of the Intergovernmental Panel on Climate Change*. Cambridge, United Kingdom: Cambridge University Press, 1–33. doi:10.1017/CBO9781107415324

Iqbal, J., Ronggui, H., Lijun, D., Lan, L., Shan, L., Tao, C., et al. (2008). Differences in Soil CO2 Flux between Different Land Use Types in Mid-subtropical China. *Soil Biol. Biochem.* 40, 2324–2333. doi:10.1016/j.soilbio.2008.05.010

Islam, S. M. M., Gaihre, Y. K., Biswas, J. C., Singh, U., Ahmed, M. N., Sanabria, J., et al. (2018). Nitrous Oxide and Nitric Oxide Emissions from lowland rice Cultivation with Urea Deep Placement and Alternate Wetting and Drying Irrigation. *Sci. Rep.* 8, 17623. doi:10.1038/s41598-018-35939-7

Lan, T., Li, M., Han, Y., Deng, O., Tang, X., Luo, L., et al. (2020). How Are Annual CH4, N2O, and NO Emissions from rice-wheat System Affected by Nitrogen Fertilizer Rate and Type?. *Appl. Soil Ecol.* 150, 103469. doi:10.1016/j.apsoil.2019.103469

Liu, Y., Lu, H., Yang, S., and Wang, Y. (2016). Impacts of Biochar Addition on rice Yield and Soil Properties in a Cold Waterlogged Paddy for Two Crop Seasons. *Field Crops Res.* 191, 161–167. doi:10.1016/j.fcr.2016.03.003

Mei, B., Zheng, X., Xie, B., Dong, H., Yao, Z., Liu, C., et al. (2011). Characteristics of Multiple-Year Nitrous Oxide Emissions from Conventional Vegetable fields in southeastern China. *J. Geophys. Res.* 116, D12113. doi:10.1029/2010jd015059

Ochoa-Hueso, R., Borer, E. T., Seabloom, E. W., Hobbie, S. E., Risch, A. C., Collins, S. L., et al. (2020). Microbial Processing of Plant Remains Is Co-limited by Multiple Nutrients in Global Grasslands. *Glob. Chang Biol.* 26, 4572–4582. doi:10.1111/gcb.15146

Pärn, J., Verhoeven, J. T. A., Butterbach-Bahl, K., Dise, N. B., Ullah, S., Aasa, A., et al. (2018). Nitrogen-rich Organic Soils under Warm Well-Drained

Conditions Are Global Nitrous Oxide Emission Hotspots. *Nat. Commun.* 9 (1), 1135. doi:10.1038/s41467-018-03540-1

Parton, W. J., Mosier, A. R., Ojima, D. S., Valentine, D. W., Schimel, D. S., Weier, K., et al. (1996). Generalized Model for N_2 and N_2O Production from Nitrification and Denitrification. *Glob. Biogeochem. Cycles* 3 (10), 401–412. doi:10.1029/96gb01455

Patrick, W. H., and Wyatt, R. (1964). Soil Nitrogen Loss as a Result of Alternate Submergence and Drying. *Soil Sci. Soc. America J.* 28, 647–653. doi:10.2136/sssaj1964.03615995002800050021x

Qiu, S., Wang, M., Wang, F., Chen, J., Li, X., Li, Q., et al. (2013). Effects of Open Drainage Ditch Design on Bacterial and Fungal Communities of Cold Waterlogged Paddy Soils. *Braz. J. Microbiol.* 44 (3), 983–991. doi:10.1590/s1517-83822013000300050

Schaufler, G., Kitzler, B., Schindlbacher, A., Skiba, U., Sutton, M. A., and Zechmeister-Boltenstern, S. (2010). Greenhouse Gas Emissions from European Soils under Different Land Use: Effects of Soil Moisture and Temperature. *Eur. J. Soil Sci.* 61 (5), 683–696. doi:10.1111/j.1365-2389.2010.01277.x

Sheng, R., Meng, D., Wu, M., Di, H., Qin, H., and Wei, W. (2013). Effect of Agricultural Land Use Change on Community Composition of Bacteria and Ammonia Oxidizers. *J. Soils Sediments* 13, 1246–1256. doi:10.1007/s11368-013-0713-3

Spott, O., Russow, R., and Stange, C. F. (2011). Formation of Hybrid N2O and Hybrid N2 Due to Codenitrification: First Review of a Barely Considered Process of Microbially Mediated N-Nitrosation. *Soil Biol. Biochem.* 43, 1995–2011. doi:10.1016/j.soilbio.2011.06.014

Wang, A., Ma, X., Xu, J., and Lu, W. (2019). Methane and Nitrous Oxide Emissions in rice-crab Culture Systems of Northeast China. *Aquacult. Fish.* 4, 134–141. doi:10.1016/j.aaf.2018.12.006

Wang, H., Guan, D., Zhang, R., Chen, Y., Hu, Y., and Xiao, L. (2014). Soil Aggregates and Organic Carbon Affected by the Land Use Change from rice Paddy to Vegetable Field. *Ecol. Eng.* 70, 206–211. doi:10.1016/j.ecoleng.2014.05.027

Wang, Y., Guo, J., Vogt, R. D., Mulder, J., Wang, J., and Zhang, X. (2017). Soil pH as the chief modifier for regional nitrous oxide emissions: New evidence and implications for global estimates and mitigation. *Global Change Biol.* 24, e617–e626.

Weller, S., Janz, B., Jörg, L., Kraus, D., Racela, H. S. U., Wassmann, R., et al. (2016). Greenhouse Gas Emissions and Global Warming Potential of Traditional and Diversified Tropical rice Rotation Systems. *Glob. Change Biol.* 22, 432–448. doi:10.1111/gcb.13099

Wissing, L., Kölbl, A., Häusler, W., Schad, P., Cao, Z.-H., and Kögel-Knabner, I. (2013). Management-induced Organic Carbon Accumulation in Paddy Soils: The Role of Organo-mineral Associations. *Soil Tillage Res.* 126, 60–71. doi:10.1016/j.still.2012.08.004

Wu, D., Dong, W., Oenema, O., Wang, Y., Trebs, I., and Hu, C. (2013). N2O Consumption by Low-Nitrogen Soil and its Regulation by Water and Oxygen. *Soil Biol. Biochem.* 60, 165–172. doi:10.1016/j.soilbio.2013.01.028

Wu, L., Tang, S., He, D., Wu, X., Shaaban, M., Wang, M., et al. (2017). Conversion from rice to Vegetable Production Increases N 2 O Emission via Increased Soil Organic Matter Mineralization. *Sci. Total Environ.* 583, 190–201. doi:10.1016/j.scitotenv.2017.01.050

Xie, K., Xu, P., Yang, S., Lu, Y., Jiang, R., Gu, W., et al. (2015). Effects of Supplementary Composts on Microbial Communities and rice Productivity in Cold Water Paddy fields. *J. Microbiol. Biotechnol.* 25, 569–578. doi:10.4014/jmb.1407.07066

Xu, X. Y., Zhang, M. M., Xiong, Y. S., Yuan, J. F., Shaaban, M., Zhou, W., et al. (2020). The Influence of Soil Temperature, Methanogens and Methanotrophs on Methane Emissions from Cold Waterlogged Paddy fields. *J. Environ. Manag.* 264, 110421. doi:10.1016/j.jenvman.2020.110421

Yan, X., Shi, S., Du, L., and Xing, G. (2000). Pathways of N2O Emission from rice Paddy Soil. *Soil Biol. Biochem.* 32 (3), 437–440. doi:10.1016/s0038-0717(99)00175-3

Yu, K. W., Wang, Z. P., and Chen, G. X. (1997). Nitrous Oxide and Methane Transport through rice Plants. *Biol. Fertil. Soils* 24 (3), 341–343. doi:10.1007/s003740050254

Zhou, M., Wang, X., Wang, Y., and Zhu, B. (2018). A Three-Year experiment of Annual Methane and Nitrous Oxide Emissions from the Subtropical Permanently Flooded rice Paddy fields of China: Emission Factor, Temperature Sensitivity and Fertilizer Nitrogen Effect. *Agric. For. Meteorol.* 250-251, 299–307. doi:10.1016/j.agrformet.2017.12.265

Zhu, K., Bruun, S., Larsen, M., Glud, R. N., and Jensen, L. S. (2014). Spatial Oxygen Distribution and Nitrous Oxide Emissions from Soil after Manure Application: a Novel Approach Using Planar Optodes. *J. Environ. Qual.* 43 (5), 1809–1812. doi:10.2134/jeq2014.03.0125

Zhu, X., Burger, M., Doane, T. A., and Horwath, W. R. (2013). Ammonia Oxidation Pathways and Nitrifier Denitrification Are Significant Sources of N2O and NO under Low Oxygen Availability. *Proc. Natl. Acad. Sci.* 110 (16), 6328–6333. doi:10.1073/pnas.1219993110

Zou, J., Huang, Y., Qin, Y., Liu, S., Shen, Q., Pan, G., et al. (2009). Changes in Fertilizer-Induced Direct N2O Emissions from Paddy fields during rice-growing Season in China between 1950s and 1990s. *Glob. Change Biol.* 15, 229–242. doi:10.1111/j.1365-2486.2008.01775.x

Conflict of Interest: The authors declare that the research was conducted in the absence of any commercial or financial relationships that could be construed as a potential conflict of interest.

frontiers in Environmental Science

ORIGINAL RESEARCH
published: 07 September 2021
doi: 10.3389/fenvs.2021.664488

Sulfur-Based Denitrification in Streambank Subsoils in a Headwater Catchment Underlain by Marine Sedimentary Rocks in Akita, Japan

Atsushi Hayakawa[1], Hitoshi Ota[1], Ryoki Asano[2], Hirotatsu Murano[3], Yuichi Ishikawa[1] and Tadashi Takahashi[1]*

[1]Department of Biological Environment, Faculty of Bioresource Sciences, Akita Prefectural University, Akita, Japan, [2]Department of Agro-Food Science, Faculty of Agro-Food Science, Niigata Agro-Food University, Tainai, Japan, [3]Department of Environmental Bioscience, Faculty of Agriculture, Meijo University, Nagoya, Japan

Sulfur-based denitrification may be a key biogeochemical nitrate (NO_3^-) removal process in sulfide-rich regions, but it is still poorly understood in natural terrestrial ecosystems. We examined sulfur-driven NO_3^- reduction using streambank soils in a headwater catchment underlain by marine sedimentary rock in Akita, Japan. In a catchment exhibiting higher sulfide content in streambed sediment, we sampled two adjacent streambank soils of streambank I (two layers) and of streambank II (eight layers). Anaerobic long-term incubation experiments (40 days, using soils of streambank I) and short-term incubation experiments (5 days, using soils of streambank II) were conducted to evaluate variations of N solutes (NO_3^-, NO_2^-, and NH_4^+), N gases (NO, N_2O), and the bacterial flora. In both experiments, two treatment solutions containing NO_3^- (N treatment), and NO_3^- and $S_2O_3^{2-}$ (N + S treatment) were prepared. In the N + S treatment of the long-term experiment, NO_3^- concentrations gradually decreased by 98%, with increases in the SO_4^{2-}, NO_2^-, NO, and N_2O concentrations and with not increase in the NH_4^+, indicating denitrification had occurred with a high probability. Temporal accumulation of NO_2^- was observed in the N + S treatment. The stoichiometric ratio of SO_4^{2-} production and NO_3^- depletion rates indicated that denitrification using reduced sulfur occurred even without additional S, indicating inherent S also served as an electron donor for denitrification. In the short-term incubation experiment, S addition was significantly decreased NO_3^- concentrations and increased NO_2^-, NO, and N_2O concentrations, especially in some subsoils with higher sulfide contents. Many denitrifying sulfur-oxidizing bacteria (*Thiobacillus denitrificans* and *Sulfuricella denitrificans*) were detected in both streambank I and II, which dominated up to 5% of the entire microbial population, suggesting that these bacteria are widespread in sulfide-rich soil layers in the catchment. We concluded that the catchment with abundant sulfides in the subsoil possessed the potential for sulfur-driven NO_3^- reduction, which could widely influence N cycling in and NO_3^- export from the headwater catchment.

Keywords: sulfur-oxidizing bacteria, ecosystem denitrification, nitrogen cycle, biogeochemistry, sulfur-based denitrification

OPEN ACCESS

Edited by:
Muhammad Shaaban, Bahauddin Zakariya University, Pakistan

Reviewed by:
Fan Chen, Harbin Institute of Technology, China
Xiangyu Xu, Hubei Academy of Agricultural Sciences, China

****Correspondence:***
Atsushi Hayakawa
hayakawa@akita-pu.ac.jp

Specialty section:
This article was submitted to Biogeochemical Dynamics, a section of the journal Frontiers in Environmental Science

Received: *05 February 2021*
Accepted: *23 August 2021*
Published: *07 September 2021*

Citation:
Hayakawa A, Ota H, Asano R, Murano H, Ishikawa Y and Takahashi T (2021) Sulfur-Based Denitrification in Streambank Subsoils in a Headwater Catchment Underlain by Marine Sedimentary Rocks in Akita, Japan. Front. Environ. Sci. 9:664488. doi: 10.3389/fenvs.2021.664488

INTRODUCTION

Human activities have dramatically increased the amount of reactive nitrogen (N) in global ecosystems and have increased food production; however, input of reactive N beyond appropriate uses can lead to eutrophication of surface water, causing degradation of aquatic ecosystems and problems such as toxic algal blooms, loss of dissolved oxygen, depletion of fish populations, and biodiversity loss (Vitousek, 1997; Galloway and Cowling, 2002). In forest ecosystems, losses of N mainly as nitrate (NO_3^-) via streams can be caused by increased levels of reactive N such as N deposition in the forest (Lovett and Goodale, 2011). Denitrification is a NO_3^- removal process and is generally performed by particular groups of ubiquitous heterotrophic bacteria that have the ability to use NO_3^- as an electron acceptor and organic carbon (C) as an electron donor during anaerobic respiration. Denitrification transforms NO_3^- to the final form (N_2 gas) via four main steps: $NO_3^- \rightarrow NO_2^- \rightarrow NO \rightarrow N_2O \rightarrow N_2$ (Tiedje, 1994). Because denitrification ultimate removes reactive N as N_2 gas from the ecosystem as one of soil functions of transforming nutrients (Adhikari and Hartemink, 2016; Lilburne et al., 2020), it is a highly valued ecosystem service in N-enriched catchments (Craig et al., 2010).

Some bacteria can use inorganic sources, such as reduced sulfur compounds and Fe^{2+}, as the electron donor to grow chemoautotrophically (Korom, 1992; Straub et al., 1996). The oxidation of such inorganic species coupled with N oxide reduction is termed autotrophic denitrification. Autotrophic denitrification can proceed through the ability of some bacteria to couple the reduction of NO_3^- to the oxidation of reduced sulfur (Burgin and Hamilton, 2007). The most used electron donors of reduced sulfur compounds include elemental sulfur, sulfide and thiosulfate (De Capua et al., 2019). Some previous studies have detected NO_3^- removal coupled with sulfide oxidation in groundwater systems (Postma et al., 1991; Schwientek et al., 2008; Jørgensen et al., 2009; Craig et al., 2010; Vaclavkova et al., 2014), riverbed sediments (Hayakawa et al., 2013; Martínez-Santos et al., 2018; Yin et al., 2019), and sediment incubated with added sulfur (Brunet and Garcia-Gil, 1996; Garcia-Gil and Golterman, 1993; Jørgensen et al., 2009; Torrentó et al., 2010, 2011). NO_3^- reduction coupled with sulfide oxidation may be widespread and biogeochemically important in freshwater sediments (Burgin and Hamilton, 2008); however, the process has been reported less in freshwater than in marine and brackish marshes and tidal ecosystems (Hu et al., 2020) and the relative importance of the electron donor in the removal process remains uncertain at catchment scales.

Typical signs of sulfur-based denitrification using sulfide as an electron donor are decreasing NO_3^- accompanied by increasing SO_4^{2-} and NO_2^- (Postma et al., 1991; Jørgensen et al., 2009; Torrentó et al., 2010; Chung et al., 2014) and the microbial stoichiometric reaction ratios of SO_4^{2-} production and NO_3^- depletion rates ($\Delta SO_4^{2-}/\Delta NO_3^-$) for sulfur-based denitrification (Hayakawa et al., 2013; Vaclavkova et al., 2014). Some bioreactor studies have reported that NO_2^- accumulation was observed during sulfur-based denitrification (Moon et al., 2004; Chung et al., 2014; Chen et al., 2018). Furthermore, a recent study has reported that accumulation of NO_2^- can also lead to build-up of NO and N_2O during the sulfur-based denitrification process (Lan et al., 2019). Microbial community analysis can provide useful information about the key players and complementary evidence of sulfur-based denitrification (Torrentó et al., 2011; Hayakawa et al., 2013; Dolejs et al., 2015; Wang et al., 2021). Therefore, to obtain evidence of sulfur-based denitrification in natural soils and sediments in freshwater ecosystems, it may be important to detect the various signs (NO_3^- reduction accompanied by SO_4^{2-} production, stoichiometric reactions inferred from the $\Delta SO_4^{2-}/\Delta NO_3^-$ ratio, accumulation of NO_2^- and gaseous forms of N, and elements of the microbial community) of sulfur-based denitrification.

The sulfur cycle is especially important in catchments that supply high concentrations of SO_4^{2-} to stream water (Szynkiewicz et al., 2012) and may be closely related to the N cycle through reactions such as sulfur-based denitrification in the catchments (Burgin and Hamilton, 2008). Reservoirs of sulfur in freshwater catchments are dominated by dissolved sulfate in water and sulfate and sulfide minerals in sediments and soils (Wynn et al., 2010; Iribar and Abalos, 2011; Hayakawa et al., 2020). In catchments suppling high levels of SO_4^{2-} to streams, it is expected to have much inherent sulfide. On one hand, the supplied SO_4^{2-} can be reduced to sulfide by the activity of dissimilatory sulfate-reducing bacteria in anoxic condition (Plugge et al., 2011), and the sulfide can be re-distributed to soils and sediments in the catchments. Reduction-oxidation reactions occur during burial because the sediments contain such reactive mixtures of oxidized and reduced components (Roberts, 2015). Some previous studies reported sulfide-driven autotrophic denitrification had occurred in sulfide-rich riverbed sediments in those catchments (Hayakawa et al., 2013; Martínez-Santos et al., 2018; Yin et al., 2019; Li et al., 2021).

Our study area, the Lake Hachiro watershed, is located along the coast of the Japan Sea, and its main surface geology consists of marine sedimentary rocks. The region was submerged beneath the sea during the Neogene Period (Shiraishi and Matoba, 1992), and sulfide minerals (easily oxidizable sulfur; EOS) in streambed sediments occur throughout the watershed, including in the forested area of the upper mountains, and may supply SO_4^{2-} to the streams from oxidation of sulfides (Hayakawa et al., 2020). High sulfide levels in streambed sediments can be reasonably expected to influence the N cycle through sulfur-based denitrification. Our previous study conducted in 35 headwater catchments in the Lake Hachiro watershed showed that in-stream NO_3^- concentrations tended to decrease with increasing EOS content in the streambed, indicating the probable occurrence of sulfur-based denitrification in the sulfide-rich catchment (Hayakawa et al., 2020). The composition of streambed sediment is affected by variations in the surface soil and geology of the catchment and has been used to identify sites with distinctive water quality (Horowitz and Elrick, 2017); thus, sulfide-rich soils are expected to be present somewhere in a catchment with a sulfide-rich streambed. In fact, soil with a high EOS content was found in a streambank

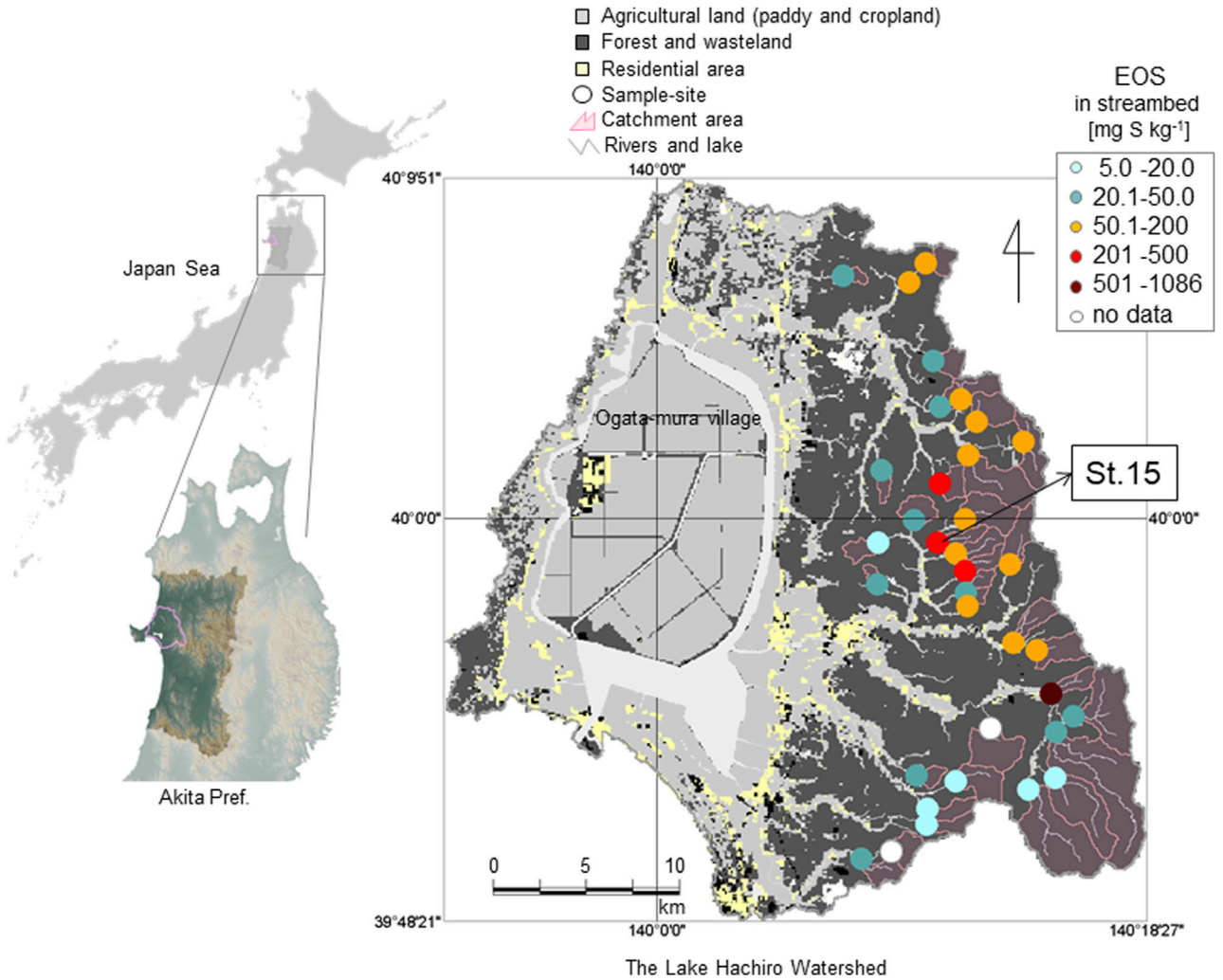

FIGURE 1 | Map of the study site and the distribution of easily oxidizable sulfur (EOS) content in streambed sediments at each headwater catchment in the Lake Hachiro watershed (Hayakawa et al., 2020). St. 15 is the study catchment.

where the EOS content in the streambed was high (Hayakawa et al., 2020). To clarify this point, we need to obtain detailed evidence of sulfide distribution and potential sulfur-based denitrification in the natural soils in the Lake Hachiro watershed.

We hypothesized that the catchment with higher sulfide content in its streambed possesses sulfide-rich soil layers and a higher potential of sulfur-based denitrification in those layers within the catchment. We focused on streambank soils because these soils constitute an interface between land and stream, and thus can influence the qualities of the streambed sediment and stream. Our main study objectives were: 1) to evaluate the vertical distribution of sulfide in streambank soils; 2) to evaluate NO_3^- reduction with production of SO_4^{2-}, NO_2^-, NO, and N_2O in sulfide-rich soils and to detect signs of sulfur-based denitrification by anaerobic incubation with and without S addition; and 3) to identify the most important sulfur-oxidizing bacteria that cause denitrification.

MATERIALS AND METHODS

Site Description and Sediment Sampling

The Lake Hachiro watershed is located in western Akita Prefecture facing the Japan Sea (**Figure 1**). The entire watershed area is 894 km^2. The geological strata of the watershed belong to the Green Tuff zone, consisting of volcanic rocks and sedimentary rocks of late Miocene age (Shiraishi, 1990). In the early part of the middle Miocene to the Pliocene (i.e., ca 13–2.5 Ma), the Akita region was drowned as a result of subsidence of the former land area (Shiraishi and Matoba, 1992). As a result, the sedimentary rocks in the watershed are mainly marine deposits and consist of thick mudstone layers (Shiraishi, 1990) with high levels of total sulfur (0.90%; Koma, 1992). Weather recordings for the region from the Gojome recording station (8 km away from the study catchment) for the period 1981-2010 (Japan Meteorological Agency, 2013) revealed that average precipitation was

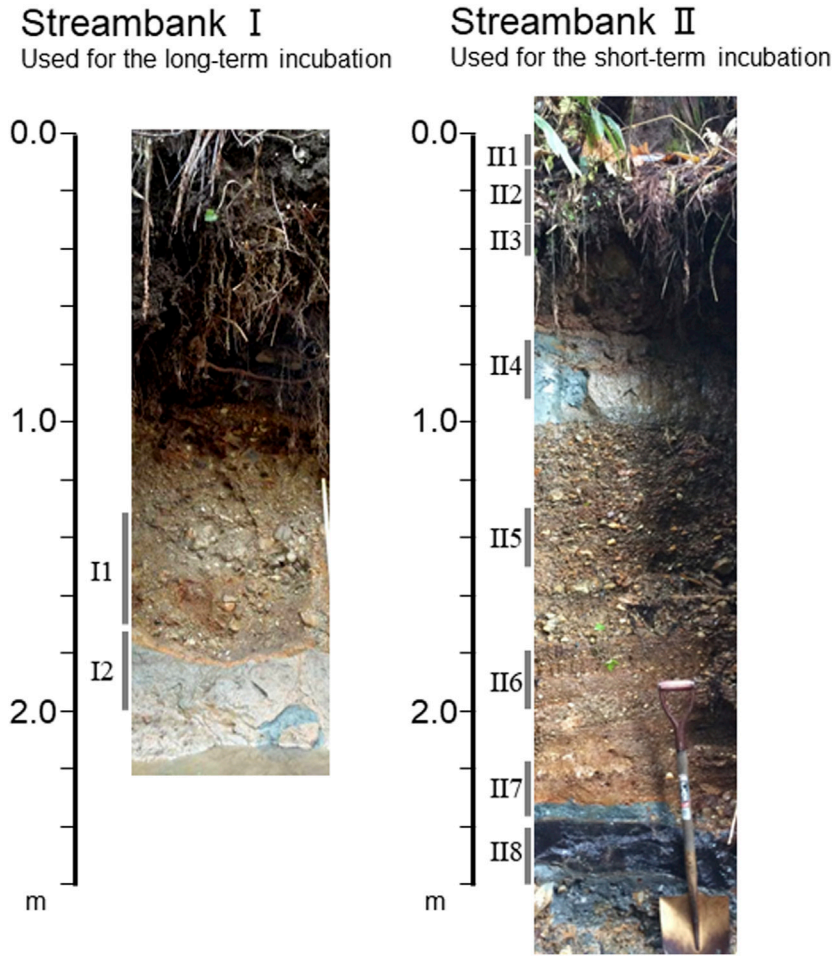

FIGURE 2 | Streambanks I and II at St. 15, and the depths of the soils sampled for the incubation experiments.

1,553 mm year^{-1} and the annual mean temperature was 10.8°C. The lowest mean monthly temperature occured in January (–0.9°C), and the highest mean monthly temperature was in August (24°C). The average maximum snow depth during winter (December–February) is 48 cm. Japanese cedar (*Cryptomeria japonica* D. Don) plantations dominated the forested area, especially in the middle and northern parts of the watershed.

The study catchment was St. 15 in the Lake Hachiro watershed (1.61 km^2, N39.9886, E140.1760), where the sulfide (EOS) content in streambed sediment is relatively high, as 0.254 g S kg^{-1} (Hayakawa et al., 2020; **Figure 1**). In a recent study, the stream-water chemistry in the catchment exhibited the highest SO_4^{2-} (18.3 mg S L^{-1}) but relatively lower NO_3^- (0.149 mg N L^{-1}) concentrations among the 35 headwater catchments in the Lake Hachiro watershed (Hayakawa et al., 2020). Bulk N deposition to the catchment was 7.5 kg N ha^{-1} year^{-1} (Hayakawa et al., 2020), higher than the threshold value of 5 kg N ha^{-1} yr^{-1} that caused N leaching to streams in China (Fang et al., 2011).

Soil sampling was conducted at two streambanks, I and II, in St. 15 in April and May 2016, respectively (**Figure 2**). Streambank I is the right streambank, and was previously studied by Hayakawa et al. (2020). Streambank II is the left bank approximately 50 m downstream from streambank I, and was newly exposed as the result of a recent flood (**Figure 2**). These streambanks might had been formed by flooding (not tidal in present) or mountain-side slope collapse, and the sediments accumulated in the streambanks may contain old and newly re-deposited reduced sulfur. Samples were collected by trowel at depths of 1.3–1.7 m (I1) and 1.7–2.0 m (I2) at streambank I for the evaluation of sulfur-based denitrification between the expected sulfide rich layer (I2) and the expected non-sulfide layer (I1). At streambank II, eight samples were collected at depths of 0–0.1 m (II1), 0.1–0.3 m (II2), 0.3–0.4 m (II3), 0.7–0.9 m (II4), 1.3–1.5 m (II5), 1.8–2.0 m (II6), 2.2–2.4 m (II7), and 2.4–2.6 m (II8). In roughly, soil textures were fine sands and silts in I2, II1, II2, II4, and II8, and were coarse sands with gravel in other layers. The bluish gray color of the soils in II2, II4, and II8 (**Figure 2**) indicated these sediments were formed reducing conditions. To avoid contact with atmospheric oxygen, the sediments were taken by ca 15 cm depth from the streambank-wall surface and were sealed in sample bags for chemical analysis and incubation experiments and in 15 ml

centrifuge tubes for bacterial analysis immediately after sampling and stored in a cooler box with ice packs. Samples for the incubation and for measurement of the bacterial community were stored at 4°C and −80°C until analysis, respectively.

Incubation Procedure

The incubation method was based on previous studies (Jørgensen et al., 2009; Hayakawa et al., 2013). Long-term incubation of soil from streambank I (I1 and I2) was conducted to evaluate changes in the NO_3^-, NO_2^-, NO, and N_2O production/depletion patterns and the bacterial community. A 120 g quantity of fresh soil and 400 ml of solution were added to 550 ml glass bottles, which were then sealed with butyl rubber septa and an aluminum crimp. Two stainless-steel needles (Terumo, Tokyo, Japan, 23G × 32 mm; GL Sciences, Tokyo, Japan, 19G × 100 mm) were inserted into each septum and fitted with sterile three-way stopcocks for gas and solution sampling. Three treatment solutions were prepared: a deionized water control, CT; KNO_3 (8 mg N L^{-1}), N; and KNO_3 + $Na_2S_2O_3$ (20 mg S L^{-1}), N + S. Thiosulfate ($S_2O_3^{2-}$) is considered to be a useful electron donor for sulfur-based denitrification (Chung et al., 2014; Qian et al., 2016). To achieve anoxic conditions, the solution and headspace in the bottles were purged with O_2-free ultrapure N_2 gas for 30 min. All bottles were prepared in triplicate and incubated at 25°C for 40 days in darkness. Because we intended to evaluate the potential of sulfur-based denitrification in the soils, the incubation was conducted in near the optimum growth temperature for sulfur denitrifying bacteria (e.g., *Thiobachillus denitrificans*, 28–32°C, Garrity et al., 2005).

Short-term incubation of soils from streambank II (II1–II8) was conducted to evaluate the vertical patterns of NO_3^-, NO_2^-, NO, and N_2O production/depletion and the bacterial community. The incubation procedure was almost same as that of the long-term incubation, but in a smaller bottle. A 15 g amount of fresh soil and 50 ml of solution were added to 150 ml glass bottles. Two treatment solutions were prepared: KNO_3 (5 mg N L^{-1}), N; and KNO_3 + $Na_2S_2O_3$ (10 mg S L^{-1}), N + S. All bottles were prepared in triplicate and incubated at 25°C for 5 days in darkness under anoxic conditions.

Water and Gas Sampling and Analysis

Water and gases in the incubation bottle were sampled eight times during the long-term incubation, at 1, 3, 6, 9, 14, 26, 30, and 40 days after the start of incubation, and twice during the short-term incubation, at 2 days (gas sample only) and 5 days after the start of incubation. In each sampling, 10- and 25 ml headspace gases in the bottle were sampled for the measurement of NO and N_2O, respectively. The NO concentration was measured immediately after the sampling by using a NOx analyzer (MODEL42-i, Thermo Fisher Scientific, Yokohama, Japan). This analysis on the principle that NO and ozone (O_3) react to produce a characteristic luminescence with an intensity linearly proportional to the NO concentration. For N_2O analysis, the headspace gas was transferred from the syringe into a 15 ml evacuated glass vial and the N_2O concentration was determined using a gas chromatograph (GC14-B, Shimadzu, Kyoto, Japan) equipped with an electron-capture detector. For water analysis, a 20 ml solution sample was extracted from the bottle with a 20 ml syringe. Immediately after the sampling, pH and electrical conductivity (EC) were measured in 5 ml of the sampled solution with a portable pH meter (B-212, HORIBA, Kyoto, Japan) and an EC meter (B-173, HORIBA, Kyoto, Japan). The remaining 15 ml of sampled solution was filtered through a 0.45 μm cellulose acetate membrane filter (DISMIC-13CP045AS, ADVANTEC, Tokyo, Japan). We measured the NO_2^-, NO_3^-, SO_4^{2-}, and $S_2O_3^{2-}$ concentrations in the solution using an ion chromatograph (DIONEX ICS-2100, Thermo Fisher Scientific, Yokohama, Japan). The detection limit for the analysis of $S_2O_3^{2-}$ concentration is 0.003 mg S L^{-1}. We determined the NH_4^+ concentration by colorimetry using the indophenol blue method with a continuous flow autoanalyzer (QuAAtro2-HR, BLTEC, Osaka, Japan). After every gas and water sampling, the same volume as the sampled gas and water of O_2-free ultrapure N_2 gas was added to the bottle by using a syringe with a needle.

Soil Analysis

We determined the total C and total S contents in the sediments using the combustion method for C (SUMIGRAPH NC-22F, SCAS, Japan) and for S (LECO S632, Tokyo, Japan). Sediment pH (H_2O) and pH (H_2O_2) were determined by using soil/solution ratios of 1:2.5 (w/v) and 1:10 (w/v) (Murano et al., 2000), respectively. If the reduced sulfur are present in soils, they are often capable of rapid oxidation by H_2O_2, causing lowered pH (H_2O_2) values. The easily oxidizable S (EOS) content in the soils was calculated as the difference between the H_2O_2-soluble S content (H_2O_2-S) and the water-soluble S content (H_2O-S) (Murano et al., 2000). EOS represents reduced sulfur such as pyrite in sediments (Murano et al., 2000).

Analysis of Bacterial Communities in the Soil

To describe the bacterial communities in the streambank soils, 16S rRNA genes were analyzed by means of PCR pyrosequencing. Total DNA was extracted from 0.5 g soil using a FastDNA SPIN Kit for Soil (MP Biomedicals, Carlsbad, CA, United States) according to the manufacturer's instructions. DNA libraries were constructed based on two-step tailed PCR for 16S rRNA V4 region using primers (515f, 5′-GTGCCAGCMGCCGCGGTAA-3'; 806r, 5′-GGACTACHVGGGTWTCTAAT-3′) with an Illumina nextera barcode (Caporaso et al., 2011, https://jp.support.illumina.com/downloads/16s_metagenomic_sequencing_library_preparation.html). The mixture for the amplification of the first step consisted of 1 × KAPA HiFi HotStart Ready Mix (Roche, Basel, Switzerland), 0.25 μM of each primer, and 10 ng template DNA in a final volume of 25 μl. The amplification conditions were as follows: 94°C for 3 min; 25 cycles at 94°C for 60 s, 50°C for 60 s, and 72°C for 105 s; and a final extension at 72°C for 10 min. After purification on Agencourt AMPure XP (Beckman Coulter, Pasadena, CA, United States), second-step PCR was performed. The mixture for the amplification of the second step consisted of 1 × KAPA HiFi HotStart Ready Mix, 0.25 μM of each primer, and 5 μl first-step PCR product in a final volume of 50 μl. After

purification on Agencourt AMPure XP, the concentrations were measured using a Qubit dsDNA BR Assay Kit (Thermo Fisher Scientific, Waltham, MA, United States). All PCR products were normalized to the same molecule concentration and mixed in equal volumes. The constructed libraries were subjected to 250-bp paired-end sequencing on an Illumina MiSeq with Miseq Reagent Kit v2 nano (500 Cycles).

Raw sequencing reads, which were divided into forward and reverse, were assembled using the Initial Process in the Ribosomal Database Project (RDP) Pyrosequencing Pipeline (http://pyro.cme.msu.edu/). Reads of 150 bp or fewer and those containing a sequence with a quality value of 20 or less were removed. Chimeric sequences were removed using Fungene chimera check Pipeline (http://fungene.cme.msu.edu/). Chimera-filtered sequences were classified phylogenetically using the RDP Classifier with a cut-off value of 0.8 (**Supplementary Figures S1, S2**). Sequences classified as belonging to sulfur-oxidizing bacteria were compared to sequences registered in the database of the DNA Databank of Japan by using the BLAST system (http://blast.ddbj.nig.ac.jp/blast/blastn?lang=en) to determine the most similar sequence type. In the sequences obtained in this study, sequences which exhibited more than 97% similarity to 16S rDNA sequences classified as SOB was, considered. The nucleotide sequence data were deposited in the DDBJ Read Archive (http://trace.ddbj.nig.ac.jp/dra/index_e.html) under accession number DRA011495.

Data Analysis

For the evaluation of NO_3^- depletion and SO_4^{2-} production rates during incubation, the accumulated number of moles n (NO_3^- and SO_4^{2-}) of element i removed from or released to the solution over time up to sampling occasion k was calculated from the measured concentration (C_{meas}) following the method of Jørgensen et al. (2009) and Vaclavkova et al. (2014):

$$n_i^k = \left[C_{i,meas}^k V_{total}^k + \sum_{s=1}^{k} C_{i,meas}^s V_{sample}^s \right] (\text{moles})$$

where V_{total}^k is the total volume of solution in the bottle after removal of the kth sample and $V_{sample}^s$is the volume of sample removed on sampling occasion k. Elemental transformation rates were calculated using linear regression against time as the independent variable and concentration as the dependent variable. Average ±standard deviation (n = 3) reaction rates (mmol per bottle) of NO_3^- depletion and SO_4^{2-} production were expressed as ΔNO_3^- and ΔSO_4^{2-}, respectively, and $\Delta SO_4^{2-}/\Delta NO_3^-$ was calculated.

The chimera-filtered sequences were divided into operational taxonomic units (OTUs) for sequences with over 97% similarity to one another by uclust method and furthest clustering algorithm using the Qiime 1.9.0 (http://qiime.org/index.html). Diversity indices, such as Chao1 and the abundance-based coverage estimate (ACE), were also calculated using Qiime (Chao and Bunge 2002) (**Supplementary Table S1**). Differences in microbial community structure among in the samples were calculated from OTUs by unweighted UniFrac using Qiime, and principal coordinate analysis was performed (**Supplementary Figure S3**).

One-way ANOVA was used followed by Bonferroni's test was used for multiple comparisons of variables among soils I1 and I2 in the long-term incubation. The Wilcoxon rank-sum test (U test) was used for comparisons between two treatments (N, N + S treatments). The Kruskal–Wallis test followed by the Steel–Dwass test were used for multiple comparisons of variables among soil layers II1 to II8, and bacterial communities among treatments in I2 during the long-term incubation. These statistical analyses were performed using R (R Development Core Team 2018; version 3.4.3).

RESULTS

Physio-Chemical Properties of Streambank Soils

The characteristics of the soils in the two streambanks are listed in **Table 1**. The pH (H_2O) was lowest in samples I2 (6.35) and II8 (5.54). The pH (H_2O_2) range was 3.04–7.08, with low values in I2, II1, II2, II4, and II8. EC was 2.9–726 mS m^{-1}, with high values in I2, II1, II4, and II8. Total carbon content was the highest (48 g kg^{-1}) in sample II1 of the surface soil. In contrast, high total sulfur contents were observed in subsoil samples I2, II4, and II8, and EOS levels were also high in those soil layers.

Long-Term Incubation Experiment

Temporal variations of the concentrations of aquatic and gaseous N species, $S_2O_3^{2-}$, and SO_4^{2-} in different soil layers (I1 and I2) and treatments (N and N + S) during the long-term incubation experiment are shown in **Figure 3**. NO_3^- concentrations decreased more with time in I2 than in I1, and in the N + S treatment than in the N treatment for each layer. On day 14 day in I2, the NO_3^- concentration was markedly different between the N and N + S treatments, with values of 6.59 ± 1.7 and 1.94 ± 3.0 mg N L^{-1}, respectively; the final values (on day 40) were 1.13 ± 0.73 and 0.22 ± 0.20 mg N L^{-1}, respectively. In I2, the decrease in the NO_3^- concentration was followed by increases in the NO_2^-, NO, and N_2O concentrations. NO_2^- accumulation was particularly observed in the first 14 days, with levels increasing to 0.76 mg N L^{-1} in the N treatment and 3.46 mg N L^{-1} in the N + S treatment. In contrast, in I1, the NO_3^- concentration did not fall markedly, but decreased more in the N + S treatment than in the N treatment. NH_4^+ was detected, but at relatively low levels (0.0–0.04 mg N L^{-1}), and exhibited no clear differences among soils and treatments.

The NO concentration increased in I2 with N + S treatment to a maximum value of 5.96 ppmv on day 14, but was almost undetectable in I1 with N treatment. N_2O was detected in both soils and treatments; the maximum values of 337 ppmv (N treatment) and 743 ppmv (N + S treatment) were observed in I2 on day 26. In I1 with N + S treatment, the maximum N_2O concentration was approximately 1/43 (17 ppmv) of that in I2 with N + S treatment. The N_2O concentration decreased rapidly after day 26, when NO_2^- and NO had almost disappeared. The $S_2O_3^{2-}$ concentration decreased rapidly in the first 10 days and was oxidized to SO_4^{2-} in both soils with N + S treatment. $S_2O_3^{2-}$ was detected at 0.83 ± 0.02 mg S L^{-1} on day 1 in I2 without S addition (N treatment) but was not detected in I1 with N treatment throughout the incubation period.

TABLE 1 | Soil chemical properties at streambanks I and II. EC, electric conductivity; T-C, total carbon; T-S, total sulfur; EOS, easily oxidizable sulfur.

Soil	depth, m	pH (H_2O)	pH (H_2O_2)	EC	T-C	T-S	EOS
	M			mS m^{-1}	g kg^{-1}	g kg^{-1}	g kg^{-1}
I1	1.3–1.7	7.11	7.08	5.5	0.89	0.14	0.004
I2	1.7–2.0	6.35	4.58	69	3.6	1.7	1.2
II1	0.0–0.1	6.97	3.37	113	48	0.75	0.073
II2	0.1–0.3	7.39	5.14	5.1	2.3	0.15	0.017
II3	0.3–0.4	6.98	5.74	5.1	1.1	0.12	0.006
II4	0.7–0.9	6.90	5.41	89	3.0	1.2	0.33
II5	1.3–1.5	6.65	6.20	3.5	1.5	0.14	0.007
II6	1.8–2.0	7.41	6.22	2.9	0.7	0.12	0.006
II7	2.2–2.4	7.26	6.15	4.2	0.7	0.15	0.007
II8	2.4–2.6	5.54	3.04	726	5.9	96	4.9

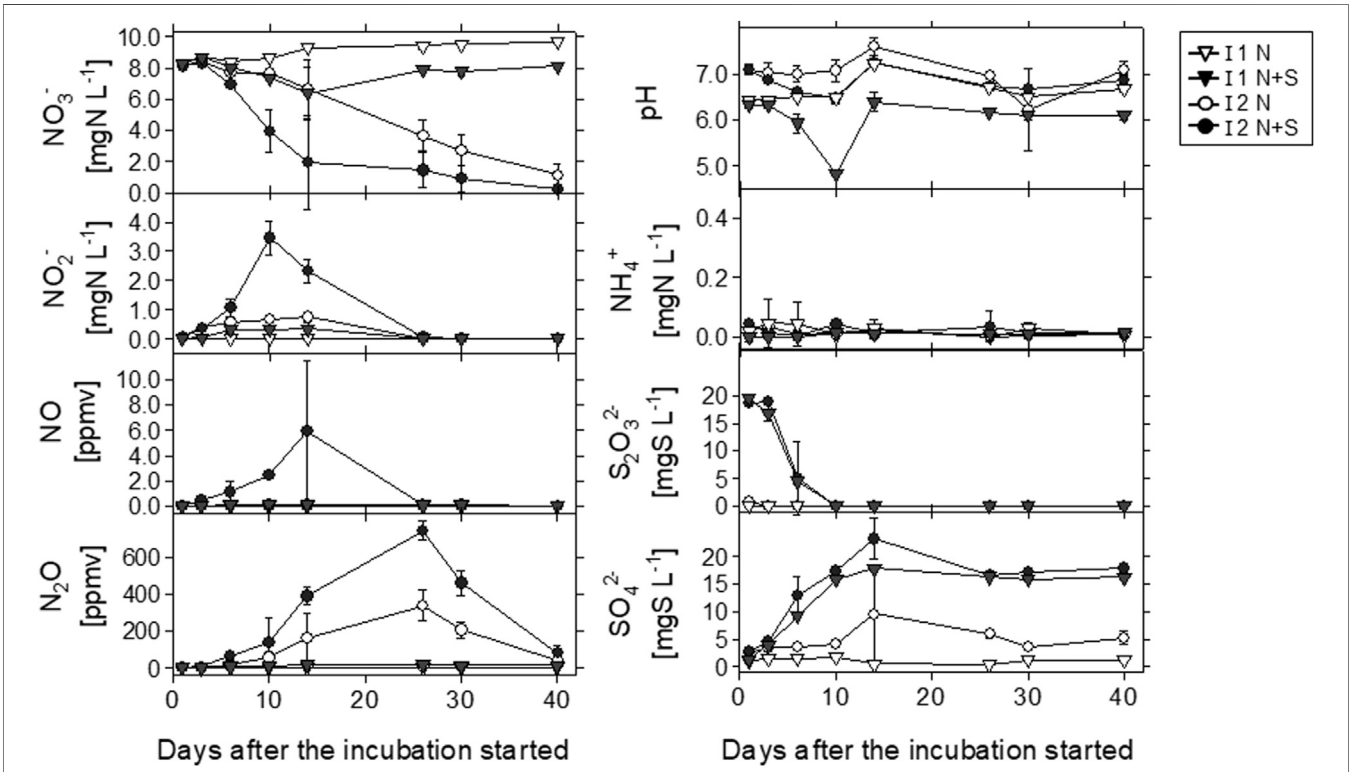

FIGURE 3 | Temporal variations of pH and the concentrations of aquatic and gaseous nitrogen species, $S_2O_3^{2-}$, and SO_4^{2-} with different soils (I1 and I2) and treatments (N and N + S) in the long-term incubation experiment. N, KNO_3 solution; N + S, KNO_3 and $Na_2S_2O_3$ solution. Error bars indicate standard deviation (n = 3).

The N + S treatment exhibited large fluctuations in water qualities and gas concentrations in sample I2 (**Figure 4**). By day 10, the NO_3^- concentration had fallen sharply, the NO_2^- concentration had increased, and the $S_2O_3^{2-}$ concentration had decreased. During this interval, the pH fell from 7.1 to 6.5. After the NO_2^- peak on day 10, the maximum NO concentration was detected on day 14, at the same time as the pH increased to 7.2, followed by the N_2O peak concentration on day 26.

Using moles data in **Supplementary Figure S4**, the results of ΔNO_3^- and ΔSO_4^{2-}, and $\Delta SO_4^{2-}/\Delta NO_3^-$ during different incubation periods are shown in **Table 2**. Since NO_3^- and SO_4^{2-} were linearly changed especially during days 1–14 (**Supplementary Figure S4**), we estimated ΔNO_3^- and ΔSO_4^{2-} values for days 1–14 and all the incubation period (1–40). In both the periods, ΔNO_3^- in I2 with N + S treatment was significantly larger than other treatments, and ΔSO_4^{2-} was significantly larger in the added S treatments (**Table 2**). On one hand, $\Delta SO_4^{2-}/\Delta NO_3^-$ did not differ between soils and treatments during days 1–14 and was significantly larger in I1 with N + S treatment during days 1–40 (**Table 2**). The relationships between ΔNO_3^- and ΔSO_4^{2-} of I1 and I2 with both treatments during different incubation periods showed that the results for I2 with N and N + S treatments plotted between the denitrification lines of $S_2O_3^{2-}$ and FeS during days 1–14 with large variations (**Figure 5A**). During days 1–40, only I2 with N + S

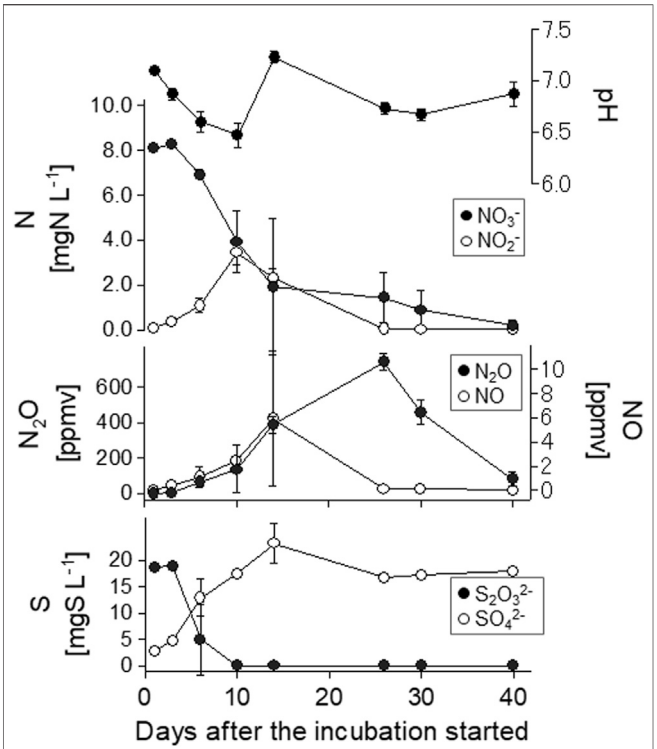

FIGURE 4 | Temporal variations of aquatic and gaseous nitrogen species and $S_2O_3^{2-}$ and SO_4^{2-} concentrations in I2 with N + S treatment in the long-term incubation experiment. N, KNO_3 solution; N + S, KNO_3, and $Na_2S_2O_3$ solution. Error bars indicate standard deviation (n = 3).

treatment plotted between these lines with small variations (**Figure 5B**). In the case of I1, relatively larger ΔSO_4^{2-} than ΔNO_3^- resulted in higher $\Delta SO_4^{2-}/\Delta NO_3^-$ in the N + S treatment. In the N treatment of I1, both ΔNO_3^- and ΔSO_4^{2-} were small; therefore, these results plotted near zero.

Short-Term Incubation Experiment

The NO_3^-, NO_2^-, NO, and N_2O levels and the pH were compared among different treatments and soil layers in the short-term incubation experiment using soils II1–8 (**Figures 6**, **7**, **Table 3**). Addition of S significantly decreased the NO_3^- concentration ($p < 0.01$) and pH ($p < 0.01$), and increased the NO_2^- ($p < 0.01$), NO ($p < 0.05$), and N_2O ($p < 0.05$) concentrations (**Figure 6**). These N species also changed markedly in the different soil layers (**Figure 7**, $p < 0.01$). NO_3^- concentrations in II4 and II8 tended to be lower, especially with added S (**Table 3**; **Figure 7**). The NO_2^- concentration rose with S addition in II4 (to 2.1 mg N L^{-1}) and II8 (to 0.57 mg N L^{-1}) (**Table 3**). SO_4^{2-} concentrations were higher in II4 (2.2 mg S L^{-1}) and II8 (10 mg S L^{-1}) without S addition (N treatment). $S_2O_3^{2-}$ was below the detection limit in any treatments or layers (data not shown). NO and N_2O concentrations after day 5 tended to be higher in II2, II4, and II8, especially with added S (**Figure 7**; **Table 3**). NO concentrations in II2, II4, and II8 with S addition increased to 12, 19, and 29 ppmv, respectively (**Table 3**); N_2O concentrations in II2, II4, and II8 with S addition increased to 84, 58, and 260 ppmv, respectively (**Table 3**). In II1, the NO_3^- concentration decreased to almost 0 mg N L^{-1} in both treatments, and NO_2^-, NO, and N_2O were also almost undetectable after day 5, but NO and N_2O clearly increased after day 2 (**Table 3**). In II3, II5, II6, and II7, the decrease in NO_3^- and the increases in NO_2^-, NO, and N_2O were relatively small.

Bacterial Communities in the Soil

The following were considered to be sulfur-oxidizing bacteria (SOB) in this study [name (Genbank accession number)]; Bacterium ML2-86 (DQ145977.1), Bacterium PE03-7G2 (AB127721.1), *Halothiobacillus* sp. SS13102 (KM979607.1), Rhodocyclaceae bacterium FTL11 (DQ451827.1), *Sulfuricella denitrificans* skB26 (AP013066.1), *Sulfuricurvum kujiense* DSM 16994 (CP002355.1), *Sulfuricurvum kujiense* YK-3 (AB080644.1), *Sulfuritalea hydrogenivorans* sk43H (AP012547.1), Sulfur-oxidizing bacterium OAII2 (AF170423.1), *Thiobacillus aquaesulis* (U58019.1), *Thiobacillus denitrificans* strain AGR/IICT/15B (LN614387.1), *Thiobacillus thioparus* strain NZ (KC542801.1), *Thiomonas arsenivorans* strain b6 (AY950676.1), *Thiomonas* sp. Ynys3 (AF387303.1). The relative abundances of SOB in I2 during the long-term incubation experiment are plotted in **Figure 8**. The significant differences ($p < 0.05$) among treatments were detected in *S. denitrificans* strain skB26 and *S. kujiense*, although no significant differences were detected any pairs of the data groups. The main SOB in the soil was *S. denitrificans* strain

TABLE 2 | Nitrate consumption (ΔNO_3^-) and sulfate production (ΔSO_4^{2-}), and $\Delta SO_4^{2-}/\Delta NO_3^-$ of the different estimation periods during long-term incubation.

Period	Layer	Treatment	ΔNO_3^-		ΔSO_4^{2-}		$\Delta SO_4^{2-}/\Delta NO_3^-$	
d			mmol		mmol			
1–14	I1	N	−0.025 (0.0032)	a	−0.0049 (0.00067)	A	0.20 (0.042)	a
	I1	N + S	0.045 (0.041)	a	0.18 (0.0036)	Bc	18 (26)	a
	I2	N	0.049 (0.026)	a	0.072 (0.083)	ab	2.2 (2.9)	a
	I2	N + S	0.15 (0.072)	b	0.22 (0.042)	c	2.1 (1.8)	a
1–40	I1	N	−0.032 (0.0026)	a	0.0015 (0.0027)	a	−0.0043 (0.080)	a
	I1	N + S	0.0090 (0.0043)	B	0.17 (0.0012)	c	22 (11)	b
	I2	N	0.15 (0.014)	C	0.032 (0.0048)	b	0.22 (0.045)	a
	I2	N + S	0.18 (0.014)	D	0.17 (0.0097)	c	0.94 (0.12)	a

Different letters indicate significant differences detected using One-way ANOVA followed by Bonferroni's test (p < 0.05).

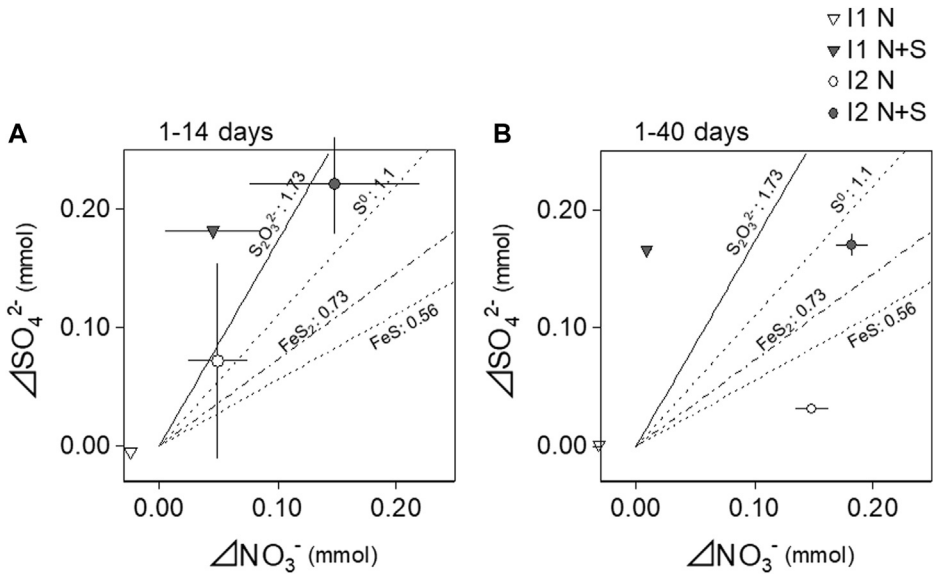

FIGURE 5 | Relationships between nitrate consumption (ΔNO_3^-) and sulfate production (ΔSO_4^{2-}) during long-term incubation. The estimation period for the consumption or the production values from days 1–14 **(A)** and from days 1–40 **(B)**. Lines in the figure indicate stoichiometric S/N of sulfur-based denitrification using different electron donors of S. $S_2O_3^{2-}$, Matsui and Yamamoto (1986); S^0, Batchelor and Lawrence (1978); FeS_2, Tong et al. (2017); FeS, Schippers and Jørgensen (2002).

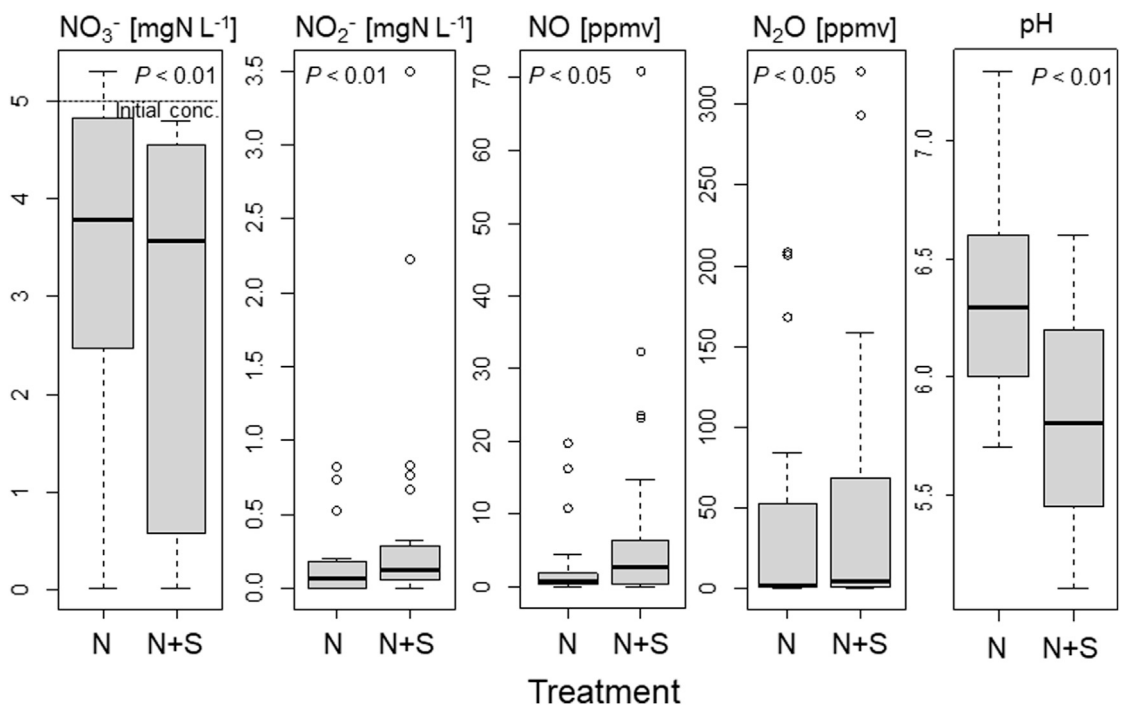

FIGURE 6 | Comparisons of NO_3^-, NO_2^-, NO, and N_2O concentrations and pH between treatments in the short-term incubation experiment using soils of streambank II. Thick line indicates median value, rectangle 25–75% of values. N, KNO_3 solution; N + S, KNO_3, and $Na_2S_2O_3$ solution.

skB26, which accounted for 55% of SOB and 0.04% of all sequences in the original soil before incubation (**Figure 8**, Ori). In the N + S treatment, *S. denitrificans* and *S. kujiense* strain YK-3increased on day 10 (N + S_10), and the combined abundance of both sequences increased to 3.3% of all bacteria. On day 30, the abundance of SOB relative to bacteria in the N + S

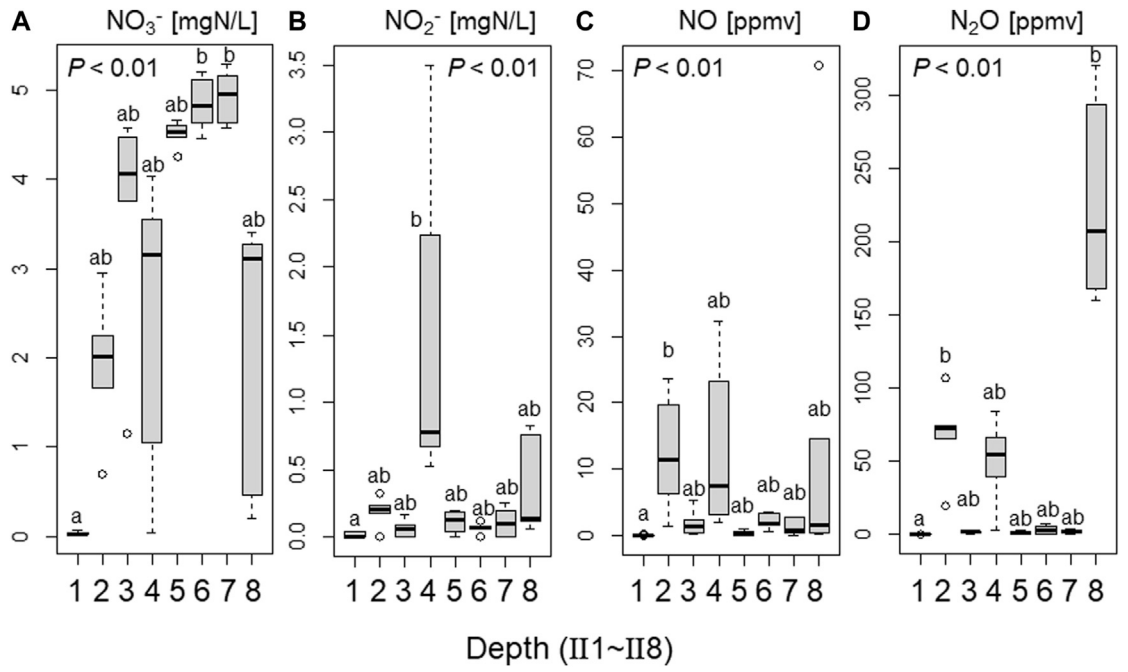

FIGURE 7 | Comparisons of NO_3^-, NO_2^-, NO, and N_2O concentrations between depths in the short-term incubation experiment using soils of streambank II. Thick line indicates median value, rectangle 25–75% of values. Different letters indicate significant differences detected using Kruskal–Wallis test followed by Steel–Dwass test ($p < 0.05$).

TABLE 3 | Summary data of the short-term incubation experiment using soils from streambank II. Values in parentheses indicate standard deviation ($n = 3$).

Layer	Treatment	pH	EC	NO_2d	NO_5d	N_2O_2d	N_2O_5d	NO_3^-	NO_2^-	SO_4^{2-}	NH_4^+
			mS m^{-1}	Ppmv	ppmv	ppmv	ppmv	mgN L^{-1}	mg N L^{-1}	mg S L^{-1}	mg N L^{-1}
II1	N	6.7 (0.1)	9.2 (0.6)	1.6 (0.6)	0.1 (0.0)	44 (33)	0.1 (0.1)	0.04 (0.02)	0 (0)	0.67 (0.07)	0.11 (0.01)
	N + S	6.5 (0.1)	12 (0.1)	1.4 (0.3)	0.1 (0.2)	43 (36)	0.1 (0.0)	0.02 (0.01)	0.03 (0.02)	6.7 (0.38)	0.12 (0.06)
II2	N	5.9 (0.1)	4.1 (0.9)	1.4 (0.3)	12 (10)	24 (10)	53 (28)	2.2 (0.67)	0.13 (0.11)	0.46 (0.05)	0.34 (0.01)
	N + S	5.4 (0.1)	7.3 (0.7)	1.6 (0.2)	12 (10)	12 (6.4)	84 (20)	1.7 (0.85)	0.25 (0.06)	6.0 (2.9)	0.30 (0.02)
II3	N	5.9 (0.1)	4.8 (0)	0.85 (0.3)	1.1 (0.9)	1.3 (0.0)	2.1 (0.5)	3.4 (2.0)	0.04 (0.03)	0.32 (0.21)	0.14 (0.03)
	N + S	5.2 (0.1)	10 (0.4)	1.1 (1.1)	2.7 (2.6)	0.8 (0.5)	1.8 (1.3)	4.0 (0.18)	0.09 (0.09)	8.6 (0.09)	0.10 (0.04)
II4	N	6.6 (0.1)	6.3 (0.4)	1.5 (0.9)	6.1 (4.1)	7.4 (2.8)	42 (41)	3.5 (0.55)	0.70 (0.15)	2.2 (0.53)	0.01 (0.005)
	N + S	6.3 (0.1)	12 (0.5)	1.5 (0.7)	19 (16)	4.1 (4.0)	58 (7.4)	1.5 (1.7)	2.1 (1.4)	11 (0.57)	0.01 (0.004)
II5	N	6.9 (0.4)	4.8 (0.4)	0.92 (0.6)	0.6 (0.4)	1.4 (0.4)	1.9 (0.7)	4.5 (0.21)	0.17 (0.04)	0.48 (0.04)	0.04 (0.003)
	N + S	5.8 (0.1)	9.9 (0.6)	0.12 (0.2)	0.1 (0.2)	0.3 (0.2)	0.5 (0.3)	4.5 (0.06)	0.05 (0.06)	8.9 (0.04)	0.004 (0.004)
II6	N	6.4 (0.1)	4.5 (0.4)	1.0 (1.1)	1.4 (0.6)	0.5 (0.2)	0.3 (0.2)	5.1 (0.11)	0.05 (0.04)	0.36 (0.02)	0.07 (0.01)
	N + S	5.8 (0.1)	10 (0.1)	2.1 (0.5)	2.9 (1.0)	1.1 (0.4)	6.1 (0.8)	4.6 (0.11)	0.09 (0.03)	8.9 (0.08)	0.10 (0.02)
II7	N	6.0 (0.1)	5.8 (0.2)	0.42 (0.4)	0.4 (0.4)	0.4 (0.2)	0.9 (0.6)	5.2 (0.01)	0.03 (0.05)	1.9 (0.06)	0.04 (0.01)
	N + S	5.6 (0.1)	10 (0.2)	0.44 (0.1)+	2.2 (1.0)	0.9 (0.1)	2.7 (0.6)	4.7 (0.11)	0.19 (0.07)	8.1 (0.07)	0.08 (0.01)
II8	N	6.3 (0.1)	11 (1.6)	3.4 (4.5)	0.9 (0.9)	33 (7.3)	190 (23)	3.3 (0.13)	0.11 (0.04)	10 (2.7)	0 (0)
	N + S	6.1 (0.1)	17 (6.1)	12 (9.4)	29 (37)	14 (14)	260 (87)	1.2 (1.6)	0.57 (0.39)	21 (7.7)	0.01 (0.02)

N, KNO_3 solution; N + S, KNO_3 and $Na_2S_2O_3$ solution.
_2d, 2 days after the start of incubation; _5d, 5 days after the start of incubation.

treatment decreased, but rose to 0.6% in the N treatment. The vertical profiles of SOB relative abundance in the soils of streambank II are plotted in **Figure 9**. The relative abundance of SOB ranged from 0.0% in II1 to 4.8% in II8. *S. denitrificans* was detected in II4, II7, and II8. Similarly, *T. denitrificans* strain AGR/IICT/15B was detected only in II8. Of the SOBs detected in the streambank II soil layers, *S. denitrificans* (II4, II7, and II8), *T. denitrificans* (II8), and *S. hydrogenivorans* (II8) all occurred in the I2 soil (**Figures 8**, **9**).

DISCUSSION

NO_3^- Reduction by Sulfur-Based Denitrification

Both the incubation experiments showed an NO_3^- reduction followed by increases in the NO_2^-, NO, and N_2O concentrations in some soils (**Figures 3**, **7**; **Table 3**), indicating that denitrification had occurred. No accumulation of NH_4^+

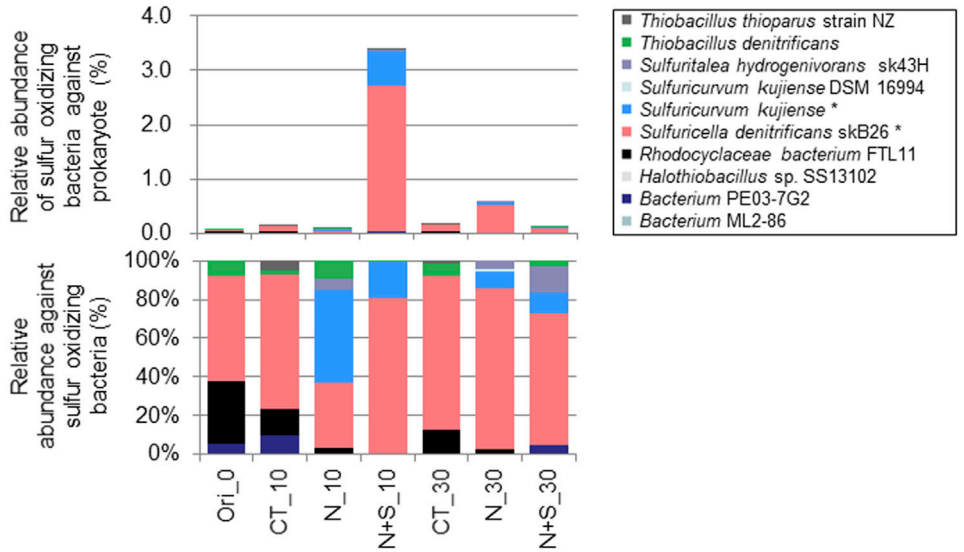

FIGURE 8 | Comparison of relative abundances of sulfur-oxidizing bacteria between treatments during the long-term incubation experiment in the I2 soil. Ori, original soil before incubation; CT, control; N, N treatment; N + S, N + S treatment. 0, 10, and 30 indicate the number of days after the start of incubation. The figure legend * indicates significant differences among treatments detected using Kruskal–Wallis test ($p < 0.05$), but no significant differences were detected any pairs of the data groups by Steel-Dwass test.

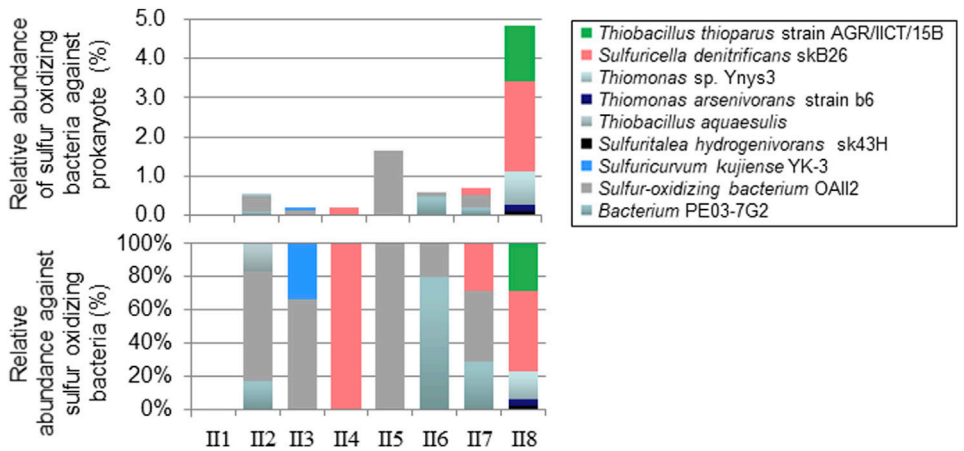

FIGURE 9 | Relative abundances of sulfur-oxidizing bacteria at different depths in the streambank II soils.

indicated dissimilatory nitrate reduction to ammonium (DNRA) (Friedl et al., 2018) was not a major NO_3^- removal process. Especially in the long-term incubation experiment in I2, the successive peaks of NO_2^-, NO, and N_2O concentrations (**Figure 4**) strongly support the occurrence of biological denitrification (Tiedje 1994; Di Capua et al., 2019). The magnitude of the decrease of NO_3^- concentration indicates that the denitrification potential was higher in the soils of I2, II1, II2, II4, and II8 (**Figures 3**, **7**). As discussed below, sulfur-based denitrification would be expected to occur predominantly in soils I2, II4, and II8, whereas other N-reduction processes such as heterotrophic denitrification could mostly take place in soils II1 and II2, depending on the availability of electron donors and/or bacteria for denitrification.

Addition of thiosulfate significantly promoted reduction of NO_3^- and production of NO2–, NO, and N_2O (**Figures 3**, **6**), indicating that sulfur-based denitrification had occurred. In I2 with N and N + S treatments, $\Delta SO_4^{2-}/\Delta NO_3^-$ for days 1–14 of incubation was large variation (2.1 ± 1.8, **Table 2**) and crossed to the denitrification line using thiosulfate, S^0, and FeS_2 as electron donors (**Figure 5**) with a decrease in pH (**Figure 4**), implying the occurrence of denitrification accompanying sulfur oxidation. II4 and II8 also exhibited relatively higher reduction of NO_3^- with added S (**Table 3**). These results indicate that sulfur-oxidizing bacteria in the soils had metabolized the added thiosulfate and

had promoted denitrification. In fact, *S. denitrificans* and *T. denitrificans*, which were relatively abundant in I2, II4, and II8, possess the ability to metabolize thiosulfate and can reduce NO_3^- (Kojima and Fukui, 2010; Shao et al., 2010). The increase in the relative proportions of *S. denitrificans* and *S. kujiense* on day 10 of I2 with N + S treatment (**Figure 8**) suggests that these bacteria were activated by the addition of thiosulfate. *S. kujiense*, which was detected in I2 and II3, also has the ability to reduce NO_3^- as the electron acceptor using thiosulfate (Kodama and Watanabe, 2004). Therefore, these bacteria are thought to be the key players in reduction of NO_3^- to NO2– by using thiosulfate.

The results of the long-term incubation also indicated that the phases controlling N reduction changed dramatically between the initial 14 day period and thereafter (**Figures 4**, **5** and **Supplementary Figure S4**). Sulfur-based denitrification may have been the predominant NO_3^- reduction process during the first 14 days in I2, and other N reduction processes such as heterotrophic denitrification may have occurred after day 14. The evidence supporting this conclusion is as follows: reduction of NO_3^- to NO2– accompanied by thiosulfate oxidation was clear during the first 14 days (**Figure 4**); the stoichiometric ratio of $\Delta SO_4^{2-}/\Delta NO_3^-$ was similar to the denitrification line using thiosulfate (Matsui and Yamamoto, 1986) during the first 14 days (**Figure 5**); and sulfur-oxidizing bacteria with NO_3^- reduction potential were detected and increased in relative abundance during this period (**Figure 8**). Chen et al. (2018) reported in a reactor study using solid S^0 as the electron donor for denitrification that the affinity of S^0 for NO_3^- was considerably higher than that for NO_2^-; they also discussed the conversion of NO_3^- to NO2–, and of NO2– to N_2, being performed by different microorganisms.

NO_2^- Accumulation and NO and N_2O Production

Temporal accumulation of NO_2^- was observed in this study (**Figure 4**; **Table 3**), as has also been demonstrated in previous bioreactor studies with added S (Moon et al., 2004; Chung et al., 2014; Liu et al., 2017; Chen et al., 2018). NO_2^- clearly accumulated during the first 10 days, particularly in I2 with S addition (**Figure 4**). Because the sum of NO_2^- and NO_3^- concentrations during this period was stable at approximately 8 mg N L^{-1}, which was equivalent to the added N concentration, NO_2^- reduction does not appear to have occurred, resulting in NO_2^- accumulation. Possible reasons for this are that the reduction of NO_2^- by sulfur-oxidizing bacteria is slower than the reduction of NO_3^- (Chung et al., 2014), and the higher affinity of sulfides for NO_3^- reduction than NO_2^- reduction, as discussed above. The S/N ratio in the added solution might also have been important for NO_2^- accumulation. Yamamoto-Ikemoto et al. (2000) observed accumulation of NO_2^- at added S/N (w/w) values of less than 4.35. Chung et al. (2014) reported that NO_2^- accumulation occurred at lower S/N ratios, possibly as a result of sulfide limitation, and complete denitrification required S/N of 5.1 (w/w). Liu et al. (2017) also observed NO_2^- accumulation at S/N values of 3.0 (w/w). In contrast, Qiu et al. (2020) reported that, in short-term batch tests in a sulfur-based denitrification system, organic supplementation accelerated NO_2^- reduction, indicating that denitrifiers likely use organics preferentially over sulfur as the electron donors to reduce NO_2^-. In our study, relatively lower added S/N (w/w) in the long-term (2.5) and short-term (2.0) incubations and probable lower available organic C in the subsoil possibly caused the temporal NO_2^- accumulation. Other possible mechanisms for NO_2^- accumulation may have to do with the abilities of sulfur-oxidizing bacteria. *S. kujiense* (detected in I2 and II3) and *T. thioparus* (detected in I2 and II8; **Figures 8**, **9**) can utilize thiosulfate as the electron donor and NO_3^- as the electron acceptor under anaerobic conditions, but can transfer NO_3^- to NO_2^- only (Kodama and Watanabe, 2004; Vaclavkova et al., 2015); thus, these bacteria, especially *S. Kujiense* detected significant change among treatments (**Figure 8**), may also contribute to NO_2^- accumulation. Another possible reason for the NO_2^- peak may be that nitrite-reducing organisms start growing after the consumption of NO_3^-. In general, bacterial growth starts after substrate consumption (Maier and Pepper, 2014). Therefore, long-term incubation studies with higher substrate addition to subsoil which is expected to be low in bacteria, slower bacterial growth-rate may not be negligible for NO_2^- accumulation.

Our results also demonstrated that S addition to the soil markedly increased the production and temporal accumulation of NO and N_2O. Especially in I2, II4, and II8, increases in NO and N_2O concentrations were observed in association with S addition (**Figures 4**, **6**, **Table 3**). This pattern may possibly result from the low added S/N ratio to the soils, the same reason as for the accumulation of NO_2^-. Lan et al. (2019) reported that a low S/N (w/w) ratio of one caused NO accumulation because competition for electrons caused incomplete denitrification (Velho et al., 2017; Pan et al., 2013). Another study reported that a high NO_2^- concentration (30 mg N L^{-1}) promoted NO accumulation (Castro-Barros et al., 2016). Our results also showed that N_2O concentration was higher with S addition, indicating enhanced N_2O production and accumulation (**Figures 4**, **6**). Lan et al. (2019) also reported N_2O accumulation in a batch reactor experiment and discussed how higher NO_2^- levels can inhibit N_2O reductase activity and cause N_2O accumulation. In fact, a rapid reduction in N_2O was observed from day 26, when NO_2^- had almost disappeared (**Figure 4**). In contrast, Yang et al. (2016) revealed that N_2O accumulation at an S/N mass ratio of 5.0 was only 4.7% of that at 3.0 S/N, and found that the N_2O reduction rate was linearly proportional to the sulfide concentration at pH 7.0. Recent study reported that the electron distribution was significantly affected by sulfide loading rate, and the electron competition among nitrogen oxide reductases was intensified with the most electrons flowing towards NO_3^- reductase, and the least electrons towards N_2O reductase under decreased sulfide loading rate, which is more directly responsible for intermediates accumulation such as NO_2^-, NO, N_2O in sulfur-based denitrification process (Oberoi et al., 2021). Therefore, considering the use of lower S/N values in our study, it seems that sulfide was predominantly used for NO_3^- reduction, after which NO_2^- accumulated because of a sulfide limitation, and the

limited sulfide and accumulated NO_2^- might also have caused NO and N_2O accumulation (**Figure 4**). Future work should incorporate experiments matching the S/N values observed in natural soils.

Sulfur-Based Denitrification Using Inherent S in Subsoil in Marine Sedimentary Rock Regions

The inherent sulfide in the subsoils might be derived from the marine sedimentary rocks, which are highly enriched in total sulfur in the Akita region (Koma, 1992), and this enrichment is likely reflected in the high EOS content in streambed sediments (**Figure 1**, Hayakawa et al., 2020) and in the subsoils in this study. The optimum growth rate of *S. kujiense* occurs in low-intensity salty conditions (Kodama and Watanabe, 2004); this species was detected in I2. The EC in the subsoil of the study area was relatively high (**Table 1**), suggesting that the subsoil remains a relatively salty environment, reflecting the influence of marine sedimentary rocks and possibly providing suitable conditions for such bacteria.

The indigenous sulfides observed in this study would be useful electron donors for ecosystem-wide sulfur-based denitrification in the subsoil. EOS represents reduced sulfur such as pyrite (Murano et al., 2000), which has been reported to act as an electron donor for sulfur-based denitrification in streambed sediments (Hayakawa et al., 2013). Because subsoils I2, II4, and II8, in which signs of sulfur-based denitrification were detected, had a high EOS content (**Table 1**), EOS in those soils could have been the electron donor for denitrification by sulfur-oxidizing bacteria. In the N treatment of I2, thiosulfate was detected at low levels on day 1, the SO_4^{2-} concentration increased even without S addition (**Figure 3**; **Table 2**), and $\Delta SO_4^{2-}/\Delta NO_3^-$ was similar to the denitrification line using thiosulfate until day 14 (**Figure 5**). These results indicate that the original EOS in the I2 soil had provided available S as an electron donor for denitrification. In addition, the SO_4^{2-} concentrations in II4 and II8 without S addition (N treatment) were higher than those in other soil layers (**Table 3**), suggesting that the inherent sulfide had been oxidized to SO_4^{2-} and might have contributed to denitrification. However, detection of thiosulfate appears to be difficult, probably because the oxidation rate of inherent sulfide to thiosulfate is slow and the thiosulfate produced is rapidly oxidized to SO_4^{2-} (**Figure 3**). Therefore, thiosulfate was not detected during the short-term incubation. HS^- and S^0 other than thiosulfate can be also electron donors for sulfur-based denitrification (De Capua et al., 2019) and iron sulfides (FeS and FeS_2) can produce HS^-, S^0 and thiosulfate in their dissolution processes (Hu et al., 2020). X-ray powder diffraction analysis showed the diffraction patterns for I2, II4, and II8 soils were likely equivalent to pyrite (FeS_2) and pentlandite [$(Fe, Ni)_9S_8$] (**Supplementary Figure S5**). Therefore, these iron sulfides might be electron donors for denitrification and the large variations of the stoichiometric ratios in I2 during days 1–14 (**Figure 5** and **Table 2**) might have included the results of the oxidation of such iron sulfides from the indigenous sulfides in the catchment. Bacteria detected in this study subsoil also possess the ability to metabolize S^0 (*S. denitrificans*, *T. denitrificans,* and *S. kujiense*) and HS^- (*T. denitrificans*), and can reduce NO_3^- (Kodama and Watanabe, 2004; Kojima and Fukui, 2010; Shao et al., 2010; De Capua et al., 2019; Cron et al., 2019).

In general, most NO_3^- is reduced by denitrifying heterotrophs rather than by chemoautotrophs such as sulfur-oxidizing bacteria because NO_3^- reduction by organic matter should thermodynamically precede reduction by sulfide (Postma et al., 1991). In the surface soil, heterotrophic denitrification was probably the dominant NO_3^- reduction process. In II1, little NO_3^-, NO_2^-, NO, and N_2O were detected after 5 days of incubation, but higher NO and N_2O concentrations were detected after 2 days (**Table 3**), indicating that denitrification had occurred rapidly. Because sulfur-oxidizing bacteria were not detected in II1 (**Figure 9**), NO_3^- was likely reduced by heterotrophs using relatively abundant organic carbon as the electron donor in the surface soil (**Table 1**). Therefore, when the conditions are suitable, denitrification will proceed more rapidly in surface soil than in the underlying soil. Carbon was also present in the subsoils (**Table 1**), but may be too old to be available for bacteria. Baker et al. (2012) suggested that pyrite was the main electron donor in subsoil because no significant decrease in organic C content was observed, likely because hardly decomposable organic C could not be exploited by heterotrophic microbes in the old sediments of the Jurassic Lincolnshire limestone. In contrast, Vaclavkova et al. (2014) found that sulfur-based denitrification co-occurred and accounted for approximately 30% of the net NO_3^- reduction, despite the presence of organic carbon, in a variety of Danish sediments. Cron et al. (2019) suggested that sulfur-oxidizing bacteria (*Sulfuricurvum kujiense,* also detected in this study) could use soluble organics to stabilize stores of bioavailable S^0 outside the cells. Recent bioreactor study reported key functional heterotrophic and autotrophic denitrifiers jointly contributed to high nitrogen removal efficiency by symbiotic relationships (Han et al., 2020). Although we did not measure organic C dynamics in this study, these symbiotic relationships may also occur in natural subsoil with lower available organic C in the study area.

The same denitrifying sulfur-oxidizing bacteria (*S. denitrificans*) were detected in the higher EOS subsoil layers I2, II4, II7, and II8 despite the different streambanks being located approximately 50 m apart (**Figure 2**), and beta diversity analysis shown that microbial communities in II4 and II8 were similar to those in I2 samples. (**Supplementary Figure S3**). *S. denitrificans* is a facultative anaerobic sulfur-oxidizing bacterium that was isolated from an anoxic layer (depth 40 m) from a freshwater lake in Japan (Kojima and Fukui, 2010). These results suggest that this bacterium is ubiquitous in the similar sulfide-containing layers in the catchments having higher EOS in riverbed sediments (**Figure 1**) and can contribute to NO_3^- reduction; in addition, because it is a freshwater bacterium, it is thought to have occurred in the soil only after the change from seawater to freshwater. However, the relative abundance of the bacterium was less than 5% of the total microbial community (**Figures 8**, **9**). A previous

sludge reactor study also reported that *T. denitrificans* accounted for less than 5% of the entire microbial population by fluorescent *in situ* hybridization, despite clear NO_3^- reduction being observed (Dolejs et al., 2015). A small number of key players may be responsible for sulfur-based denitrification, especially in natural subsoils and sediments.

CONCLUSIONS

We detected multiple signs of sulfur-based denitrification in streambank subsoils in a headwater catchment underlain by marine sedimentary rock. Specifically, NO_3^- reduction accompanied by SO_4^{2-} production; a microbial stoichiometric $\Delta SO_4^{2-}/\Delta NO_3^-$ ratio indicative of denitrification using thiosulfate; accumulation of NO_2^-, NO, and N_2O; and sulfur-oxidizing bacteria with the ability to reduce NO_3^- were detected in the subsoils with higher sulfide contents. The key player of sulfur-based denitrification in the subsoils appeared to be *S. denitrificans*, which is widespread and can exploit the inherent sulfide in those soils. These results revealed that the subsoils possess the potential for sulfur-based denitrification; therefore, sulfur-based denitrification in the subsoil is an important process for NO_3^- reduction and might control NO_3^- in the catchment. Further information on the quantity and three-dimensional distribution of sulfides and the functions associated with sulfur-oxidizing bacteria are required for better understanding and estimation of ecosystem-wide denitrification in sulfide-rich regions.

DATA AVAILABILITY STATEMENT

The datasets presented in this study can be found in online repositories. The names of the repository/repositories and accession number(s) can be found below: https://www.ddbj.nig.ac.jp/, DRA011495.

AUTHOR CONTRIBUTIONS

AH: Conceptualization, methodology, investigation, writing-reviewing and editing of this study. HO: Investigation, analysis of soil and gas, and writing-original draft preparation. RA: Bacterial community analysis. HM: Methodology of soil analysis especially easily oxidizable sulfur. TI: Investigation and reviewing. TT: Supervision of this study.

FUNDING

This study was partly supported by a Grant-in-Aid for Research (B), No. 26281011, provided by the Japan Society for the Promotion of Science (JSPS).

SUPPLEMENTARY MATERIAL

The Supplementary Material for this article can be found online at: https://www.frontiersin.org/articles/10.3389/fenvs.2021.664488/full#supplementary-material.

REFERENCES

Adhikari, K., and Hartemink, A. E. (2016). Linking soils to ecosystem services - A global review. *Geoderma* 262, 101–111. doi:10.1016/j.geoderma.2015.08.009

Baker, K. M., Bottrell, S. H., Hatfield, D., Mortimer, R. J. G., Newton, R. J., Odling, N. E., et al. (2012). Reactivity of pyrite and organic carbon as electron donors for biogeochemical processes in the fractured Jurassic Lincolnshire limestone aquifer, UK. *Chem. Geology.* 332-333, 26–31. doi:10.1016/j.chemgeo.2012.07.029

Batchelor, B., and Lawrence, A. W. (1978). Autotrophic Denitrification Using Elemental Sulfur. *Journal (Water Pollution Control Federation)* 50, 1986–2001.

Brunet, R. C., and Garcia-Gil, L. J. (1996). Sulfide-induced dissimilatory nitrate reduction to ammonia in anaerobic freshwater sediments. *FEMS Microbiol. Ecol.* 21, 131–138. doi:10.1016/0168-6496(96)00051-710.1111/j.1574-6941.1996.tb00340.x

Burgin, A. J., and Hamilton, S. K. (2007). Have we overemphasized the role of denitrification in aquatic ecosystems? A review of nitrate removal pathways. *Front. Ecol. Environ.* 5, 89–96. doi:10.1890/1540-9295(2007)5[89:hwotro]2.0.co;2

Burgin, A. J., and Hamilton, S. K. (2008). NO3 −-Driven SO4 2− Production in Freshwater Ecosystems: Implications for N and S Cycling. *Ecosystems* 11, 908–922. doi:10.1007/s10021-008-9169-5

Caporaso, J. G., Lauber, C. L., Walters, W. A., Berg-Lyons, D., Lozupone, C. A., Turnbaugh, P. J., et al. (2011). Global patterns of 16S rRNA diversity at a depth of millions of sequences per sample. *Proc. Natl. Acad. Sci.* 108, 4516–4522. doi:10.1073/pnas.1000080107

Castro-Barros, C. M., Rodríguez-Caballero, A., Volcke, E. I. P., and Pijuan, M. (2016). Effect of nitrite on the N2O and NO production on the nitrification of low-strength ammonium wastewater. *Chem. Eng. J.* 287, 269–276. doi:10.1016/j.cej.2015.10.121

Chao, A., and Bunge, J. (2002). Estimating the number of species in a stochastic abundance model. *Biometrics* 58 (3), 531–539. doi:10.1111/j.0006-341x.2002.00531.x

Chen, F., Li, X., Gu, C., Huang, Y., and Yuan, Y. (2018). Selectivity control of nitrite and nitrate with the reaction of S0 and achieved nitrite accumulation in the sulfur autotrophic denitrification process. *Bioresour. Tech.* 266, 211–219. doi:10.1016/j.biortech.2018.06.062

Chung, J., Amin, K., Kim, S., Yoon, S., Kwon, K., and Bae, W. (2014). Autotrophic denitrification of nitrate and nitrite using thiosulfate as an electron donor. *Water Res.* 58, 169–178. doi:10.1016/j.watres.2014.03.071

Craig, L., Bahr, J. M., and Roden, E. E. (2010). Localized zones of denitrification in a floodplain aquifer in southern Wisconsin, USA. *Hydrogeol J.* 18, 1867–1879. doi:10.1007/s10040-010-0665-2

Cron, B., Henri, P., Chan, C. S., Macalady, J. L., and Cosmidis, J. (2019). Elemental Sulfur Formation by Sulfuricurvum kujiense Is Mediated by Extracellular Organic Compounds. *Front. Microbiol.* 10, 2710. doi:10.3389/fmicb.2019.02710

Di Capua, F., Pirozzi, F., Lens, P. N. L., and Esposito, G. (2019). Electron donors for autotrophic denitrification. *Chem. Eng. J.* 362, 922–937. doi:10.1016/j.cej.2019.01.069

Dolejs, P., Paclík, L., Maca, J., Pokorna, D., Zabranska, J., and Bartacek, J. (2015). Effect of S/N ratio on sulfide removal by autotrophic denitrification. *Appl. Microbiol. Biotechnol.* 99, 2383–2392. doi:10.1007/s00253-014-6140-6

Fang, Y., Gundersen, P., Vogt, R. D., Koba, K., Chen, F., Chen, X. Y., et al. (2011). Atmospheric deposition and leaching of nitrogen in Chinese forest ecosystems. *J. For. Res.* 16, 341–350. doi:10.1007/s10310-011-0267-4

Friedl, J., De Rosa, D., Rowlings, D. W., Grace, P. R., Müller, C., and Scheer, C. (2018). Dissimilatory nitrate reduction to ammonium (DNRA), not

denitrification dominates nitrate reduction in subtropical pasture soils upon rewetting. *Soil Biol. Biochem.* 125, 340–349. doi:10.1016/j.soilbio.2018.07.024

Galloway, J. N., and Cowling, E. B. (2002). Reactive Nitrogen and the World: 200 Years of Change. *AMBIO: A J. Hum. Environ.* 31, 64–71. doi:10.1579/0044-7447-31.2.64

Garcia-Gil, L. J., and Golterman, H. L. (1993). Kinetics of FeS-mediated denitrification in sediments from the Camargue (Rhone delta, southern France). *FEMS Microbiol. Ecol.* 13, 85–91. doi:10.1111/j.1574-6941.1993.tb00054.x

Garrity, G. M., Bell, J. A., and Lilburn, T. (2005). "Genus Thiobacillus," In *Bergey's manual of systematic bacteriology*. Vol. 2,2edn, PartB. Edited by G. M. Garrity 58–59. New York: Springer.

Han, F., Zhang, M., Shang, H., Liu, Z., and Zhou, W. (2020). Microbial community succession, species interactions and metabolic pathways of sulfur-based autotrophic denitrification system in organic-limited nitrate wastewater. *Bioresour. Tech.* 315, 123826. doi:10.1016/j.biortech.2020.123826

Hayakawa, A., Funaki, Y., Sudo, T., Asano, R., Murano, H., Watanabe, S., et al. (2020). Catchment topography and the distribution of electron donors for denitrification control the nitrate concentration in headwater streams of the Lake Hachiro watershed. *Soil Sci. Plant Nutr.* 66, 906–918. doi:10.1080/00380768.2020.1827292

Hayakawa, A., Hatakeyama, M., Asano, R., Ishikawa, Y., and Hidaka, S. (2013). Nitrate reduction coupled with pyrite oxidation in the surface sediments of a sulfide-rich ecosystem. *J. Geophys. Res. Biogeosci.* 118, 639–649. doi:10.1002/jgrg.20060

Horowitz, A. J., and Elrick, K. A. (2017). The use of bed sediments in water quality studies and monitoring programs. *Proc. IAHS* 375, 11–17. doi:10.5194/piahs-375-11-2017

Hu, Y., Wu, G., Li, R., Xiao, L., and Zhan, X. (2020). Iron sulphides mediated autotrophic denitrification: An emerging bioprocess for nitrate pollution mitigation and sustainable wastewater treatment. *Water Res.* 179, 115914. doi:10.1016/j.watres.2020.115914

Iribar, V., and Ábalos, B. (2011). The geochemical and isotopic record of evaporite recycling in spas and salterns of the Basque Cantabrian basin, Spain. *Appl. Geochem.* 26, 1315–1329. doi:10.1016/j.apgeochem.2011.05.005

Japan Meteorological Agency (2013). Information of meteorological statistics. Accessed April 19 2013 http://www.data.jma.go.jp/obd/stats/etrn/index.php.

Juncher Jørgensen, C., Jacobsen, O. S., Elberling, B., and Aamand, J. (2009). Microbial oxidation of pyrite coupled to nitrate reduction in anoxic groundwater sediment. *Environ. Sci. Technol.* 43, 4851–4857. doi:10.1021/es803417s

Kodama, Y., and Watanabe, K. (2004). *Sulfuricurvum kujiense* gen. nov., sp. nov., a facultatively anaerobic, chemolithoautotrophic, sulfur-oxidizing bacterium isolated from an underground crude-oil storage cavity. *Int. J. Syst. Evol. Microbiol.* 54, 2297–2300. doi:10.1099/ijs.0.63243-0

Kojima, H., and Fukui, M. (2010). *Sulfuricella denitrificans* gen. nov., sp. nov., a sulfur-oxidizing autotroph isolated from a freshwater lake. *Int. J. Syst. Evol. Microbiol.* 60, 2862–2866. doi:10.1099/ijs.0.016980-0

Koma, T. (1992). Studies on depositional environments from chemical components of sedimentary rocks-with special reference to sulfur abundance-. *Bull. Geol. Surv. Jpn.* 43, 473–548.

Korom, S. F. (1992). Natural denitrification in the saturated zone: A review. *Water Resour. Res.* 28, 1657–1668. doi:10.1029/92wr00252

Lan, L., Zhao, J., Wang, S., Li, X., Qiu, L., Liu, S., et al. (2019). NO and N2O accumulation during nitrite-based sulfide-oxidizing autotrophic denitrification. *Bioresour. Tech. Rep.* 7, 100190. doi:10.1016/j.biteb.2019.100190

Li, E., Deng, T., Yan, L., Zhou, J., He, Z., Deng, Y., et al. (2021). Elevated nitrate simplifies microbial community compositions and interactions in sulfide-rich river sediments. *Sci. Total Environ.* 750, 141513. doi:10.1016/j.scitotenv.2020.141513

Lilburne, L., Eger, A., Mudge, P., Ausseil, A.-G., Stevenson, B., Herzig, A., et al. (2020). The Land Resource Circle: Supporting land-use decision making with an ecosystem-service-based framework of soil functions. *Geoderma* 363, 114134. doi:10.1016/j.geoderma.2019.114134

Liu, C., Li, W., Li, X., Zhao, D., Ma, B., Wang, Y., et al. (2017). Nitrite accumulation in continuous-flow partial autotrophic denitrification reactor using sulfide as electron donor. *Bioresour. Tech.* 243, 1237–1240. doi:10.1016/j.biortech.2017.07.030

Lovett, G. M., and Goodale, C. L. (2011). A New Conceptual Model of Nitrogen Saturation Based on Experimental Nitrogen Addition to an Oak Forest. *Ecosystems* 14, 615–631. doi:10.1007/s10021-011-9432-z

Maier, R. M., and Pepper, I. L. (2014). "Chapter3-Bacterial Growth," in *Environmental Microbiology*. Editors I. L. Pepper, C. P. Gerba, and T. J. Gentry. Third Edition (Amsterdam: Elsevier), 37–56.

Martínez-Santos, M., Lanzén, A., Unda-Calvo, J., Martín, I., Garbisu, C., and Ruiz-Romera, E. (2018). Treated and untreated wastewater effluents alter river sediment bacterial communities involved in nitrogen and sulphur cycling. *Sci. Total Environ.* 633, 1051–1061. doi:10.1016/j.scitotenv.2018.03.229

Matsui, S., and Yamamoto, R. (1986). A New Method of Sulphur Denitrification for Sewage Treatment by a Fluidized Bed Reactor. *Water Sci. Tech.* 18, 355–362. doi:10.2166/wst.1986.0308

Moon, H. S., Ahn, K.-H., Lee, S., Nam, K., and Kim, J. Y. (2004). Use of autotrophic sulfur-oxidizers to remove nitrate from bank filtrate in a permeable reactive barrier system. *Environ. Pollut.* 129, 499–507. doi:10.1016/j.envpol.2003.11.004

Murano, H., Yamanaka, T., and Mizota, C. (2000). Origin of sulfides and associated sulfates in Neogene sediments along the Kitakami River basin from northeast Japan—Sulfur isotopic characterization and implications for land consolidation. *Pedologist* 44, 81–90. (in Japanese with English summary). doi:10.18920/pedologist.44.2_81

Oberoi, A. S., Huang, H., Khanal, S. K., Sun, L., and Lu, H. (2021). Electron distribution in sulfur-driven autotrophic denitrification under different electron donor and acceptor feeding schemes. *Chem. Eng. J.* 404, 126486. doi:10.1016/j.cej.2020.126486

Pan, Y., Ye, L., and Yuan, Z. (2013). Effect of H2S on N2O Reduction and Accumulation during Denitrification by Methanol Utilizing Denitrifiers. *Environ. Sci. Technol.* 130710143655002, 130710143655002. doi:10.1021/es401632r

Plugge, C. M., Zhang, W., Scholten, J. C. M., and Stams, A. J. M. (2011). Metabolic Flexibility of Sulfate-Reducing Bacteria. *Front. Microbio.* 2, 81. doi:10.3389/fmicb.2011.00081

Postma, D., Boesen, C., Kristiansen, H., and Larsen, F. (1991). Nitrate Reduction in an Unconfined Sandy Aquifer: Water Chemistry, Reduction Processes, and Geochemical Modeling. *Water Resour. Res.* 27, 2027–2045. doi:10.1029/91WR00989

Qian, J., Zhou, J., Zhang, Z., Liu, R., and Wang, Q. (2016). Biological Nitrogen Removal through Nitritation Coupled with Thiosulfate-Driven Denitritation. *Sci. Rep.* 6, 27502. doi:10.1038/srep27502

Qiu, Y.-Y., Zhang, L., Mu, X., Li, G., Guan, X., Hong, J., et al. (2020). Overlooked pathways of denitrification in a sulfur-based denitrification system with organic supplementation. *Water Res.* 169, 115084. doi:10.1016/j.watres.2019.115084

Roberts, A. P. (2015). Magnetic mineral diagenesis. *Earth-Science Rev.* 151, 1–47. doi:10.1016/j.earscirev.2015.09.010

Schippers, A., and Jørgensen, B. B. (2002). Biogeochemistry of pyrite and iron sulfide oxidation in marine sediments. *Geochimica et Cosmochimica Acta* 66, 85–92. doi:10.1016/S0016-7037(01)00745-1

Schwientek, M., Einsiedl, F., Stichler, W., Stögbauer, A., Strauss, H., and Maloszewski, P. (2008). Evidence for denitrification regulated by pyrite oxidation in a heterogeneous porous groundwater system. *Chem. Geology.* 255, 60–67. doi:10.1016/j.chemgeo.2008.06.005

Shao, M.-F., Zhang, T., and Fang, H. H.-P. (2010). Sulfur-driven autotrophic denitrification: Diversity, biochemistry, and engineering applications. *Appl. Microbiol. Biotechnol.* 88, 1027–1042. doi:10.1007/s00253-010-2847-1

Shiraishi, T. (1990). Holocene geologic development of the Hachiro-gata lagoon, Akita Prefecture, Northeast Honshu, Japan. *Mem. Geol. Soc. Jpn.* 36, 47–69. (in Japanese with English summary).

Shiraishi, T., and Matoba, Y. (1992). Neogene paleogeography and paleoenvironment in Akita and Yamagata Prefectures, Japan Sea side of northeast Honshu, Japan. *Mem. Geol. Soc. Jpn.* 37, 39–51. (in Japanese with English summary).

Straub, K. L., Benz, M., Schink, B., and Widdel, F. (1996). Anaerobic, nitrate-dependent microbial oxidation of ferrous iron. *Appl. Environ. Microbiol.* 62, 1458–1460. doi:10.1128/aem.62.4.1458-1460.1996

Szynkiewicz, A., Johnson, A. P., and Pratt, L. M. (2012). Sulfur species and biosignatures in Sulphur Springs, Valles Caldera, New Mexico-Implications for Mars astrobiology. *Earth Planet. Sci. Lett.* 321-322, 1–13. doi:10.1016/j.epsl.2011.12.015

Tiedje, J. M. (1994). "Denitrifiers," in *Methods of Soil Analysis. Part 2. SSSA Book Ser. 5.* Editor R. W. Weaver (Madison: Soil Science Society of America), 245–257.

Tong, S., Rodriguez-Gonzalez, L. C., Feng, C., and Ergas, S. J. (2017). Comparison of particulate pyrite autotrophic denitrification (PPAD) and sulfur oxidizing denitrification (SOD) for treatment of nitrified wastewater. *Water Sci. Tech.* 75, 239–246. doi:10.2166/wst.2016.502

Torrentó, C., Cama, J., Urmeneta, J., Otero, N., and Soler, A. (2010). Denitrification of groundwater with pyrite and Thiobacillus denitrificans. *Chem. Geology.* 278, 80–91. doi:10.1016/j.chemgeo.2010.09.003

Torrentó, C., Urmeneta, J., Otero, N., Soler, A., Viñas, M., and Cama, J. (2011). Enhanced denitrification in groundwater and sediments from a nitrate-contaminated aquifer after addition of pyrite. *Chem. Geology.* 287, 90–101. doi:10.1016/j.chemgeo.2011.06.002

Vaclavkova, S., Jørgensen, C. J., Jacobsen, O. S., Aamand, J., and Elberling, B. (2014). The Importance of Microbial Iron Sulfide Oxidation for Nitrate Depletion in Anoxic Danish Sediments. *Aquat. Geochem.* 20, 419–435. doi:10.1007/s10498-014-9227-x

Vaclavkova, S., Schultz-Jensen, N., Jacobsen, O. S., Elberling, B., and Aamand, J. (2015). Nitrate-Controlled Anaerobic Oxidation of Pyrite byThiobacillusCultures. *Geomicrobiology J.* 32, 412–419. doi:10.1080/01490451.2014.940633

Velho, V. F., Magnus, B. S., Daudt, G. C., Xavier, J. A., Guimarães, L. B., and Costa, R. H. R. (2017). Effect of COD/N ratio on N2O production during nitrogen removal by aerobic granular sludge. *Water Sci. Tech.* 76, 3452–3460. doi:10.2166/wst.2017.502

Vitousek, P. M. (1997). Human Domination of Earth's Ecosystems. *Science* 277, 494–499. doi:10.1126/science.277.5325.494

Wang, J.-J., Xu, L.-Z. -J., Huang, B.-C., Li, J., and Jin, R.-C. (2021). Multiple electron acceptor-mediated sulfur autotrophic denitrification: Nitrogen source competition, long-term performance and microbial community evolution. *Bioresour. Tech.* 329, 124918. doi:10.1016/j.biortech.2021.124918

Wynn, J. G., Sumrall, J. B., and Onac, B. P. (2010). Sulfur isotopic composition and the source of dissolved sulfur species in thermo-mineral springs of the Cerna Valley, Romania. *Chem. Geology.* 271, 31–43. doi:10.1016/j.chemgeo.2009.12.009

Yamamoto-Ikemoto, R., Komori, T., Nomuri, M., Ide, Y., and Matsukami, T. (2000). Nitrogen removal from hydroponic culture wastewater by autotrophic denitrification using thiosulfate. *Water Sci. Tech.* 42, 369–376. doi:10.2166/wst.2000.0405

Yang, W., Zhao, Q., Lu, H., Ding, Z., Meng, L., and Chen, G.-H. (2016). Sulfide-driven autotrophic denitrification significantly reduces N2O emissions. *Water Res.* 90, 176–184. doi:10.1016/j.watres.2015.12.032

Yin, H., Yang, P., and Kong, M. (2019). Effects of nitrate dosing on the migration of reduced sulfur in black odorous river sediment and the influencing factors. *Chem. Eng. J.* 371, 516–523. doi:10.1016/j.cej.2019.04.095

Conflict of Interest: The authors declare that the research was conducted in the absence of any commercial or financial relationships that could be construed as a potential conflict of interest.

Publisher's Note: All claims expressed in this article are solely those of the authors and do not necessarily represent those of their affiliated organizations, or those of the publisher, the editors and the reviewers. Any product that may be evaluated in this article, or claim that may be made by its manufacturer, is not guaranteed or endorsed by the publisher.

Advantages of publishing in Frontiers

OPEN ACCESS
Articles are free to read for greatest visibility and readership

FAST PUBLICATION
Around 90 days from submission to decision

HIGH QUALITY PEER-REVIEW
Rigorous, collaborative, and constructive peer-review

TRANSPARENT PEER-REVIEW
Editors and reviewers acknowledged by name on published articles

Frontiers
Avenue du Tribunal-Fédéral 34
1005 Lausanne | Switzerland

Visit us: www.frontiersin.org
Contact us: frontiersin.org/about/contact

REPRODUCIBILITY OF RESEARCH
Support open data and methods to enhance research reproducibility

DIGITAL PUBLISHING
Articles designed for optimal readership across devices

FOLLOW US
@frontiersin

IMPACT METRICS
Advanced article metrics track visibility across digital media

EXTENSIVE PROMOTION
Marketing and promotion of impactful research

LOOP RESEARCH NETWORK
Our network increases your article's readership